Estudio del tráfico intracelular del transportador neuronal de glicina GlyT2: Modulación por lipid rafts, ubiquitinación e interacción con Na/K ATPasa.

Tesis doctoral
/2013

Estudio del tráfico intracelular del transportador neuronal de glicina GlyT2: Modulación por lipid rafts, ubiquitinación e interacción con Na/K ATPasa.

Jaime de Juan Sanz

Universidad Autónoma de Madrid
Facultad de Ciencias
Departamento de Biología Molecular

Memoria presentada por el licenciado Jaime de Juan Sanz para optar al título de Doctor en Ciencias

Director de la tesis:
Dra. Carmen Aragón Rueda

Codirector de la tesis:
Dra. Beatriz López-Corcuera

Este trabajo ha sido realizado en el Departamento de Biología Molecular, Centro de Biología Molecular "Severo Ochoa" (C.S.I.C - U.A.M)

Introducción

Artículos compendiados

Introducción

A.1 El sistema nervioso, neuronas y sinápsis.

El sistema nervioso (SN) tiene la capacidad de recibir, procesar e interpretar estímulos externos e internos para determinar una respuesta rápida del organismo a cambios en su entorno. Esto está estrechamente ligado a la supervivencia y, por tanto, evolutivamente el sistema nervioso ha ido perfeccionándose para conseguir respuestas más finas, rápidas y coherentes. Anatómicamente el SN se divide en sistema nervioso periférico (SNP), constituido por los nervios craneales y espinales, responsable de la recepción de estímulos (internos y externos) y sistema nervioso central (SNC), formado por encéfalo y médula espinal, encargado de la integración de las señales aferentes y de la respuesta motora final. Ambos, SNP y SNC, se componen principalmente de dos tipos celulares: la neuroglia (o únicamente glia) y las neuronas, especializadas en la transmisión eléctrica de información a lo largo del cuerpo.

Las neuronas comparten con el resto de tipos celulares los orgánulos más comunes (retículo endoplasmático, aparato de Golgi, citoesqueleto, mitocondrias, lisosomas, etc…) pero poseen una diferenciación morfológica, celular y proteómica única que les permite recibir e integrar una señal eléctrica y transmitirla a lo largo de su membrana plasmática.

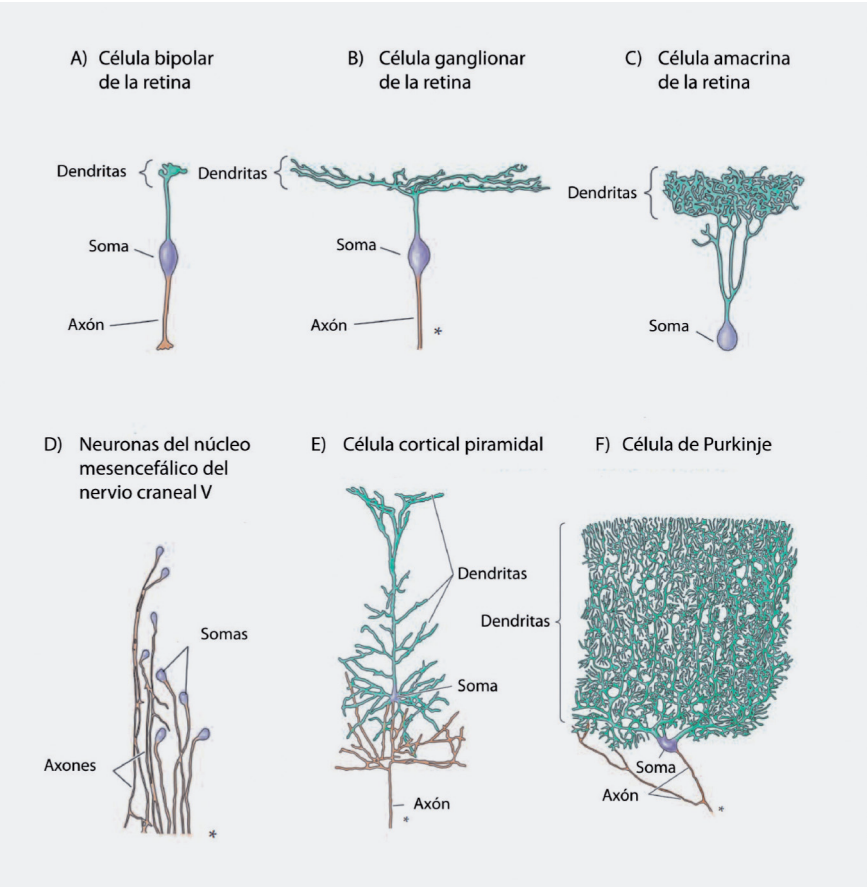

Figura1
Variabilidad neuronal existente en el SN.
Los ejemplos mostrados son: A) célula bipolar de la retina, B) célula ganglionar de la retina, C) célula amadrina de la retina, D) neuronas del núcleo mesencefálico del nervio craneal V, E) célula cortica piramidal y F) célula de Purkinje. Nótese la limitada arborización dendrítica de las neuronas bipolares de la retina (A), que permite una menor integración de las señales externas, mientras que, por ejemplo, las células de Purkinje poseen un árbol dendrítico mucho mayor que permite la recepción de información desde muchos más contactos sinápticos.

Generalmente las neuronas se componen de soma (cuerpo celular), dendritas y axón pero la subespecialización neuronal determina enormes diferencias, por ejemplo, en la longitud del axón o en la ramificación del árbol dendrítico (figura 1), así como en la expresión de unas proteínas u otras, lo que conlleva la existencia de diferentes subtipos neuronales que pueden llevar a cabo diferentes funciones relacionadas con la transmisión de información.

Esta transmisión de información se lleva a cabo gracias a la sinápsis, una diferenciación morfológica y funcional constituida por la terminación del axón de una neurona que se ensancha para formar el botón presináptico, en aposición a una región de una dendrita (o menos frecuentemente del soma) de otra neurona, que recibe el nombre de región postsináptica. Entre la membrana presináptica y la postsináptica existe un espacio denominado hendidura sináptica que tiene una anchura de 20 a 50 nm y donde a través de unas sustancias químicas llamadas neurotransmisores se produce la comunicación interneuronal.

Los principales neurotransmisores pueden ser de distintos tipos: 1) Derivados de aminas (dopamina, serotonina, norepinefrina…), 2) aminoácidos (glutamato, glicina, ácido γ-aminobutírico…), 3) purinas (ATP, adenosina), 4) pequeños péptidos de entre 3 y 30 aminoácidos (sustancia P, somatostatina…) o 5) pequeñas moléculas (acetilcolina). Pero todos tienen en común el mecanismo de acción: Liberación del neurotransmisor, unión al receptor postsináptico específico, activación (o inhibición) de la neurona postsináptica y terminación de esta señal llevada a cabo principalmente por la recaptación de neurotransmisor a través de transportadores específicos neuronales y gliales.

B.1 La glicina como neurotransmisor.

La glicina, que desde el punto de vista estructural es el aminoácido proteinogenético más simple, es el principal neurotransmisor inhibidor en áreas caudales del sistema nervioso central, estando muy implicado en el procesamiento de la información sensorial y motora (1). Así, se ha descrito su papel en el procesamiento de la información auditiva a través del núcleo coclear, el complejo olivar superior y el colículo inferior (2), en el procesamiento de la información visual en las células ganglionares de la retina (3 y 4) y en la percepción del dolor neuropático e inflamatorio (5).

En el tallo cerebral y médula espinal la glicina es liberada por interneuronas glicinérgicas que controlan la generación de ritmos motores, la coordinación de respuestas reflejas espinales y el procesamiento de señales sensoriales. En concreto, las interneuronas espinales glicinérgicas del tipo Ia median circuitos reflejos de inhibición recíproca y permiten, de esta forma, la relajación de músculos antagónicos y la contracción coordinada de músculos agonistas, mientras que las interneuronas de Renshaw regulan la excitabilidad de motoneuronas mediante la producción de señales inhibitorias recurrentes a través de un sistema de retroalimentación negativa (1).

De este modo, anatómicamente las interneuronas glicinérgicas se encuentran en el tallo cerebral y médula espinal formando una serie de contactos sinápticos locales con neuronas aferentes sensitivas, interneuronas excitadoras e inhibidoras y con proyecciones neuronales provenientes de las áreas superiores del SNC mediante las cuales se transmite la información al cerebro. Esta red de contactos locales interneuronales se ha determinado como un primer punto de control de la transmisión sensitiva, ya que pueden favorecer o no la propagación de la información. Es lo que se ha denominado Compuerta Espinal en la teoría de la Compuerta o Puerta de Entrada propuesta por Melzack y Wall en 1965 (6).

El mecanismo de acción de la glicina se lleva a cabo mediante la liberación del neurotransmisor al espacio sináptico y la posterior unión a su receptor sensible a estricnina, GlyR, en la postsinápsis produciendo la entrada de iones cloruro y generando un potencial postsináptico inhibidor (PPSI) que hiperpolariza la membrana, lo que inhibe la posible excitación de la neurona postsináptica (figura 2). Los receptores de glicina pertenecen a la superfamilia de los canales iónicos activados por ligando cuya estructura es heteropentamérica. Este pentámero se creía formado por 3 subunidades alfa y dos subunidades beta (α3:β2) (7), pero recientemente se ha determinado por microscopía de fuerza atómica que se compone por una estructura α2:β3 siguiendo una distribución β-α-β-α-β (8). Las subunidades α y β comparten una misma estructura formada por un largo extremo amino terminal, cuatro dominios transmembrana (TM1-4) y un gran bucle intracelular entre los TM3 y

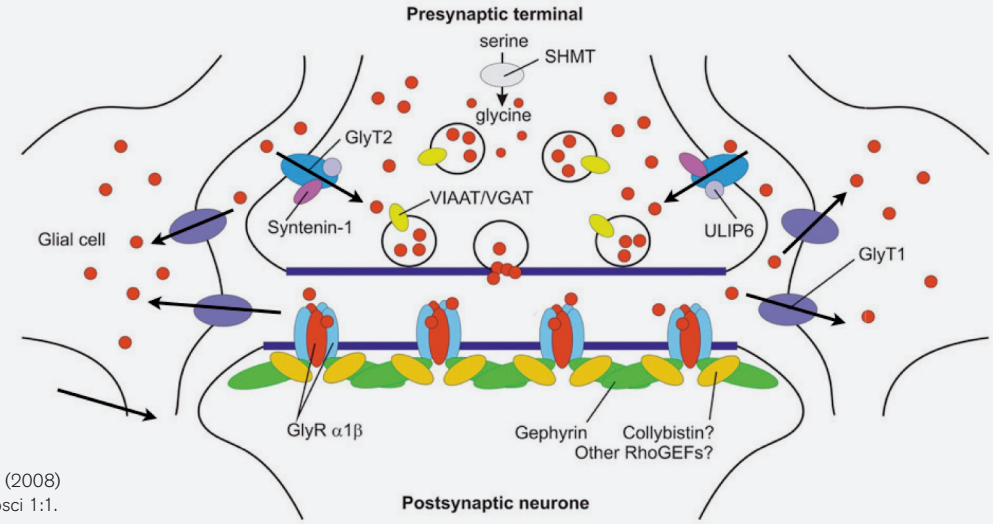

Harvey RJ et. al. (2008)
Front Mol Neurosci 1:1.

Figura 2

Esquema de la neurotransmisión glicinérgica inhibidora.

A partir del aminoácido serina se sintetiza el neurotransmisor glicina que se libera al espacio sináptico tras la fusión de las vesículas sinápticas con la membrana plasmática presináptica. El neurotransmisor se une en la neurona postsináptica al receptor de glicina GlyR compuesto por 3 subunidades β y 2 α. La localización del receptor en la postsinápsis es posible gracias a las proteínas de andamiaje gefirina y colibistina. La acivación del receptor permite la entrada de iones cloruro que hiperpolarizan la neurona postsináptica. Esta señalización inhibidora es finalizada gracias al transporte activo de GlyT1, expresado en células gliales y GlyT2, expresado en la neurona presináptica. GlyT2 interacciona con sintenina, que parece ser necesaria para su correcta localización sináptica, y con ULIP6 cuya función aún está por determinar. La reintroducción de la glicina al interior de las vesículas se lleva a cabo por el transportador vesicular VIAAT que permite la reutilización del neurotransmisor.

TM4 (figura 3) (9, 10). Esta región tiene la capacidad de unir gefirina, una proteína de andamiaje necesaria para la correcta posición del receptor en la postsinápsis. En cuanto al mecanismo de apertura del receptor tras la unión de glicina son necesarios los segmentos TM2 de cada monómero que se orientan hacia el interior del pentámero para formar un canal selectivo a iones cloruro produciendo la hiperpolarización de la neurona postsináptica.

Esta acción inhibidora es finalizada gracias a la recaptación de la glicina del espacio sináptico por dos transportadores específicos, GlyT1 (isoforma mayoritariamente glial) y GlyT2 (isoforma neuronal) (11). GlyT2 recaptura glicina hacia el terminal presináptico para facilitar su reincorporación de nuevo a vesículas sinápticas, ayudando a preservar su contenido cuántico y permitiendo de este modo su reutilización (3). La reintroducción de la glicina en las vesículas sinápticas se lleva a cabo por el transportador vesicular VIAAT (*Vesicular Inhibitory Amino Acid Transporter*), responsable también de la reincorporación vesicular del ácido γ-aminobutírico (GABA), el principal neurotransmisor inhibidor en áreas superiores del SNC. VIAAT posee una reducida afinidad por glicina requiriendo por tanto una elevada concentración de este neurotransmisor para un eficiente transporte del mismo al interior de la vesícula de la neurona presináptica (12)(figura 2).

Aparte de su papel inhibidor en la neurotransmisión glicinérgica, la glicina puede actuar como neurotransmisor excitador al ser un co-agonista obligado del receptor de glutamato NMDA. Estos receptores forman heterómeros conteniendo subunidades NR1 y NR2 (NR2A-D) y en ocasiones subunidades NR3 (NR3A o NR3B). La glicina se une específicamente a la subunidad NR1 mientras que el glutamato se une a la subunidad NR2 y la unión de ambos provoca la apertura eficiente del canal (13). Además, para que tenga lugar la máxima activación del receptor de glutamato NMDA, se requiere aparentemente la unión de dos moléculas de glutamato y dos de glicina (14, 15). Durante las últimas décadas ha emergido una intensa investigación sobre la región en NR1 que reconoce glicina, ya que la modulación de la actividad del receptor NMDA mediante agonistas o antagonistas específicos de esta región puede resultar interesante como aproximación terapéutica en algunas enfermedades como la esquizofrenia (16).

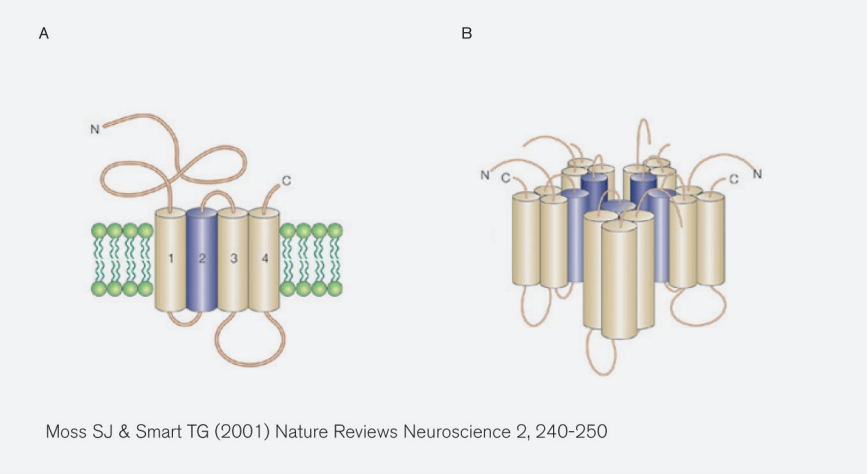

Moss SJ & Smart TG (2001) Nature Reviews Neuroscience 2, 240-250

Figura 3
Estructura del receptor postsináptico de glicina GlyR.
A) Las subunidades α y β comparten una misma estructura, formada por un largo extremo amino terminal, cuatro dominios transmembrana (TM1-4), y un gran bucle intracelular entre los TM3 y TM4. Esta región tiene la capacidad de unir gefirina, una proteína de andamiaje necesaria para la correcta posición del receptor en la postsinápsis. Se señalan en morado los segmentos TM2 de cada monómero, que son necesarios para formar un canal selectivo a la entrada de iones cloruro al orientarse hacia el interior del pentámero.
B) El receptor está formado por un pentámero que se compone de α2:β3, siguiendo una distribución β-α-β-α-β.

B.2 Transportadores de glicina: Expresión, variantes y genes codificantes.

Los trasportadores de glicina (GlyTs, *Glycine Transporters*) pertenecen a la familia génica *SLC6* (*Solute Carrier 6*), también denominada NSS (*neurotransmitter:sodium symporter family*), que engloba a los transportadores de neurotransmisores para serotonina (5-hidroxitriptamina), dopamina, norepinefrina y GABA (17). Los transportadores de neurotransmisores de esta familia poseen 12 dominios transmembrana (TM) conectados por 5 bucles intracelulares y 6 extracelulares (de los cuales el bucle extracelular 2 generalmente posee multiple N-glicosilación) y presentan los extremos amino y carboxilo terminal orientados hacia el interior celular.

Se han identificado dos subtipos de GlyTs, GlyT1 y GlyT2, que comparten aproximadamente el 65% de su secuencia de aminoácidos, pero que difieren en la farmacología que les afecta y en su distribución tisular y celular (18, 19). GlyT1 se expresa a lo largo del SNC, principalmente en astrocitos (20), aunque puede ser hayado en determinadas poblaciones neuronales, como por ejemplo en neuronas glutamatérgicas de hipocampo (21). Además de expresarse en el SNC, GlyT1 también se localiza en hígado, pancreas e intestino. Por el contrario, GlyT2 se expresa exclusivamente en regiones ricas en sinápsis glicinérgicas en el SNC, como son el tallo cerebral y médula espinal y únicamente es detectado en interneuronas glicinérgicas (22).

Ambos GlyTs presentan diferentes variantes derivadas de "*splicing*" alternativo del ARN mensajero o de un uso alternativo de distintos promotores. El gen humano de GlyT1 (*SLC6A9*) se compone de 14 exones distribuidos a lo largo de 44,1 mega bases (Mb) y está localizado en el cromosoma 1 (p31.3–p32) (23). Hasta la fecha, en humanos y otros mamíferos, solamente se han detectado 3 variantes de GlyT1 (GlyT1a-c) que difieren en su extremo amino terminal (18, 19). Mientras que GlyT1a y GlyT1b se generan por un uso alternativo de promotores, GlyT1c es un producto derivado del "*splicing*" producido sobre el ARN mensajero de GlyT1b, conteniendo un segmento inicial de 15 residuos (común con GlyT1b) seguido por una secuencia única de 54 residuos que no aparece en las otras dos variantes (24). Además, en bovinos (subfamilia *Bovinae*) se han descrito dos variantes de "*splicing*" del extremo carboxilo terminal (GlyT1d, e) que hasta la fecha no se han encontrado en otras especies (25) (figura 4a (i)).

El gen humano que codifica para GlyT2 (*SLC6A5*) se compone de 16 exones distribuidos a lo largo de 20,6 mega bases (Mb) y está localizado en el cromosoma 11 (p15.1–15.2) (26). Sobre el tránscrito que produce se han descrito 3 variantes de "*splicing*" efectuadas sobre el extremo amino terminal que producen tres variantes, GlyT2a-c. Únicamente hay 5 aminoácidos de diferencia entre GlyT2a y GlyT2b/c, por lo que en la literatura lo más común es hablar de GlyT2 y englobar las tres isoformas. Entre GlyT2b y GlyT2c no exiten diferencias en la secuencia de aminoácidos y lo

único que se ha encontrado son diferencias en las regiones 5' no codificantes (5'-UTR, del inglés "*untranslated region*") de sus respectivos ARNm. (27) (figura 4a (ii))

GlyT2 presenta además una característica poco común: posee un extremo amino terminal hacia el interior celular mucho más grande que el observado en el resto de proteínas pertenecientes a la familia NSS, llegando a alcanzar los 200 aminoácidos lo que significa que es aproximadamente tres veces más largo que el del resto de transportadores de neurotransmisores. Sin embargo, la expresión en células HEK293 de GlyT2 sin la región N-terminal mantiene el 100% de la función de transporte (28), por lo que es probable que su función esté relacionada con la regulación del transportador.

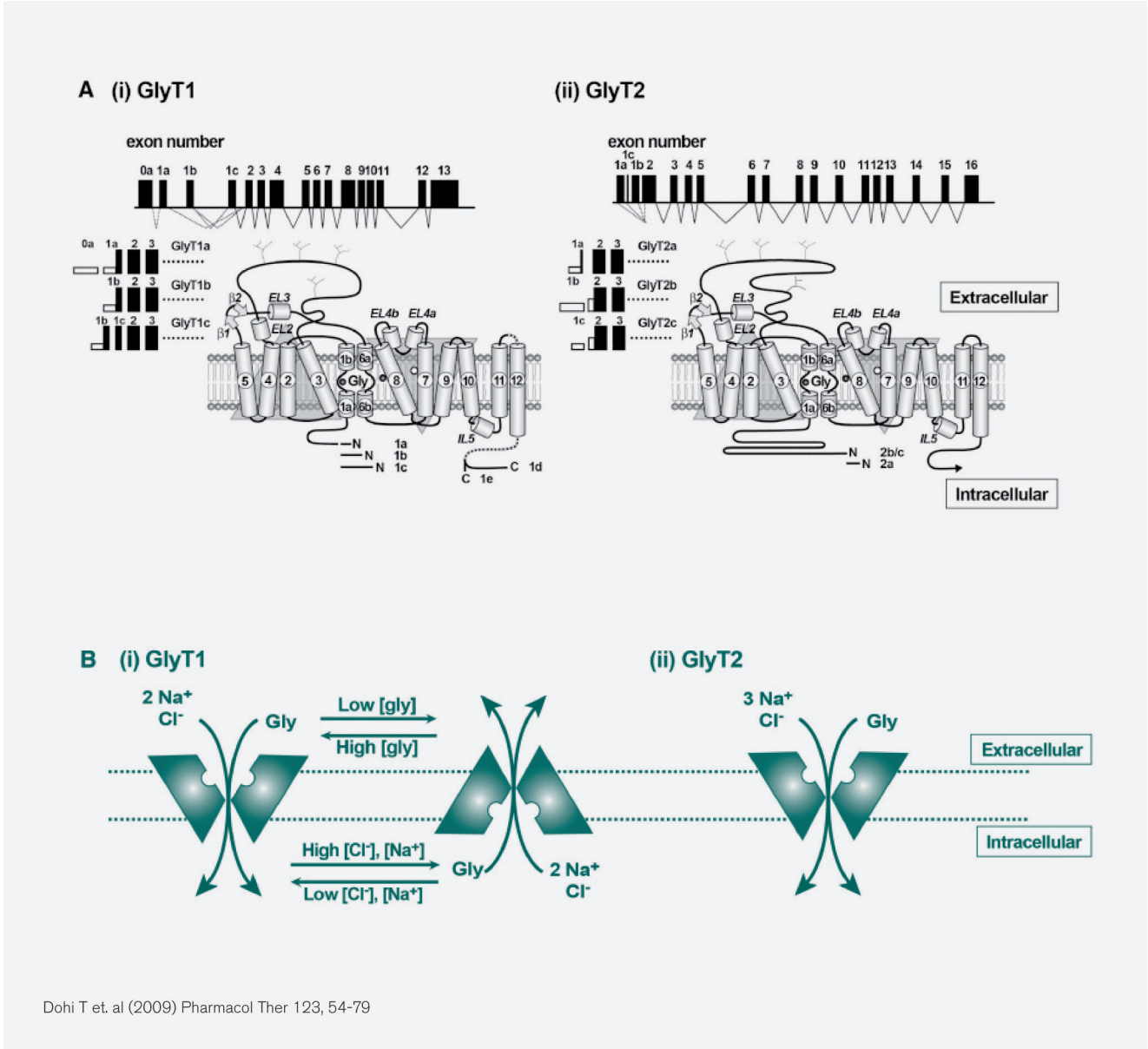

Dohi T et. al (2009) Pharmacol Ther 123, 54-79

Figura 4

Diferencias estructurales, génicas y de transporte entre GlyT1 y GlyT2.

A) Estructura del gen de GlyT1 (*SLC6A9*, 14 exones) y GlyT2 (*SLC6A5*, 16 exones). GlyT1 posee tres variantes de "*splicing*" que difieren en su N-terminal (GlyT1a-c) y dos variantes que difieren en su C-terminal (GlyT1d-e) mientras que GlyT2 sólo posee tres variantes en su N-terminal (GlyT2a-c). Nótese la mayor longitud del extremo amino terminal de GlyT2 que posee unos 200 aminoácidos. B) Diferencias en el ciclo de transporte de glicina por GlyT1 y GlyT2. Mientras que GlyT1 acopla el transporte a 2 iones Na^+, GlyT2 necesita cotransportar 3 iones Na^+. Esta diferencia en el acoplamiento iónico implica que GlyT1 necesita menor fuerza motriz para el transporte que GlyT2, lo que le permite funcionar en modo reverso dependiendo de los cambios en la concentración extracelular de sustrato o gradientes iónicos, mientras que GlyT2 carece de esta posibilidad.

B.3 El ciclo de transporte de glicina: diferencias entre GlyT1 y GlyT2

La introducción de glicina hacia el interior celular llevada a cabo por los GlyTs es dependiente de cloruro y está acoplada energéticamente al gradiente electroquímico de sodio, que es generado y mantenido por la Na/K-ATPasa. La glicina se une en la cara extracelular de los transportadores junto con los iones Na^+ y Cl^-, lo que induce un cambio conformacional desde el estado "hacia fuera" al estado "hacia dentro" (en inglés, "*outward*" e "*inward*" respectivamente). Esto expone el sitio de unión de la glicina al citosol, lo que permite la liberación del neurotransmisor y los iones. Ahora el transportador se encuentra "vacío", de tal modo que vuelve a la conformación "hacia fuera" permitiendo un nuevo ciclo de transporte (figura 5).

Pese a que las fases del ciclo de transporte son iguales, la estequiometría sustrato/iones es diferente entre GlyT1 y GlyT2. GlyT1 co-transporta $2Na^+/1Cl^-$/1glicina, mientras que GlyT2 co-transporta $3Na^+/1Cl^-$/1glicina (figura 4b (i, ii) (29). Esta diferencia en el acoplamiento iónico implica que GlyT1 necesita menor fuerza motriz para el transporte que GlyT2, lo que le permite funcionar en modo reverso en función de los cambios en la concentración extracelular de sustrato, gradientes iónicos o en el potencial de membrana. Este mecanismo permitiría la liberación de glicina de una manera independiente de calcio (Ca^{2+}), probablemente durante una intensa actividad inhibidora glicinérgica, permitiendo extender el periodo o la concentración de glicina en el espacio sináptico en estas condiciones (30).

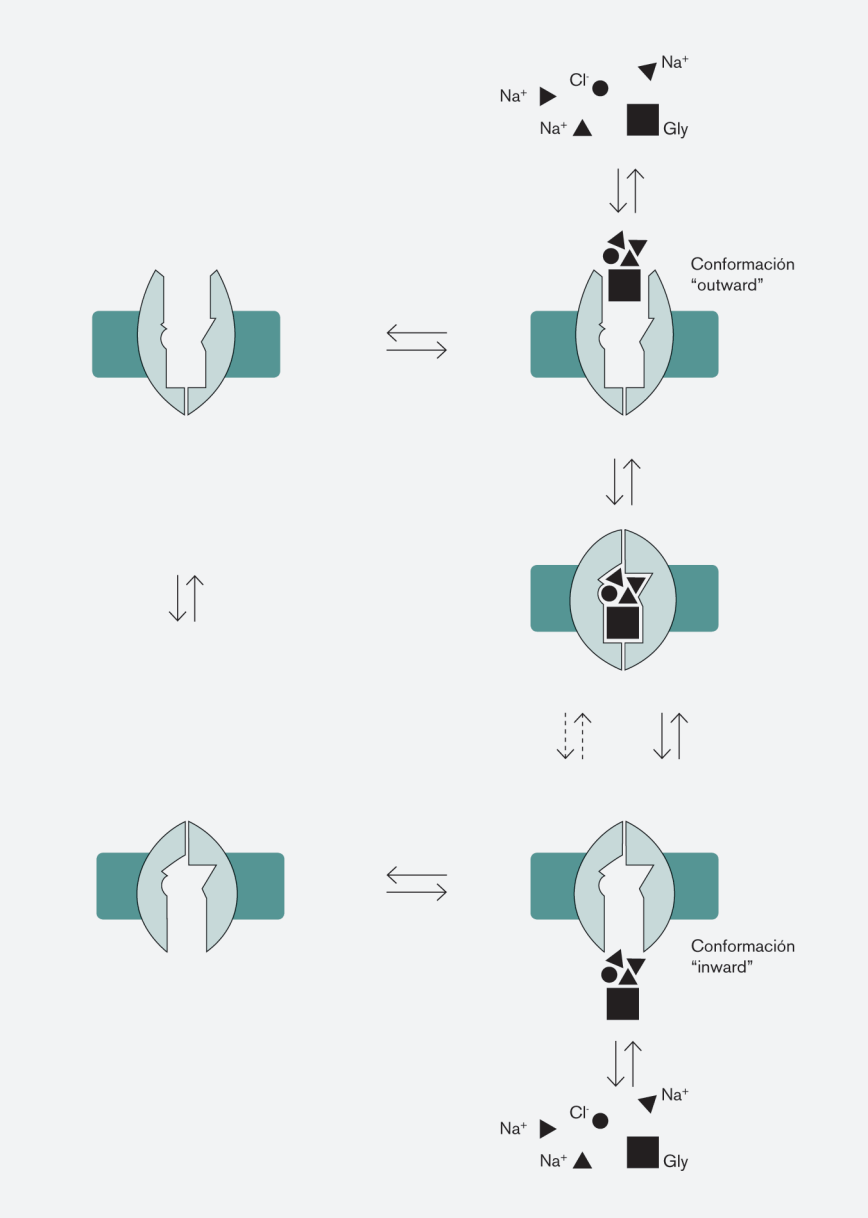

Figura 5
Ciclo de transporte de glicina de GlyT2.
El transportador en conformación "hacia fuera" (*outward*) tiene la capacidad de unir glicina, 3 iones Na^+ y un ion Cl^-. Tras esta unión se produce un cambio conformacional en la proteína. Esto expone los sitios de unión a glicina e iones hacia el interior celular, (conformación hacia dentro o *inward*) lo que permite su liberación al citosol, El transportador vacío en conformación *inward* tiene la capacidad de volver a la conformación *outward* para permitir un nuevo ciclo de transporte de glicina.

B.4 GlyT2 y Na/K-ATPasa.

El transporte de glicina mediado por GlyT2 requiere el correcto funcionamiento de la Na/K-ATPasa que mantiene el gradiente electroquímico de Na^+. De este modo, la inhibición de la Na/K-ATPasa por esteroides cardiotónicos (del inglés "*cardiotonic steroids*" (CTS)) produce una inhibición paralela del transporte de glicina por falta de gradiente. La Na/K-ATPasa es una proteína integral de membrana que acopla la hidrólisis de ATP a un transporte activo de 3 iones Na^+ al medio extracelular a cambio de la introducción de dos iones K^+ en cada ciclo enzimático. En neuronas, los gradientes de Na^+ y K^+ son especialmente importantes para el mantenimiento de la excitabilidad neuronal, la conducción del potencial de acción, la regulación del volumen celular, la concentración de Ca^{2+} y el mantenimiento del pH (31). La Na/K-ATPasa se compone de una subunidad catalítica, denominada α, que contiene los sitios de unión a esteroides cardiotónicos, una subunidad β, que está ampliamente glicosilada y en algunos tejidos se puede encontrar la subunidad γ, que pertenece a la familia FXYD. Existen 4 tipos de subunidades α, que se expresan en distintos tejidos (α1, α2,

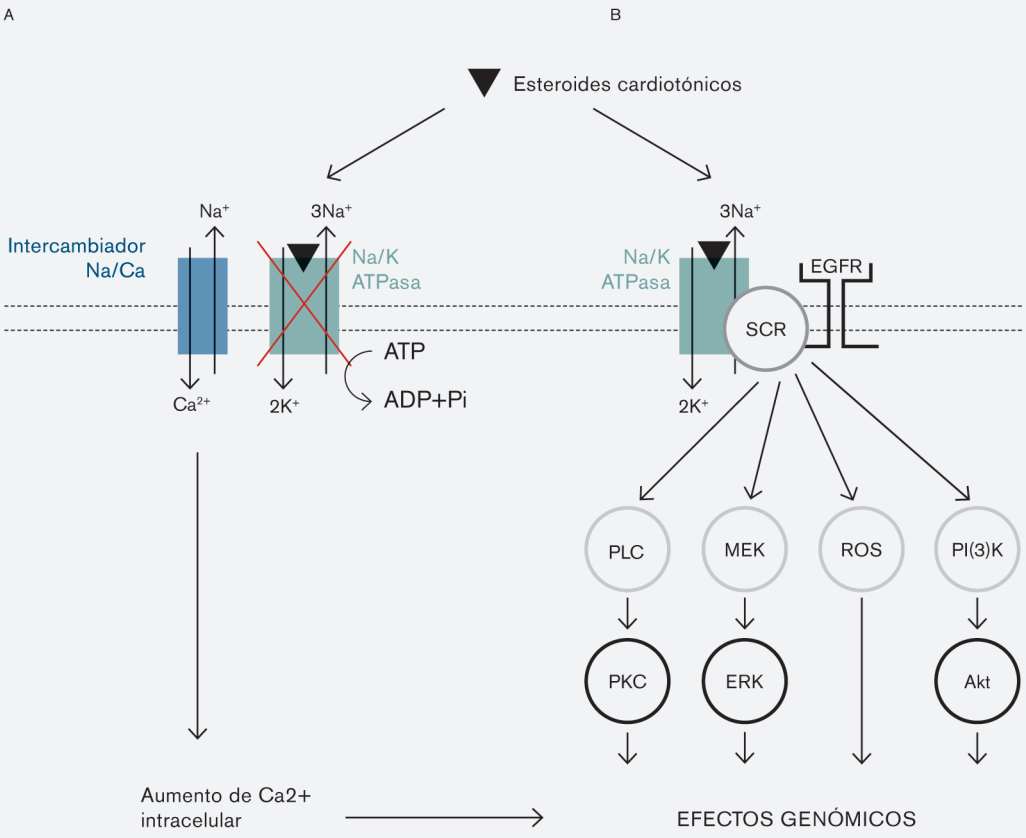

Figura 6

Transducción de señales mediada por la Na/K-ATPasa tras la unión de esteroides cardiotónicos.

A-B) La figura muestra las diferentes cascadas de señalización llevadas a cabo por la Na/K ATPasa tras la unión de ouabaína. A) Esta unión produce, por una parte, una inhibición del transporte de Na y K, lo que determina un amuento del Na intracelular. Esto activa al cotransportador Na/Ca que introduce Ca para liberar Na y mantener el gradiente de este último, lo que implica un aumento en el Ca citosólico que produce, entre otros efectos, cambios genómicos. B) La Na/K ATPasa, tras unir ouabaína, produce una transactivación del receptor del factor de crecimiento epidérimco EGFR a través de la tirosina quinasa SRC. Este cambio es capaz de producir la activación de varias cascadas de señalización que terminan produciendo efectos sobre distintas proteínas y sobre el genoma. Entre estas vías se encuentran: 1) Activación de PLC, y posterior activación de PKC, 2) Activación de PI3K y posterior activación de Akt, 3) Activación de la vía de las MAPK (activación de MEK, y posterior activación de ERK1/2) y 4) producción de especies reactivas de oxígeno (del inglés "*reactive oxigen species*", ROS)

α3 y α4) y que están codificadas por 4 genes diferentes: *ATP1A1*, *ATP1A2*, *ATP1A3* y *ATP1A4*. La subunidad α1 es ubicua, la α2 se expresa en músculo (esquelético, liso y cardiaco), cerebro, pulmones y adipocitos, la α3 es principalmente neuronal (aunque se ha encontrado en ovarios) y la α4 se expresa exclusivamente en testículos.

Además del importantísimo papel en el mantenimiento de los gradientes iónicos de Na^+ y K^+, investigaciones realizadas en la última década han determinado que la Na/K-ATPasa puede actuar además como un receptor que media múltiples eventos de señalización intracelular tras la unión de ouabaína, incluso a concentraciones nanomolares en las que no se ve interrumpida su actividad. De hecho, recientemente se han detectado concentraciones nanomolares circulantes de oubaína y esteroides relacionados producidos endógenamente en hipótalamo, glándulas adrenales y sistema cardiovacular. Cuando la ouabaína se une a la Na/K-ATPasa se produce una activación de la tirosina quinasa Src y del receptor del factor de crecimiento epidérmico (EGFR), a lo que sigue la activación de varias cascadas de señalización que terminan produciendo efectos en el genoma. Entre estas vías se encuentran: 1) Activación de PLC, y posterior activación de PKC, 2) Activación de PI3K y posterior activación de Akt, 3) Activación de la vía de las MAPK (activación de MEK, y posterior activación de ERK1/2) y 4) producción de especies reactivas de oxígeno (del inglés "*reactive oxigen species*", ROS). Además, la inhibición de la actividad Na/K-ATPasa produce un aumento de Na^+ intracelular. Esto induce un mecanismo compensatorio en el que el intercambiador de Na^+ y Ca^{2+} (NCX) introduce un ión Ca^{2+} para expulsar $3Na^+$, lo que produce un aumento del Ca^{2+} intracelular, que entre otros efectos contribuye a producir cambios genómicos (figura 6).

Estos mecanismos de señalización han sido estudiados principalmente en células renales y musculares cardíacas. Sin embargo, la función como receptor de la Na/K-ATPasa en neuronas está mucho menos caracterizada. A pesar de su papel como proteína de andamiaje propuesto en otros tipos celulares (32), son escasas las interacciones descritas entre la Na/K-ATPasa y proteínas de membrana que participan en la neurotransmisión en el SNC. Hasta la fecha, se han descrito interacciones con los receptores de dopamina D1 y D2 (33), con el transportador de glutamato GLT1 (34) y con el receptor de glutamato AMPAR (35). Dosis altas de ouabaína (que producen una inhibición del 50% de la actividad ATPasa) inducen una internalización y degradación de AMPAR, lo que determina una supresión de la actividad sináptica mediada por glutamato en estas neuronas. En el caso de GLT1, Rose et. al proponen un complejo Na/K-ATPasa/Src/GLT1 que operaría como una unidad funcional reguladora de la neurotransmisión glutamatérgica. Estos resultados implican que la Na/K-ATPasa es necesaria en el SNC por su doble papel como bomba de Na^+/K^+ y como receptor que media señalización intracelular; este último efecto hasta ahora no se había implicado en la función y estabilidad de GlyT2.

B.5 Función fisiológica de los transportadores de glicina.

Gracias a la generación de los ratones deficientes en los transportadores GlyT1 y GlyT2 por el grupo de Heinrich Betz, en el Max-Planck Institute for Brain Research en Alemania, se ha podido determinar con mayor exactitud la función fisiológica de ambos transportadores.

Ambos ratones deficientes (que denominaremos $GlyT1^{-/-}$ y $GlyT2^{-/-}$) presentan un aspecto físico relativamente normal al nacer, lo que sugiere que la expresión de ambas proteínas parece no ser necesaria para un correcto desarrollo embrionario. Sin embargo, los ratones $GlyT1^{-/-}$ mueren generalmente durante el día del nacimiento debido a que presentan grandes fallos motosensoriales caracterizados por letargia, hipotonía, baja capacidad de respuesta al entorno y una grave deficiencia respiratoria que conlleva largos periodos de apnea (36).

Los ratones deficientes en GlyT2 también presentan un fenotipo que resulta letal pero la muerte ocurre generalmente durante la segunda semana postnatal y después de haber desarrollado grandes fallos neuromotores, claramente distintos a los que sufren los ratones $GlyT1^{-/-}$. Los ratones $GlyT2^{-/-}$ muestran un claro temblor en sus extremidades, signos de rigidez muscular y son incapaces de adoptar una posición normal si se les coloca de espaldas, indicando una reducida coordinación motora (37).

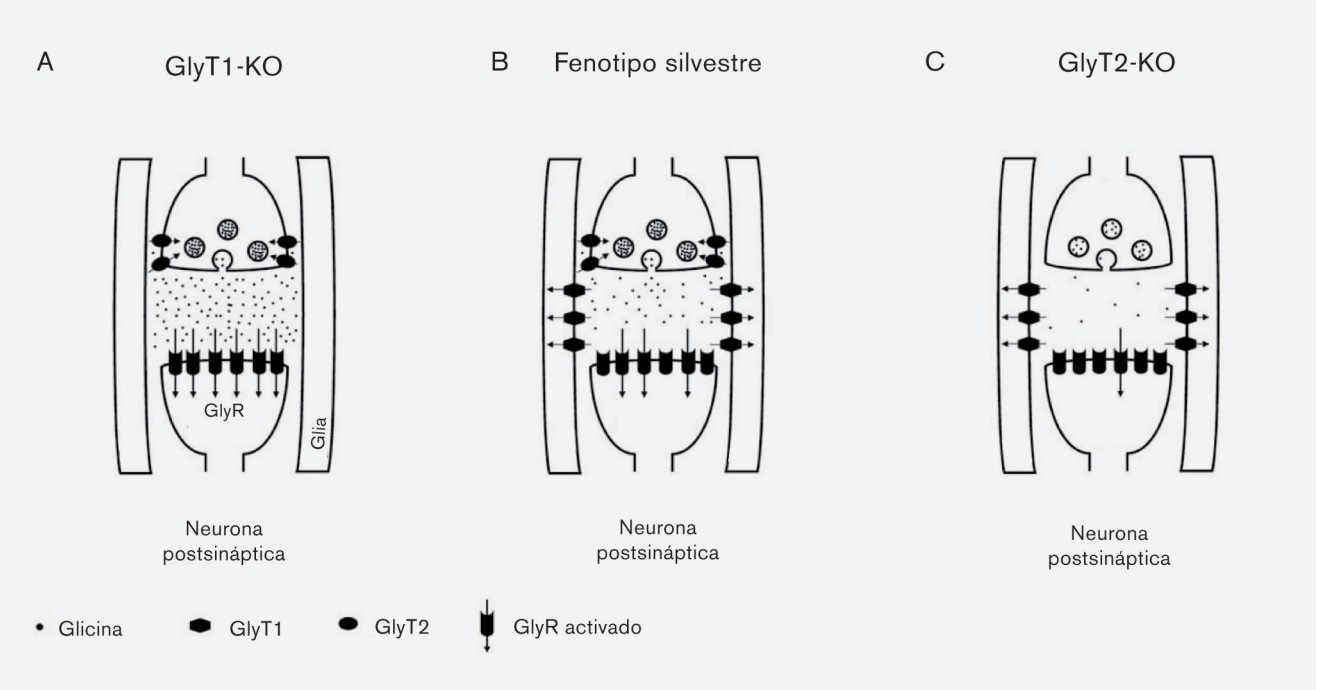

Figura 7

Modelos de la estructura sináptica en ratones deficientes en transportadores de glicina.

El esquema muestra diferentes sinápsis glicinérgicas. A) En ratones deficientes en GlyT1, B) en ratones con fenotipo silvestre y C) en ratones deficientes en GlyT2. En el fenotipo silvestre se observa que GlyT2 es esencial para la recaptación de glicina hacia la neurona presináptica, lo que permite el rellenado de las vesículas y que GlyT1 está retirando la glicina del espacio sináptico hacia las células gliales manteniendo una baja concentración de glicina en la hendidura sináptica. En el caso del ratón deficiente en GlyT1 (A), la ausencia de este transportador produce un aumento de la concentración en la hendidura sináptica, lo que resulta en una inhibición continuada de la neurona postsináptica. En el caso del ratón deficiente en GlyT2 (C), se observa un fallo en la reutilización de la glicina liberada al espacio sináptico, lo que se traduce en una deficiencia en el rellenado de vesículas. De este modo, cuando se produce una liberación de neurotransmisor la cantidad de glicina liberada es mucho menor, lo que implica que la inhibición sobre la neurona postsináptica está claramente disminuida comparada con la producida en el caso del fenotipo silvestre.

Estas diferencias, junto con medidas adicionales de corrientes inhibitorias postsinápticas glicinérgicas (IPSCs, *inhibitory postsynaptic currents*), sugieren consecuencias prácticamente opuestas en la neurotransmisión glicinérgica. De este modo se propone que la ausencia de GlyT1 provoca una situación de hiperglicinergia (con un fenotipo hipotónico y letargia), mientras que la ausencia de GlyT2 provoca hipoglicinergia (con un fenotipo de descoordinación y espasticidad muscular). Gomeza et. al proponen el modelo que sugiere el papel de cada transportador en la neurotransmisión glicinérgica: GlyT1 elimina la glicina del espacio sináptico y mantiene bajas las concentraciones extracelulares de este neurotransmisor a lo largo de las áreas caudales del SNC, lo que previene la excesiva activación de los receptores GlyR y GlyT2 recapta y recicla la glicina liberada hacia la presinápsis, lo que permite el rellenado de vesículas sinápticas y la posibilidad de liberación de neurotransmisor en futuros ciclos de neurotransmisión glicinérgica (figura 7).

C.1 Aspectos fisiopatológicos de GlyT2 en la neurotransmisión glicinérgica: hiperplexia y dolor.

Al igual que en ratones, la deficiencia de la actividad de GlyT2 en humanos produce severos trastornos fisiológicos: rigidez de tronco y extremidades, puños apretados, frecuentes temblores, y sobresaltos enérgicos y generalizados en respuesta a estímulos triviales generalmente acústicos o táctiles. El conjunto de estos síntomas derivados de la hipofunción glicinérgica constituyen la denominada enfermedad del sobresalto o hiperplexia hereditaria (OMIM 149400), también conocida como “síndrome del bebé entumecido”. Se trata de una enfermedad rara que se manifiesta muy pronto tras el nacimiento (o incluso durante el periodo intrauterino) y aunque

no es necesariamente letal como en ratones existe un alto riesgo de muerte súbita del bebé como consecuencia de fallos cardiorrespiratorios y espasmos laríngeos (38).

Un alto porcentaje de neuronas glicinérgicas son además GABAérgicas, es decir, son capaces de liberar ambos neurotransmisores inhibidores. En la actualidad esta característica se utiliza en el tratamiento de la hiperplexia humana, ya que la administración de clonazepam (inhibidor de la recaptación de GABA) produce un aumento de la concentración efectiva de GABA en las sinápsis glicinérgicas/GABAérgicas y es capaz de compensar, al menos en parte, la deficiente neurotransmisión glicinérgica (39).

Mutaciones en el gen de GlyT2 (*SLC6A5*) son la segunda causa responsable de producir esta enfermedad, sólo superada por mutaciones en el gen codificante para la subunidad α1 del receptor de glicina GlyR (*GLRA1*) (26, 40-44), lo que resalta la importancia de este transportador en la fisiología humana y la necesidad de su correcto funcionamiento.

Se han descrito diferentes mutaciones (la mayoría de carácter recesivo) a lo largo de los 16 exones que forman el gen de GlyT2. Algunas de estas mutaciones producen una proteína truncada debido a un cambio en el patrón de lectura o a una sustitución sin sentido (del inglés "*non-sense mutation*") (W151X, Y297X, Y377X, R439X, V432F+fs97, Q630X, P108L+fs25). Otras mutaciones con cambio de sentido ("*missense mutations*") producen transportadores no funcionales que sí son capaces de alcanzar correctamente la superficie celular pero que poseen modificaciones en residuos importantes para el ciclo de transporte, como en sitios de unión a Na^+ (N509S, A275T), Cl^- (S513I), glicina (W482R), o en otras regiones posiblemente necesarias para los cambios conformacionales necesarios durante el ciclo de transporte (L237P, L243T, E248K, T425M, Y491C, N511S, F547S o Y656H) (26, 40, 41).

Dentro de este grupo de mutaciones con cambio de sentido se han descrito también sustituciones aminoacídicas que modifican la actividad del transportador debido a defectos en el tráfico intracelular de la proteína. Una de estas mutaciones, que provoca la sustitución de una serina por una arginina en la posición 512 (S512R), ha sido propuesta como la única mutación en *SLC6A5* con herencia autosómica dominante. Estudios realizados en el laboratorio (Arribas-González E. et. al, sin publicar) demuestran que efectivamente el mutante S512R sufre una retención intracelular y mediante la interacción directa con el fenotipo silvestre retiene también a este impidiendo su llegada a la membrana plasmática, ejerciendo por tanto un efecto dominante negativo sobre la proteína silvestre.

Recientemente en nuestro laboratorio, junto al laboratorio del Dr. Cecilio Giménez y en colaboración con el grupo del Dr. Robert Harvey (de la UCL School of Pharmacy del Reino Unido), hemos descrito una nueva mutación dominante asociada a hiperplexia con defectos de tráfico y alteraciones bioquímicas. La sustitución Y705C (c.2114A→G) encontrada en el exón 15 de pacientes de España y del Reino Unido muestra una reducida actividad de transporte debido a la suma de dos efectos, 1) una alteración del tráfico intracelular que provoca una retención intracelular del transportador y 2) una disminución de la actividad de transporte (45). Tras distintos estudios bioquímicos hemos determinado que la introducción de esta nueva cisteína en la posición 705 de GlyT2 da lugar a la formación de nuevos puentes disulfuro aberrantes con el par de cisteínas C311 y C320 del bucle extracelular 2, lo que modifica la movilidad intramolecular de la proteína y limita su actividad de transporte. La adición de agentes reductores como el DTT permite recuperar la actividad al impedir la formación de estos enlaces aberrantes.

Sin embargo no todas las mutaciones encontradas en el gen *SLC6A5* en pacientes de hiperplexia poseen un fenotipo claramente inactivo. Tras la expresión y ensayo en sistemas heterólogos de los mutantes A89E y G767R no se han encontrado diferencias significativas respecto al fenotipo silvestre, lo que podría indicar que estos mutantes presentan fallos no detectables en estos sistemas de expresión (39). Por tanto, son necesarios estudios futuros de expresión en sistemas neuronales para determinar las razones por las que producen un fenotipo hiperpléxico en humanos.

A continuación se muestra una tabla que resume todas las mutaciones encontradas hasta la fecha en el gen *SLC6A5* y que están asociadas a hiperplexia (tabla 1).

TABLA 1

Genotipo	Herencia	Segundo alelo por determinar	Exon	Modificación en la proteína	Localización Subcelular	Actividad Transporte	Ref.
C1131A	AR	NO	7	Y377X	CITOPLASMA	NO	26
G1294T + Ins[T]1295	AR		8	V432F+FS97	CITOPLASMA	NO	26
C1131A (H)	AR	NO	7	Y377X (H)	CITOPLASMA	NO	34
A1472G	AR	NO	9	Y491C	MEMBRANA PLASMÁTICA	NO	26
C1888T	AR		13	Q630X	CITOPLASMA	NO	
DelC{319–324}	AR	NO	2	P108L+FS25	CITOPLASMA	NO	26
T1444C	AR		9	W482R	MEMBRANA PLASMÁTICA	NO	
C916G	AR	NO	5	L306V	MEMBRANA PLASMÁTICA	NO	26
A1526G	AR		10	N509S	MEMBRANA PLASMÁTICA	NO	
C1274T (H)	AR	SI	8	T425M	MEMBRANA PLASMÁTICA	NO	26
--	--		--	--	--	--	
T1530G	AD	NO	10	S510R	CITOPLASMA	NO	26
			--	--		--	
C2299T	AR	NO	16	G767R	MEMBRANA PLASMÁTICA	SI (100%)	34
En GLRA1	AR			I244T EN GLYRα1	DESCONOCIDO.	--	
C266A	AR	SI	2	A89E	MEMBRANA PLASMÁTICA	SI (100%)	34
--	--		--	--	--	--	
IVS14 + 1 ΔG (H)	AR	NO	14	ALTERACIÓN "SPLICING" (H)	NO ESTUDIADO	NO	35
C727A (H)	AR	NO	4	P243T (H)	NO ESTUDIADO	NO	35
C891A (H)	AR	NO	5	Y297X (H)	NO ESTUDIADO	NO	35
C1315T (H)	AR	NO	8	R439X (H)	NO ESTUDIADO	NO	35
C1315T	AR	NO	8	R439X	NO ESTUDIADO	NO	35
IVS13 + 1 G>T	AR		13	ALTERACIÓN "SPLICING"	NO ESTUDIADO	NO	
T1640C	AR	NO	11	F547S	NO ESTUDIADO	NO	35
T1966C	AR		13	Y656H	NO ESTUDIADO	NO	
G742A	AR	NO	4	E248K	NO ESTUDIADO	NO	35
IVS8 + 1 G>A	AR		8	ALTERACIÓN "SPLICING"	NO ESTUDIADO	NO	
ΔCT [1460–1467]	AR	NO	9	S489F + FS39	NO ESTUDIADO	NO	35
G1970C	AR		14	G657A	NO ESTUDIADO	NO	
C571T	AR	NO	3	R191X	NO ESTUDIADO	NO	35
ΔTG [593–594] (M)	AR		3	L198R + FS123	NO ESTUDIADO	NO	
G452A	AR	SI	2	W151X	NO ESTUDIADO	NO	35
--	--		--	--	--	--	
C1315T	AR	SI	8	R439X	NO ESTUDIADO	NO	35
--	--		--	--	--	--	
G823A	AR	SI	5	A275T	MEMBRANA PLASMÁTICA	SI (60%)	35
--	--		--	--	--	--	
ΔC [319–323]	AR	NO	2	P108L + FS25	NO ESTUDIADO	NO	35
ΔT [1994]	AR		14	I665K + FS1	NO ESTUDIADO	NO	
ΔTG [593–594]	AR	NO	3	L198R + FS123	NO ESTUDIADO	NO	35
T710C	AR		4	L237P	NO ESTUDIADO	NO	
G1538T	AR	SI	10	S513I	NO ESTUDIADO	NO	35
--	--		--	--	--	--	
A2114G	AD	NO	15	Y705C	60% EN MEMBRANA	SI (60%)	39
			--	--	--	--	

** (H) significa homozigótico para esa mutación / ** (--) significa por determinar*

Debido a la importancia fisiopatológica del correcto funcionamiento de GlyT2 en la sinápsis, nuestro laboratorio y otros grupos han tratado de profundizar durante los últimos años en el estudio de posibles mecanismos moduladores de la actividad de este transportador. Así, los primeros compuestos descritos con acción inhibitoria sobre GlyT2 (amoxapina y etanol) fueron determinados por nuestro laboratorio en el año 2000 (46, 47) pero debido a su baja afinidad y/o especificidad no han permitido el desarrollo de posteriores estudios farmacológicos. En los siguientes años se han desarrollado algunos compuestos con una alta afinidad y especificidad por GlyT2, entre los que se incluyen Org-25543 (48), ALX-1393 (49) y el recientemente publicado Oleil-L-Carnitina (50). ALX-1393 es el más ensayado hasta la fecha, habiéndose testado incluso *in vivo* en ratas gracias a lo cual se está considerando a GlyT2 como una interesante diana farmacológica para reducir el dolor, ya que la inyección intratecal de este compuesto reduce en ratas la respuesta asociada a dolor neuropático (18).

C.2 Tráfico intracelular de proteínas.

La densidad y número de receptores de neurotransmisores o de transportadores en una sinápsis resulta crucial para determinar la fuerza e importancia de su respuesta. Así un mayor número de receptores permite una mayor respuesta de la neurona postisináptica al neurotransmisor liberado, mientras que un mayor número de transportadores producirá una recaptación más rápida del neurotransmisor, limitando su tiempo de acción en la sinápsis. Cambios en la cantidad de receptores y transportadores en la sinápsis son la base de la plasticidad sináptica. La actividad de estas moléculas puede ser regulada de una manera rápida y versátil mediante su tráfico intracelular (51, 52) resultante del equilibrio entre exocitosis (llegada a la membrana plasmática) y endocitosis (retirada desde la membrana plasmática).

La endocitosis es un mecanismo presente en todas las células que regula la composición lipídica y proteica de la membrana plasmática, lo que modifica la manera en la que una célula puede reaccionar a su entorno. Existen diversos mecanismos de endocitosis que coexisten en las células de mamíferos y que normalmente se definen en función de la dependencia de distintas proteínas y/o lípidos. La tabla 2 muestra un resumen de los procesos de endocitosis a pequeña escala (del inglés "*microscale-endocytosis*") conocidos hasta la fecha. Más información sobre procesos de endocitosis a gran escala ("*macroscale-endocytosis*") como fagocitosis o macropinocitosis se puede encontrar en las ref. 53 y 54.

TABLA 2

Mecanismo de endocitosis	Endocitosis mediada por clatrina	Endocitosis mediada por caveolina	IL-2Rβ	GEEC	Endocitosis mediada por flotilina	Dependiente de Arf6
Tamaño y morfología	Vesicular 150-200 nm	Langeniforme, ~120 nm	Vesicular, 50-100 nm	Tubular	Vesicular	Tubular
Proteína de recubrimiento	Clatrina	Caveolina	Ninguna	Ninguna	Ninguna	Ninguna
¿Dep. Dinamina?	Si	Si	Si	No	No	No
GTPasas implicadas	Rab5	Sin establecer	RhoA, Rac1	ARF1, Cdc42	–	Arf6
Otras proteínas asociadas	AP2, AP180, Eps15, Epsin, Amfifisin	PTRF, src, SDPR, Actina	PAK1 y 2	Actina, GRAF1 GBF1 ARHGAP10	Flotillinas-1 y 2	–

C.3 Endocitosis mediada por clatrina en la sinápsis.

De todos los mecanismos de endocitosis el mejor caracterizado hasta la fecha es la endocitosis mediada por clatrina (EMC). Este proceso es básico para el correcto funcionamiento de la sinápsis, ya que en el terminal presináptico es responsable de la retirada y reciclaje de membrana plasmática de las vesículas sinápticas tras su fusión durante la liberación de neurotransmisor. Además, regula la cantidad de numerosos tipos de receptores postsinápticos y transportadores de neurotransmisores gliales y neuronales (55, 56). El mecanismo de endocitosis mediada por clatrina consta de 5 pasos (figura 8):

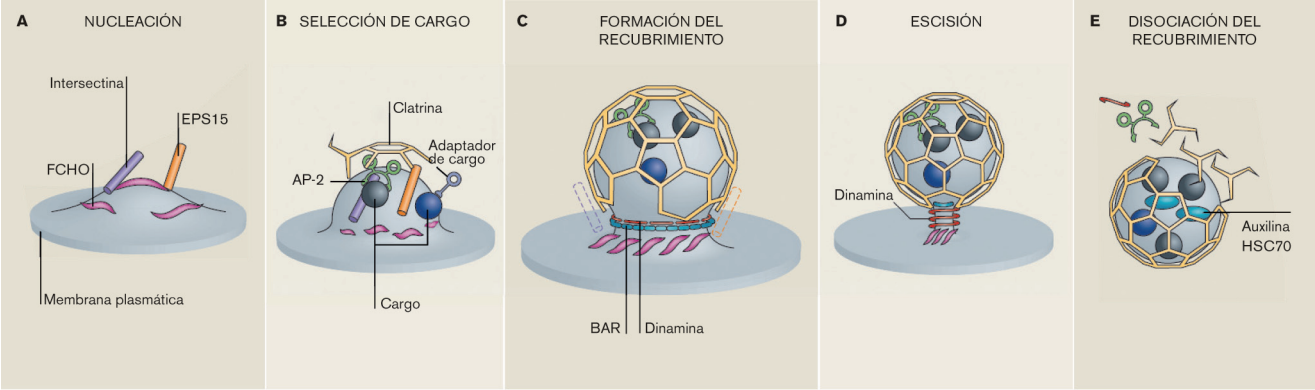

Figura 8
Fases de la endocitosis mediada por clatrina.
A) Nucleación: Primer paso para la formación de la vesícula endocítica gracias a la acción de las proteínas de la familia de las FCHO que reclutan epsinas, intersectinas y EPS15, comenzando la curvatura de la membrana. B) Selección de cargo: Se reclutan al complejo adaptadores específicos de los cargos que serán endocitados gracias a la presencia de AP-2, que también facilita el comienzo de la formación del recubrimiento clatrina. C) Formación del recubrimiento: Se van acoplando distintas moléculas de triskelion de clatrina, polimerizando en forma de hexágonos y pentágonos que recubren por completo la vesícula. D) Escisión: La GTPasa dinamina se localiza en el cuello de la vesícula y produce la escisión de la misma. E) La vesícula internalizada pierde el recubrimiento gracias a la acción de auxilinas y HSC70.

1. Nucleación: Las proteínas FCHO (del inglés "*FCH domain only*") unen fosfatidilinositol bifosfato (PtdIns(4,5)P2 o PIP2) y reclutan proteínas de la familia de las epsinas a través de su dominio ENTH, junto con otras proteínas como son EPS15 y EPS15R (*EPS15-related*) y las denominadas intersectinas, lo que inicia la curvatura de la membrana.
2. Selección de cargo: En este punto se decide qué moléculas endocitarán (denominadas cargo) a través de la futura vesícula. Este paso se da gracias a la llegada de AP-2 ("*adaptor protein 2*") al complejo a través de las intersectinas. AP-2 recluta adaptadores específicos de las moléculas cargo que mediante interacción directa determinan las moléculas que van a endocitar. Estas interacciones se basan en el reconocimiento de diferentes motivos existentes en la secuencia de la proteína cargo: basado en tirosinas, basado en di-leucinas o el motivo NPXY. Además, en colaboración con AP-2 otros adaptadores reconocen modificaciones en las proteínas cargo, como mono/multi-ubiquitinación (por parte de epsinas y Eps15) y fosforilación (por ejemplo el reconocimientro de GPCRs por β-arrestin) (57).
3. Formación del recubrimiento: Se recluta el triskelion de clatrina por AP-2 que polimeriza formando hexágonos y pentágonos que recubren la incipiente invaginación de la membrana.
4. Escisión: La GTPasa dinamina se situa en el cuello de la vesícula donde polimeriza (proceso que requiere hidrólisis de GTP) e induce la escisión de la vesícula de la membrana plasmática.
5. Disociación del recubrimiento: Las auxilinas reclutan la proteína HSC70 para desensamblar el recubrimiento de clatrina y dan lugar a la vesícula endocítica como tal que contiene los cargos específicos seleccionados antes de la endocitosis.

La pérdida de función de cualquiera de los componentes centrales de la EMC (clatrina, AP2, epsina o dinamina) produce letalidad embrionaria. Como resultado no es esperable que mutaciones severas (que produzcan pérdida de función) en estas proteínas estén relacionadas con enfermedades

humanas. Sin embargo, se han descrito muchas perturbaciones en estas proteínas relacionadas con numerosas enfermedades como son el cáncer, miopatías, neuropatías, síndromes metabólicos y enfermedades neurodegenerativas (58).

C.4 Endocitosis independiente de clatrina. Implicaciones de las balsas lipídicas (*lipid rafts*).

Las balsas lipídicas (del inglés "*lipid rafts*"), o más recientemente denominadas balsas de membrana ("*membrane rafts*"), son subdominios especializados de las membranas celulares enriquecidos en colesterol, esfingolípidos y proteínas ancladas a la membrana por medio de glicosilfosfatidilinositol (GPI). Estas balsas además tienen una asociación especial con el citoesqueleto y se definen por su resistencia a su solubilización en frío por detergentes no iónicos, lo que determinó que se definiesen en un principio como membranas resistentes a detergente (del inglés "*detergent resitant membranes*" o DRMs).

Existen dos tipos de balsas lipídicas, 1) las caveolas, pequeñas invaginaciones langeniformes que contienen proteínas de la familia de las caveolinas y 2) las denominadas balsas lipídicas planas ("*planar lipid rafts*"), que como su nombre indica no producen invaginaciones, y contienen proteínas de la familia de las flotilinas. Las caveolinas son el componente mayoritario de las caveolas y se expresan a lo largo del sistema nervioso en microvasos, células endoteliales, astrocitos, oligodendrocitos, células de Schwann, en los ganglios de la raíz dorsal y en neuronas de hipocampo. Sin embargo, las caveolinas no están presentes en la mayoría de tipos neuronales (59) cuyos *lipid rafts* son balsas lipídicas planas enriquecidas en flotilinas, también denominadas reggies, que pertenecen a la superfamilia de las SPFHs (Stomatin/Prohibitin/Flotillin/HflK). Existen dos tipos de flotilinas, flotilina-1 (reggie-2) y flotilina-2 (reggie-1) que se expresan en la mayoría de tipos celulares, están altamente conservadas y parecen definir los dominios *raft* a los que se encuentran asociadas por miristoilación y/o palmitoilación (60).

Los *lipid rafts* median un gran número de funciones celulares. Por ejemplo, sirven como plataformas de señalización celular al contener ciertas moléculas que no se encuentran en otras zonas de la membrana, modulando su actividad mediante el desplazamiento lateral entre dominios *raft*/*no raft*. Este fenómeno parece de especial importancia en la sinápsis ya que varios receptores de neurotransmisores se localizan en *rafts* (GABA, NMDA, AMPA, nACh y P2X) y su acción es dependiente de la integridad de estos subdominios, ya que es necesaria para mantener la óptima actividad de NMDA (61) y $GABA_A$ (62), la estabilidad del receptor AMPA en la superficie (63) y la estabilidad y actividad del receptor de acetilcolina en "*clusters*" (64). Estas variaciones de actividad por compartimentalización diferencial permiten que mediante desplazamientos laterales desde y hacia estos subdominios en la superficie celular se pueda regular la actividad de muchas proteínas. Además, modificaciones postraduccionales como fosforilación o ubiquitinación, así como interacciones proteína-proteína se producen diferencialmente en estos subdominios.

Otra función de los *lipid rafts* es la regulación del tráfico intracelular de proteínas que se encuentren en estos subdominios. Como se indica en la tabla 2, dentro de la endocitosis mediada por *lipid rafts* existen 2 tipos de internalización: 1) la endocitosis mediada por flotilina y 2) la endocitosis mediada por caveolina. La primera es independiente de la GTPasa de escisión dinamina, no posee proteínas de recubrimiento y al producir la endocitosis forma una invaginación vesicular. La segunda sí depende de la escisión por dinamina, utiliza a las caveolinas como proteínas de recubrimiento y al producir la endocitosis forma una invaginación langeniforme. En el laboratorio se consiguen inhibir ambos procesos por agentes quelantes de colesterol que lo retiran de estos dominios y producen su desestructuración limitando la capacidad de internalización mediada por la balsa lipídica.

C.5 Papel de la ubiquitinación en la endocitosis de proteínas en la sinápsis.

La ubiquitinación es un proceso mediante el cual se une covalentemente una o varias moléculas de ubiquitina (proteína de 76 aminoácidos) a otra proteína. Se ha propuesto que esta modificación postraduccional puede estar implicada en prácticamente todos los procesos celulares debido a que

regula la degradación de proteínas. En un principio se describió como un proceso asociado directa y únicamente a la degradación proteasomal de proteínas citosólicas, pero en la última década se ha descrito la existencia del ESCRT (del inglés "*endosomal sorting complex required for transport*"), un complejo sistema que regula la degradación de proteínas transmembrana ubiquitinadas por el lisosoma (65).

Además de su función en la degradación de proteínas proteasomal y lisosomal, la ubiquitinación juega un importante papel en la regulación transcripcional, activación de quinasas implicadas en señalización celular, interacciones proteína-proteína, localización de proteínas y en la endocitosis de proteínas (66). Esto resulta de gran importancia para la función normal de la sinápsis, ya que se ha descrito que la ubiquitinación controla la estabilidad, actividad y localización de receptores y transportadores de neurotransmisores, por lo que se propone como un mecanismo necesario para la actividad y plasticidad de las conexiones sinápticas (67, 68).

El proceso de unión covalente de una molécula de ubiquitina está finamente regulado por un cascada multienzimática que implica a tres proteínas: 1) Enzima activadora de ubiquitina (E1),

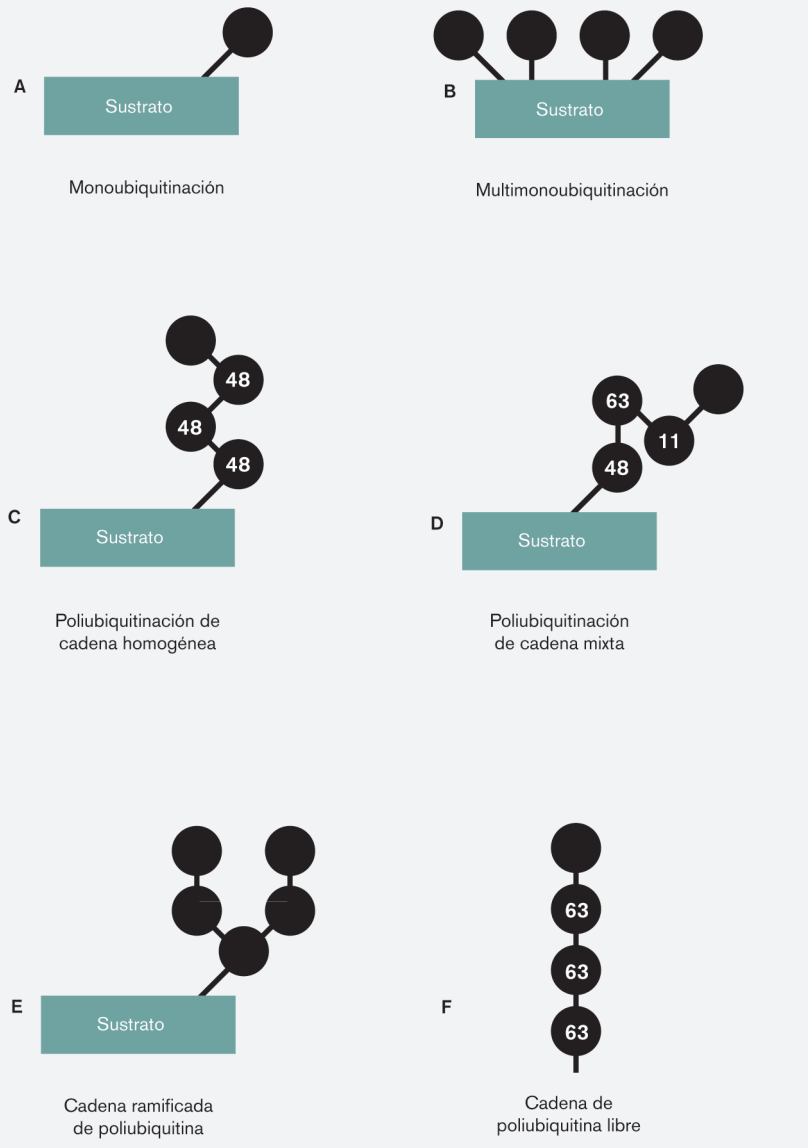

Figura 9
Diferentes variantes de ubiquitinación.
A-F) La figura muestra las diferentes posibilidades de adición de moléculas de ubiquitina al sustrato.

A) Monoubiquitinación: la adición de una única molécula de ubiquitina en una lisina concreta, o en una lisina perteneciente a un grupo de residuos. Generalmente asociada a regulación del tráfico de proteínas.
B) Multimonoubiquitinación: la adición de varias moléculas de ubiquitina en diferentes lisinas pero sin formar nunca una cadena mediante uniones entre varias ubiquitinas. Generalmente asociada a regulación del tráfico de proteínas.
C) Cadena homogénea de poliubiquitina: Adición de una molécula de ubiquitina al sustrato, sobre la que se añaden otras ubiquitinas formando una cadena a través de un único residuo, por ejemplo, la lisina K48. Asociado a regulaciones de trafico (K63) o a degradación de proteínas (K48).
D) Cadena mixta de poliubiquitina: Proceso similar al descrito en [C], pero formando la cadena de poliubiquitina a través de cualquier residuo de esta proteína. Asociado a modulación de interacciones proteína-proteína, endocitosis y degradación de proteínas.
E) Cadenas ramificadas de poliubiquitina: Tras la adición de la primera molécula de ubiquitina al sustrato, sobre esta es pueden producir otras uniones a través de distintos residuos, formando cadenas de poliubiquitina que se ramifican. Su significado fisiológico hasta la fecha no está claro.
F) Cadenas de poliubiquitina libres: sin estar unidas a ningún sustrato, se han encontrado cadenas de poliubiquitina libres en la células. Su función está aún por determinar, aunque parecen estar relacionadas con el mantenimiento de la estabilidad de los reservorios de ubiquitina libre.

2) enzima conjugadora de ubiquitina (E2) y ubiquitin ligasa (E3). Estas enzimas catalizan la formación de un enlace isopeptídico entre el extremo carboxilo terminal de la ubiquitina y una lisina de la proteína diana, lo que da lugar a la monoubiquitinación (figura 9a) que puede ocurrir en una lisina única en una posición concreta (por ejemplo la lisina 619 en GlyT1) o en una lisina perteneciente a conjunto de lisinas. Si se produce monoubiquitinación en varias lisinas a la vez se denomina multimonoubiquitinación (figura 9b).

Las moléculas de ubiquitina unidas a la proteína diana dejan libre su extremo amino terminal y otros residuos de lisinas, que a su vez se pueden unir a nuevas moléculas dando lugar a cadenas poliméricas de ubiquitina denominadas poliubiquitinación. Estos enlaces se producen sobre una de las siete lisinas de la molécula de ubiquitina en las posiciones K6, K11, K27, K29, K33, K48 y K63, dando lugar a cadenas cortas (de 2 moléculas de ubiquitina) o cadenas largas de más de 10 enlaces. Los enlaces más comunes se producen a través de K11, K48, o K63, pudiendo producir una cadena homogénea que mantiene un tipo de enlace (figura 9c), o produciéndose una cadena mixta que alterna diferentes posiciones (figura 9d). En algunas ocasiones se producen ramificaciones en las que una ubiquitina se une a otras en varias posiciones, o incluso se han observado cadenas de poliubiquitina libres, aunque la función de ambas de momento no está clara (figura 9e, f). En general, cadenas homogéneas con enlaces sobre la lisina K48 determinan degradación proteasomal de la proteína marcada, mientras que enlaces sobre la lisina K63 poseen varias funciones como autofagia, reparación del ADN o tráfico endosomal. En cuanto a la endocitosis, parecen estar también implicadas las señales de monoubiquitinación y multimonoubiquitinación.

C.6 Adición selectiva de una o varias moléculas de ubiquitina a la proteína diana.

Un paso crucial en el proceso de ubiquitinación es la especificidad del sistema para marcar únicamente la proteína de interés en el momento adecuado. Esto es posible gracias a la acción de las ubiquitin ligasas (E3) al final del proceso, que pueden pertenecer a dos familias: 1) Ubiquitin ligasas con motivos de dedos de zinc RING (del inglés "*RING Finger Ubiquitin Ligases*") y 2) Ubiquitin ligasas con dominios HECT (del inglés "*HECT Domain Ubiquitin Ligases*"). Las primeras obtienen su especificidad gracias a su unión simultánea a la enzima E2 y al sustrato, transfiriendo la ubiquitina desde la enzima conjugadora de ubiquitina a la proteína diana. La segunda familia cataliza la formación de un enlace tioéster con la ubiquitina y la transfiere entonces al sustrato.

Parece ser que el reconocimiento específico de la proteína diana puede ser mediado por su fosforilación o por la fosforilación de la ubiquitin ligasa, pero hasta la fecha se conoce muy poco sobre la regulación de la longitud de la cadena de moléculas de ubiquitina, lo que puede determinar muy diferentes destinos para la proteína diana. Se especula que la longitud de la cadena puede depender del tiempo de unión entre la ubiquitin ligasa y la proteína diana, de tal modo que se adicionan mayor número de moléculas si la interacción es más estable.

Por otro lado, la longitud de estas cadenas de ubiquitina puede ser editada o eliminada por las enzimas denominadas deubiquitinasas (DUBs) que tienen la función de romper enlaces ubiquitina-ubiquitina o ubiquitina-proteína para editar/anular la señal mediada por la ubiquitinación y liberar moléculas de ubiquitina libre monomérica para su reutilización.

En el genoma humano se han identificado 95 genes potenciales de DUBs (69) que se dividen en 5 clases en función de su homología de dominios catalíticos. Del mismo modo que las enzimas E3, las DUBs necesitan reconocer proteínas ubiquitinadas de manera específica, con lo que se especula que la edición/eliminación de la ubiquitinación de una determinada proteína diana se llevará a cabo por una DUB concreta. Esto implica que varias DUBs median funciones específicas y fallos en su actividad se relacionan con la aparición de enfermedades. La tabla 3 muestra un ejemplo de las funciones neuronales mas importantes de algunas DUBs conocidas hasta la fecha.

Una de las DUBs más importantes en el sistema nervioso es UCHL1 (del inglés "*Ubiquitin carboxyl-terminal hydrolase L1*") ya que regula la estabilidad de la sinápsis y está implicada en la supervivencia neuronal, habiendo sido asociada en algunas enfermedades neurodegenerativas como por ejemplo en la enfermedad de Parkinson (70, 71). La función de UCHL1 resulta crucial en el mantenimiento

TABLA 3

DUB	Función en el sistema nervioso	Enfermedades asociadas
UCHL1	Implicada en la generación de repositorios de ubiquitina libre en la sinápsis, es necesaria para la correcta función y mantenimiento de la sinápsis. La deficiencia en UCHL1 causa distrofia axonal grácil en ratones y mutaciones en su gen codificante se han asociado a la enfermedad de Parkinson.	
UCHL3	Mutaciones en el gen que la codifica se han asociado a deficits en el aprendizaje espacial y en la memoria operativa en ratones, además de degeneración muscular y de la retina. UCHL3 podría proteger ante el estrés oxidativo relacionado a las mitocondrias en retina.	
USP14	Esencial para el mantenimiento de los repositorios de ubiquitina libre, al igual que UCHL1. De hecho, existe una compensación génica entre ambas enzimas, de tal modo que el ratón deficiente en UCHL1 expresa una mayor cantidad de USP14, y viceversa. La expresión de USP14 parece ser esencial para el correcto desarrollo de las uniones neuromusculares.	
USP18	Ratones deficientes en esta DUB sufren necrosis en las células ependimales e hidrocefalia, mostrando temblores, convulsiones, y pérdida de equilibrio.	
USP24	Desconocida.	Puede jugar un papel en la susceptibilidad a padecer enfermedad de Parkinson, según la predicción de análisis genéticos de ligamiento.
USP40	Desconocida.	Al igual que USP24, puede jugar un papel en la susceptibilidad a padecer enfermedad de Parkinson, según la predicción de análisis genéticos de ligamiento.
Ataxin-3	DUB implicada en la edición de cadenas de ubiquitina, relacionado con el control de calidad de las proteínas. Necesaria durante estrés proteotóxico en cultivos celulares humanos y de ratón.	Expansión en la región de poliglutaminas (poliQ) de la ataxina-3 produce neurodegeneración y ataxia espincerebelosa tipo 3.
OTUB1	Desconocida.	Aparece en los cuerpos de Lewy en pacientes analizados postmortem con enfermedad de Parkinson.

de la homeostasis de ubiquitina monomérica libre, necesaria para asegurar la disponibilidad de esta para otros procesos de ubiquitinación en la neurona (72, 73). El mantenimiento de un nivel adecuado de moléculas de ubiquitina libre resulta crucial para la función sináptica ya que permite la ubiquitinación, y por tanto la regulación, de las proteínas neuronales. De hecho se ha comprobado que su limitación mediante la deficiencia o la inhibición farmacológica de UCHL1 produce grandes defectos en la plasticidad sináptica al alterar los procesos de degradación y tráfico de las proteínas implicadas (73, 74).

C.7 Ubiquitinación y tráfico intracelular de transportadores de neurotransmisores.

Dado que la ubiquitinación es un proceso crucial para la regulación de la función sináptica, durante la última década se ha realizado un gran esfuerzo en determinar su posible implicación en la regulación de transportadores de neurotransmisores. El mecanismo más conocido y mejor caracterizado de regulación de estas proteínas es la modulación de su tráfico intracelular (75), de tal modo que el nivel de expresión en la membrana plasmática en un momento dado será el principal determinante de su actividad funcional. Como proteínas de membrana, los transportadores de neurotransmisores están sujetos a un tráfico constitutivo, resultante del equilibrio exocitosis/endocitosis. Se ha demostrado que para la mayoría de los neurotransportadores (GLT1, DAT, GAT1, GlyT1, GlyT2, SERT y NET) la activación de las distintas isoformas de PKC por el éster de forbol 12-miristato 13-acetato (PMA o TPA) produce un desplazamiento de este equilibrio hacia una mayor endocitosis con la consiguiente disminución de la presencia y actividad del transportador (77-86). El mecanismo de la endocitosis regulada por PKC se ha relacionado con procesos de ubiquitinación para algunos de los transportadores, como GlyT1, GLT1 y DAT, tras haberse observado un considerable aumento de su grado de ubiquitinación tras la activación de PKC (78, 79, 87).

En estos procesos resulta de gran interés la identificación de la ubiquitin ligasa responsable, ya que intervenciones farmacológicas sobre esta pueden modificar la función de los transportadores en la sinápsis. Recientemente se ha descrito que la enzima E3 denominada Nedd4-2 ("*neural precursor cell expressed, developmentally downregulated 4-2*") es responsable de la ubiquitinación de GLT1 (77) y DAT (87) tras la activación de PKC, mientras que para el resto de transportadores aún está por determinar la enzima responsable. Otro aspecto clave del proceso es la identificación de los residuos de lisina ubiquitinados. Su sustitución por otro aminoácido, además de abolir la ubiquitinación, permite conocer el papel que ésta modificación postraduccional desempeña en otros aspectos del "*turnover*" celular de la proteína. Así, la endocitosis inducida por PKC de GLT1 requiere la ubiquitinación de las 7 lisinas del extremo carboxilo terminal (78), de GlyT1 la ubiquitinación de la última lisina (K619) del extremo carboxilo terminal (79) y de DAT la ubiquitinación del conjunto de 3 lisinas del extremo amino terminal (88).

Por otro lado, como cualquier proteína transmembrana, los transportadores de neurotrasmisores endocitan consititutivamente como parte de su reciclaje continuo. Esta endocitosis constitutiva requiere también de la ubiquitinación en algunos transportadores, como es el caso de GLT1 (89) y GlyT1 (78), mientras que otros, como DAT, endocita sin necesitar ubiquitinación (90). De esto se deduce que los mecanismos de endocitosis consititutiva pueden diferir entre los distintos transportadores de neurotransmisores, pudiendo la ubiquitinación estar o no involucrada en el proceso dependiendo de la proteína. En el caso de GlyT2, a pesar de su importancia fisiopatológica, no se conocía el papel que la ubiquitinación pudiera desempeñar en su endocitosis constitutiva y regulada por PKC.

D.1 Tráfico intracelular del transportador GlyT2: antecedentes.

Como para el resto de transportadores de neurotransmisores, la presencia de GlyT2 en la membrana plasmática debe estar controlada acorde a la actividad sináptica de la neurona. Así, nuestro laboratorio ha demostrado que durante la liberación de glicina al espacio sináptico se produce un aumento transitorio de GlyT2 en la membrana, de acuerdo a la mayor necesidad momentánea de recaptación de glicina (91). Esta rápida llegada de GlyT2 a la superficie es dependiente de Ca^{2+} y de sintaxina 1A (proteína que nuestro laboratorio previamente había descrito que interacciona con GlyT2) (92), lo que llevó a sugerir que GlyT2 podría traficar, al menos en parte, en vesículas sinápticas. Mediante microscopía electrónica se examinó esta posibilidad y se pudo comprobar que el transportador se encuentra intracelularmente en pequeñas vesículas similares a vesículas sinápticas, que denominamos "*small synaptic-like vesicles*" (91), que contienen sinaptofisina, Rab11 y VIAAT (93). En la actualidad, mediante estudios de proteómica y posterior comprobación por otras técnicas, estamos confirmando la interacción y colocalización de GlyT2 con otras proteínas de vesículas sinápticas, como SNAP-25, SV2, sinaptobrevina y sinaptotagmina (de Juan-Sanz et. al, sin publicar).

En el estado estacionario, una notable proporción de GlyT2 se encuentra en compartimentos intracelulares, tanto en sistemas de expresión heterólogos como en tejido nervioso (93, 94). Al igual que otros transportadores de la familia *SLC6*, GlyT2 recicla constitutivamente entre estos compartimentos y la membrana plasmática, pudiendo la activación de PKC acelerar e incrementar la endocitosis del transportador al interior celular (95, 96)

Por otra parte, nuestro laboratorio ha demostrado que GlyT2 se asocia a balsas lipídicas en la membrana plasmática. Estos subdominios de membrana son ricos en colesterol y esfingolípidos, lo que da lugar a un entorno lipídico ordenado de una manera diferencial. En el caso de GlyT2 este entorno lipídico produce variaciones en su actividad de transporte, de tal modo que alcanza su máxima actividad cuando reside en estos subdominios, pero si se produce una desestructuración de las balsas lipídicas por agentes quelantes de colesterol, su actividad se reduce hasta un 50% (97). Además, la activación de PKC se ha visto que produce un desplazamiento de GlyT2 desde los dominios *raft* a los *no raft* en la membrana, con la consiguiente disminuición de actividad del transportador (96).

E.1 Introducción de los trabajos presentados y aportación original del autor.

Dado que: 1) una gran proporción de las mutaciones en el gen de GlyT2 asociadas a hiperplexia producen alteraciones en su tráfico intracelular (ver tabla 1) y 2) y la regulación del equilibrio exocitosis/endocitosis ha demostrado ser el método más eficaz para modular la actividad de los neurotransportadores (75), resulta de gran interés profundizar en el estudio de la modulación endógena de la actividad de GlyT2 a través de su presencia/ausencia en membrana plasmática. Pese al gran esfuerzo realizado en el estudio del tráfico intracelular de GlyT2 en la última década (91-97), varias cuestiones clave permanecían sin determinar hasta la publicación de los trabajos presentados en esta tesis. Una de estas cuestiones, básica para estudios futuros sobre el tráfico de esta proteína, es la descripción del mecanismo de endocitosis utilizado por el transportador, ya que permite predecir qué moléculas están implicadas en el proceso y pueden llegar a regularlo. En este sentido, hemos descrito la dependencia de la GTPasa dinamina y la utilización de la vía dependiente de clatrina, tanto en la endocitosis constitutiva como en la endocitosis regulada por PKC. Como se describe anteriormente, la endocitosis mediada por clatrina se relaciona con la internalización de proteínas ubiquitinadas, ya que ciertos adaptadores del triskelion de clatrina, como epsinas y Eps15, reconocen proteínas mono/multimonoubiquitinadas. Por tanto, quisimos investigar la implicación de la ubiquitinación en la endocitosis de GlyT2. Mediante la sustitución de residuos de lisina por arginina por mutagénesis dirigida hemos sido capaces de demostrar que: 1) La activación de PKC produce un aumento en la ubiquitinación del transportador que se pierde al mutar la última lisina del carboxilo terminal en la posición K791. Este aumento en la ubiquitinación coincide con un aumento de moléculas de GlyT2 en endosomas tardíos Rab7-positivos y una aceleración de la degradación de la proteína. Además el mutante K791R es incapaz de endocitar tras la activación de PKC, pero internaliza constitutivamente de una manera similar al fenotipo silvestre. 2) La endocitosis constitutiva necesita de la ubiquitinación simultánea de las 4 últimas lisinas del extremo carboxilo terminal (K751, K773 ,K787, K791), ya que el mutante 4KR (en el que se produce la sustitución de estas 4 lisinas por argininas) no es capaz de internalizar constitutivamente, mientras que cualquiera de los mutantes puntuales si que poseen esta característica. Como consecuencia, el mutante 4KR presenta una estabilidad y vida media claramente incrementadas respecto al fenotipo silvestre dado que la falta de ubiquitinación en estas lisinas impide su llegada a endosomas tardíos Rab7-positivos y su posterior degradación.

Parece por tanto que GlyT2 necesita de un correcto funcionamiento de su sistema de ubiquitinación para un adecuado tráfico intracelular. Esto se ha comprobado mediante el uso de Pyr41, un inhibidor de la actividad de las enzimas activadoras de ubiquitina E1 que bloquea, por tanto, los procesos de ubiquitinación en la célula. En estas condiciones disminuye la forma ubiquitinada de GlyT2 y se produce una reducción significativa de la internalización del transportador. De acuerdo con estos resultados, la reducción de los reservorios de ubiquitina libre monomérica en neuronas por la inhibición de la deubiquitinasa UCHL1 (y en menor medida de UCHL3), disminuye la capacidad de ubiquitinación de GlyT2, lo que produce una inhibición de su tráfico confirmando la necesidad de esta modificación postraduccional para su correcta internalización.

Por otra parte, como se ha descrito previamente, GlyT2 se encuentra asociado a balsas lipídicas o *lipid rafts*. Estos subdominios de membrana median un gran número de funciones celulares, entre las que se encuentran la compartimentalización de proteínas o la regulación del tráfico de proteínas (vías de endocitosis dependientes de flotilina o caveolina) (98). En el artículo #1 contribuimos a esclarecer el papel de la presencia de GlyT2 en estos microdominos: Hemos comprobado mediante estudios denominados "*antibody feeding*" que GlyT2 endocita constitutivamente manteniendo su asociación a dominios *raft*. Además, en el artículo #1 hemos comprobado en neuronas que el desplazamiento de GlyT2 desde dominios *raft* a dominios *no raft* en la superficie celular tras la activación de PKC se produce como un paso previo a la endocitosis. Este desplazamiento lateral es un mecanismo rápido de inhibición del transporte adicional a la endocitosis.

El adecuado funcionamiento del tráfico intracelular de GlyT2, estrechamente regulado por la ubiquitinación y su asociación a *rafts*, resulta clave para el funcionamiento normal de la neurotransmisión glicinérgica. Mutaciones en el gen humano de GlyT2 están asociadas a la enfermedad denominada hiperplexia. En el articulo #3 presentado en esta tesis hemos descrito una nueva mutación dominante asociada a hiperplexia con defectos de tráfico intracelular y alteraciones

bioquímicas. La sustitución Y705C (c.2114A→G) presenta una reducida actividad de transporte debido a la suma de dos efectos, 1) una alteración del tráfico que provoca una retención intracelular del transportador y 2) una disminución de la actividad de transporte. Este artículo contribuye a demostrar la importancia de este transportador en humanos, ya que mutaciones como la que hemos descrito producen una deficiencia en la neurotransmisión glicinérgica inhibidora.

Dada la relevancia de la función de GlyT2 en el SNC resulta clave la identificación de mecanismos reguladores de su actividad en la membrana plasmática. Uno de los mecanismos más comunes que regulan la actividad de muchas proteínas son las interacciones con otras moléculas, por lo que en el artículo #4 presentado en esta tesis decidimos utilizar técnicas de proteómica para identificar el interactoma de GlyT2 desde un inmunoprecipitado de sinaptosomas provenientes de cordón espinal de rata adulta. Esto nos ha permitido identificar la interacción entre GlyT2 y la Na/K-ATPasa, proteína encargada de la generación y mantenimiento de los gradientes iónicos de Na^+ y K^+ en la membrana que permiten, entre otros procesos, el transporte de glicina acoplado a Na^+ llevado a acabo por GlyT2. Esta interacción está sujeta a compartimentalización mediada por *lipid rafts* ya que únicamente se observa en estos subdominios de la superficie celular.

En la última década se ha demostrado que la Na/K-ATPasa puede actuar como un receptor de esteroides cardiotónicos, entre los que se encuentra la ouabaína, que se produce de manera endógena en el organismo. La unión de estos compuestos a bajas concentraciones (nM) a la subunidad α activa distintas vías de señalización sin apenas alterar su actividad catalítica. Estas vías son principalmente:1) Activación de PLC y posterior activación de PKC, 2) Activación de PI3K y posterior activación de Akt, 3) Activación de la vía de las MAPK (activación de MEK, y posterior activación de ERK1/2), además de la producción de especies reactivas de oxígeno (del inglés "*reactive oxigen species*", ROS). En el artículo #4 presentamos resultados que muestran que la adición de ouabaína a neuronas de médula espinal y tallo cerebral produce una endocitosis y degradación del reservorio de transportadores GlyT2 asociado a *lipid rafts* que no ocurre con otros transportadores de la familia (GAT1 o SERT), describiendo así un nuevo mecanismo de regulación de este transportador. Este efecto además se reproduce *in vivo* en ratas tras la administración intramedular de ouabaína, lo que pone de manifiesto la relevancia de este mecanismo de regulación de la neurotransmisión glicinérgica en el organismo completo.

Dado que este efecto mayoritariamente se produce sobre las moléculas de GlyT2 asociadas a *lipid rafts* y que la interacción GlyT2-Na/K-ATPasa está compartimentalizada en estos subdominios, en el artículo #4 hemos realizado una proteómica desde fracciones aisladas de dominios *raft* y *no raft* para determinar posibles nuevos interactores que medien este efecto. Los resultados confirman la especificidad de la interacción en estos subdominios, pero no muestran ningún candidato descrito en la bibliografía implicado en estos procesos, por lo que estudios posteriores son necesarios para la determinación de otras moléculas implicadas en este mecanismo que sean responsables de la señalización intracelular que media este efecto.

A continuación se resume la aportación original del autor mediante los trabajos presentados en esta tesis.

1 Determinación de la endocitosis mediada por clatrina como la vía principal de internalización constitutiva y regulada por PKC del transportador neuronal de glicina GlyT2. (Artículo #1)

2 Contribución a esclarecer el sentido celular de la presencia de GlyT2 en *lipid rafts*. Implicaciones sobre su tráfico: Existen diferencias entre la endocitosis constitutiva (GlyT2 permanece asociado a *rafts*) y regulada por PKC (GlyT2 abandona los dominios *raft* como un paso previo de inactivación a la endocitosis). (Artículo #1)

3 Determinación del papel esencial de la ubiquitinación en el tráfico intracelular de GlyT2. Identificación de los residuos de lisina ubiquitinados en la endocitosis inducida por PKC (K791) y en la endocitosis constitutiva (K751, K773 ,K787, K791). La falta de ubiquitinación producida al sustituir estas cuatro lisinas aumenta considerablemente la estabilidad y vida media de GlyT2 (Artículos #1 y #2)

4 Necesidad de reservorios de ubiquitina libre monomérica para la endocitosis de GlyT2. Implicaciones de la deubiquitinasas UCHL1/3 como moduladores indirectos del tráfico del transportador en neuronas. (Artículo #2)

5 Descripción de una nueva mutación en el gen de GlyT2 (*SLC6A5*) que produce defectos en el tráfico del transportador y que está asociada a hiperplexia humana. (Artículo #3)

6 Determinación de la interacción en *lipid rafts* entre GlyT2 y las subunidades α1, α2 y α3 de la Na/K-ATPasa. (Artículo #4)

7 La bomba Na/K-ATPasa al actuar como receptor de ouabaína activa una serie de cascadas de señalización que inducen la endocitosis y degradación del reservorio de GlyT2 asociado a *lipid rafts* en neuronas. (Artículo #4)

F.1 Referencias de los artículos compendiados

Artículo #1

de Juan-Sanz J, Zafra F, López-Corcuera B, Aragón C. (2011) Endocytosis of the Neuronal Glycine Transporter GLYT2. Role of Membrane Rafts and Protein Kinase C-dependent Ubiquitination. *Traffic*. 12:1850-67.

Artículo #2

de Juan-Sanz J, Nunez E, López-Corcuera B, Aragón C. (2013) Constitutive endocytosis and turnover of the neuronal glycine transporter GlyT2 is dependent on ubiquitination of a C-terminal lysine cluster. *PLOS ONE*. 7 Feb 2013. doi: 10.1371/journal.pone.0058863

Artículo #3

Giménez C, Pérez-Siles G, Martínez-Villarreal J, Arribas-González E, Jiménez E, Núñez E, **de Juan-Sanz J**, Fernández-Sánchez E, García-Tardón N, Ibáñez I, Romanelli V, Nevado J, James VM, Topf M, Chung SK, Thomas RH, Desviat LR, Aragón C, Zafra F, Rees MI, Lapunzina P, Harvey RJ, López-Corcuera B. (2012) A novel dominant hyperekplexia mutation Y705C alters trafficking and biochemical properties of the presynaptic glycine transporter GlyT2. *J Biol Chem*. 287(34):28986-9002.

Artículo #4

de Juan-Sanz J, Nunez E, Villarejo-López L, Rodriguez-Fraticelli AE, Pérez-Hernández D, López-Corcuera B, Vazquez J, Aragón C. Na/K ATPase is a new interacting partner for the neuronal glycine transporter GlyT2 that downregulates its expression *in vitro* and *in vivo*.
In preparation.

Artículo #1

Endocytosis of the Neuronal Glycine Transporter GLYT2. Role of Membrane Rafts and Protein Kinase C-dependent Ubiquitination.

de Juan-Sanz J, Zafra F, López-Corcuera B, Aragón C. (2011). *Traffic*. 12:1850-67.

Traffic 2011

doi:10.1111/j.1600-0854.2011.01278.x

Endocytosis of the Neuronal Glycine Transporter GLYT2: Role of Membrane Rafts and Protein Kinase C-Dependent Ubiquitination

Jaime de Juan-Sanz[1,2], Francisco Zafra[1,2], Beatriz López-Corcuera[1,2] and Carmen Aragón[1,2,*]

[1]Departamento de Biología Molecular and Centro de Biología Molecular ''Severo Ochoa'' (CSIC-UAM), Universidad Autónoma de Madrid, Madrid, Spain
[2]Centro de Investigación Biomédica en Red de Enfermedades Raras (CIBERER), ISCIII, Madrid, Spain
**Corresponding author: Carmen Aragón, caragon@cbm.uam.es*

Glycinergic neurotransmission is terminated by sodium- and chloride-dependent plasma membrane transporters. The neuronal glycine transporter 2 (GLYT2) supplies the terminal with substrate to refill synaptic vesicles containing glycine. This crucial process is defective in human hyperekplexia, a condition that can be caused by mutations in GLYT2. Inhibitory glycinergic neurotransmission is modulated by the GLYT2 exocytosis/endocytosis equilibrium, although the mechanisms underlying the turnover of this transporter remain elusive. We studied GLYT2 internalization pathways and the role of ubiquitination and membrane raft association of the transporter in its endocytosis. Using pharmacological tools, dominant-negative mutants and small-interfering RNAs, we show that the clathrin-mediated pathway is the primary mechanism for constitutive and regulated GLYT2 endocytosis in heterologous cells and neurons. We show that GLYT2 is constitutively internalized from cell surface lipid rafts, remaining associated with rafts in subcellular recycling structures. Protein kinase C (PKC) negatively modulates GLYT2 via rapid and dynamic redistribution of GLYT2 from raft to non-raft membrane subdomains and increasing ubiquitinated GLYT2 endocytosis. This biphasic mechanism is a versatile means to modulate GLYT2 behavior and hence, inhibitory glycinergic neurotransmission. These findings may reveal new therapeutic targets to address glycinergic pathologies associated with alterations in GLYT2 trafficking.

Key words: clathrin, endocytosis, glycine, GLYT2, transport, ubiquitin

Received 28 March 2011, revised and accepted for publication 8 September 2011, uncorrected manuscript published online 12 September 2011

Glycine is the main inhibitory neurotransmitter in posterior areas of the vertebrate central nervous system, like the brainstem and spinal cord, where it participates in motor, visual and acoustic functions. Its inhibitory action is terminated by reuptake through sodium- and chloride-dependent plasma membrane glycine transporters, GLYTs, which belong to the neurotransmitter:sodium symporter (NSS) family (*SLC6* gene family) that also contains transporters for neurotransmitters such as serotonin, dopamine, norepinephrine and Gamma-Aminobutyric Acid (GABA) (1). By mediating the synaptic recycling of glycine, the neuronal transporter GLYT2 preserves the quantal glycine content in synaptic vesicles and it assists GLYT1 in regulating glycine levels at the synaptic cleft. Gene deletion studies have suggested that modification of GLYT activity may be beneficial in treating several human disorders, including neuromotor deficiencies (startle disease, myoclonus), pain and epilepsy (2–4). Indeed, missense mutations in the gene encoding GLYT2 can cause hyperekplexia in humans and congenital muscular dystonia type 2 in calves (5,6). Hence, understanding the mechanisms that modulate GLYT2 activity could reveal possible therapeutic targets for the treatment of these conditions.

Protein trafficking plays a fundamental role in the control of neuronal activity and it has been identified as a primary regulatory mechanism for several plasma membrane neurotransmitter transporters (7). The surface expression of GLYT2 during exocytosis is regulated by a Ca^{2+}-dependent SNARE-mediated mechanism in synaptosomes, facilitating the tight coupling of glycine release and reuptake (8). GLYT2 is recycled between the cell surface and the cell interior via constitutive and protein kinase C (PKC)-regulated trafficking pathways (9,10). Thus, different stimuli can control GLYT2 surface expression by influencing GLYT2 trafficking, thereby influencing glycinergic neurotransmission. In fact, a large proportion of GLYT2 resides in intracellular structures of both heterologous systems and nervous tissue under steady-state conditions (11).

We recently examined the subcellular localization of GLYT2 in rat brainstem and identified vesicles containing GLYT2 beside synaptophysin, Rab11 and the GABA and glycine vesicular transporter Vesicular Inhibitory Amino Acid Transporter (VIAAT), as a subset of Rab11-positive endosomal membranes (12). Furthermore, we reported that GLYT2 resides in membrane rafts in primary neurons and synaptosomes (13). Membrane rafts are specialized, heterogeneous, highly dynamic, cholesterol- and sphingolipid-enriched membrane subdomains that compartmentalize cellular processes (14). Several proteins, including neurotransmitter transporters, preferentially

associate with membrane rafts (15,16), which are more tightly packed than surrounding non-raft regions and that serve as mobile platforms in which membrane components can be organized. In neurons, membrane rafts participate in axon guidance (17), establishment of cell polarity (18), receptor signaling (19) and membrane protein trafficking (20), and they contribute to the structural maintenance and plasticity of the synapse (21). As optimal transport activity is achieved when GLYT2 is located in plasma membrane lipid rafts, its interaction with lipids represents a new mechanism through which GLYT2 function and trafficking can be modulated (13).

In eukaryotic cells, endocytosis is a complex process through which molecules can be internalized along multiple routes. Recent findings have highlighted the importance of this process, pointing to endocytosis and trafficking as components of a superior cellular organization or 'cellular master plan' (22). Clathrin-mediated endocytosis is the best characterized pathway by which cells internalize molecules (23–27), although several heterogeneous mechanisms of non-clathrin-mediated routes have been reported (26,28–31). These pathways mainly differ in terms of kinetics, associated protein machinery and the cargo transported (30), but its classification is hampered by overlapping molecular requirements. Furthermore, growing evidence suggests that the same cargo may be internalized via multiple endocytic pathways, depending on the cell type or cellular environment, hindering a clear delineation of the molecular mechanisms for specific cargoes.

Recent evidence has revealed the importance of ubiquitination in the endocytosis of several membrane proteins and is the proposed mechanism for PKC-dependent endocytosis of neurotransmitter transporters (32–37). This post-translational modification consists of the addition of the polypeptide ubiquitin to some free amino groups in proteins, mainly on the ε-amino of lysines, and is catalyzed by the sequential action of three enzymes (E1, E2 and E3). The E3 ligase is the enzyme responsible for the transfer of ubiquitin to the specific substrate (38).

This work reveals the molecular mechanisms of endocytosis of GLYT2, a crucial protein in the physiology and pathology of glycinergic neurotransmission. We have used different approaches to study the molecular pathways involved in the endocytic trafficking of GLYT2, the significance of its association with membrane rafts in this process and the ubiquitination dependence of PKC-induced endocytosis. Our results suggest that clathrin-mediated endocytosis is the main mechanism driving constitutive and regulated GLYT2 internalization and that GLYT2 is constitutively endocytosed from membrane rafts, remaining associated with rafts in subcellular recycling structures. Furthermore, we show that PKC negatively modulates GLYT2 through two different events, a rapid and dynamic GLYT2 redistribution at the cell surface and an increased ubiquitination-dependent GLYT2 endocytosis. Our mutational analysis points to the lysine 791 in the C-terminal tail of GLYT2 as the major determinant for PKC-induced internalization.

Results

We previously showed that GLYT2 is distributed between the cell surface and the cell interior in both heterologous cells and native systems in proportions characteristic of each particular system. The steady-state distribution of transporters is controlled by constitutive intracellular traffic and it can be altered by regulatory stimuli, such as neuronal activity or PKC activation (8–11). To further define the endocytotic pathways used by GLYT2, we studied these pathways in Madin–Darby canine kidney (MDCK) and occasionally COS7 cells. As described previously, polarized MDCK cells express GLYT2 asymmetrically on the apical surface, reflecting the distribution of native GLYT2 in axonal and nerve terminal plasma membranes (39). To facilitate the detection of the GLYT2 protein when expressed in heterologous cells and to monitor its endocytosis, we generated N-terminal epitope-tagged GLYT2 transporters. The NGFR-GLYT2 construct consists of the extracellular and transmembrane domains of the p75 NGFR (nerve growth factor receptor) fused to the NH_2 terminus of GLYT2. This construct enables antibody feeding experiments to be performed in living cells (scheme in Figure 1A). In addition, a GFP-GLYT2 construct was used that was characterized previously in MDCK and PC12 cells (10,11). We found that both tagged proteins were fully functional and exhibited similar glycine transport kinetic parameters to the untagged GLYT2 (Figure 1B). Then, we examined the time–course of constitutive NGFR-GLYT2 (Figure 1C) and GFP-GLYT2 (Figure 1E) endocytosis in MDCK cells. Using antibodies against the extracellular NGFR epitope and a fluorescent secondary antibody, the transporter was labeled at the cell surface in living cells at 4°C (Figure 1C) and the cells were chased at 37°C for the indicated periods of time to follow internalization. The quantification of NGFR-GLYT2 membrane fluorescence for each of the times tested shows the progressive increase of the internalized GLYT2 (Figure 1D). The kinetics of GFP-GLYT2 endocytosis were studied in the presence of the H^+-ionophore monensin, an inhibitor of transport via acidic endosomal compartments, which blocks the recycling of the protein back to the plasma membrane, resulting in the accumulation of endocytosed protein in endosomes (Figure 1E). This is a common experimental strategy used to study the constitutive endocytosis of membrane proteins (32,37,40–42). As expected, monensin (35 μM) promoted the intracellular accumulation of GFP-GLYT2 with a concomitant decrease in protein content in the plasma membrane, as indicated by E-cadherin labeling (plasma membrane marker) (Figure 1E). Moreover, both GLYT2 constructs display similar constitutive and phorbol 12-myristate 13-acetate (PMA)-induced endocytosis as the fluorescence of both constructs overlaps extensively (Figure 1F). This endocytic pattern is also shared by the untagged GLYT2

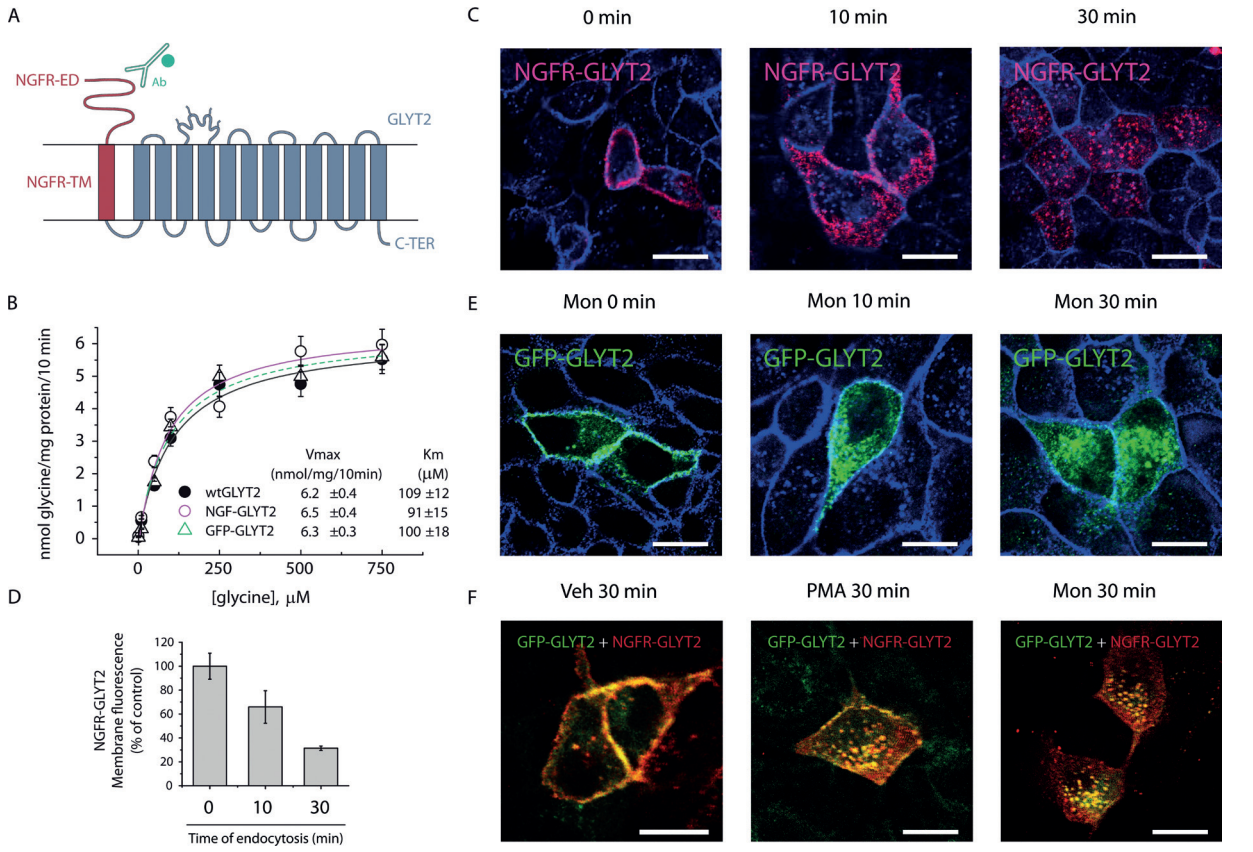

Figure 1: Functional and endocytic characteristics of epitope-tagged GLYT2 constructs in MDCK cells. A) Scheme of the chimeric NGFR-GLYT2 protein constructed with the extracellular and transmembrane domains of the p75 NGFR (NGFR-ED and NGFR-TM) plus the full-length GLYT2 (GLYT2). The binding of anti-NGFR (Ab) to NGFR-ED and that of the Alexa 488-labeled secondary antibody is represented by a Y and a green filled circle, respectively. B) MDCK cells were transfected with either untagged wild-type GLYT2, NGFR-GLYT2 or GFP-GLYT2 and the glycine kinetic parameters of each transporter were determined. The glycine concentration range used was from 1 to 750 μM. Bars represent SEM of triplicates. C) MDCK cells expressing NGFR-GLYT2 were labeled at 4°C with an anti-NGFR antibody and the fluorescent secondary antibody. They were then either fixed directly (0 min) or incubated at 37°C for 10 or 30 min. D) Quantification of NGFR-GLYT2 fluorescence at the cell surface is shown in (C) (using E-cadherin as a membrane marker). Fluorescence intensity was quantified as described in *Materials and Methods*. The histogram represents the mean ± SEM ($n = 3$; on average, 50 cells per condition were analyzed in each experiment). E) MDCK cells expressing GFP-GLYT2 were either fixed (0 min) or incubated at 37°C for 10 or 30 min in the presence of 35 μM monensin (Mon). F) MDCK cells were cotransfected with NGFR-GLYT2 plus GFP-GLYT2 and incubated at 37°C for 30 min in the presence of vehicle (Veh), 1 μM PMA or 35 μM monensin (Mon). Total NGFR-GLYT2 fluorescence was detected after cell permeabilization as in (C). The cells were analyzed by confocal microscopy. E-cadherin labeling (plasma membrane marker) is shown in blue. Scale bar, 15 μm.

in MDCK cells (10). Alternatively, we have performed reversible biotinylation experiments to study the constitutive endocytosis of GLYT2 (Figure S1). In this assay, the biotinylation of surface proteins of living cells is followed by the protein internalization and stripping of biotin from plasma membrane-residing proteins (see *Materials and Methods*). Surprisingly, we have found that when 4°C biotinylated living cells are incubated for 30 min at 37°C to permit internalization, a significant decrease (27.10 ± 3.41% SEM) in GLYT2 transport activity, with respect to the control living cells (30 min, 37°C incubation in the absence of sulfo-NHS-SS-biotin), is observed (Figure S1A). This result could indicate that this biotinylation procedure induces an increased internalization of the transporter with the consequent loss of functional GLYT2 from the cell surface. Regardless of this observed effect, the amount of internalized transporter that is recovered by streptavidin precipitation and further detected by immunoblotting, at least in our hands, is always very low (Figure S1B) for any GLYT2 construct (GLYT2wt, GFP-GLYT2 or NGFR-GLYT2) and cellular system assayed (MDCK or primary neurons). The densitometric quantification of GLYT2 immunoblots obtained by reversible biotinylation and monensin treatment approaches to monitor constitutive endocytosis (as the representative one displayed) indicates that only the 10.53 ± 2.73% SEM of internalized GLYT2 is recovered by reversible biotinylation procedure with respect to the monensin method, suggesting that 89.47% of endocytosed transporter is lost. Similar drawbacks with this procedure in living cells

have also been observed by other authors (32). The low recovery of internalized GLYT2 could be due to the behavior of the cleavable linker of sulfo-NHS-SS-biotin in the reducing intracellular environment. In these conditions, the cleavage of the disulfide bond between protein and biotin could prevent the complete isolation of biotinylated proteins, making difficult its use for constitutive internalization studies.

Constitutive and regulated endocytosis of GLYT2 are dynamin 2-dependent

To define the pathway through which GLYT2 is endocytosed, we used dominant-negative mutants of several proteins involved in specific stages of the endocytic process. The large GTPase dynamin is involved in both clathrin-dependent and clathrin-independent pathways (29), fulfilling an essential role in vesicle scission at the plasma membrane during internalization. The dynamin 2 K44A dominant-negative mutant (GTP-binding-deficient) is a commonly used tool to efficiently block this essential endocytic step (43). MDCK cells were cotransfected with untagged wild-type GLYT2 plus GFP-tagged wild-type dynamin 2 (Figure 2B,E,H) or untagged wild-type GLYT2 plus GFP-tagged K44A mutant (Figure 2C,F,I), and the effect on constitutive (monensin) and regulated (PMA, active phorbol ester) transporter endocytosis was observed by immunofluorescence microscopy. The GFP-K44A mutant (DN-Dyn) blocked both PMA- and monensin-induced internalization of GLYT2 (Figure 2F,I). To confirm the effect of the dynamin 2 dominant-negative mutant on transporter endocytosis, we performed a [^{3}H]-glycine uptake assay to measure the level of functional GLYT2 remaining in the plasma membrane (Figure 2L). The reduction of GLYT2 transport activity by PMA treatment (1 μM) was negligible in the presence of the dominant-negative dynamin 2 mutant. As previously noted elsewhere (32,44), transport activity cannot be accurately measured in the presence of monensin as its cationophore action can affect the electrogenic and Na^+- and Cl^--dependent transport of glycine by GLYT2, leading to erroneous interpretations of GLYT2 surface expression. Thus, we performed quantitative biotinylation of cell surface transporter. Monensin (35 μM) and PMA treatments exerted a similar decrease in the plasma membrane GLYT2 levels, but this effect was not observed in cells coexpressing the dominant-negative dynamin 2 mutant (Figure 2J). Moreover, the similar GLYT2 downregulation exerted by PMA and monensin raises the question of whether PMA, as monensin, could be blocking the recycling of GLYT2 to the membrane. Nevertheless, we previously reported (10) that the combined addition of both compounds produces a higher decrease in plasma membrane GLYT2 than either PMA or monensin alone, suggesting that different trafficking steps are involved in the action of each compound.

Together, these data indicate that both constitutive and regulated GLYT2 endocytosis occur via dynamin-dependent routes.

GLYT2 endocytosis in MDCK cells and primary neurons is clathrin-dependent

The dynamin dependency of GLYT2 internalization mainly confines endocytosis to the pathways mediated by caveolae, clathrin and Ras homolog gene family, member A (RhoA) (29). We initially examined the effect of a dominant-negative mutant of caveolin-1/S80E on GLYT2 internalization in MDCK cells. This mutant retains caveolae in the endoplasmic reticulum (ER) and consequently inhibits their formation at the cell surface (45). Coexpression of myc-tagged cav1/S80E and GFP-GLYT2 (Figure 3D–F) did not prevent GLYT2 internalization, as results from immunofluorescence microscopy (Figure 3A–F), biotinylation labeling (Figure 3G) and glycine transport activity (Figure 3H) approaches show, suggesting that both constitutive and regulated GLYT2 endocytosis are caveolin-1-independent processes (Figure 3). Next, we performed caveolin-1 and clathrin heavy chain (CHC) knockdown by RNA interference [small-interfering RNA (siRNA)] to specifically deplete the endogenous expression of these proteins in MDCK cells, and we examined the effect on GLYT2 endocytosis. Immunofluorescence (Figure 4A–G) revealed that knockdown of caveolin-1, a protein strongly expressed by MDCK cells, did not impede GLYT2 endocytosis. The efficient depletion of caveolin-1 (94.73 ± 2.21% SEM, Figure 4H) together with the activity of GLYT2 (Figure 4I) was consistent with the results obtained with the cav1/S80E mutant (Figure 3). Additional biotinylation approach supported these findings (Figure S2A). As clathrin is involved in many intracellular trafficking steps, we wonder whether the clathrin depletion may also affect clathrin-independent endocytosis. Therefore, we assayed the internalization of labeled albumin as a marker for caveolar endocytosis (Figure S3) (46). Using two distinct siRNA sequences (see *Materials and Methods*), CHC expression was efficiently reduced (94.33 ± 1.13% SEM) relative to cells nucleofected with scrambled siRNA (Figures 5H, S2D and S3B). As shown, the endocytosis of albumin is not altered, despite the high depletion of clathrin achieved (Figure S3A). Immunofluorescence analysis revealed that CHC knockdown produced a large reduction in both constitutive and regulated GLYT2 endocytosis (Figure 5A–G). The strong correlation between the surface GLYT2 immunofluorescence, transport activity and biotinylation assays following CHC depletion (Figures 5 and S2C,D) highlights the clathrin pathway as the primary mechanism of GLYT2 endocytosis. Collectively, the results of our siRNA experiments indicate that regulated and constitutive GLYT2 endocytosis occur via the clathrin-mediated pathway and rule out the caveolar route as a mechanism of GLYT2 internalization in MDCK cells.

As GLYT2 is specifically expressed in neurons, we next sought to determine whether endogenously expressed neuronal GLYT2 is endocytosed through this clathrin-dependent route, as seen in heterologous cells. To this end, we examined the effect of clathrin and caveolar/raft pathways on GLYT2 internalization in primary neuronal cultures from the brainstem (16 DIV). We used the membrane

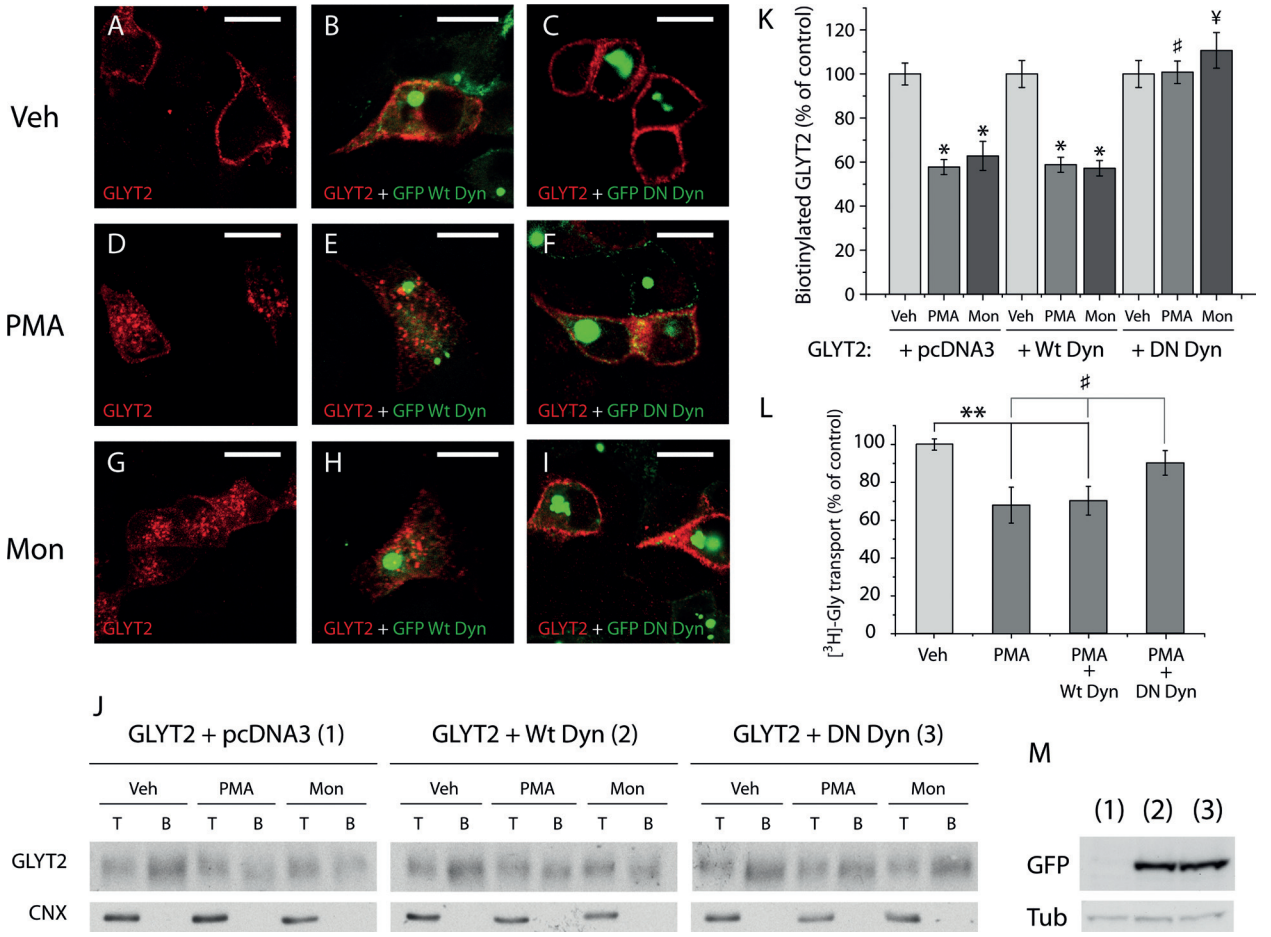

Figure 2: Constitutive and regulated internalization of wild-type GLYT2 are dynamin 2-dependent. A–I) MDCK cells were transfected with wild-type GLYT2 plus the empty pcDNA3 vector (A, D and G) or the wild-type dynamin 2 fused to GFP (Wt-Dyn) (B, E and H) or the dominant-negative K44A mutant of dynamin 2 fused to GFP (DN-Dyn) (C, F and I). After 48 h, the cells were exposed to the vehicle alone (A–C), PMA (1 μM, 30 min: D–F) or monensin (35 μM, 30 min: G–I). After treatment, the cells were fixed with 4% paraformaldehyde, immunostained to visualize GLYT2 (red) and analyzed by confocal microscopy. Note the blockage of transporter endocytosis in (F) and (I) but not in (D, E, G and H). Scale bar, 15 μm. J) Representative immunoblot of MDCK cells expressing wild-type GLYT2 or GLYT2 plus Wt-Dyn or GLYT2 plus DN-Dyn. The cells were treated with the vehicle alone, PMA or monensin as above. The cell surface proteins were labeled with sulfo-NHS-SS-biotin and the biotinylated proteins were pulled down with streptavidin-agarose beads, and GLYT2 expression was analyzed in western blots. Calnexin immunodetection was used as a non-biotinylated protein control. B, biotinylated protein (20 μg); T, total protein (10 μg). K) Densitometric analysis of three independent western blots as in (J). The values are represented as the percentage of the control values (Veh). Bars represent SEM of triplicates. *, significantly different from control, $p < 0.05$; #, significantly different from other PMA-treated samples, $p < 0.05$; ¥, significantly different from other monensin-treated samples, $p < 0.05$ by ANOVA with Tukey's *post hoc* test. L) Transport activity was measured in MDCK cells expressing wild-type GLYT2 or GLYT2 plus Wt-Dyn or GLYT2 plus DN-Dyn after PMA treatment. The data are represented as the mean ± SEM of three triplicate experiments and they are presented as the percentage of control activity, which was 3.44 ± 0.16 nmol of glycine/mg of protein/10 min for wild-type GLYT2. **, significantly different from control, $p < 0.01$; #, significantly different from PMA and PMA + Wt-dyn, $p < 0.05$ by ANOVA with Tukey 's *post hoc* test. M) The cells used in (J) were lysed and analyzed in western blots with an anti-GFP antibody to detect specifically Wt-Dyn or DN-Dyn expression (fused to GFP). Tubulin (Tub) was used as a protein loading control.

impermeable sulfo-NHS-SS-biotin to detect changes in cell surface levels of GLYT2. While PMA induced a 44.27 ± 11.54% SEM reduction in GLYT2 at the neuron surface (Figure 6C), exposing neurons to monensin for 30 min at 37°C induced a decrease of 37.03 ± 8.43% SEM in biotinylated transporter (Figure 6D), as expected when recycling back to the plasma membrane is impaired. These results are consistent with the data obtained in MDCK cells (Figures 2–5), and show the fine tuning of GLYT2 endocytosis by PKC in neurons. The presence of selective inhibitors of the clathrin pathway (chlorpromazine, monodansylcadaverine and concanavalin) or selective blockers of caveolar/raft pathways (filipin or nystatin) (47) had different consequences on the GLYT2 internalization. A reduction in GLYT2 at the neuronal surface provoked by both monensin and PMA was markedly attenuated by inhibitors

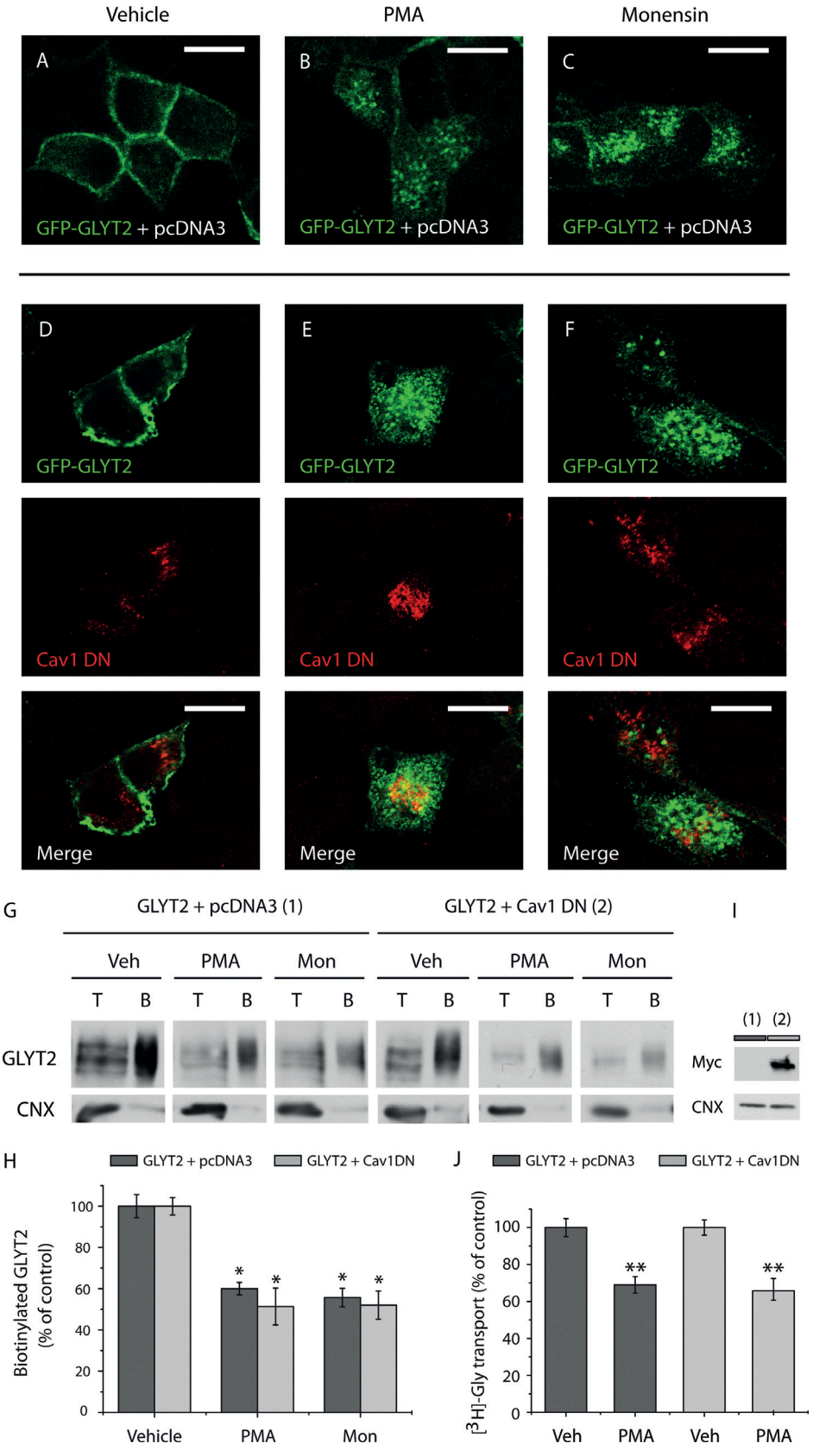

Figure 3: Legend on next page.

of the clathrin pathway. By contrast, GLYT2 internalization was not affected by blockers of caveolar/raft pathways (Figure 6A–D). Together, these findings indicate that constitutive and regulated endocytosis of endogenous GLYT2 in neurons are predominantly mediated by clathrin, which appears to constitute the primary mechanism of GLYT2 endocytosis in diverse cellular systems.

Ubiquitination mediates the PKC-induced endocytosis of GLYT2

As ubiquitination has been implicated in the regulated endocytosis of various membrane proteins including the transporters for dopamine, glutamate and glycine neurotransmitters (DAT, GLT1, GLYT1b) (32–37), we investigated whether the regulated internalization of GLYT2 might depend on its ubiquitination. To know if the level of functional GLYT2 in the plasma membrane was affected by the ubiquitination process, we first performed glycine transport assays in the presence of 4-[4-(5-nitro-furan-2-ylmethylene)-3,5-dioxo-pyrazolidin-1-yl]-benzoicacid ethyl ester (PYR-41), a cell permeable inhibitor of the E1 ubiquitin-activating enzyme that catalyzes the first and critical step in the protein ubiquitination pathway (48). MDCK cells expressing wild-type GLYT2 were pretreated with or without 50 μM PYR-41 for 1 h followed by 30 min in the presence or absence of 1 μM PMA before the glycine transport assay. As Figure 7A shows, the reduction of GLYT2 transport activity by PMA was abolished by PYR-41 treatment, suggesting that ubiquitination is involved. The recent identification of the lysine cluster of the C-terminal as the ubiquitination site required for regulated endocytosis of the highly homologous transporter GLYT1b (37) prompted us to generate mutants to arginine of the four lysines present in the C-terminal of GLYT2 (K751, K773, K787 and K791). Functional results of each single mutant (Figure 7B) showed that the inhibition of GLYT2 activity derived from PMA-induced endocytosis was only abolished by substitution of lysine 791, suggesting that ubiquitination required for GLYT2-regulated endocytosis mainly takes place on this residue. Consistent with the functional results, mutation of K791 but no K751, K773 or K787 substitutions was also effective in removing the PMA-induced internalization as revealed by immunofluorescence (Figure 7C). According to the transport activity and immunofluorescence data, quantitative biotinylation assays showed that the decrease in biotinylated wild-type GLYT2 by PMA was efficiently inhibited when the lysine 791 was mutated (Figure 7D). Moreover, direct evidence of K791 ubiquitination as the main mechanism underlying the PKC-induced GLYT2 endocytosis was provided by immunoprecipitation experiments (Figure 7E,F). MDCK cells expressing wild-type GLYT2 or K791R mutant were treated with or without PMA and the ubiquitinated transporters were immunoprecipitated from cell lysates with agarose-conjugated anti-multiubiquitin (clone FK2), an antibody that recognizes poly- and monoubiquitinated proteins (49), and samples were analyzed by western blot with anti-GLYT2 antibodies. Treatment of PMA increased 2.7-fold the amount of ubiquitinated GLYT2, but similar levels of K791R mutant were detected in either conditions. Together, these data show a direct relationship between ubiquitination of GLYT2 and its PKC-dependent endocytosis and point to the ubiquitination of the lysine 791 in the C-terminal of the transporter as a crucial event in this process.

GLYT2 endocytosis and membrane rafts

We recently reported that GLYT2 displays optimal transport activity when associated with plasma membrane rafts, where it resides in primary neurons and synaptosomes from the rat brainstem, as well as in heterologous cells. Indeed, as well as GLYT2 internalization of PMA induces a redistribution of GLYT2 from raft to non-raft membrane domains (13). Hence, we studied the role of lipid rafts in constitutive and/or regulated GLYT2 endocytosis. The NGFR-GLYT2 construct enabled antibody feeding experiments to be performed in living cells (Figure 8), assays that were performed in COS7 cells instead of MDCK cells due to the technical difficulty of detecting transferrin (Tfn)–fluorophore binding by fluorescence microscopy on the cell surface of MDCK cells, this serving as a marker of non-raft membrane fractions (44). The B

Figure 3: Effect of dominant-negative caveolin-1/S80E mutant on constitutive and regulated internalization of GLYT2. A–F) MDCK cells were transfected with GFP-GLYT2 and the pcDNA3 vector (A–C), or GFP-GLYT2 and the dominant-negative caveolin-1/S80E mutant fused to the myc epitope (Cav1DN: D–F). Two days after transfection, the cells were exposed to the vehicle alone (A and D), PMA (1 μM, 30 min: B and E) or monensin (35 μM, 30 min: C and F). Subsequently, the cells were fixed and labeled with the corresponding primary and secondary antibodies and the fluorescence was visualized by confocal microscopy. GFP-GLYT2 (A–F) was detected by GFP fluorescence, whereas the Cav1DN was detected with the anti-myc antibody and is shown in red (D–F). Scale bar, 15 μm. G) Representative immunoblot of MDCK cells expressing wild-type GLYT2 or GLYT2 plus Cav1DN. The cells were treated with the vehicle alone, PMA or monensin as above. The cell surface proteins were labeled with sulfo-NHS-SS-biotin and the biotinylated proteins were pulled down with streptavidin-agarose beads. GLYT2 expression was analyzed in western blots and calnexin immunodetection was used as a non-biotinylated protein control. B, biotinylated protein (30 μg); T, total protein (10 μg). H) Densitometric analysis of three independent western blots as in (G). The values are represented as the percentage of the control values (Veh). Bars represent SEM of triplicates. *, significantly different from control, $p < 0.05$ by ANOVA with Tukey's *post hoc* test. I) The cells used in (G) were lysed and analyzed in western blots with an anti-myc antibody to detect specifically Cav1DN expression (fused to the myc epitope). J) Transport activity was measured in MDCK cells expressing GLYT2 or GLYT2 plus Cav1DN after PMA treatment. The data are represented as the mean ± SEM of three triplicate experiments and they are presented as the percentage of control activity, which was 3.58 ± 0.17 nmol of glycine/mg of protein/10 min for GFP-GLYT2 plus vector and 2.07 ± 0.08 nmol of glycine/mg of protein/10 min for GFP-GLYT2 plus Cav1DN. **, significantly different from control, $p < 0.01$, Student's *t*-test.

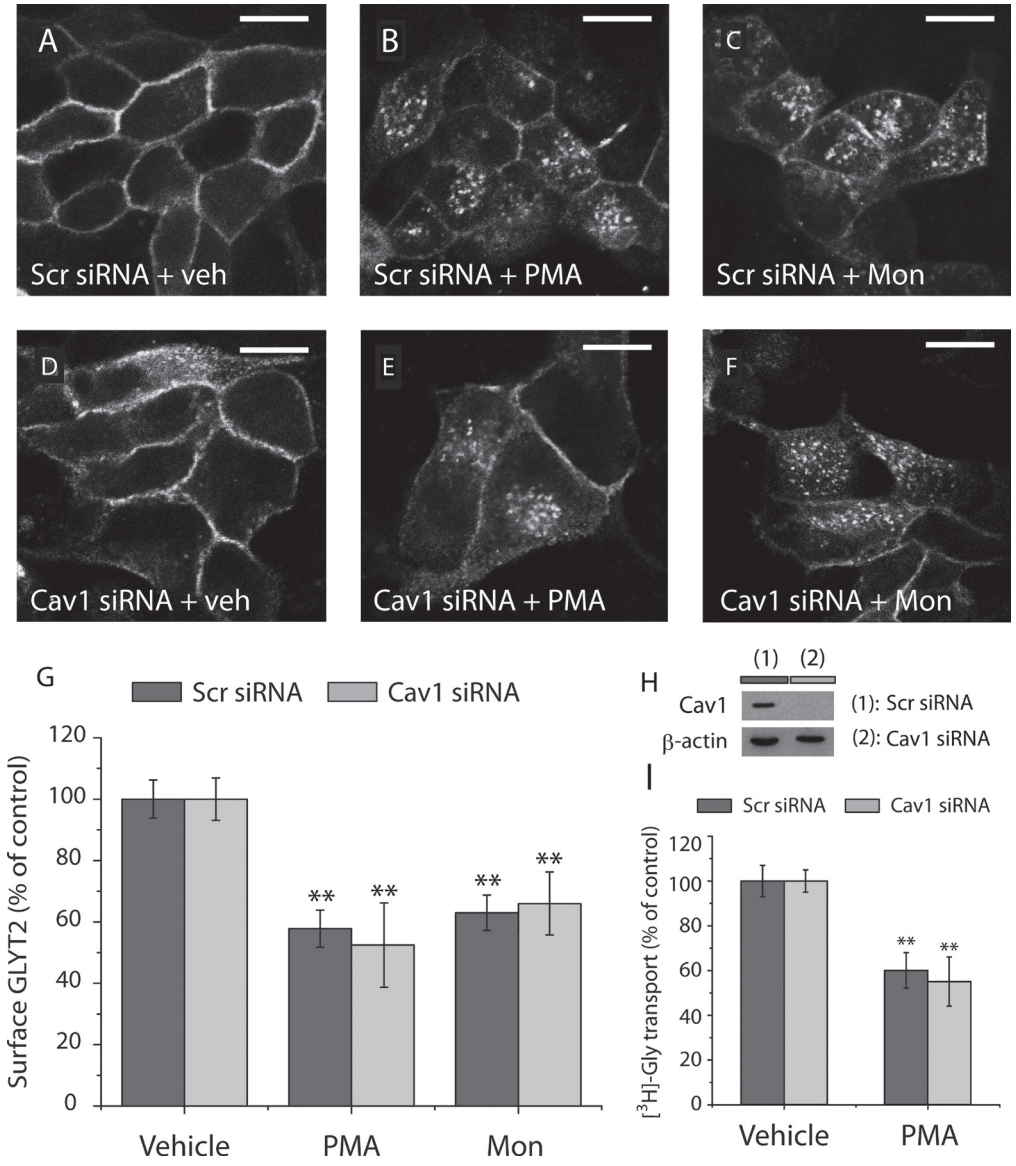

Figure 4: Effect of caveolin-1 knockdown on the endocytosis of GFP-GLYT2. A–F) MDCK cells were nucleofected either with a scrambled siRNA (A–C) or with a caveolin-1 siRNA (D–F), and 1 day after nucleofection, the cells were transfected with GFP-GLYT2. Two days after transfection (and 3 days after nucleofection), the cells were exposed to the vehicle alone (A and D), PMA (1 μM, 30 min: B and E) or monensin (35 μM, 30 min: C and F). Subsequently, the cells were fixed and analyzed by confocal microscopy. Scale bar, 15 μm. G) Quantification of GFP-GLYT2 fluorescence at the cell surface (using E-cadherin as a membrane marker). Fluorescence intensity was quantified as described in *Materials and Methods*. The histogram represents the mean ± SEM ($n = 3$; on average, 60 cells per condition were analyzed in each experiment). **, significantly different from control, $p < 0.01$ by ANOVA with Tukey's *post hoc* test. H) MDCK cells expressing GFP-GLYT2 and nucleofected with the caveolin-1 siRNA or a scrambled siRNA were lysed and immunoblotted using β-actin as a control for protein loading. I) [^{3}H]-Glycine uptake was measured in cells pretreated as in (A, D and B, E). The data represent the means ± SEM of three triplicate experiments and they are presented as the percentage of control activity, which was 3.19 ± 0.22 nmol of glycine/mg of protein/10 min for GFP-GLYT2 cotransfected with scrambled siRNA, and 2.11 ± 0.10 nmol of glycine/mg of protein/10 min for GFP-GLYT2 cotransfected with caveolin-1 siRNA. PMA values were compared with the values obtained with the vehicle alone (**$p < 0.01$, Student's *t*-test).

subunit of cholera toxin (Alexa 488-CTB) was used as a lipid raft marker, which specifically binds to the GM1 ganglioside present in these rafts (17). COS7 cells transiently expressing NGFR-GLYT2 were preincubated with the NGFR antibody, Alexa 594-Tfn and Alexa 488-CTB for 30 min at 4°C and washed with cold PBS. Cells were then chased for 0 and 30 min at 37°C to stimulate internalization and they were then immediately treated with 0.5% Triton-X-100 at 4°C prior to fixation with cold 4% paraformaldehyde. This experimental approach has

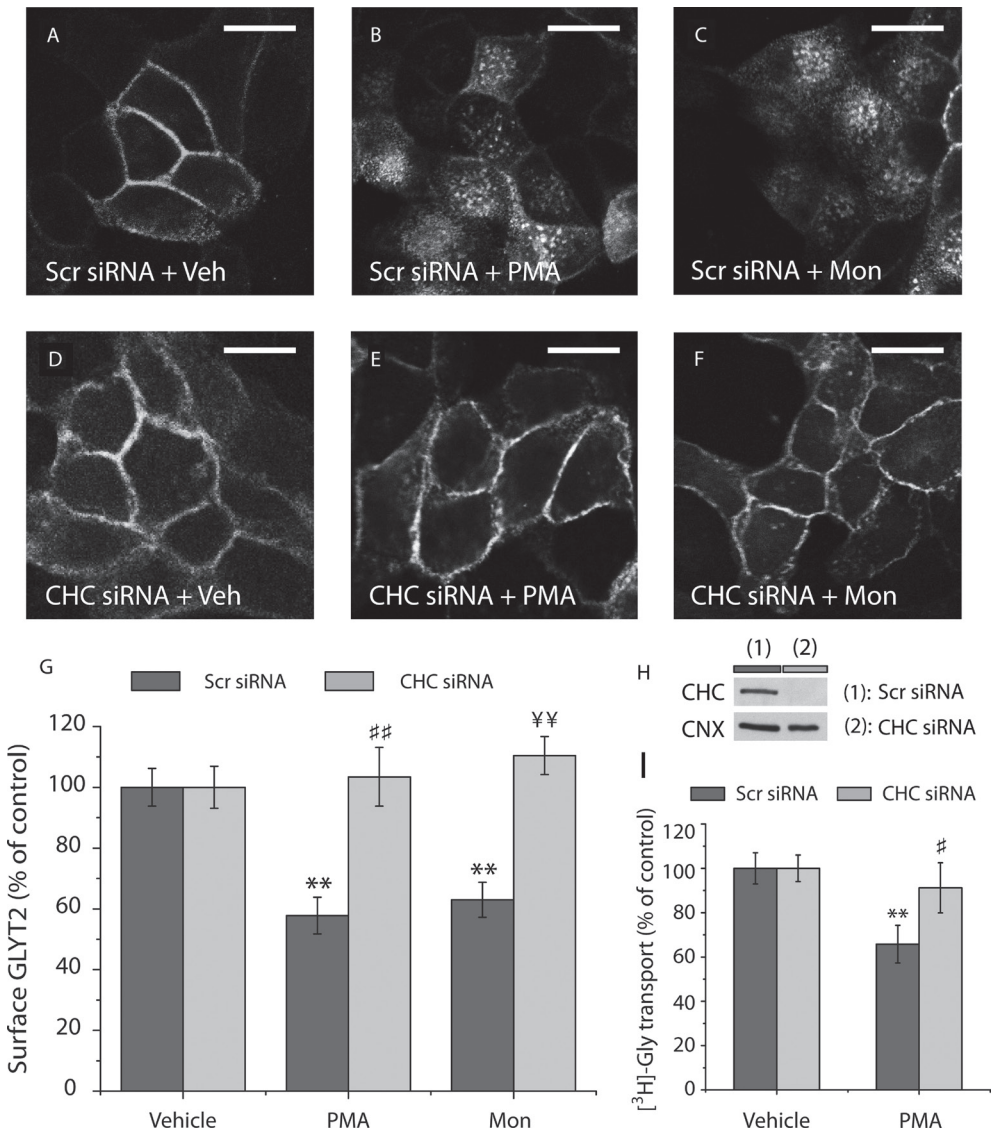

Figure 5: Effect of clathrin knockdown on the endocytosis of GFP-GLYT2. A–F) MDCK cells were nucleofected either with a scrambled (Scr) siRNA (A–C) or with a CHC siRNA (D–F), and a day after nucleofection, the cells were transfected with GFP-GLYT2. Two days after transfection (and 3 days after nucleofection), the cells were exposed to the vehicle alone (A and D),PMA (1 μM, 30 min: B and E) or monensin (35 μM, 30 min: C and F). Subsequently, the cells were fixed and analyzed by confocal microscopy. Note the blockage of transporter endocytosis in (E) and (F) but not in (B) and (C).G) Quantification of GFP-GLYT2 fluorescence at the cell surface (using E-cadherin as a membrane marker). The fluorescence intensity was quantified as described in *Materials and Methods*. The histogram represents the mean ± SEM ($n = 3$; on average, 70 cells per condition were analyzed in each experiment). **, significantly different from control, $p < 0.01$; ##, significantly different from PMA-treated samples, $p < 0.01$; ¥¥, significantly different from Mon-treated samples, $p < 0.01$ by ANOVA with Tukey's *post hoc* test. H) MDCK cells expressing GFP-GLYT2 and nucleofected with a CHC siRNA or a scrambled siRNA were lysed and immunoblotted using calnexin (CNX) as a control for protein loading. I) [^{3}H]-Glycine uptake was measured in cells pretreated as in (A, D and B, E). The data represent the means ± SEM of three triplicate experiments and they are presented as the percentage of control activity, which was 3.19 ± 0.22 nmol of glycine/mg of protein/10 min for GFP-GLYT2 cotransfected with a scrambled siRNA, and 2.11 ± 0.10 nmol of glycine/mg of protein/10 min for GFP-GLYT2 cotransfected with a CHC siRNA. The PMA values were compared with those obtained with the vehicle alone (**$p < 0.01$), and the CHC siRNA values with those with scrambled siRNA values (#, $p < 0.05$, Student's *t*-test). Scale bar, 15 μm.

been used previously to study the movement of other raft-associated proteins (50,51). Representative cells were analyzed by confocal microscopy under identical settings. Exposure to Triton-X-100 completely extracted the Alexa 594-Tfn bound to the cell surface while CTB staining and antibody-bound NGFR-GLYT2 were resistant to detergent extraction (Figure 8C), as expected if the majority of GLYT2 at the surface is associated with rafts (13).

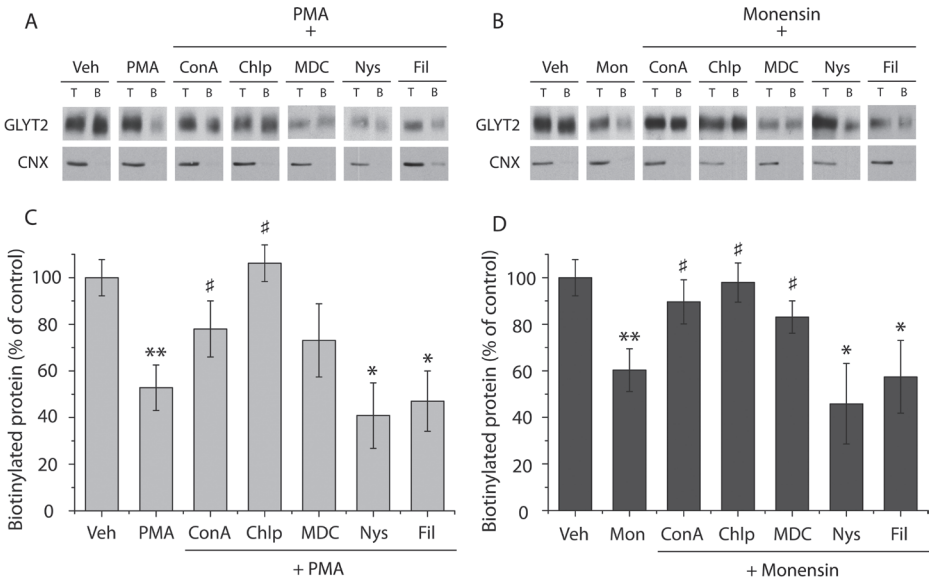

Figure 6: Constitutive and regulated internalization of endogenous GLYT2 in neuronal brainstem cultures use the clathrin-dependent pathway. A) Representative immunoblot of primary neuronal cultures. Cells were treated with the vehicle alone, PMA (1 μM, 30 min) or PMA (1 μM, 30 min) plus the indicated inhibitors of endocytosis. B) Representative immunoblot of primary neuronal cultures. The cells were treated with the vehicle alone,monensin (35 μM, 30 min) and monensin (35 μM, 30 min) plus the indicated inhibitors of endocytosis. The cell surface proteins were labeled with sulfo-NHS-SS-biotin and the biotinylated proteins were pulled down with streptavidin-agarose beads. GLYT2 expression was analyzed in western blots. The inhibitors used to block the clathrin endocytic pathway were concanavalin A (ConA, 0.25 mg/mL), chlorpromazine (Chlp, 15 μM) and monodansylcadaverine (MDC, 200 μM). The inhibitors used to block the caveolar/raft pathway were nystatin (Nys, 20 μM) and filipin (Fil, 5 μg/mL). Calnexin immunodetection was used as a non-biotinylated protein control. B, biotinylated protein (20 μg); T, total protein (10 μg). C and D) Densitometric analysis of three independent western blots as in (A) and (B). The values are represented as the percentage of the control values (Veh). The data represent the means ± SEM. **, significantly different from control, $p < 0.01$; *, significantly different from control, $p < 0.05$; #, significantly different from single PMA/monensin-treated samples, $p < 0.05$ by ANOVA with Tukey's *post hoc* test. Note the blockage of regulated (PMA) and constitutive (monensin) endocytosis of the transporter in the presence of clathrin endocytotic pathway inhibitors (especially in the presence of chlorpromazine) but not in the presence of inhibitors of the caveolar/raft pathway.

After internalization (30 min), Triton-X-100 treatment of living cells totally solubilized the endocytosed Alexa 594-Tfn, whereas the internalized Alexa 488-CTB and NGFR-GLYT2–antibody complex remained resistant to detergent (Figure 8D), indicating that NGFR-GLYT2 was present in the membrane raft subdomains of recycling endosomes (12). Alternative immunostaining of endogenous Tfn receptor confirmed its extraction by the detergent, which rules out the release of Tfn from the receptor after Triton-X-100 treatment as the cause that accounts for the disappearance of the Tfn fluorescence (Figure 8E–H). These results suggest that GLYT2 located in membrane rafts remains associated with the raft during and after constitutive clathrin-mediated endocytosis.

As we previously showed that PKC activation by PMA induces endocytosis as well as shifting GLYT2 from raft to non-raft domains (10), we sought to determine whether the PMA-stimulated endocytosis of GLYT2 acts on transporters associated with rafts or those in other membrane domains. We also investigated whether lateral displacement and internalization are directly coupled phenomena or two independent modulatory steps. As both constitutive and regulated endocytosis occur simultaneously upon PKC stimulation, the assay used in Figure 8 does not permit to address this issue. We used an alternative approach based on a biotinylation procedure in combination with detergent-resistant membrane (DRM) isolation and different endocytosis inhibition methods. In MDCK cells expressing the dynamin 2 K44A dominant-negative mutant (DN-Dyn), the GLYT2 endocytosis induced by PMA was efficiently prevented (Figure 9A and also Figure 2). By contrast, the exit of GLYT2 from membrane rafts at the cell surface after PMA addition was unaffected, despite blocking endocytosis (Figure 9B). Similar results were obtained for endogenous GLYT2 in cultured brainstem neurons (Figure 10) when clathrin-mediated endocytosis of GLYT2 was inhibited with chlorpromazine. Under these conditions, biotinylation of GLYT2 revealed that, despite the lack of internalization (Figure 10A), PMA treatment displaced GLYT2 from neuron membrane raft domains (Figure 10B). As the raft marker flotillin-1 distributes into the low- and high-density fractions from sucrose gradient, the non-raft marker Tfn receptor was used to show a suitable separation between the two fractions. Together, these results suggest that GLYT2 migration from rafts on the cell surface and clathrin-mediated GLYT2 endocytosis induced by PKC

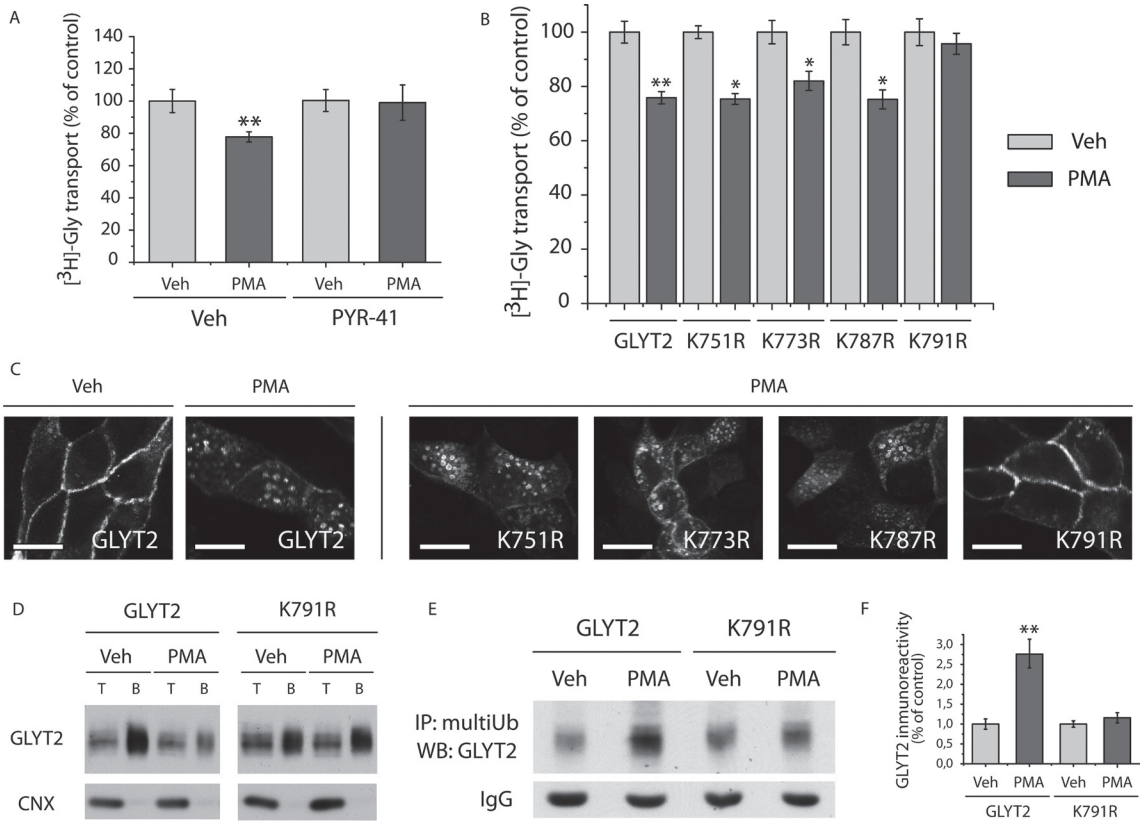

Figure 7: Effect of PKC activation on ubiquitination and endocytosis of GLYT2. A) MDCK cells expressing wild-type GLYT2 were preincubated with the vehicle alone or with 50 μM PYR-41 for 1 h followed by an incubation with 1 μM PMA for 30 min, and then glycine transport activity was measured. The data are represented as the mean ± SEM of four triplicate experiments, and they are presented as the percentage of control activity, which was 3.90 ± 0.33 nmol of glycine/mg of protein/10 min for GLYT2 (Veh) and 4.75 ± 0.32 nmol of glycine/mg of protein/10 min for GLYT2 (Veh + PYR-41) in the presence of PYR-41. **, significantly different from control, $p < 0.01$ by Student's *t*-test. B) [^{3}H]-Glycine uptake was measured in MDCK cells expressing wild-type GLYT2 or the mutants indicated after the treatment with the vehicle alone or PMA as in (A). The results represent the means ± SEM of five triplicate experiments, and they are presented as the percentage of control activity, which was 3.76 ± 0.32 (GLYT2), 3.97 ± 0.12 (K751R), 4.20 ± 0.33 (K773R), 3.88 ± 0.15 (K787R) and 4.03 ± 0.17 (K791R) nmol of glycine/mg of protein/10 min. **, significantly different from control, $p < 0.01$; *, significantly different from control, $p < 0.05$ by Student's *t*-test. C) MDCK cells expressing wild-type GLYT2 or the mutants indicated were exposed to the vehicle alone or PMA (1 μM, 30 min). Cells were then fixed and analyzed by confocal microscopy. To simplify the figure, only the GLYT2 wild-type control (Veh) is displayed. (The rest of controls were highly similar.) Scale bar, 15 μm. D) Representative immunoblot of MDCK cells expressing wild-type GLYT2 or the K791R mutant. The cells were treated with the vehicle alone or PMA as above. The cell surface proteins were labeled with sulfo-NHS-SS-biotin and the biotinylated proteins were pulled down with streptavidin-agarose beads. GLYT2 expression was analyzed in western blots and calnexin immunodetection was used as a non-biotinylated protein control. B, biotinylated protein (30 μg); T, total protein (10 μg). E) MDCK cells expressing wild-type GLYT2 or the K791R mutant were incubated with vehicle or PMA as above. Cells were lysed, and the ubiquitinated transporters were immunoprecipitated with agarose-conjugated anti-multiubiquitin antibody. Then, immunoprecipitates were probed with anti-GLYT2 antibodies. Quantification of three experiments performed identically to the representative experiment is shown in (F). Bars represent the mean ± SEM of the amount of ubiquitinated transporter (PMA) to the normalized amount of ubiquitinated transporter (Veh). **$p < 0.01$ by ANOVA with Tukey's *post hoc* test.

activation are not simultaneous events, but rather that the exit of GLYT2 from surface rafts precedes its internalization to recycling compartments.

Discussion

We previously showed that GLYT2 recycles between the cell surface and the cell interior through constitutive and PKC-regulated trafficking, such that in steady-state conditions a large proportion of transporter resides in intracellular structures of both heterologous systems and nervous tissue (10–12). Recently, we identified GLYT2-containing subcellular structures as a subset of Rab11-positive endosomes, thereby confirming the existence of dynamic and active recycling of GLYT2 in nerve terminals of the brainstem and spinal cord (12). GLYT2 trafficking represents a critical means of controlling inhibitory glycinergic neurotransmission, allowing the rate of exocytosis/endocytosis of the recruitable GLYT2 internal pool to

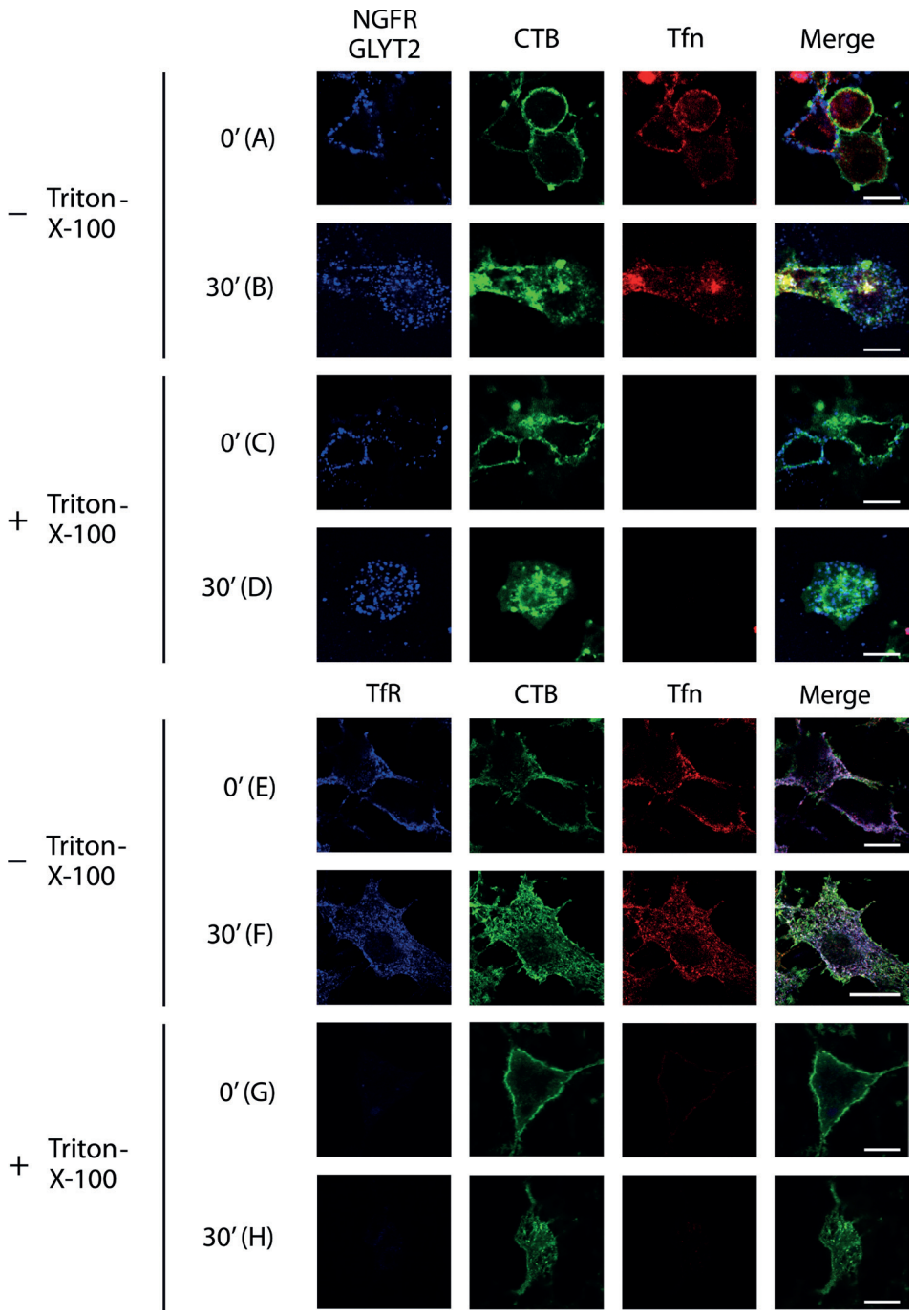

Figure 8: Constitutive internalization of NGFR-GLYT2 takes place from membrane rafts. A and B) COS7 cells expressing NGFR-GLYT2 were incubated at 4°C for 30 min with an anti-NGFR antibody (blue), cholera toxin B-Alexa 488 (CTB-488, green) and transferrin Alexa-594 (Tfn-594, red), fixed and the NGFR antibody was detected with an Alexa 647-conjugated secondary antibody (bound) and visualized by confocal microscopy (A). For internalization (30 min: B), the cells incubated at 4°C (as in A) were further chased for 30 min at 37°C and then fixed and labeled as in (A). C and D) The cells were treated as in (A) and (B), respectively, and then treated with 0.5% Triton-X-100 prior to fixation, as described in *Materials and Methods*. Note that non-raft membrane fractions are solubilized *in vivo* (disappearance of Tfn-594, red fluorescence) but CTB-488 (raft marker) and GLYT2-NGFR are resistant to detergent solubilization before and after internalization. E–H) COS7 cells were incubated at 4°C for 30 min with cholera toxin B-Alexa 488 (CTB-488, green) and transferrin Alexa 594 (Tfn-594, red), fixed, immunostained to visualize transferrin receptor (TfR) (blue) and visualized by confocal microscopy (E). For internalization (30 min: F), the cells incubated at 4°C (as in E) were further chased for 30 min at 37°C and then fixed and labeled as in (E). G and H) The cells were treated as in (E) and (F), respectively, and then treated with 0.5% Triton-X-100 prior to fixation. Scale bar, 15 μm.

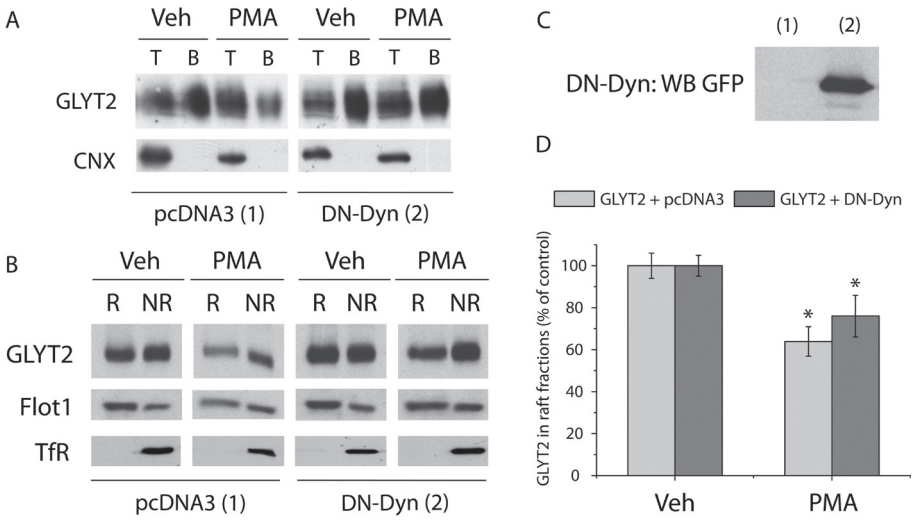

Figure 9: Biphasic mechanism of GLYT2-regulated endocytosis in MDCK cells. A–C) Cells were transfected either with wild-type GLYT2 plus the empty pcDNA3 vector (1) or with wild-type GLYT2 plus the K44A dominant-negative mutant of dynamin 2 fused to GFP, DN-Dyn (2). The cells were exposed to the vehicle alone (Veh) or PMA (1 μM, 30 min; PMA: A and B). A) Subsequently, the cells were biotinylated and GLYT2 expression was analyzed as described in Figure 6. B, biotinylated protein (20 μg); T, total protein (10 μg). Calnexin is shown as a non-biotinylated protein control. Note that DN-Dyn blocks the GLYT2 internalization induced by PMA. B) After treatment and biotinylation as in (A), the cells were lysed and subjected to membrane raft isolation as described in *Materials and Methods*. Raft (R) and non-raft (NR) fractions were collected and pulled down with streptavidin-agarose beads, and GLYT2 expression was analyzed in western blots of each fraction (30 μg). Note that the R to NR GLYT2 displacement produced by PMA in (1) also occurs in (2), where GLYT2 endocytosis is blocked by DN-Dyn as shown in (A). Thus, lateral movement at the cell surface occurs before GLYT2 endocytosis. Transferrin receptor (TfR) is a non-raft protein and flotillin-1 was used as a raft marker and as a protein loading control. C) The cells used in (A and B) were lysed and analyzed in western blots with an anti-GFP antibody to detect specifically DN-Dyn expression (fused to GFP). D) Quantification of GLYT2 immunoreactivity in raft (R) fractions calculated as the ratio R/(R + NR) and normalized as the percentage of control. Data represent the means ± SEM of three experiments (*$p < 0.05$, Student's *t*-test).

be modulated to and from the cell surface, and potentially facilitating the rapid and efficient neuronal adaptation to changes in synaptic neurotransmitter concentrations. As GLYT2 supplies glycine to refill synaptic vesicles in the inhibitory nerve terminal and mutations in the *GLYT2* gene have been identified as the major presynaptic defect in human hyperekplexia patients (5), this transporter represents an important therapeutic target for the treatment of neuromotor disorders (hyperekplexia, myoclonus), pain or epilepsy (4). Hence, understanding the molecular mechanisms involved in the endocytic trafficking of GLYT2 and the significance of its association with membrane rafts in this process is of considerable interest.

With the aid of a novel epitope-tagged GLYT2 construct, NGFR-GLYT2, we studied here the constitutive endocytosis of this transporter in living cells using the antibody feeding assay. We also used a previously described GFP-tagged GLYT2 construct in the presence of monensin, an ionophore commonly used in membrane protein trafficking studies (32,37,40–42). Regulated internalization was induced by the active phorbol ester, PMA, and constitutive and PMA-induced GLYT2 endocytosis were dependent on dynamin 2 as both processes are blocked by a dominant-negative mutant of this GTPase, K44A (52). The involvement of dynamin 2 and the presence of GLYT2 in membrane rafts (13) suggest that GLYT2 may be internalized through the caveolar/raft pathway. However, neither overexpression of a dominant-negative mutant of caveolin-1/S80E nor knockdown of endogenous caveolin-1 by specific siRNA in MDCK cells prevented GLYT2 internalization, ruling out a role for caveolin-1 in GLYT2 endocytosis. By contrast, siRNA targeting of the CHC strongly reduced constitutive and regulated GLYT2 endocytosis, indicating that the primary route of GLYT2 endocytosis in MDCK cells is clathrin-mediated. Pharmacological inhibition of either clathrin or caveolar/raft pathways in cultured brainstem neurons showed the involvement of the clathrin pathway in constitutive and regulated endocytosis of endogenous GLYT2. Together, our results indicate that clathrin-mediated endocytosis is the main pathway for GLYT2 internalization, apparently independent of cell type.

With regard to the molecular mechanism of the PKC-dependent GLYT2 endocytosis, our data show a correlation between the stimulation of GLYT2 endocytosis by PKC activation and increased ubiquitination of the transporter, suggesting that ubiquitination of GLYT2 represents an internalization signal for this process. Similar observations have been reported for DAT, GLT1 and GLYT1b neurotransporters (32–37). Our mutagenesis analysis have identified lysine 791, one of a cluster of four lysines in the C-terminal tail of GLYT2, as the site of ubiquitination required for PKC-dependent

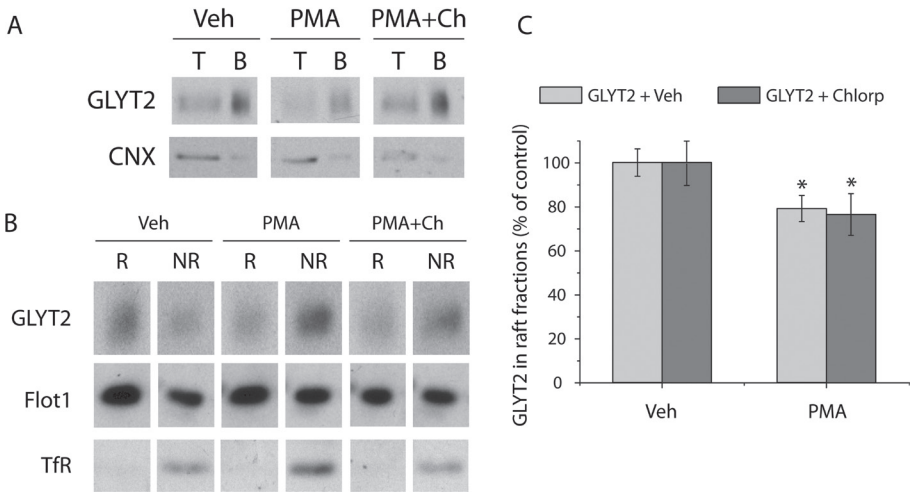

Figure 10: Regulated endocytosis mechanism of endogenous GLYT2 in neurons. A and B) Primary brainstem and spinal cord neuron cultures were exposed to the vehicle alone (Veh), PMA (1 μM, 30 min: PMA) or PMA plus chlorpromazine (1 μM plus 15 μM, respectively, for 30 min: PMA + Ch). A) Subsequently, the neurons were biotinylated and GLYT2 expression was analyzed as described in Figure 6. B, biotinylated protein (20 μg); T, total protein (10 μg). Calnexin is shown as a non-biotinylated protein control. B) After treatment and biotinylation as in (A), the cells were lysed and membrane rafts were isolated as described in *Materials and Methods*. Raft (R) and non-raft (NR) fractions were collected and pulled down with streptavidin-agarose beads, and GLYT2 expression was analyzed in western blots of each fraction (30 μg). Note that the lateral displacement of GLYT2 produced by PMA also occurs when internalization is blocked by chlorpromazine, indicating that it occurs prior to and independent of transporter internalization. Transferrin receptor (TfR) is a non-raft protein and flotillin-1 was used as a raft marker and as a protein loading control. C) Quantification of GLYT2 immunoreactivity in raft (R) fractions calculated as the ratio R/(R + NR) and normalized as the percentage of control. Data represent the means ± SEM of three experiments (*$p < 0.05$, Student's *t*-test).

GLYT2 endocytosis. Lysine residues located in the intracellular tail of transporters have been previously reported as common targets for ubiquitin recruitment involved in the PKC-dependent endocytosis. Thus, a cluster of three lysines in the N-terminal domain of the dopamine transporter, DAT (35), and a cluster of several lysines in the C-terminal of the glutamate transporter, GLT1, have been reported (36). A recent study of the highly homologous GLYT1b identified one residue, the lysine 619 in the C-terminal, as the main target for PKC-dependent ubiquitination (37). In this regard, GLYT2 behavior resembles that of GLYT1b because our results identify lysine 791 (the most terminal lysine of GLYT2 as the lysine 619 in GLYT1b) as the ubiquitination target following PKC activation. The ubiquitin bind to K791 of GLYT2 might be the platform on which the clathrin network is assembled. Our present results and the previously reported contribute to the hypothesis that ubiquitination is the general mechanism by which PKC activation accelerates endocytosis of various transporters and probably other membrane proteins.

Moreover, we previously reported that the activity of GLYT2 and its modulation by PKC are dependent on its localization to cell surface rafts (10,13). Modulating the ratio of raft-associated to non-raft-associated transporter may control the rate and level of neurotransmitter uptake at the synapse (19). Although many neurotransporters undergo redistribution from lipid rafts to other membrane domains by PKC, these domains are not necessarily involved in the regulated endocytic mechanism of the transporter (32). Growing evidence suggests that proteins located in lipid rafts are endocytosed via clathrin-dependent pathways (50,53–60). Our demonstration of the continued association of GLYT2 with lipid rafts during constitutive endocytosis is consistent with recent findings from our laboratory that indicate recycling endosomes are the major subcellular compartment in which GLYT2 resides in the steady state (12). Recycling endosomes are more enriched in lipid and protein raft components than the late/lysosomal compartment (44,61). Lipid rafts appear to be restricted from entering the degradative lysosomal compartment, and once internalized, raft components are returned to the cell surface from the recycling endosomes (61,62). In this sense, the increased ubiquitination and the shift to non-rafts of GLYT2 by PKC could direct a pool of GLYT2 resident in recycling endosomes to the degradative lysosomal pathway, hindering the recycling to the membrane and thereby decreasing the amount of functional transporter at the cell surface.

We have proposed that GLYT2 associates with synaptic vesicles at some stages during its recycling in the nerve terminal, in agreement with the proposed role of synaptic vesicles in the trafficking of plasma membrane proteins (63). This is consistent with the enrichment of raft-associated proteins in synaptic vesicles (64,65). In addition, a raft-based sorting mechanism for apical/axonal proteins has been proposed in polarized epithelial and neuronal cells that operate along the recycling pathway,

contributing to the maintenance of cell polarity (44,66,67). Therefore, in basal conditions raft-associated GLYT2 undergoes constitutive internalization to maintain a readily available functional transporter pool that can repopulate the cell surface to maintain basal glycine transport. Our previous (10) and present results confirm that the functional inhibition of GLYT2 by PKC is dependent on the localization of GLYT2 in membrane rafts and occurs through two independent events: the shift of GLYT2 from raft to non-raft subdomains at the plasma membrane and the increase in endocytosis. These two processes, which are uncoupled by inhibiting clathrin-mediated endocytosis, may be sequential, suggesting that surface GLYT2 is shifted to non-raft domains and then endocytosed from this location. A similar modulatory mechanism involving independent raft exit and clathrin-mediated endocytosis has been described for other membrane raft proteins, such as epidermal growth factor receptor (EGFR) (68), the α_{1a} adrenergic receptor (59) and tetanus toxin (69). Following transfer to cell surface non-raft domains, GLYT2 may be inactive or less active for some time before undergoing endocytosis. Alternatively, it may be rapidly transported back to plasma membrane rafts, where it can exert optimal activity (13), or as discussed above, irreversibly directed to the degradative lysosomal compartment, a transporter pool that may represent the non-raft-associated transporter described previously (10,12,13). This circuit could involve additional modulatory steps as the recycling of functional GLYT2 to the surface is dependent on its inclusion in rafts, probably through *trans* Golgi network (TGN) trafficking and axonal/apical sorting. We propose that GLYT2 pools associated with different membrane subdomains may be maintained by constitutive or regulated dynamic trafficking.

In summary, we propose that PKC can negatively modulate GLYT2 via two mechanisms, through the rapid and dynamic redistribution of the transporter at the cell surface and through increased internalization of the ubiquitinated transporter via clathrin-mediated endocytosis. These events may represent different spatial and temporal aspects of a plastic mechanism responsible for the dynamic and versatile modulation of GLYT2 to modify glycine neurotransmission in pathophysiological situations. Future studies will be necessary to identify raft lipids and/or proteins that interact with GLYT2, facilitating its dynamic association/dissociation with the membrane, and the maintenance of an active GLYT2 recycling pool capable of fulfilling the demand for synaptic glycine reuptake. Defining these interactions is of particular relevance to understand the altered trafficking of human GLYT2 mutants responsible for hyperekplexia and to identify further targets for therapeutic intervention.

Materials and Methods

Materials

Wistar rats were bred in standard conditions at the 'Centro de Biología Molecular S.O.' in accordance with current guidelines regarding the use of animals in Neuroscience research. Ubiquitin E1 inhibitor, PYR-41, was from Calbiochem. All other chemicals were purchased from Sigma-Aldrich. Antibodies against the following proteins were used: GLYT2 [rabbit and rat: (12,70)], E-cadherin (kindly provided by Dr A. Cano, CIB), calnexin (Stressgen), caveolin-1 (Abcam), CHC (BD Transduction), flotillin-1 (BD Biosciences), β-actin (Sigma-Aldrich) and NGFR (Oncogene). Agarose-conjugated anti-multiubiquitin (monoclonal antibody, clone FK2) was from MBL International. The Tfn receptor and GFP were purchased from Invitrogen and myc was from Roche Applied Sciences. Tfn, CTB or albumin conjugated to Alexa Fluor 594, Fluor 488 or Fluor 555 was purchased from Invitrogen and the fluorophore-coupled secondary antibodies were from Molecular Probes.

Cell growth and transfection

COS7 and MDCK II cells (American Type Culture Collection) were grown at 37°C and 5% CO_2 in high-glucose DMEM supplemented with 10% fetal bovine serum. Transient expression was achieved using Neofectin™ (COS7 cells) or Lipofectamine™ 2000 (MDCK cells) from Mid Atlantic Biolabs and Invitrogen, respectively, following the manufacturer's instructions. Reproducible results were obtained with 60–70% confluent cells on a 60-mm dish using 6 μg of total DNA. Cells were incubated for 48 h at 37°C until they were used.

Plasmid constructs and generation of mutants

GLYT2 fused to GFP in the pEGFPC1 vector was constructed as described elsewhere (GFP-GLYT2:11). An expression vector for the fusion protein NGFR-GLYT2 (pCDNA3-NGFR-GLYT2) was prepared by polymerase chain reaction (PCR) using a two-step strategy. First, a fragment encoding the 298 N-terminal residues of the rat NGFR was amplified with primers AAGCTTATGAGGAGGGCAGGTGCT and GAATTCCGCTGTTCAACCTCTTGAAAGC using the full-length NGFR as a template (donated by Dr G. Dechant). This fragment was cloned in the *Hind*III/*Eco*RI sites of pCDNA3 to produce the construct pCDNA3-NGFR. The complete open reading frame (ORF) of GLYT2 was then amplified using the oligonucleotide primers GAATTCACATGGATTGCAGTGCTCCC and TCTAGACTAGCACTGGGTGCCCAGTTCC and cloned in frame with NGFR at the *Eco*RI/*Xba*I sites of pCDNA3-NGFR. The reverse primer contained a stop codon to halt transcription. The Cav1/S80E-myc plasmid was kindly provided by Dr J. E. Pessin (Albert Einstein College of Medicine) and GFP wild-type dynamin 2 and GFP K44A dynamin 2 plasmids were provided by Dr M. A. Alonso (CBMSO). The fidelity of these constructs was confirmed by DNA sequencing. Substitution mutants were generated with the QuickChange Site-Directed Mutagenesis kit (Stratagene), using the rat GLYT2 in pCDNA3 as reported (71).

RNA-mediated interference and western blots

siRNA oligonucleotides were purchased from Sigma and two CHC siRNA duplexes were used: 5′-UAAUCCAAUUCGAAGACCAAU-3′ and 5′-GUAUGAUGCUGCUAAACUA-3′ (72). The caveolin-1 siRNA duplex was 5′-AAGAUGUGAUUGCAGAACCAGUU-3′ (73) and a scrambled siRNA (Sigma) was used as the control. The siRNAs (625 ng of each siRNA) were transfected into MDCK cells (0.5×10^6 cells) by nucleofection by Amaxa electroporation using the A-24 program of the Nucleofector device, according to the manufacturer's instructions (Lonza Group Ltd). The cells were then plated at 80% confluence and experiments were performed 3 days after nucleofection. Cell lysates containing 25 μg of protein were analyzed by SDS–PAGE and immunoblotting to detect the expression of CHC or Cav1. The signals obtained were normalized to calnexin or β-actin immunoreactivity.

Immunocytochemistry and confocal imaging

MDCK II and COS7 cells grown on glass coverslips were transfected with the corresponding expression vectors using Lipofectamine™ 2000 and Neofectin™, respectively, according to the manufacturer's instructions. Immunostaining was performed as described previously (9,12). Cells were visualized by confocal microscopy on a Microradiance microscope (BioRad) using a vertical Axioskop 2 microscope (Zeiss) or an LSM510 META

confocal microscope coupled to an inverted microscope AXIOVERT 200 (Zeiss). IMAGEJ (National Institutes of Health) and LSM image browsers (Carl Zeiss, Inc) were used for image processing.

Anti-multiubiquitin immunoprecipitation

Three hundred micrograms of scraped and washed MDCK II cells were lysed at 1 mg of protein/mL concentration in TN buffer (25 mM Tris–HCl and 150 mM NaCl, pH 7.4) containing 0.05% Nonidet P-40 (NP-40), 50 mM *N*-ethylmaleimide and protease inhibitors [PIs; 0.4 mM phenylmethylsulfonyl fluoride (PMSF) + Sigma cocktail] for 30 min at room temperature. Then, 12 μL of agarose-conjugated anti-multiubiquitin (MBL International) was added and incubated for 1 h at room temperature. The beads were collected by mild centrifugation and washed 3× with lysis buffer. Finally, beads were pelleted and ubiquitinated proteins were eluted in 75°C Laemmli buffer during 10 min. Samples were run on an SDS/PAGE gel (7.5% gel), subjected to western blot with enhanced chemiluminescence (ECL) detection and quantified on a GS-710 calibrated imaging densitometer from Bio-Rad.

Antibody uptake and Triton-X-100 treatment of living cells

Transiently transfected COS7 cells were incubated in serum-free DMEM for 4 h (or overnight), followed by incubation with the anti-NGFR (1:250) antibody for 30 min at 4°C. The cells were then washed twice with cold PBS and incubated with anti-mouse Alexa 647, Tfn Alexa 594 (50 μg/mL) and CTB Alexa 488 (5 μg/mL) for 30 min at 4°C. After washing the cells twice with PBS at 4°C, they were fixed in cold 4% paraformaldehyde in PBS for 20 min or further incubated at 37°C for the indicated periods to facilitate trafficking. The cells were solubilized at the times indicated with 0.5% Triton-X-100 in PBS for 30 seconds at 4°C and after *in vivo* solubilization, they were washed once with PBS at 4°C, fixed with cold 4% paraformaldehyde in PBS for 20 min and visualized by confocal microscopy.

Primary cultures of brainstem neurons and surface biotinylation

Brainstems from 16-day-old Wistar rat fetuses were isolated in Hank's Balanced Salt Solution (HBSS) buffer (Invitrogen) and dissociated with trypsin as described previously (71). Surface proteins of primary brainstem neurons (16 DIV) were labeled with the non-permeable sulfo-NHS-SS-biotin reagent (Thermo Fisher Scientific) as described previously (11). The labeled proteins were resolved by SDS–PAGE and visualized by ECL detection and quantified on a GS-710 calibrated imaging densitometer from Bio-Rad with QUANTITY ONE software, using film exposures in the linear range. Standard errors were calculated after densitometry from at least three separate experiments.

Endocytosis of biotinylated proteins

Surface proteins of primary brainstem neurons (16 DIV) were labeled with the non-permeable sulfo-NHS-SS-biotin reagent (Thermo Fisher Scientific) with 2.5 mg/mL sulfo-NHS-SS-biotin. Following biotinylation, one set of cells was washed with PBS and maintained at 4°C to determine the total initial surface GLYT2 and MesNa strip efficiencies. Endocytosis was initiated by washing cells with prewarmed PBS and incubating them for the indicated times at 37°C. After stopping endocytosis, placing plates in an ice bath and washing them with ice-cold PBS, residual biotinylated proteins were stripped with freshly prepared 50 mM MesNa in NT buffer [150 mM NaCl, 1 mM ethylenediaminetetraacetic acid (EDTA), 0.2% bovine serum albumin, 20 mM Tris, pH 8.6] for 30 min at 4°C and then washed twice in ice-cold PBS containing 5 mg/mL iodoacetamide. All the wells were then solubilized in RIPA buffer (50 mM Tris-HCl pH 7.4, 150 mM NaCl, 5 mM EDTA, 1% Triton X-100, 0,25% Sodium Deoxycholate and 0,1% SDS), biotinylated proteins were pulled down with streptavidin-agarose beads and GLYT2 internalization was analyzed in western blots.

Isolation of detergent-resistant membranes

Membrane rafts from primary cultures of brainstem neurons or from transfected MDCKII and COS7 cells were isolated as described previously (13), with minor modifications. In short, washed cells were scraped and lysed in TNE buffer (25 mM Tris–HCl, 5 mM EDTA and 150 mM NaCl, pH 7.4) containing 0.35–0.5% Triton-X-100 and PIs (0.4 mM PMSF + Sigma cocktail). Cells were solubilized by passing them through a 25-gauge needle and then incubated for 30 min at 4°C. Equal volumes of 70% (w/v) sucrose were added and the lysates were mixed thoroughly before the samples (1 mL) in 35% sucrose were overlaid with 2 mL of 30% and then 1 mL of 5% sucrose (in TNE + PI) in a TST 60.4 ultracentrifuge tube (Beckman). After centrifugation at 200000 × ***g*** (TST 60.4 rotor, Beckman) for 16 h at 4°C, two fractions were collected. The first fraction was from the 5–30% discontinuity (insoluble fraction, containing the DRMs) and the second from the bottom of the tube (soluble fraction). The proteins in each fraction were precipitated with 10% ice-cold trichloroacetic acid, subjected to SDS/PAGE (10% gel) and then immunoblotting.

Glycine transport assay

[^{3}H]-Glycine transport in MDCK cells was measured as described previously (12).

Immunofluorescence quantification of plasma membrane GLYT2

To quantify the proportion of GLYT2 fluorescence in the plasma membrane, E-cadherin was used as a membrane marker and two channel confocal images were obtained (green for GLYT2, red for E-cadherin). The regions occupied by E-cadherin were considered plasma membrane and those inside the cadherin staining were considered intracellular, as measured with the Region of Interest (ROI) manager of IMAGEJ software. After applying an automatic threshold to adjust the images, the fluorescence intensity was measured separately for the membrane and intracellular regions, and the percentage of GLYT2 in the plasma membrane was calculated. This process was performed on at least 60 cells per condition, and the p values were calculated with the Student's *t*-test, comparing vehicle treatment with PMA or monensin treatment.

Acknowledgments

This work was supported by the Spanish 'Ministerio de Ciencia e Innovación' (SAF2008-05436), the Comunidad Autónoma de Madrid (S-SAL-0253/2006) and by an institutional grant from the 'Fundación Ramón Areces'. We thank Dr G. Dechant (Max-Planck-Institute of Neurobiology) for the NGFR plasmid, Dr M. A. Alonso (Centro de Biología Molecular 'Severo Ochoa') for the GFP-dynamin 2 (K44A) plasmid and Dr J. E. Pessin (Albert Einstein College of Medicine of Yeshiva University) for the caveolin-1 (S80E)-myc plasmid. We also thank Enrique Núñez for his excellent technical assistance and Clara Cassinello for her excellent graphic design advices.

Supporting Information

Additional Supporting Information may be found in the online version of this article:

Figure S1: GLYT2 reversible biotinylation and monensin treatment of live cells. A) Living primary cultured neurons (15 DIV) were treated with sulfo-NHS-biotin (+biotin) or vehicle (–biotin) for 30 min at 4°C and then incubated for 30 min at 37°C to permit internalization before the performance of glycine transport assay. The data are represented as the mean ± SEM of three triplicate experiments and they are presented as the percentage of control activity (–biotin), which was 1.7 nmol/mg prot/10 min. B) Living primary cultured neurons were surface-biotinylated with sulfo-NHS-SS-biotin, incubated for different times at 37°C, washed and stripped with cell-impermeant MesNa. Biotinylated GLYT2 was isolated with avidin and internalized GLYT2 was quantified following western blot analysis [0: cell surface GLYT2 at time 0 without stripping, C: cell surface GLYT2 at time 0 with stripping (stripping control), 15: endocytosis permitted during 15 min, 30: endocytosis permitted during 30 min]. C) Living primary cultured neurons (16 DIV) were treated with 35 μM monensin at various times (0, 15 and 30 min) and then incubated with sulfo-NHS-SS-biotin for 30 min at 4°C. Biotinylated proteins were

pulled down with streptavidin-agarose beads and GLYT2 internalization was analyzed in western blots, and compared with values obtained in reversible biotinylation assays.

Figure S2: Cell surface GLYT2 biotinylation in caveolin- or clathrin-depleted cells. A) MDCK cells were nucleofected either with a scrambled siRNA or with a caveolin-1 siRNA, and 1 day after nucleofection, the cells were transfected with GLYT2. Two days after transfection (and 3 days after nucleofection), the cells were exposed to the vehicle alone, PMA (1 μM, 30 min) or monensin (35 μM, 30 min). Subsequently, the cell surface proteins were labeled with sulfo-NHS-SS-biotin and the biotinylated proteins were pulled down with streptavidin-agarose beads. GLYT2 expression was analyzed in western blots and calnexin immunodetection was used as a non-biotinylated protein control. B, biotinylated protein (20 μg); T, total protein (10 μg). B) MDCK cells expressing GLYT2 and nucleofected with the caveolin-1 siRNA or a scrambled siRNA were lysed and immunoblotted using calnexin (CNX) as a control for protein loading. C) MDCK cells were nucleofected either with a scrambled (Scr) siRNA or with a CHC siRNA, and a day after nucleofection, the cells were transfected with GLYT2. Two days after transfection (and 3 days after nucleofection), the cells were exposed to the vehicle alone, PMA (1 μM, 30 min) or monensin (35 μM, 30 min). Subsequently, the cell surface proteins were labeled with sulfo-NHS-SS-biotin and the biotinylated proteins were pulled down with streptavidin-agarose beads. GLYT2 expression was analyzed in western blots and calnexin immunodetection was used as a non-biotinylated protein control. B, biotinylated protein (20 μg); T, total protein (10 μg). Note the blockage of transporter internalization in CHC siRNA-nucleofected cells (C), but not in Cav1 siRNA-nucleofected cells (A). D) MDCK cells expressing GLYT2 and nucleofected with the CHC siRNA or a scrambled siRNA were lysed and immunoblotted using tubulin (Tub) as a control for protein loading. E) Densitometric analysis of three independent western blots as in (A) and (C). The values are represented as the percentage of the control values (Veh). Bars represent SEM of triplicates. *, significantly different from control, $p < 0.05$; #, significantly different from scr siRNA PMA-treated samples, $p < 0.05$; ¥, significantly different from scr siRNA monensin-treated samples, $p < 0.05$ by ANOVA with Tukey's *post hoc* test.

Figure S3: Endocytosis of albumin in clathrin-depleted cells. A) MDCK cells were nucleofected either with a scrambled siRNA (1) or with a CHC siRNA (2) as in Figures 5 and S1C, and 3 days after nucleofection, cells were incubated at 4°C for 30 min with albumin Alexa 555, fixed and red fluorescence visualized by confocal microscopy. For internalization, cells incubated at 4°C were further chased for 30 min at 37°C and then fixed and analyzed by confocal microscopy. B) MDCK cells nucleofected with scrambled siRNA (1) or CHC siRNA (2) were lysed and immunoblotted using calnexin (CNX) as a control for protein loading.

Please note: Wiley-Blackwell are not responsible for the content or functionality of any supporting materials supplied by the authors. Any queries (other than missing material) should be directed to the corresponding author for the article.

References

1. Aragon C, Lopez-Corcuera B. Structure, function and regulation of glycine neurotransporters. Eur J Pharmacol 2003;479:249–262.
2. Gomeza J, Hulsmann S, Ohno K, Eulenburg V, Szoke K, Richter D, Betz H. Inactivation of the glycine transporter 1 gene discloses vital role of glial glycine uptake in glycinergic inhibition. Neuron 2003;40:785–796.
3. Gomeza J, Ohno K, Hulsmann S, Armsen W, Eulenburg V, Richter DW, Laube B, Betz H. Deletion of the mouse glycine transporter 2 results in a hyperekplexia phenotype and postnatal lethality. Neuron 2003;40:797–806.
4. Aragon C, Lopez-Corcuera B. Glycine transporters: crucial roles of pharmacological interest revealed by gene deletion. Trends Pharmacol Sci 2005;26:283–286.
5. Rees MI, Harvey K, Pearce BR, Chung SK, Duguid IC, Thomas P, Beatty S, Graham GE, Armstrong L, Shiang R, Abbott KJ, Zuberi SM, Stephenson JB, Owen MJ, Tijssen MA et al. Mutations in the gene encoding GlyT2 (SLC6A5) define a presynaptic component of human startle disease. Nat Genet 2006;38:801–806.
6. Harvey RJ, Topf M, Harvey K, Rees MI. The genetics of hyperekplexia: more than startle! Trends Genet 2008;24:439–447.
7. Blakely RD, Bauman AL. Biogenic amine transporters: regulation in flux. Curr Opin Neurobiol 2000;10:328–336.
8. Geerlings A, Nunez E, Lopez-Corcuera B, Aragon C. Calcium- and syntaxin 1-mediated trafficking of the neuronal glycine transporter GLYT2. J Biol Chem 2001;276:17584–17590.
9. Fornes A, Nunez E, Aragon C, Lopez-Corcuera B. The second intracellular loop of the glycine transporter 2 contains crucial residues for glycine transport and phorbol ester-induced regulation. J Biol Chem 2004;279:22934–22943.
10. Fornes A, Nunez E, Alonso-Torres P, Aragon C, Lopez- Corcuera B. Trafficking properties and activity regulation of the neuronal glycine transporter GLYT2 by protein kinase C. Biochem J 2008;412:495–506.
11. Geerlings A, Nunez E, Rodenstein L, Lopez-Corcuera B, Aragon C. Glycine transporter isoforms show differential subcellular localization in PC12 cells. J Neurochem 2002;82:58–65.
12. Nunez E, Perez-Siles G, Rodenstein L, Alonso-Torres P, Zafra F, Jimenez E, Aragon C, Lopez- Corcuera B. Subcellular localization of the neuronal glycine transporter GLYT2 in brainstem. Traffic 2009;10:829–843.
13. Nunez E, Alonso-Torres P, Fornes A, Aragon C, Lopez-Corcuera B. The neuronal glycine transporter GLYT2 associates with membrane rafts: functional modulation by lipid environment. J Neurochem 2008;105:2080–2090.
14. Pike LJ. Rafts defined: a report on the Keystone Symposium on lipid rafts and cell function. J Lipid Res 2006;47:1597–1598.
15. Butchbach ME, Tian G, Guo H, Lin CL. Association of excitatory amino acid transporters, especially EAAT2, with cholesterol-rich lipid raft microdomains: importance for excitatory amino acid transporter localization and function. J Biol Chem 2004;279:34388–34396.
16. Jayanthi LD, Samuvel DJ, Ramamoorthy S. Regulated internalization and phosphorylation of the native norepinephrine transporter in response to phorbol esters. Evidence for localization in lipid rafts and lipid raft-mediated internalization. J Biol Chem 2004;279:19315–19326.
17. Guirland C, Suzuki S, Kojima M, Lu B, Zheng JQ. Lipid rafts mediate chemotropic guidance of nerve growth cones. Neuron 2004;42:51–62.
18. Ledesma MD, Simons K, Dotti CG. Neuronal polarity: essential role of protein-lipid complexes in axonal sorting. Proc Natl Acad Sci U S A 1998;95:3966–3971.
19. Allen JA, Halverson-Tamboli RA, Rasenick MM. Lipid raft microdomains and neurotransmitter signalling. Nat Rev Neurosci 2007;8:128–140.
20. Bruses JL, Chauvet N, Rutishauser U. Membrane lipid rafts are necessary for the maintenance of the (alpha)7 nicotinic acetylcholine receptor in somatic spines of ciliary neurons. J Neurosci 2001;21:504–512.
21. Hering H, Lin CC, Sheng M. Lipid rafts in the maintenance of synapses, dendritic spines, and surface AMPA receptor stability. J Neurosci 2003;23:3262–3271.
22. Scita G, Di Fiore PP. The endocytic matrix. Nature 2010;463:464–473.
23. Sorkin A. Cargo recognition during clathrin-mediated endocytosis: a team effort. Curr Opin Cell Biol 2004;16:392–399.
24. Mousavi SA, Malerod L, Berg T, Kjeken R. Clathrin-dependent endocytosis. Biochem J 2004;377:1–16.
25. Traub LM. Common principles in clathrin-mediated sorting at the Golgi and the plasma membrane. Biochim Biophys Acta 2005;1744:415–437.
26. Doherty GJ, McMahon HT. Mechanisms of endocytosis. Ann Rev Biochem 2009;78:857–902.
27. Wieffer M, Maritzen T, Haucke V. SnapShot: endocytic trafficking. Cell 2009;137:382.e1–382.e3
28. Kirkham M, Parton RG. Clathrin-independent endocytosis: new insights into caveolae and non-caveolar lipid raft carriers. Biochim Biophys Acta 2005;1746:349–363.
29. Parton RG, Simons K. The multiple faces of caveolae. Nat Rev Mol Cell Biol 2007;8:185–194.
30. Mayor S, Pagano RE. Pathways of clathrin-independent endocytosis. Nat Rev Mol Cell Biol 2007;8:603–612.
31. Glebov OO, Bright NA, Nichols BJ. Flotillin-1 defines a clathrin-independent endocytic pathway in mammalian cells. Nat Cell Biol 2006;8:46–54.

32. Sorkina T, Hoover BR, Zahniser NR, Sorkin A. Constitutive and protein kinase C-induced internalization of the dopamine transporter is mediated by a clathrin-dependent mechanism. Traffic 2005;6:157–170.
33. Miranda M, Wu CC, Sorkina T, Korstjens DR, Sorkin A. Enhanced ubiquitylation and accelerated degradation of the dopamine transporter mediated by protein kinase C. J Biol Chem 2005;280:35617–35624.
34. Sorkina T, Miranda M, Dionne KR, Hoover BR, Zahniser NR, Sorkin A. RNA interference screen reveals an essential role of Nedd4-2 in dopamine transporter ubiquitination and endocytosis. J Neurosci 2006;26:8195–8205.
35. Miranda M, Dionne KR, Sorkina T, Sorkin A. Three ubiquitin conjugation sites in the amino terminus of the dopamine transporter mediate protein kinase C–dependent endocytosis of the transporter. Mol Biol Cell 2007;18:313–323.
36. Gonzalez-Gonzalez I, Garcia-Tardón N, Gimenez C, Zafra F. PKC-dependent endocytosis of the GLT1 glutamate transporter depends on ubiquitylation of lysines located in a C-terminal cluster. GLIA 2008;56:963–974.
37. Fernandez-Sanchez E, Martinez-Villarreal J, Gimenez C, Zafra F. Constitutive and regulated endocytosis of the glycine transporter GLYT1Bb is controlled by ubiquitination. J Biol Chem 2009;284: 19482–19492.
38. Kaiser P, Fon EA. Expanding horizons at Big Sky. Symposium on ubiquitin and signaling. EMBO Rep 2007;8:817–822.
39. Martinez-Maza R, Poyatos I, Lopez-Corcuera B, Núñez E, Gimenez C, Zafra F, Aragon C. The role of N-glycosylation in transport to the plasma membrane and sorting of the neuronal glycine transporter GLYT2. J Biol Chem 2001;276:2168–2173.
40. Dang VC, Williams, JT. Chronic morphine treatment reduces recovery from opioid desensitization. J Neurosci 2004;24:7699–7706.
41. Michaely P, Zhao Z, Li WP, Garuti R, Huang LJ, Hobbs HH, Cohen JC. Identification of a VLDL-induced, FDNPVY independent internalization mechanism for the LDLR. EMBO J 2007;26:3273–3282.
42. Magalhaes AC, Holmes KD, Dale LB, Comps-Agrar L, Lee D, Yadav PN, Drysdale L, Poulter MO, Roth BL, Pin JP, Anisman H, Ferguson SS. CRF receptor 1 regulates anxiety behaviour via sensitization of 5-HT2 receptor signaling. Nat Neurosci 2010;13:622–629.
43. McNiven MA, Cao H, Pitts KR, Yoon Y. The dynamin family of mechanoenzymes: pinching in new places. Trends Biochem Sci 2000;25:115–120.
44. Gagescu R, Demaurex N, Parton RG, Hunziker W, Huber LA, Gruenberg J. The recycling endosome of Madin-Darby canine kidney cells is a mildly acidic compartment rich in raft components. Mol Biol Cell 2000;11:2775–2791.
45. Shigematsu S, Watson RT, Khan AH, Pessin JE. The adipocyte plasma membrane caveolin functional/structural organization is necessary for the efficient endocytosis of GLUT4. J Biol Chem 2003;278:10683–10690.
46. Singh RD, Marks DL, Pagano RE. Using fluorescent sphingolipid analogs to study intracellular lipid trafficking. Curr Protoc Cell Biol 2007;35:24.1.1–24.1.19.
47. Ivanov AI. Pharmacological inhibition of endocytic pathways: is it specific enough to be useful? Methods Mol Biol 2008;440:15–33.
48. Yang Y, Kitagaki J, Dai RM, Tsai YC, Lorick KL, Ludwig RL, Pierre SA, Jensen JP, Davydov IV, Oberoi P, Li CC, Kenten JH, Beutler JA, Vousden KH, Weissman AM. Inhibitors of ubiquitin-activating enzyme (E1), a new class of potential cancer therapeutics. Cancer Res 2007;67:9472–9481.
49. Fujimoro M, Yokosawa H. Production of antipolyubiquitin monoclonal antibodies and their use for characterization and isolation of polyubiquitinated proteins. Methods Enzymol 2005;399:75–86.
50. Masuyama N, Kuronita T, Tanaka R, Muto T, Hirota Y, Takigawa A, Fujita H, Aso Y, Amano J, Tanaka Y. HM1.24 is internalized from lipid rafts by clathrin-mediated endocytosis through interaction with alpha-adaptin. J Biol Chem 2009;284:15927–15941.
51. Fattakhova G, Masilamani M, Borrego F, Gilfillan AM, Metcalfe DD, Coligan JE. The high-affinity immunoglobulin-E receptor (FcepsilonRI) is endocytosed by an AP-2/clathrin-independent, dynamin-dependent mechanism. Traffic 2006;7:673–685.
52. Damke H, Baba T, Warnock DE, Schmid SL. Induction of mutant dynamin specifically blocks endocytic coated vesicle formation. J Cell Biol 1994;127:915–934.
53. Cuitino L, Matute R, Retamal C, Bu G, Inestrosa NC, Marzolo MP. ApoER2 is endocytosed by a clathrin-mediated process involving the adaptor protein Dab2 independent of its Rafts' association. Traffic 2005;6:820–838.
54. Puri C, Tosoni D, Comai R, Rabellino A, Segat D, Caneva F, Luzzi P, Di Fiore PP, Tacchetti C. Relationships between EGFR signaling-competent and endocytosis-competent membrane microdomains. Mol Biol Cell 2005;16:2704–2718.
55. Taylor DR, Watt NT, Perera WS, Hooper NM. Assigning functions to distinct regions of the N-terminus of the prion protein that are involved in its copper-stimulated, clathrin-dependent endocytosis. J Cell Sci 2005;118:5141–5153.
56. Stoddart A, Jackson AP, Brodsky FM. Plasticity of B cell receptor internalization upon conditional depletion of clathrin. Mol Biol Cell 2005;16:2339–2348.
57. Wang H, Traub LM, Weixel KM, Hawryluk MJ, Shah N, Edinger RS, Perry CJ, Kester L, Butterworth MB, Peters KW, Kleyman TR, Frizzell RA, Johnson JP. Clathrin-mediated endocytosis of the epithelial sodium channel. Role of epsin. J Biol Chem 2006;281: 14129–14135.
58. Rollason R, Korolchuk V, Hamilton C, Schu P, Banting G. Clathrin-mediated endocytosis of a lipid-raft-associated protein is mediated through a dual tyrosine motif. J Cell Sci 2007;120:3850–3858.
59. Morris DP, Lei B, Wu YX, Michelotti GA, Schwinn DA. The alpha1a-adrenergic receptor occupies membrane rafts with its G protein effectors but internalizes via clathrin-coated pits. J Biol Chem 2008;283:2973–2985.
60. Sarnataro D, Caputo A, Casanova P, Puri C, Paladino S, Tivodar SS, Campana V, Tacchetti C, Zurzolo C. Lipid rafts and clathrin cooperate in the internalization of PrP in epithelial FRT cells. PloS One 2009;4:e5829.
61. Simons K, Gruenberg J. Jamming the endosomal system: lipid rafts and lysosomal storage diseases. Trends Cell Biol 2000;10:459–462.
62. Kobayashi T, Gu F, Gruenberg J. Lipids, lipid domains and lipid-protein interactions in endocytic membrane traffic. Semin Cell Dev Biol 1998;9:517–526.
63. Takamori S, Holt M, Stenius K, Lemke EA, Gronborg M, Riedel D, Urlaub H, Schenck S, Brugger B, Ringler P, Muller SA, Rammner B, Grater F, Hub JS, De Groot BL et al. Molecular anatomy of a trafficking organelle. Cell 2006;127:831–846.
64. Lang T, Bruns D, Wenzel D, Riedel D, Holroyd P, Thiele C, Jahn R. SNAREs are concentrated in cholesterol-dependent clusters that define docking and fusion sites for exocytosis. EMBO J 2001;20:2202–2213.
65. Fortin DL, Troyer MD, Nakamura K, Kubo S, Anthony MD, Edwards RH. Lipid rafts mediate the synaptic localization of alpha-synuclein. J Neurosci 2004;24:6715–6723.
66. Roper K, Corbeil D, Huttner WB. Retention of prominin in microvilli reveals distinct cholesterol-based lipid micro-domains in the apical plasma membrane. Nat Cell Biol 2000;2:582–592.
67. Simons K, Ikonen E. Functional rafts in cell membranes. Nature 1997;387:569–572.
68. Mineo C, Gill GN, Anderson RG. Regulated migration of epidermal growth factor receptor from caveolae. J Biol Chem 1999;274:30636–30643.
69. Deinhardt K, Berninghausen O, Willison HJ, Hopkins CR, Schiavo G. Tetanus toxin is internalized by a sequential clathrin-dependent mechanism initiated within lipid microdomains and independent of epsin1. J Cell Biol 2006;174:459–471.
70. Zafra F, Aragon C, Olivares L, Danbolt NC, Gimenez C, Storm-Mathisen J. Glycine transporters are differentially expressed among CNS cells. J Neurosci 1995;15:3952–3969.
71. Jimenez E, Zafra F, Perez-Sen R, Delicado EG, Miras-Portugal MT, Aragon C, Lopez-Corcuera B. P2Y purinergic regulation of the glycine neurotransmitter transporters. J Biol Chem 2011;286:10712–10724.
72. Deborde S, Perret E, Gravotta D, Deora A, Salvarezza S, Schreiner R, Rodriguez-Boulan E. Clathrin is a key regulator of basolateral polarity. Nature 2008;452:719–723.
73. Manninen A, Verkade P, Le Lay S, Torkko J, Kasper M, Fullekrug J, Simons K. Caveolin-1 is not essential for biosynthetic apical membrane transport. Mol Cell Biol 2005;25:10087–10096.

Artículo #2

Constitutive endocytosis and turnover of the neuronal glycine transporter GlyT2 is dependent on ubiquitination of a C-terminal lysine cluster.

de Juan-Sanz J, Nunez E, López-Corcuera B, Aragón C (2013). *PLOS ONE*. 7 Feb 2013. doi: 10.1371/journal.pone.0058863

Constitutive endocytosis and turnover of the neuronal glycine transporter GlyT2 is dependent on ubiquitination of a C-terminal lysine cluster

Jaime de JUAN-SANZ*†‡, Enrique NÚÑEZ*†‡,
Beatriz LÓPEZ-CORCUERA*†‡ and Carmen ARAGÓN*†‡[1]

*Centro de Biología Molecular "Severo Ochoa", Universidad Autónoma de Madrid, Consejo Superior de Investigaciones Científicas, Madrid, Spain.
†Centro de Investigación Biomédica en Red de Enfermedades Raras (CIBERER), ISCIII; ‡IdiPAZ-Hospital Universitario La Paz, Madrid, Spain.

[1]Corresponding author: Carmen Aragón, Centro de Biología Molecular "Severo Ochoa", Universidad Autónoma de Madrid, Madrid, Spain.
Telephone: +34-91-1964632; Fax: +34-91-1964420; Email: caragon@cbm.uam.es

ABSTRACT

Inhibitory glycinergic neurotransmission is terminated by sodium and chloride-dependent plasma membrane glycine transporters (GlyTs). The mainly glial glycine transporter GlyT1 is primarily responsible for the completion of inhibitory neurotransmission and the neuronal glycine transporter GlyT2 mediates the reuptake of the neurotransmitter that is used to refill synaptic vesicles in the terminal, a fundamental role in the physiology and pathology of glycinergic neurotransmission. Indeed, inhibitory glycinergic neurotransmission is modulated by the exocytosis and endocytosis of GlyT2. We previously reported that constitutive and Protein Kinase C (PKC)-regulated endocytosis of GlyT2 is mediated by clathrin and that PKC accelerates GlyT2 endocytosis by increasing its ubiquitination. However, the role of ubiquitination in the constitutive endocytosis and turnover of this protein remains unexplored. Here, we show that ubiquitination of a C-terminus four lysine cluster of GlyT2 is required for constitutive endocytosis, sorting into the slow recycling pathway and turnover of the transporter. Ubiquitination negatively modulates the turnover of GlyT2, such that increased ubiquitination driven by PKC activation accelerates transporter degradation rate shortening its half-life while decreased ubiquitination increases transporter stability. Finally, ubiquitination of GlyT2 in neurons is highly responsive to the free pool of ubiquitin, suggesting that the deubiquitinating enzyme (DUB) ubiquitin C-terminal hydrolase-L1 (UCHL1), as the major regulator of neuronal ubiquitin homeostasis, indirectly modulates the turnover of GlyT2. Our results contribute to the elucidation of the mechanisms underlying the dynamic trafficking of this important neuronal protein which has pathological relevance since mutations in the GlyT2 gene (*SLC6A5*) are the second most common cause of human hyperekplexia.

Key words: Trafficking, transport, glycinergic neurotransmission, endocytosis, ubiquitination

INTRODUCTION

Inhibitory glycine neurotransmission is terminated by specific transporters, GlyTs (GlyT1 and GlyT2), which mediate the reuptake of glycine from the synaptic cleft. GlyTs belong to the neurotransmitter:sodium symporter family (SLC6 gene family), which includes transporters for most of the neurotransmitters (serotonin, dopamine, norepinephrine and GABA) in the central nervous system (CNS) [1]. By mediating the synaptic recycling of glycine, the neuronal transporter GlyT2 preserves the quantal glycine content in synaptic vesicles and assists GlyT1 in regulating glycine levels at the synaptic cleft. Gene deletion studies suggest that modification of glycine transporter activity may be beneficial in several human disorders, including neuromotor deficiencies (startle disease, myoclonus), pain and epilepsy [2-4]. Indeed, missense, nonsense, frameshift, and splice site mutations in the gene encoding GlyT2 can induce hyperekplexia in humans and congenital muscular dystonia type 2 (CMD2) in Belgian Blue cattle [5-9]. In addition, a microdeletion in SLC6A5 as cause of startle disease in Irish Wolfhounds has been reported [10].

Protein trafficking plays a fundamental role in the control of neuronal activity and it has been identified as a primary regulatory mechanism for several plasma membrane neurotransmitter transporters, providing a rapid means to modulate their activity [11]. The surface expression of GlyT2 is controlled by a variety of stimuli that influence its trafficking, including PKC and syntaxin 1A [12, 13]. GlyT2 is recycled between the cell surface and the cell interior along constitutive and PKC-regulated trafficking pathways [14], and a large proportion of GlyT2 resides in intracellular endosomal membranes of rat brainstem neurons and heterologous cells under steady-state conditions [15, 16].

Recent findings have demonstrated the importance of ubiquitination in the endocytosis of several membrane proteins, suggesting

that the attached ubiquitin molecule may act as a platform for the recruitment of the clathrin-dependent endocytic machinery [17, 18]. In fact, ubiquitination is the mechanism proposed to mediate PKC-dependent endocytosis of neurotransmitter transporters [19-22]. Accordingly, we recently demonstrated that clathrin-mediated endocytosis is the main mechanism driving constitutive and regulated GlyT2 internalization and the lysine 791 in the C-terminal tail of GlyT2 was proposed to be the major determinant of PKC-induced internalization [23]. However, the role of ubiquitination in the constitutive endocytosis of membrane neurotransporters is less clear. Indeed, the dopamine transporter DAT is constitutively internalized in an ubiquitination-independent manner [24], while the constitutive endocytosis of GlyT1 and the glutamate transporter GLT1 requires the ubiquitination of several lysines. Hence, it appears that the requirement of ubiquitination is not a general condition for constitutive endocytosis of these transporters [19, 25].

In the present study, we investigated the possible role of ubiquitination in the constitutive internalization of neuronal GlyT2 and its sorting to recycling and/or degradation pathways. Our results show that constitutive endocytosis of GlyT2 is dependent on the ubiquitination of the cytoplasmic C-terminal lysine cluster (K751, K773, K787 and K791). The dynamic ubiquitination/deubiquitination process controls GlyT2 turnover through constitutive sorting mainly to the recycling pathway and targeting the transporter primarily to the degradation pathway via PKC-mediated ubiquitination. In neurons, the ubiquitination status of GlyT2 is highly responsive to the free ubiquitin pool, which is mainly controlled by UCHL1 deubiquitinase [26, 27]. Thus, UCHL1 activity may indirectly modulate the turnover of neuronal GlyT2. These findings demonstrate the requirement of ubiquitination in the regulation of neuronal GlyT2, a key protein in the physiology and pathology of glycinergic neurotransmission.

MATERIALS and METHODS

Materials

Male wistar rats were bred under standard conditions at the Centro de Biología Molecular Severo Ochoa. All animal work performed in this study was carried out in accordance with procedures approved in the Directive 86/609/EEC of the European Union with approval of the Ethics Committee of the Universidad Autónoma de Madrid. PYR-41 (4-[4-(5-nitro-furan-2-ylmethylene)-3,5-dioxo-pyrazolidin-1-yl]-benzoic acid ethyl ester), and inhibitors of UCH-L1 [LDN-57444 (LDN)] and ubiquitin C-terminal hydrolase-L3 (UCH-L3) (4, 5, 6, 7-tetrachloroindan-1,3-dione, TCID) were purchased from Calbiochem (San Diego, CA). All other chemicals were purchased from Sigma-Aldrich. Antibodies against GlyT2 (rabbit and rat: [28, 16]), calnexin (Stressgen), syntenin-1 (Abcam), tubulin (Sigma-Aldrich) and syntaxin1A and Ubiquitin (Clone P4D1) (Santa Cruz) were used. Agarose-conjugated anti-multiubiquitin (monoclonal antibody, clone FK2) was purchased from MBL International. Fluorophore-coupled secondary antibodies were acquired from Molecular Probes. Multiple sequence alignment was performed with CLUSTAL 2.1 multiple sequence alignment software, using the rat GlyT2 sequence as the query at www.ebi.ac.uk.

Primary cultures of neurons

The brainstem and spinal cord from 16-day-old Wistar rat fetuses or the hippocampus from 18-day-old Wistar rat fetuses were isolated in Hank's Balanced Salt Solution buffer (Invitrogen), dissociated with trypsin as described previously [29] and grown in culture plates. After 2 days, cytosine arabinoside (2.5 μM) was added to inhibit further glial growth and the primary neurons were studied after 14 days in culture.

Transfection of MDCK cells and hippocampal neurons

Madin–Darby canine kidney II (MDCK II) cells (American Type Culture Collection) were grown at 37ºC and 5% CO_2 in minimal essential medium supplemented with 10% fetal bovine serum. Transient expression was achieved using Lipofectamine™ 2000 (Invitrogen) following the manufacturer's instructions. Reproducible results were obtained with 50-60% confluent cells in a 60 mm dish using 6 μg of total DNA. The cells were incubated for 48 h at 37ºC before the experiment was performed. Hippocampal neurons were obtained as described above. The cells (DIV10) were transfected with Effectene (Qiagen) following manufacturer's instructions using 10μl of Effectene per 1μg of DNA in a 12mm dish.

Generation of mutants

Substitution mutants were generated with the QuikChange Site-Directed Mutagenesis kit (Stratagene), using the rat GlyT2 in pCDNA3 as described previously [29]. The 4KR mutant (GlyT2 mutant in which all the C-terminal lysines are substituted by arginines) was created via four consecutive rounds of Polymerase Chain Reaction (PCR) site-directed mutagenesis, one for each C-terminal lysine-to-arginine mutation. All point mutations were verified by sequencing.

Immunocytochemistry and confocal imaging

MDCK II cells and hippocampal neurons were grown on glass coverslips and transfected with the corresponding expression vectors as indicated above. Immunostaining was performed as described previously [23] and the cells were visualized by confocal microscopy on a Microradiance microscope (BioRad) using a vertical Axioskop 2 microscope (Zeiss), or with a LSM510 META confocal microscope coupled to an inverted AXIOVERT 200 microscope (Zeiss). IMAGEJ (National Institutes of Health) software and LSM image browsers (Carl Zeiss Inc.) were used for image processing.

Anti-multiubiquitin immunoprecipitation

Brainstem and spinal cord primary neurons (100 μg) or MDCK II cells were lysed for 30 min at room temperature (RT) at a concentration of 1 mg of protein/ml in TN buffer (25 mM TrisHCl and 150 mM NaCl, pH 7.4) containing 0.25% Nonidet P-40 (NP-40), 50 mM N-ethylmaleimide and protease inhibitors (PIs: 0.4 mM phenylmethylsulfonyl fluoride [PMSF] + Sigma cocktail). Agarose-conjugated anti-multiubiquitin (12 μl) was added and incubated for 1 h at RT. The beads were collected by mild centrifugation and washed 3 times for 5 minutes with lysis buffer. Finally, the beads were pelleted and the ubiquitinated proteins were eluted in Laemmli buffer at 75°C for 10 min, resolved in sodium dodecyl Sulfate Polyacrylamide Gel electrophoresis (SDS/PAGE) gels (7.5%), detected in Western blots with enhanced chemiluminescence (ECL) and quantified on a GS-710 calibrated imaging densitometer (Bio-Rad).

Cell surface labelling with Sulfo-NHS-SS-biotin

Surface proteins of transfected MDCK II cells or primary brainstem and spinal cord neurons (14 DIV) were washed with 1.0 ml of Phosphate Buffered Saline (PBS) at 4°C and incubated for 40 min at 4ºC with 1 mg/ml of non-permeable sulfo-NHS-SS-biotin reagent (Thermo Fisher Scientific) in PBS. Cells were then washed

3 times with 1 ml of the same solution supplemented with 100 mM lysine and scraped in 50 mM Tris-HCl [pH 7.4], 150 mM NaCl (TN) buffer plus 0.4 mM phenylmethylsulfonylfluoride (PMSF) and protease inhibitor mixture (Sigma). Total proteins were solubilized for 30 min at 4°C in RIPA buffer (150 mM NaCl, 5 mM EDTA, 1% Triton X-100, 1% SDS and 0.25% sodium deoxycholate). Streptavidin-agarose beads (40 µl per sample: Sigma) were added and incubated for 1 h at 4°C with agitation. Bead-bound biotinylated proteins (B) were eluted for 15 min at 70°C with Laemmli buffer (40 mM Tris [pH 6.8], 2% SDS, 10% glycerol, 0.1 mM dithiothreitol and 0.01% bromophenol blue). Total protein (T; 10 µg) and biotinylated protein (B; 30 µg) were run on a 7.5% SDS-polyacrylamide gel and after analyzed by Western blot with specific GlyT2 antibodies, the bands were visualized by ECL and quantified in the linear range on a GS-710 calibrated imaging densitometer (Bio-Rad) with Quantity One software. Calnexin immunoreactivity was used as a non-biotinylated protein control. The standard error of the mean (S.E.M) was calculated after densitometric analysis of at least three separate experiments.

Glycine transport assay

Transport assays in MDCK cells were performed at 37°C in PBS plus 10 mM glucose, containing 2 µCi/ml [^{3}H]-labelled glycine (1.6 TBq/mmol; PerkinElmer) diluted to a final glycine concentration of 10 µM, as described previously [23]. Reactions were terminated after 10 min by aspiration and transport was quantified by subtracting the glycine accumulated in mock-transfected MDCK cells from that of the transporter-transfected cells and normalized to the protein concentration.

Quantification of co-localization and cell surface rates from immunofluorescence microscopy images

To perform the quantification of co-localization, Pearson´s value was analyzed with IMAGEJ software (National Institutes of Health), using at least 30 images for each condition. Images were processed with a 2.0 pixel median filter, and threshold used was automatically determined by JACoP plugin [30]. Pearson´s value was obtained with JACoP by comparing the two thresholded channels and measuring the correlation between them. The value can range from -1 to 1, being 1 the maximal co-localization possible (two identical images), and usually values from 0.5 to 1.0 can be considered as a valid co-localization [31]. The quantification of cell surface GlyT2 was performed as described previously [23].

Data Analysis

All statistical analyses were performed using SPSS 19.0 (SPSS Inc., Chicago, IL) and graphs and curves were generated with Origin 8.0 (OriginLab Corp, MA). One-way analysis of variance (ANOVA) was used to compare multiple groups, with subsequent Tukey's post-hoc test to determine the significant differences between samples. The Student's *t*-test was used to compare two separate groups. p values <0.05 were considered significant.

RESULTS

The constitutive endocytosis of GlyT2 is regulated by ubiquitination of its C-terminal lysines

Ubiquitination is a well-described post-translational modification involved in the PKC-induced endocytosis of various membrane proteins, including dopamine, glutamate and glycine transporters (DAT, GLT1, GlyT1b, GlyT2). However, its role in the constitutive endocytosis of these proteins is less understood. We recently demonstrated a direct relationship between the ubiquitination of lysine 791 in the C-terminus of the neuronal glycine transporter GlyT2 and its PKC-dependent endocytosis. Hence, in the present study we investigated whether the constitutive endocytosis of GlyT2 was also ubiquitin-dependent, initially using the MDCK cell line, a suitable background for our immunofluorescence studies due to the efficient and uniform expression of transfected GlyT2 at the cell surface of these cells, as described previously [23]. To study the constitutive endocytosis of GlyT2 we used the cationophore monensin, an experimental strategy commonly employed to analyze the constitutive endocytosis of membrane proteins. Monensin is an inhibitor of transport via acidic endosomal compartments and thus, interferes with the intracellular trafficking of proteins. Monensin does not prevent endocytosis but rather, by blocking protein recycling to the plasma membrane and likely degradation, it promotes the accumulation of endocytosed membrane proteins [23, 32-34].

We first examined the effect of PYR41, a cell-permeable specific inhibitor of the E1 ubiquitin-activating enzyme that catalyzes an initial and critical step in the protein ubiquitination pathway [35]. As expected, monensin promoted the intracellular accumulation of GlyT2 (Fig. 1A, B) with a concomitant marked decrease in protein levels in the plasma membrane (Fig. 1B, E). When cells were pretreated with PYR-41 (50 µM) and then incubated with monensin (35 µM), a considerable reduction of GlyT2 endocytosis with a substantial amount of the transporter remaining at the cell surface was observed (Fig. 1D, E). Immunoprecipitation experiments provided direct evidence that inhibition of GlyT2 ubiquitination underlies the reduction in GlyT2 endocytosis (Fig. 1F, G). MDCK cells expressing wild-type GlyT2 were maintained in the presence or absence of PYR41 and the ubiquitinated transporter was immunoprecipitated from cell lysates with agarose-conjugated anti-multiubiquitin (clone FK2), an antibody that recognizes poly- and mono-ubiquitinated proteins [36], and samples were then analyzed by Western blot with anti-GlyT2 antibodies. Indeed, the inhibition of E1 ubiquitin-activating enzyme by PYR41 clearly reduced the amount of ubiquitinated GlyT2 (56.97 ± 6.30% SEM, Fig. 1G), indicating a positive correlation between ubiquitination and constitutive GlyT2 internalization.

Lysine clusters in different cytosolic domains have been identified as ubiquitination sites required for endocytosis of GLT1 [20] and DAT [17] neurotransporters. To investigate this phenomenon in GlyT2, we first examined the contribution of each residue (K751, K773, K787 and K791) present in the C-terminus of GlyT2 to its constitutive endocytosis by immunofluorescence confocal microscopy and biotinylation assays. These GlyT2 lysine residues are evolutionarily conserved in most animal species (as evident in sequence alignments: Fig. 2A, in red), suggesting an important role in GlyT2 function. Mutants in which each of the four lysine residues was substituted individually to arginine displayed similar constitutive internalization to that observed for the wild-type protein when assessed by confocal microscopy (Fig. 2B). Likewise, quantitative biotinylation revealed similar levels of remaining transporter at the cell surface in the presence of monensin for each mutant and the wild-type transporter (Fig. 2C, D), suggesting that ubiquitination of the individual K751, K773, K787 and K791 residues contributed weakly to GlyT2 constitutive endocytosis. [^{3}H]-glycine uptake assays depicted in fig. 2E showed

similar transport activity levels for every mutant and wild-type GlyT2. Next, we generated a GlyT2 mutant in which all four C-terminal lysines are simultaneously substituted by arginines (4KR mutant) and the constitutive endocytosis was assayed as above. As immunofluorescence pictures show, in contrast to wild-type GlyT2, the 4KR mutant predominantly remained at the cell surface in the presence of monensin, suggesting a role for the C-terminal lysine cluster in the constitutive internalization of the transporter (Fig. 3A-D). These findings were further supported by quantification of transporter levels at the cell surface by biotinylation (Fig. 3E, F). In addition, immunoprecipitation experiments provided direct evidence that lysine cluster ubiquitination is a critical requirement for the constitutive endocytosis of GlyT2 (Fig. 3G, H). Fig 3G and H shows that 4KR mutant was around 32% less ubiquitinated than the wild-type transporter but it still remained ubiquitinated. Redundancy in ubiquitination sites has been frequently reported [33], such that other lysines are ubiquitinated in the absence of the main conjugation sites. This may account for the residual ubiquitination of the 4KR mutant. Alternatively, other intracellular lysine residues may be ubiquitinated, but in either case its contribution to the constitutive endocytosis does not appear to be functionally relevant. [^{3}H]-glycine uptake assays showed similar transport activity for 4KR mutant and wild-type GlyT2 (Fig. 3I). Together, these results point to C-terminal K751, K773, K787 and K791 of GlyT2 as targets of the ubiquitination required for its constitutive endocytosis.

Neuronal localization of GlyT2 is not impaired by substitution of the C-terminal lysine cluster

Regarding the synaptic localization of the transporter, C-terminus region of GlyT2 has been suggested to be important for synaptic localization of the transporter since modification of its C-terminal type III PDZ domain binding motif reduces co-localization of GlyT2 with different synaptic markers [37]. To test if the C-terminal lysine cluster was also implicated in the neuronal localization of transporter we transfected primary hippocampal neurons with GlyT2 wild-type and 4KR mutant constructs and measured co-localization with syntenin-1, a PDZ domain protein, and syntaxin1A, a Soluble NSF Attachment Protein REceptor (SNARE) complex component (Fig 4) We have selected syntenin-1 and syntaxin1A because they are the only proteins whose interaction with GlyT2 has been described in nervous tissue preparations [38, 13]. In agreement with previous results [37] no GlyT2 immunostaining was detected in non-transfected neurons (data not shown), indicating that the fluorescence was derived from the exogenous constructs of GlyT2. As figure 4 shows, both GlyT2 and 4KR present similar punctate distribution pattern (Fig. 4A-B) and similar levels of co-localization with syntaxin1A and syntenin-1 (Fig. 4C), indicating that the C-terminal lysine cluster appears not to be implicated in the synaptic localization of GlyT2. Together these results suggest that simultaneous substitution of C-terminal K751, K773, K787 and K791 residues does not affect GlyT2 interactions with syntaxin1A and syntenin-1, and therefore neither the proper neuronal localization of GlyT2.

Ubiquitination modulates the intracellular distribution and degradation of GlyT2

To further investigate whether deficient ubiquitination alters the intracellular localization of GlyT2 we co-expressed wild-type or 4KR GlyT2 with different Rab proteins fused to green fluorescent protein in MDCK cells. Small Rab GTPases are well-known organizers of intracellular trafficking of membrane proteins in eukaryotic cells and they serve as markers of distinct endosomal compartments [39]. We previously showed that at steady state, most intracellular GlyT2 resides in a subset of Rab11-positive recycling endosomes in nerve terminals and neurons [16]. Accordingly, double immunofluorescence images revealed that at the steady state also in MDCK cells, intracellular GlyT2 mainly co-localized with Green Fluorescent Protein (EGFP)-Rab11, a marker of slow recycling endosomes. By contrast, we observed a small co-localization with EGFP-Rab7, a marker of late endosomes (Fig. 5A, C, I). The 4KR mutant accumulated on the cell surface and no intracellular vesicles expressing this transporter were detected (Fig. 5E, G). Moreover, the abundant EGFP-Rab11 and GlyT2-positive vesicles observed after 30 min of monensin treatment, suggest that GlyT2 is constitutively mainly sorted to the slow recycling pathway (Fig. 5D, I). In accordance with the reduced endocytosis of the 4KR mutant, only a few vesicles were observed containing both the 4KR transporter and EGFP-Rab11 (Fig. 5H, I).

In recent years, the importance of ubiquitination in controlling endocytosis and degradation of plasma membrane proteins has been established. Thus, we investigated whether ubiquitination affects the stability of GlyT2. We compared the degradation rate of wild-type GlyT2 and the ubiquitin-deficient 4KR mutant in untreated and PMA-treated cells in the presence of cycloheximide, a blocker of protein synthesis (Fig. 6). As we recently reported that PKC-dependent GlyT2 endocytosis is mediated by increased GlyT2 ubiquitination [23], PMA was used to establish the opposite scenario to that seen in the ubiquitin-deficient 4KR mutant. Quantification of Western blots revealed that the wild type protein decreased rapidly after 2 hours, with only 54.44 ± 9.72% of initial protein remaining after 6 h. By contrast, the 4KR mutant protein was more stable and persisted longer in these cells. Exposure to Phorbol 12-Myristate 13-Acetate (PMA) markedly accelerated the degradation of GlyT2 and after 6 h, protein levels had fallen by 73.56 ± 6.39% of initial amount (Fig. 6A, B). Increased degradation by PMA has been previously observed for DAT which is completely degraded within 2 h of PKC activation [40]. In accordance with the absence of the major target of PKC-induced ubiquitination (lysine 791, [23]), the 4KR mutant was stable through 2 h of PMA treatment. After longer PMA exposure time a small degradation was observed (Fig. 6A, B), probably as result of ubiquitination of other intracellular lysine residues when K791 is absent, as indicated above (see comments to Fig. 3G, H). Indeed, immunofluorescence assays showed a significant increase in GlyT2 and EGFP-Rab7 colocalization after PMA treatment (Fig 6F, G) further supporting that acceleration of GlyT2 endocytosis by PKC-mediated ubiquitination directs the transporter mainly to degradation pathway.

In conclusion, our data demonstrate that in MDCK cells GlyT2 primarily resides at steady state and after constitutive endocytosis in slow recycling pathway endosomes. Ubiquitination modulates the GlyT2 turnover, in such that enhanced ubiquitination increases the transporter degradation shortening its half-life, while decreased ubiquitination promotes its stability.

The ubiquitination status of GlyT2 in neurons is highly responsive to the free ubiquitin pool

The intracellular location of GlyT2 in recycling endosomes implies that a mechanism of deubiquitination exists that permits GlyT2 to return to the cell surface. Like many other post-translational

modifications, ubiquitination is reversible and deubiquitination is accomplished by deubiquitinating enzymes (DUBs). DUBs are fundamental in the regulation of protein ubiquitination, they influence in crucial functions in the nervous system and its dysfunction is involved in some neurodegenerative diseases [26, 27, 41]. The availability of ubiquitin to target proteins towards different cellular pathways is essential to maintain the homeostasis and activity of the nervous system. Indeed, ubiquitin carboxyl-terminal hydrolases, UCHL1 and UCHL3, are abundantly expressed in the CNS, where they play important roles in the generation and modulation of free monomeric ubiquitin [26, 27, 41, 42]. Given the specific expression of GlyT2 in neurons, we used primary cultures of brainstem neurons to study the effect of inhibiting UCHL1 and UCHL3 on the ubiquitination and constitutive endocytosis of endogenous GlyT2.

Specific inhibition of UCHL1 with LDN-57444 and of UCHL3 with TCID diminished GlyT2 ubiquitination, which was more pronounced when UCHL1 was inhibited and when cells were exposed to these inhibitors for longer periods (Fig. 7A, B). The relevant control exerted by these DUBs on ubiquitin homeostasis may account for these effects since pharmacological blocking of UCHL1 or UCHL3 reduced the monomeric ubiquitin pool, in turn restricting the ubiquitination of GlyT2 in neurons (Fig. 7C). When we investigated the effect of UCH-L1 inhibition on the constitutive endocytosis of GlyT2, the decrease in biotinylated GlyT2 induced by monensin was notably attenuated after exposure to the UCHL1 inhibitor for 2 h (Fig 8A, B), an effect that was paralleled by a significant reduction in ubiquitination of the transporter (Fig 8C, D). Together, these data indicate a strict dependence of constitutive endocytosis on ubiquitination of GlyT2 in neurons, supporting our findings in MDCK cells. Furthermore, these results suggest that although GlyT2 seems not to be directly deubiquitinated by UCHL1 and UCHL3, both DUBs indirectly modulate the dynamics of GlyT2 ubiquitination/deubiquitination, by controlling monomeric ubiquitin homeostasis in neurons.

DISCUSSION

We previously demonstrated that GlyT2 is recycled between the cell surface and cell interior via constitutive and PKC-regulated clathrin-dependent endocytosis, resulting in the localization of a large proportion of the transporter in a subset of Rab11-positive endosomes in CNS nerve terminals under steady-state conditions [14, 16]. The C-terminal tail of other SLC6 family members is known to play a critical role in transporter trafficking, stability and degradation [19, 20, 22, 25, 43] and, in agreement with that, we have described an increase in the ubiquitination of GlyT2 in lysine 791 in the C-terminal tail as the major determinant of PKC-induced GlyT2 endocytosis [23]. Ubiquitination of neuronal membrane proteins controls their internalization and endocytic sorting to recycling and/or degradation pathways, and is thus an important mechanism for neuronal development and function [44]. Whereas ubiquitination is proposed as the mechanism for PKC-dependent endocytosis of several neurotransmitter transporters [17, 19, 20] its role in constitutive endocytosis appears to be specific for each transporter [19, 24, 25].

In the present study, we sought to elucidate the putative role of ubiquitination in the constitutive internalization and sorting to recycling and/or degradation pathways of neuronal GlyT2. Our results demonstrate that constitutive GlyT2 endocytosis is dependent on ubiquitination, as indicated by the decreased ubiquitination and concomitant accumulation of GlyT2 at the cell surface following inhibition of E1 ubiquitin-activating enzyme. This enzyme is the first component of the multi-step enzymatic process (E1s, E2s and E3s) that mediates the transfer of ubiquitin to lysine residues on target proteins. Indeed, substituting the C-terminal cluster of lysine residues significantly inhibited GlyT2 internalization, pointing to the K751, K773, K787 and K791 residues as major targets of ubiquitination in constitutive GlyT2 endocytosis. Similarly, ubiquitination of cytosolic lysine clusters has been implicated in the constitutive endocytosis of the glutamate neurotransporter (GLT1) [25]. The partial decrease of 4KR mutant ubiquitination suggests a basal level of ubiquitination of GlyT2, or alternatively, redundant ubiquitination of other lysines when the main conjugation sites are removed [33]. In this regard, GlyT2 sequence contains additional potential sites for ubiquitination such as six lysine residues of its long intracellular N-terminal domain, unique structural characteristic that distinguishes GlyT2 of other members of the neurotransmitter:sodium symporter family (SLC6 gene family). Further site-mutagenesis studies will be necessary to discern between these possibilities.

Moreover, the mutation of the C-terminal lysine cluster does not alter the neuronal localization of GlyT2 as indicated by the similar co-localization levels between 4KR mutant and GlyT2 wild type with the PDZ protein syntenin-1 and the SNARE protein component syntaxin1A in hippocampal neurons. Both proteins interact with GlyT2 and have been involved in the regulation of its presynaptic localization and trafficking [37, 38, 13].

In addition to promoting internalization, ubiquitination of neuronal membrane proteins can also dynamically control the post-endocytic sorting to the recycling or lysosomal degradation pathways [44]. Members of the small GTPase Rab family are known organizers of intracellular membrane protein trafficking in eukaryotic cells [39]. Our immunofluorescence studies reveal that most GlyT2 is targeted to the recycling pathway after constitutive endocytosis, reflected in the high level of co-localization of GlyT2 and Rab11, a protein that modulates slow recycling of proteins to the plasma membrane via the pericentriolar recycling compartment (or 'long loop': [45]). The low co-localization of GlyT2 with the late endosomal marker Rab7 after 30 min of endocytosis indicates that a small proportion of GlyT2 is targeted to the lysosomal degradation pathway. These data support our previous findings regarding the steady state localization of GlyT2 in nervous tissue [16], and demonstrate that GlyT2 undergoes continuous and efficient turnover between the plasma membrane and the intracellular compartment. The requirement of ubiquitination for constitutive GlyT2 endocytosis and the subsequent sorting demonstrated here contrasts with the pattern described for the related dopamine transporter DAT. Constitutive DAT endocytosis has been previously studied [43] and recent data have demonstrated that DAT sorting to degradation and recycling pathways occurs independently of N-terminal lysine ubiquitination [24], suggesting distinct outcomes following the ubiquitination of different membrane proteins. In addition, the analyses of the degradation rate indicated that ubiquitination negatively modulates GlyT2 turnover, as witnessed by the correlation between ubiquitination status and GlyT2 stability. Increased PKC-mediated ubiquitination therefore directs GlyT2 mainly to the degradation pathway leading to an efficient down-regulation of the protein, whereas reduced C-terminal lysine ubiquitination increases its stability.

The availability of ubiquitin to target proteins in distinct cellular pathways is essential for nervous system function and DUBs contribute to ubiquitin homeostasis by recycling ubiquitin from lysosomal and proteasomal substrates. The human genome encodes nearly 95 DUBs [46], although their specific substrates and physiological roles are still poorly understood [27]. Presynaptic ubiquitin pools are particularly sensitive to variations in ubiquitin availability to be away from the site of synthesis [47]. UCHL1 is abundantly expressed in neurons and is one of the main mediators of ubiquitin homeostasis, accounting for 60% of hippocampal deubiquitination [26, 48]. The significant reduction in neuronal monomeric ubiquitin levels following pharmacological blockade of UCHL1 and UCHL3 observed in our assays and also described by other authors [26] may account for the significant decrease in GlyT2 ubiquitination described here. However, we cannot rule out the possibility that ubiquitin depletion by UCHL1 inhibition results in the up-regulation of DUBs acting on GlyT2. Compensatory mechanisms have been described in every UCH-L1 and Usp14-deficient mice where the lowered ubiquitin pool by the suppression of either DUB induced an increase in mRNA and protein levels of each other [49]. However, the rapid reduction in GlyT2 ubiquitination observed only 1 hour after of pharmacological UCHL1 blockade is not consistent with this genetic mechanism. Thus, our findings suggest that constitutive internalization of GlyT2 in neurons depends on ubiquitination, and that its ubiquitination status is highly sensitive to ubiquitin homeostasis.

It should be noted that ubiquitination is an important regulatory mechanism for inhibitory synaptic neurotransmission through control of the trafficking and turnover of glycine and GABA receptors [50-52]. In this regard, the modulation of GlyT2 turnover by ubiquitination described here (through endocytosis, recycling and degradation) contributes to our understanding of how inhibitory neurotransmission is regulated. As GlyT2 supplies glycine to refill synaptic vesicles in inhibitory nerve terminals, the regulation of dynamic and active GlyT2 cellular trafficking is critical for inhibitory glycinergic neurotransmission. This is evident through the disruption in transporter membrane trafficking associated with certain GlyT2 gene *(SLC6A5)* mutations associated with hyperekplexia [5, 9]. Modulation of the recruitable GlyT2 internal pool facilitates rapid and efficient neuronal adaptation to changes in synaptic neurotransmitter concentrations. Thus, GlyT2 modulation through ubiquitination increases our knowledge in the processes that control glycinergic inhibitory neurotransmission. A better understanding of the molecular mechanisms that underlie functional processes is a requirement for a more specific and precise future clinical intervention strategies in glycinergic neuromotor disorders including hyperekplexia and myoclonus, or other dysfunctions as neuropathic pain or epilepsy.

ACKNOWLEDGEMENTS

We thank Dr. Jose A. Esteban (Centro de Biología Molecular Severo Ochoa) for the EGFP-Rab7 and EGFP-Rab11 plasmids and Dr. Francisco Zafra for his valuable suggestions.

REFERENCES

1. Aragón C, Lopez-Corcuera B (2003) Structure,function and regulation of glycine neurotransporters. Eur J Pharmacol 479: 249-262.
2. Aragón C, López-Corcuera B (2005) Glycine transporters: crucial roles of pharmacological interest revealed by gene deletion. Trends Pharmacol Sci 26: 283-286.
3. Gomeza J, Hulsmann S, Ohno K, Eulenburg V, Szoke K, et al. (2003) Inactivation of the glycine transporter 1 gene discloses vital role of glial glycine uptake in glycinergic inhibition. Neuron 40: 785-796.
4. Gomeza J, Ohno K, Hulsmann S, Armsen W, Eulenburg V, et al. (2003) Deletion of the mouse glycine transporter 2 results in a hyperekplexia phenotype and postnatal lethality. Neuron 40: 797-806.
5. Rees MI, Harvey K, Pearce BR, Chung SK, Duguid IC, et al. (2006) Mutations in the gene encoding GlyT2 (SLC6A5) define a presynaptic component of human startle disease. Nat Genet 38: 801-806.
6. Harvey RJ, Topf M, Harvey K, Rees MI (2008) The genetics of hyperekplexia: more than startle!. Trends Genet 24: 439-47.
7. Harvey RJ, Carta E, Pearce BR, Chung SK, Supplisson S, et al. (2008) A critical role for glycine transporters in hyperexcitability disorders. Front Mol Neurosci 1:1.
8. Carta E, Chung SK, James VM, Robinson A, Gill JL, et al. (2012) Mutations in the GlyT2 gene (SLC6A5) are a second major cause of startle disease. J Biol Chem 287: 28975-85.
9. Gimenez C, Perez-Siles G, Martinez-Villarreal J, Arribas-Gonzalez E, Jimenez E, et al. (2012) A novel dominant hyperekplexia mutation Y705C alters trafficking and biochemical properties of the presynaptic glycine transporter GlyT2. J Biol Chem 287: 28986-29002.
10. Gill JL, Capper D, Vanbellinghen JF, Chung SK, Higgins RJ, et al. (2011) Startle disease in Irish wolfhounds associated with a microdeletion in the glycine transporter GlyT2 gene. Neurobiol Dis 43, 184-189.
11. Blakely RD, Bauman, AL (2010) Biogenic amine transporters: regulation in flux. Curr Opin Neurobiol 10: 328-336.
12. Fornes A, Nunez E, Aragon C, Lopez-Corcuera B (2004) The second intracellular loop of the glycine transporter 2 contains crucial residues for glycine transport and phorbol ester-induced regulation. J Biol Chem 279: 22934-22943.
13. Geerlings A, Nunez E, Lopez-Corcuera B, Aragon C (2001) Calcium- and syntaxin1A- mediated trafficking of the neuronal glycine transporter GlyT2. J Biol Chem 276: 17584-17590.
14. Fornes A, Nunez E, Alonso-Torres P, Aragon C, Lopez-Corcuera B (2008) Trafficking properties and activity regulation of the neuronal glycine transporter GlyT2 by protein kinase C. Biochem J 412: 495-506.
15. Geerlings A, Nunez E, Rodenstein L, Lopez-Corcuera B, Aragon C (2002) Glycine transporter isoforms show differential subcellular localization in PC12 cells. J Neurochem 82: 58-65.
16. Nunez E, Perez-Siles G, Rodenstein L, Alonso-Torres P, Zafra F (2009) Subcellular localization of the neuronal glycine transporter GlyT2 in brainstem. Traffic 10: 829-843.
17. Miranda M, Dionne KR, Sorkina T, Sorkin A (2007) Three ubiquitin conjugation sites in the amino terminus of the dopamine transporter mediate protein kinase C-dependent endocytosis of the transporter. Mol Biol Cell 18: 313–323.
18. Traub LM, Lukacs GL (2007) Decoding ubiquitin sorting signals for clathrin-dependent endocytosis by CLASPs. J Cell Sci 120: 543–553.
19. Fernandez-Sanchez E, Martinez-Villarreal J, Gimenez C, Zafra F (2009) Constitutive and regulated endocytosis of the glycine transporter GlyT1Bb is controlled by ubiquitination. J Biol Chem 284: 19482-19492.
20. Gonzalez-Gonzalez IM, Garcia-Tardón N, Gimenez C, Zafra F (2008) PKC-Dependent Endocytosis of the GLT1 Glutamate Transporter Depends on Ubiquitylation of Lysines Located in a C-Termi-

nal Cluster. Glia 56: 963–974.
21. Miranda M, Wu CC, Sorkina T, Korstjens DR, Sorkin A (2005) Enhanced Ubiquitylation and Accelerated Degradation of the Dopamine Transporter Mediated by Protein Kinase C. J Biol Chem 280: 35617–35624.
22. Sorkina T, Miranda M, Dionne KR, Hoover BR, Zahniser NR, et al. (2006) RNA interference screen reveals an essential role of Nedd4-2 in dopamine transporter ubiquitination and endocytosis. J Neurosci 26: 8195-205.
23. de Juan-Sanz J, Zafra F, López-Corcuera B, Aragón C (2011) Endocytosis of the neuronal glycine transporter GlyT2: role of membrane rafts and protein kinase C-dependent ubiquitination. Traffic 12: 1850–1867.
24. Eriksen J, Bjørn-Yoshimoto WE, Jørgensen TN, Newman AH, Gether U (2010) Postendocytic sorting of constitutively internalized dopamine transporter in cell lines and dopaminergic neurons. J Biol Chem 285: 27289–27301.
25. Martínez-Villarreal J, García-Tardón N, Ibáñez I, Giménez C, Zafra F (2012) Cell Surface Turnover of the Glutamate Transporter GLT-1 Is Mediated by Ubiquitination/Deubiquitination. Glia doi: 10.1002/glia.22354.
26. Cartier AE, Djakovic SN, Salehi A, Wilson SM, Masliah E, et al. (2009) Regulation of Synaptic Structure by Ubiquitin C-Terminal Hydrolase L1. J Neurosci 29: 297857–297868.
27. Todi SV, Paulson HL (2009) Balancing act: deubiquitinating enzymes in the nervous system. Trends Neurosci 34: 370–382.
28. Zafra F, Aragon C, Olivares L, Danbolt NC, Gimenez C, et al. (1995) Glycine transporters are differentially expressed among CNS cells. J Neurosci 15: 3952–3969.
29. Jimenez E, Zafra F, Perez-Sen R, Delicado EG, Miras-Portugal MT, et al. (2011) P2Y purinergic regulation of the glycine neurotransmitter transporters. J Biol Chem 286: 10712–1072427.
30. Bolte S, Cordelières FP (2006) A guided tour into subcellular colocalization analysis in light microscopy. J Microsc 224: 213-32.
31. Zinchuk V, and Zinchuk O (2008) Quantitative colocalization analysis of confocal fluorescence micro scopy images. Curr Protoc Cell Biol. Chapter 4, Unit 4.19.
32. Magalhaes AC, Holmes KD, Dale LB, Comps-Agrar L, Lee D, et al. (2010) CRF receptor 1 regulates anxiety behaviour via sensitization of 5 HT2 receptor signaling. Nat Neurosci 13: 622-629.
33. Miranda M, Sorkin A (2007) Regulation of receptors and transporters by ubiquitination: new insights into surprisingly similar mechanisms. Mol Interv 7: 157-67.
34. Michaely P, Zhao Z, Li WP, Garuti R, Huang LJ, et al. (2007) Identification of a VLDL induced FDNPVY independent internalization mechanism for the LDLR. EMBO J 26: 3273–3282.
35. Yang Y, Kitagaki J, Dai RM, Tsai YC, Lorick KL, et al. (2007) Inhibitors of ubiquitin-activating enzyme (E1), a new class of potential cancer therapeutics. Cancer Res 67: 9472–9481.
36. Fujimoro M, Yokosawa H (2005) Production of antipolyubiquitin monoclonal antibodies and their use for characterization and isolation of polyubiquitinated proteins. Methods Enzymol 399: 75-86.
37. Armsen W, Himmel B, Betz H, Eulenburg V (2007) The C-terminal PDZ-ligand motif of the neuronal glycine transporter GlyT2 is required for efficient synaptic localization. Mol Cell Neurosci 36: 369-380.
38. Ohno K, Koroll M, El Far O, Scholze P, Gomeza J, et al. (2004) The neuronal glycine transporter 2 interacts with the PDZ domain protein syntenin-1. Mol Cell Neurosci. 26: 518-529.
39. Zerial M, McBride H (2001) Rab proteins as membrane organizers. Nat Rev Mol Cell Biol 2: 107–117. 40. Daniels GM, Amara SG (1999). Regulated trafficking of the human dopamine transporter. Clathrin mediated internalization and lysosomal degradation in response to phorbol esters. J Biol Chem 274: 35794-801.
41. Kurihara LJ, Kikuchi T, Wada K, Tilghman SM (2001) Loss of Uch-L1 and Uch-L3 leads to neurodegeneration, posterior paralysis and dysphagia. Hum Mol Genet 10: 1963-1970.
42. Osaka H, Wang YL, Takada K, Takizawa S, Setsuie R, et al. (2003) Ubiquitin carboxy-terminal hydrolase L1 binds to and stabilizes monoubiquitin in neuron. Hum Mol Genet 12: 1945-1958.
43. Boudanova E, Navaroli DM, Stevens Z, Melikian HE (2008) Dopamine transporter endocytic determinants: carboxy terminal residues critical for basal and PKC-stimulated internalization. Mol Cell Neurosci 39: 211-217.
44. Schwarz LA, Patrick GN (2012) Ubiquitin-dependent endocytosis, trafficking and turnover of neuronal membrane proteins. Mol Cell Neurosci 49: 387-393.
45. Jones MC, Caswell PT, Norman JC (2006) Endocytic recycling pathways: emerging regulators of cell migration. Curr Opin Cell Biol 18: 549–557.
46. Nijman SM, Luna-Vargas MP, Velds A, Brummelkamp TR, Dirac AM M, et al. (2005) A genomic and functional inventory of deubiquitinating enzymes. Cell 123: 773–786.
47. Chen PC, Bhattacharyya BJ, Hanna J, Minkel H, Wilson JA, et al. (2011) Ubiquitin Homeostasis Is Critical for Synaptic Development and Function. J Neurosci 31: 17505–17513.
48. Gong B, Cao Z, Zheng P, Vitolo OV, Liu S, et al. (2006) Ubiquitin hydrolase Uch-L1 rescues beta-amyloid induced decreases in synaptic function and contextual memory. Cell 126: 775–788.
49. Walters BJ, Campbell SL, Chen PC, Taylor AP, Schroeder DG, et al. (2008) Differential effects of Usp14 and Uch-L1 on the ubiquitin proteasome system and synaptic activity. Mol Cell Neurosci 39: 539-548.
50. Arancibia-Cárcamo IL, Yuen EY, Muir J, Lumb, MJ, Michels G, et al. (2009) Ubiquitin-dependent lysosomal targeting of GABA(A) receptors regulates neuronal inhibition. Proc Natl Acad Sci USA 573: 17552–17557.
51. Büttner C, Sadtler S, Leyendecker A, Laube B, Griffon N, et al. (2001) Ubiquitination precedes internalization and proteolytic cleavage of plasma membrane-bound glycine receptors. J Biol Chem 276**:** 42978-42985.
52. Saliba RS, Michels G, Jacob TC, Pangalos MN, Moss SJ (2007) Activity-dependent ubiquitination of GABA(A) receptors regulates their accumulation at synaptic sites. J Neurosci 27 (48): 13341–13351.

LEGEND TO FIGURES

Figure 1: Pharmacological inhibition of the E1 ubiquitin-activating enzyme activity reduces constitutive GlyT2 endocytosis. A-D) MDCK cells were transfected to express wild-type GlyT2, and were preincubated for 2 h with vehicle (A, B) or PYR-41 (50 μM) (C,D). Then were incubated for 30 min with vehicle (A, C) or monensin (35 μM) (B, D) maintaining the previous pretreatment. The cells were then fixed with 4% paraformaldehyde, immunostained to visualize GlyT2 and analyzed by confocal microscopy. Scale bar = 15 μm. Note the reduction in constitutively endocytosed GlyT2 in the presence of monensin and PYR-41 (D). E) Quantification of GlyT2 fluorescence intensity at the cell surface was performed as described in Materials and Methods. The histogram represents the mean ± SEM (n = 4; on average, 30 cells per condition were analyzed in each experiment). **, significantly different, $p < 0.01$ by

ANOVA with Tukey's post hoc test. n.s., not statistically significant. F) MDCK cells expressing wild-type GlyT2 were incubated with PYR-41 or the vehicle alone, as described above, the cells were lysed and the ubiquitinated transporters were immunoprecipitated with agarose-conjugated anti-multiubiquitin antibody. The immunoprecipitates were probed with an anti-GlyT2 antibody. Ub, anti-multiubiquitin immunoprecipitation (75 µg); T, total protein (10 µg). G) Quantification of three experiments performed as described in (F). Bars represent the mean ± SEM levels of PYR-41-treated ubiquitinated transporter relative to those of ubiquitinated transporter in control cells exposed to the vehicle alone. *, significant difference relative to controls; $p < 0.05$ (Student's t-test).

Figure 2: Mutation of each lysine of the GlyT2 C-terminal does not impair GlyT2 constitutive endocytosis.

A) Multiple sequence alignment of rat GlyT2 C-terminus region (740-799) from different species was obtained with the CLUSTAL 2.1 multiple sequence alignment method. Identical conserved lysines from different species are shown in red. B-C) MDCK cells expressing wild-type GlyT2 or one of four different point mutants (K751R, K773R, K787R or K791R) were exposed for 30 min to monensin (35 µM) at 37ºC or the vehicle alone, fixed with 4% paraformaldehyde, immunostained to visualize GlyT2 and analyzed by confocal microscopy. To simplify the figure, only the wild-type GlyT2 control (Veh) is displayed (all other controls were comparable). Scale bar = 15 µm. C) Representative immunoblot of MDCK cells expressing wild-type GlyT2 or the indicated mutants. Cells were treated with monensin or the vehicle alone, as described above. The cell surface proteins were labeled with sulfo-NHS-SS-biotin and biotinylated proteins were pulled down with streptavidin-agarose beads. GlyT2 expression was analyzed in Western blots and calnexin immunodetection was used as a non-biotinylated protein control. B, biotinylated protein (30 µg); T, total protein (10 µg). D) Densitometric analysis of three independent Western blots as shown in (C), relative to the control values (Veh). E) [^{3}H]-Glycine uptake during 10 minutes was measured in MDCK cells expressing wild-type GlyT2 or the mutants indicated and transport activity is denoted in nmol of glycine/mg of protein. The data represent the means ± SEM and no significant differences respect to vehicle were observed performing ANOVA analysis (with Tukey's post-hoc test).

Figure 3: The 4KR GlyT2 mutant exhibits impaired endocytosis and lower basal ubiquitination than wild-type GlyT2.

A-D) MDCK cells were transfected with wild-type GlyT2 or with 4KR mutant cDNAs (GlyT2 with lysines in positions 751, 773, 787 and 791 mutated to arginines). After 48 h the cells were exposed for 30 min to monensin (35 µM) at 37ºC or the vehicle alone, fixed with 4% paraformaldehyde, immunostained to visualize GlyT2 and analyzed by confocal microscopy. Scale bar = 15 µm. Note that endocytosis of the 4KR mutant is blocked in the presence of monensin (D). E) Representative immunoblot of MDCK cells expressing wild-type GlyT2 or the 4KR mutant. Cells were treated for 30 min with the vehicle alone or with monensin (35 µM) at 37ºC. Cell surface proteins were labeled with sulfo-NHS-SS-biotin and the biotinylated proteins were pulled down with streptavidin-agarose beads. GlyT2 expression was analyzed in Western blots and calnexin immunodetection was used as a non-biotinylated protein control. B, biotinylated protein (30 µg); T, total protein (10 µg). F) Densitometric analysis of four independent Western blots as in (E) relative to the control values (veh). Data represent means ± SEM. **, significant difference with respect to control, $p < 0.01$ (ANOVA with Tukey's post-hoc test). Note that constitutive endocytosis of the 4KR mutant is blocked in the presence of monensin. G) MDCK cells expressing wild-type GlyT2 or the 4KR mutant were lysed, ubiquitinated proteins were immunoprecipitated with agarose-conjugated anti-multiubiquitin antibodies, and GlyT2 was analyzed in Western blots. Ub, anti-multiubiquitin immunoprecipitation (50 µg); T, total protein (10 µg). H) Quantification of four experiments performed as described in (G). Bars represent the mean ± SEM of the amount of 4KR mutant ubiquitinated transporter relative to the amount of wild-type ubiquitinated transporter. *, significant difference with respect to control, $p < 0.05$ (Student's t-test). I) [^{3}H]-Glycine uptake during 10 minutes was measured in MDCK cells expressing wild-type GlyT2 or the 4KR mutant and transport activity is denoted in nmol of glycine/mg of protein. The data represent the means ± SEM and no significant differences respect to vehicle were observed performing student's t-test.

Figure 4: Mutation of the C-terminal lysine cluster of GlyT2 does not impair its neuronal localization in transfected hippocampal neurons.

A-C) Hippocampal neurons were transfected with wild type GlyT2 or with the 4KR mutant at 10 DIV. Three days after transfection, the cultures were fixed in pre-cooled 100% methanol at -20 ºC and stained for GlyT2 (green), syntaxin1A (red) and syntenin-1 (blue) specific antibodies. General scale bar, 40 **µm**. Scale bar in detailed images, 5 **µm**. C) Quantification of co-localization between syntaxin1A and GlyT2, or between syntenin-1 and GlyT2, was performed using Pearson´s value of correlation as described in Materials and Methods. Note there is no significant difference in the neuronal localization between GlyT2 and 4KR mutant, by Student's T-test. The histogram represents the mean ± SEM (n = 3; on average, 30 images per condition were analyzed in each experiment).

Figure 5: Endocytosed GlyT2 co-localizes with GFP-Rab11, whereas the 4KR mutant fails to internalize and accumulates in the surface.

A-H) MDCK cells were transfected with wild-type GlyT2 and GFP-Rab7 (A, B) or GFP-Rab11 (C, D), or with the 4KR mutant and GFP-Rab7 (E, F) or GFP-Rab11 (G, H). After 48 h the cells were incubated for 30 min with monensin (35 µM) or the vehicle alone and fixed with 4% paraformaldehyde. GFP-Rab7 and GFP-Rab11 were visualized by GFP fluorescence (green), whereas GlyT2 was detected with the anti-GlyT2 antibody (shown in red). Note the increase in intracellular vesicles in monensin-treated cells expressing wild-type GlyT2 (B,D), which colocalizes with GFP-Rab11 (D) but not GFP-Rab7 (B). This increase was not observed in cells expressing the 4KR mutant transporter (F, H). Scale bar = 15 µm. I) Quantification of colocalization using Pearson´s value was performed as described in Materials and Methods. Note the increase of colocalization between Rab11 and wild type GlyT2 in the presence of monensin, which cannot be observed with 4KR mutant. The histogram represents the mean ± SEM (n = 3; on average, 30 images per condition were analyzed in each experiment). **, significantly different, $p < 0.01$ by ANOVA with Tukey's post hoc test.

Figure 6: Reduction of GlyT2 C-terminal ubiquitination increases its constitutive stability and attenuates PMA-induced degradation.

A) Representative immunoblot of MDCK cells expressing wild-type GlyT2 or the 4KR mutant. Cells were treated with cyclo-

heximide (CHX: 10 µg/ml) or CHX plus PMA (1 µM) for the times indicated. The cells were then harvested, lysed and whole cell lysates (20 µg/lane) were resolved by SDS-PAGE and analyzed by immunoblotting with the anti-GlyT2 antibody. As a loading control, blots were reprobed with anti-tubulin. B) Degradation curves were generated by measuring GlyT2 band densities and normalizing them to corresponding tubulin band densities, designating time zero as 100%. Black curves correspond to CHX + DMSO conditions and grey curves correspond to CHX + PMA conditions. Densitometric analysis of three independent Western blots as in (A) was performed with the data representing the means ± SEM. C - F) MDCK cells were transfected with wild-type GlyT2 and GFP-Rab11 (C, D) or GFP-Rab7 (E, F). After 48 h the cells were incubated for 2 hours with PMA (1 µM) or the vehicle and fixed with 4% paraformaldehyde. GFP-Rab7 and GFP-Rab11 were visualized by GFP fluorescence (green), whereas GlyT2 was detected with the anti-GlyT2 antibody (shown in red). Note the increase in intracellular vesicles in PMA-treated cells expressing wild-type GlyT2 (D, F) which colocalizes with GFP-Rab7 (F). Scale bar = 15 µm. G) Quantification of colocalization using Pearson´s value was performed as described in Materials and Methods. The histogram represents the mean ± SEM (n = 3; on average, 30 images per condition were analyzed in each experiment). **, significantly different, $p < 0.01$ by ANOVA with Tukey's post hoc test.

Figure 7: Basal ubiquitination of GlyT2 in neurons decreases when the pool of free monomeric ubiquitin is reduced

A) Brainstem and spinal cord primary neurons were treated with DMSO, UCHL1 inhibitor (10 µM) or UCHL3 inhibitor (10 µM) for the times indicated at 37ºC. After lysis, the ubiquitinated proteins were immunoprecipitated with agarose-conjugated anti-multiubiquitin antibodies and the endogenous GlyT2 was analyzed in Western blots. Ub, anti-multiubiquitin immunoprecipitation (50 µg); T, total protein (5 µg). B) Quantification of three experiments performed identically to the representative experiment shown in (A). Bars represent mean ± SEM of the amount of ubiquitinated transporter relative to total GlyT2 expression. *, significant difference with respect to control, $p < 0.05$, ** $p<0.01$ (ANOVA with Tukey's post-hoc test). C) Primary neurons were treated identically as in (A) for 2h at 37ºC. The cells were then harvested, lysed and whole cell lysates (40 µg/lane) were resolved by SDS-PAGE and analyzed by immunoblotting with anti-Ubiquitin antibody (clone P4D1). As a loading control, blots were reprobed with anti-tubulin.

Figure 8: UCHL1 inhibition impairs Glyt2 constitutive endocytosis in neurons.

A) Representative immunoblot of brainstem and spinal cord primary neurons. Cells were pretreated for 2 h with vehicle (DMSO) or *LDN*-57444 (UCHL1 inhibitor: 10 µM) and were then exposed to monensin (35 µM, 30 min) or the vehicle alone (EtOH), in the presence or absence of UCHL1. Cell surface proteins were labeled with sulfo-NHS-SS-biotin and the biotinylated proteins were pulled down with streptavidin-agarose beads. GlyT2 expression was analyzed in Western blots using calnexin immunodetection as a control of intracellular non-biotinylated protein. B, biotinylated protein (30 µg); T, total protein (10 µg). B) Densitometric analysis of four independent Western blots as in (A) relative to the control values (Veh). Data represent the means ± SEM. **, significant difference with respect to control; $p < 0.01$ (ANOVA with Tukey's post-hoc test). C) Primary neurons were incubated with vehicle or *LDN*-57444 as described above, the cells were lysed and the ubiquitinated GlyT2 was immunoprecipitated with agarose-conjugated anti-multiubiquitin antibody. The immunoprecipitates were probed with anti-GlyT2 antibody. Ub, anti-multiubiquitin immunoprecipitation (75 µg); T, total protein (10 µg). D) Quantification of four experiments performed as described in (C). Bars represent the mean ± SEM level of *LDN*-57444-treated ubiquitinated transporter relative to that of ubiquitinated transporter in vehicle-treated cells. *, significant difference with respect to control; $p < 0.05$ (Student's t-test).

Figure 1

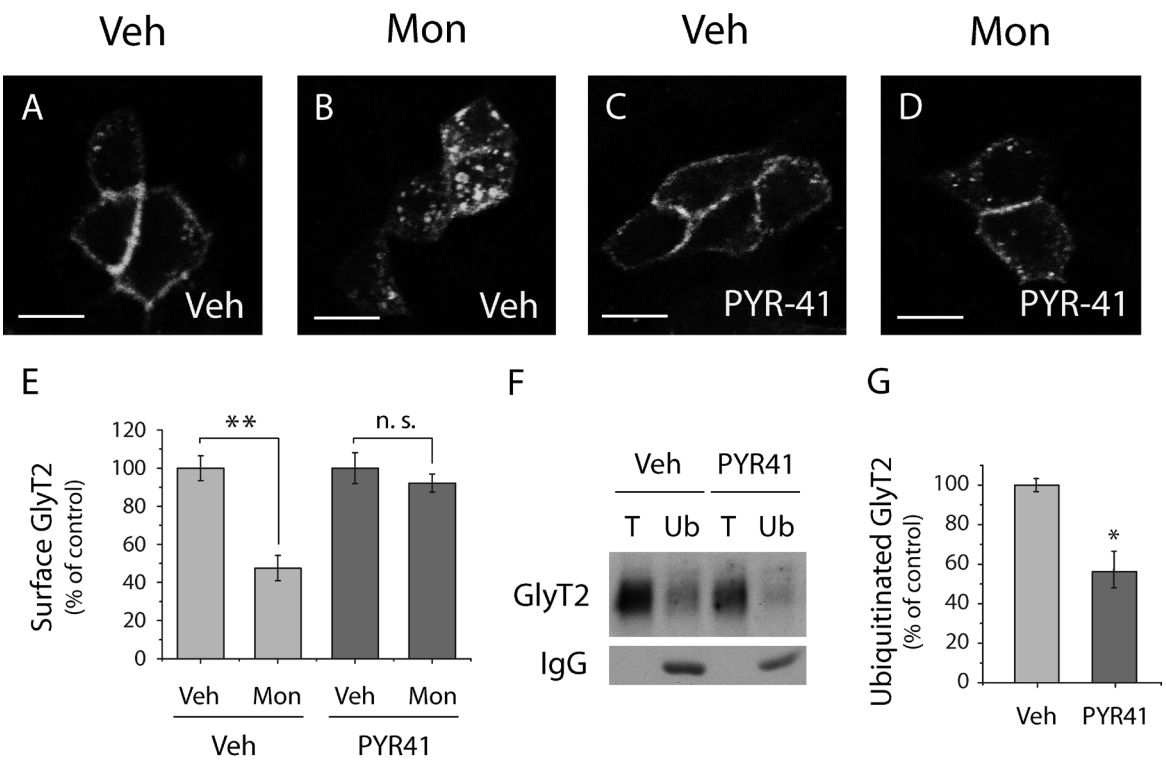
Veh
Mon
Veh
Mon
A
Veh
B
Veh
C
PYR-41
D
PYR-41
E
Surface GlyT2
(% of control)
120
100
80
60
40
20
0
**
n. s.
Veh
Mon
Veh
Mon
Veh
PYR41
F
Veh
PYR41
T
Ub
T
Ub
GlyT2
IgG
G
Ubiquitinated GlyT2
(% of control)
100
80
60
40
20
0
*
Veh
PYR41

Figure 2

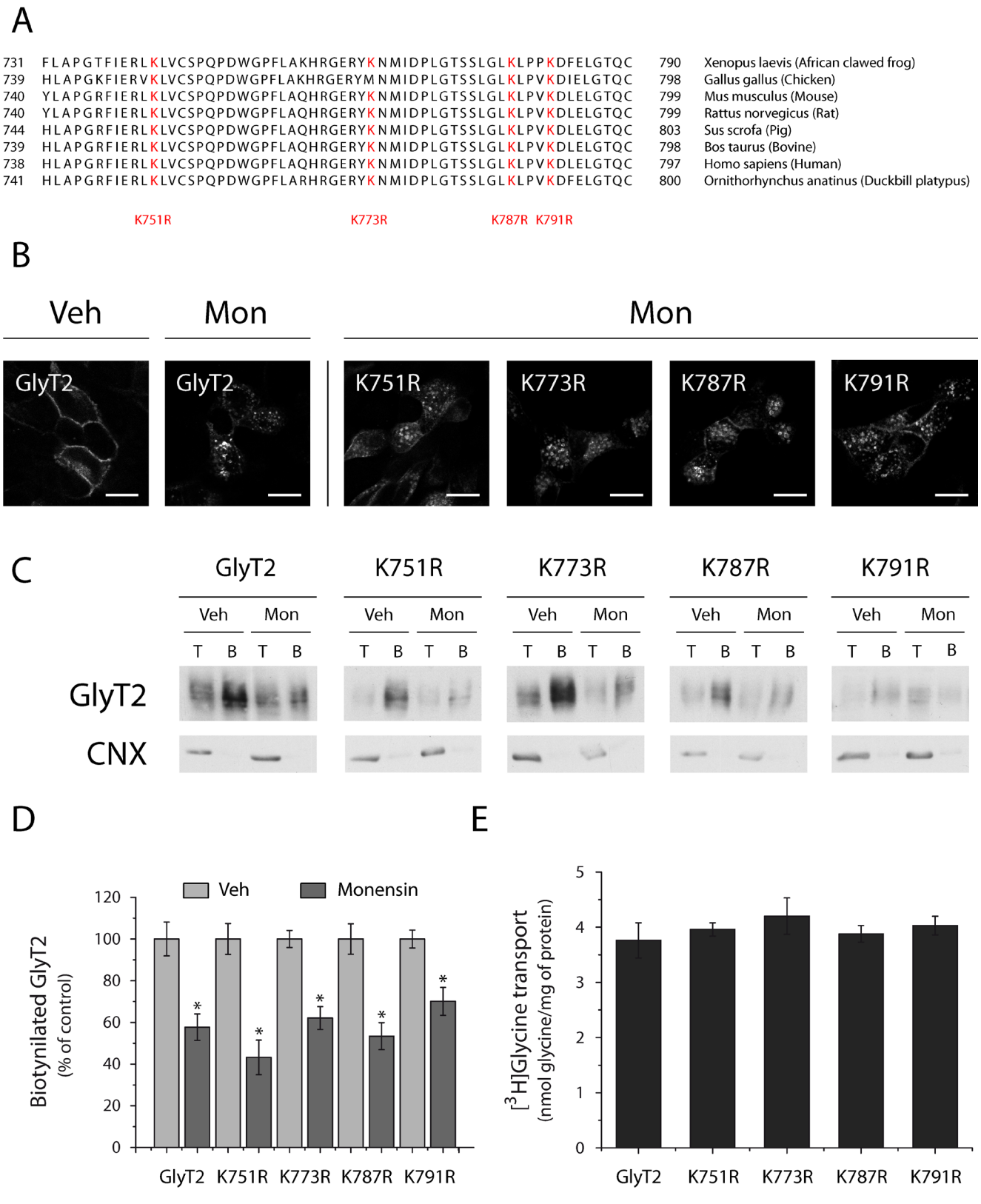
A
731 FLAPGTFIERLKLVCSPQPDWGPFLAKHRGERYKNMIDPLGTSSLGLKLPPKDFELGTQC 790 Xenopus laevis (African clawed frog)
739 HLAPGKFIERVKLVCSPQPDWGPFLAKHRGERYMNMIDPLGTSSLGLKLPVKDIELGTQC 798 Gallus gallus (Chicken)
740 YLAPGRFIERLKLVCSPQPDWGPFLAQHRGERYKNMIDPLGTSSLGLKLPVKDLELGTQC 799 Mus musculus (Mouse)
740 YLAPGRFIERLKLVCSPQPDWGPFLAQHRGERYKNMIDPLGTSSLGLKLPVKDLELGTQC 799 Rattus norvegicus (Rat)
744 HLAPGRFIERLKLVCSPQPDWGPFLAQHRGERYKNMIDPLGTSSLGLKLPVKDLELGTQC 803 Sus scrofa (Pig)
739 HLAPGRFIERLKLVCSPQPDWGPFLAQHRGERYKNMIDPLGTSSLGLKLPVKDLELGTQC 798 Bos taurus (Bovine)
738 HLAPGRFIERLKLVCSPQPDWGPFLAQHRGERYKNMIDPLGTSSLGLKLPVKDLELGTQC 797 Homo sapiens (Human)
741 HLAPGRFIERLKLVCSPQPDWGPFLARHRGERYKNMIDPLGTSSLGLKLPVKDFELGTQC 800 Ornithorhynchus anatinus (Duckbill platypus)
K751R
K773R
K787R K791R
B
Veh
Mon
Mon
GlyT2
GlyT2
K751R
K773R
K787R
K791R
C
GlyT2
K751R
K773R
K787R
K791R
Veh Mon Veh Mon Veh Mon Veh Mon Veh Mon
T B T B T B T B T B T B T B T B T B T B
GlyT2
CNX
D
Veh
Monensin
Biotynilated GlyT2 (% of control)
120
100
80
60
40
20
0
GlyT2 K751R K773R K787R K791R
E
[3H]Glycine transport (nmol glycine/mg of protein)
5
4
3
2
1
0
GlyT2 K751R K773R K787R K791R

Figure 3

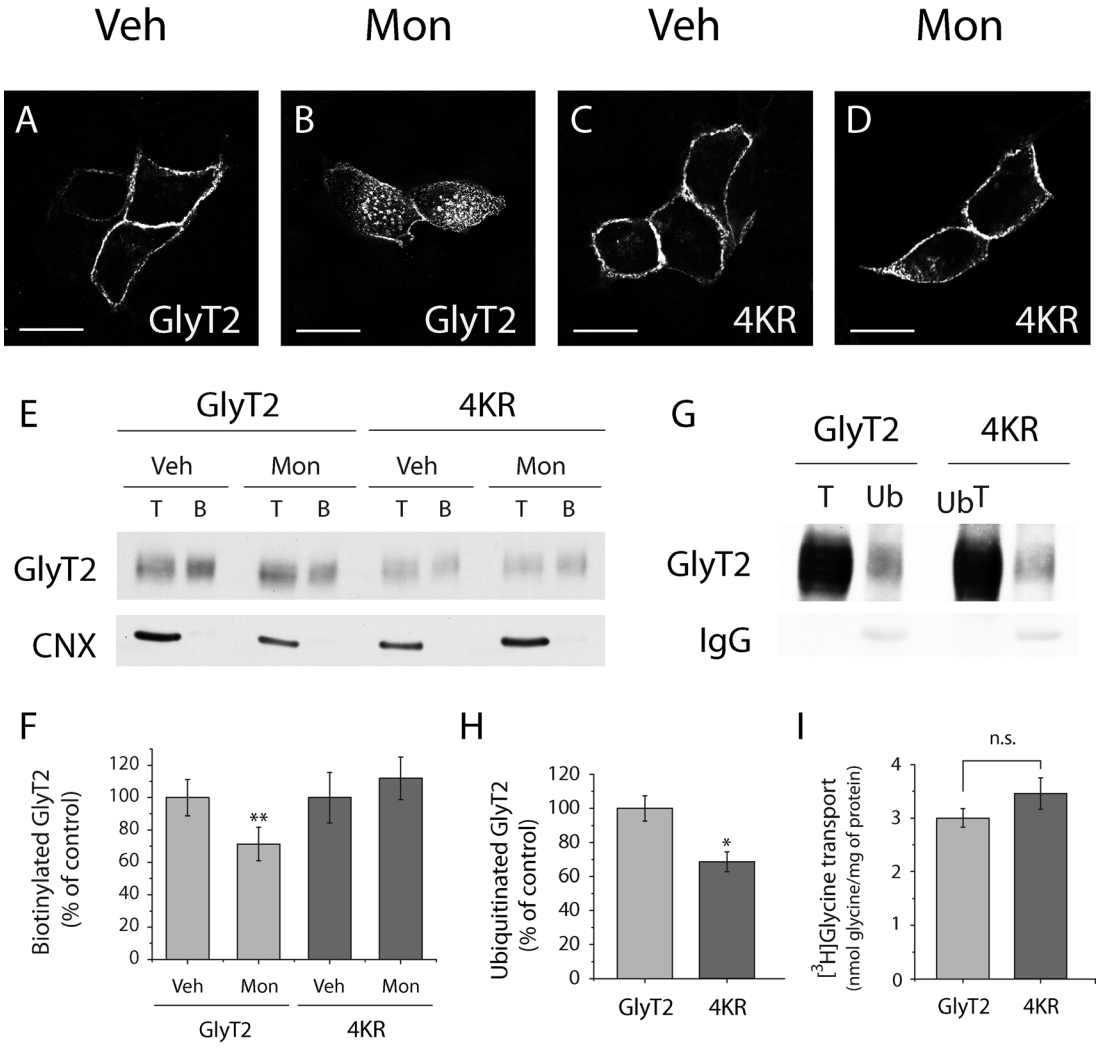
Veh
Mon
Veh
Mon
A
GlyT2
B
GlyT2
C
4KR
D
4KR
E
GlyT2
4KR
Veh
Mon
Veh
Mon
T B T B T B T B
GlyT2
CNX
G
GlyT2
4KR
T Ub UbT
GlyT2
IgG
F
Biotinylated GlyT2 (% of control)
120
100
80
60
40
20
0
**
Veh
Mon
Veh
Mon
GlyT2
4KR
H
Ubiquitinated GlyT2 (% of control)
120
100
80
60
40
20
0
*
GlyT2
4KR
I
n.s.
[3H]Glycine transport (nmol glycine/mg of protein)
4
3
2
1
0
GlyT2
4KR

Figure 4

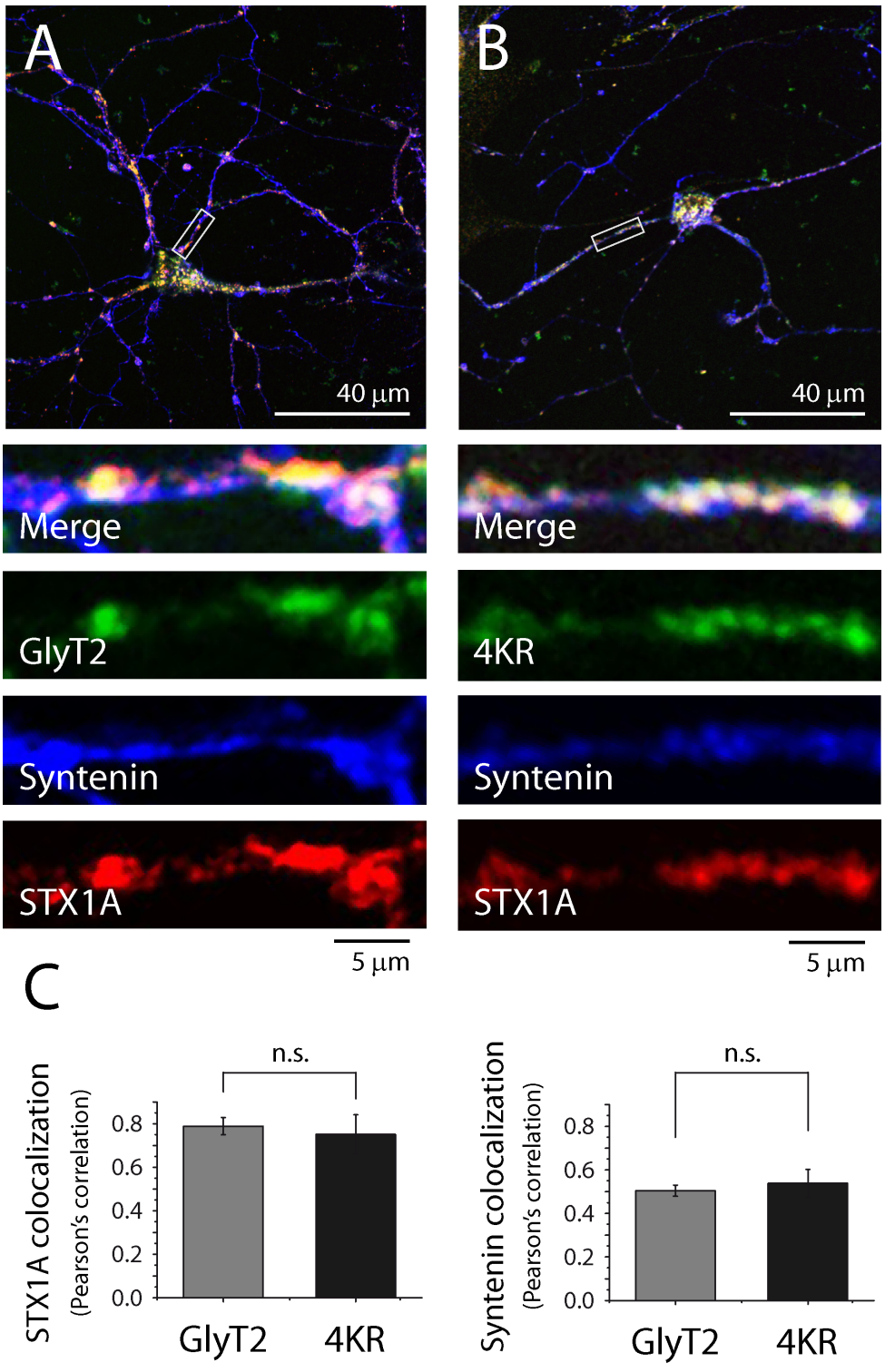
A
B
40 µm
40 µm
Merge
Merge
GlyT2
4KR
Syntenin
Syntenin
STX1A
STX1A
5 µm
5 µm
C
STX1A colocalization
(Pearson's correlation)
n.s.
0.0
0.2
0.4
0.6
0.8
GlyT2
4KR
Syntenin colocalization
(Pearson's correlation)
n.s.
0.0
0.2
0.4
0.6
0.8
GlyT2
4KR

Figure 5

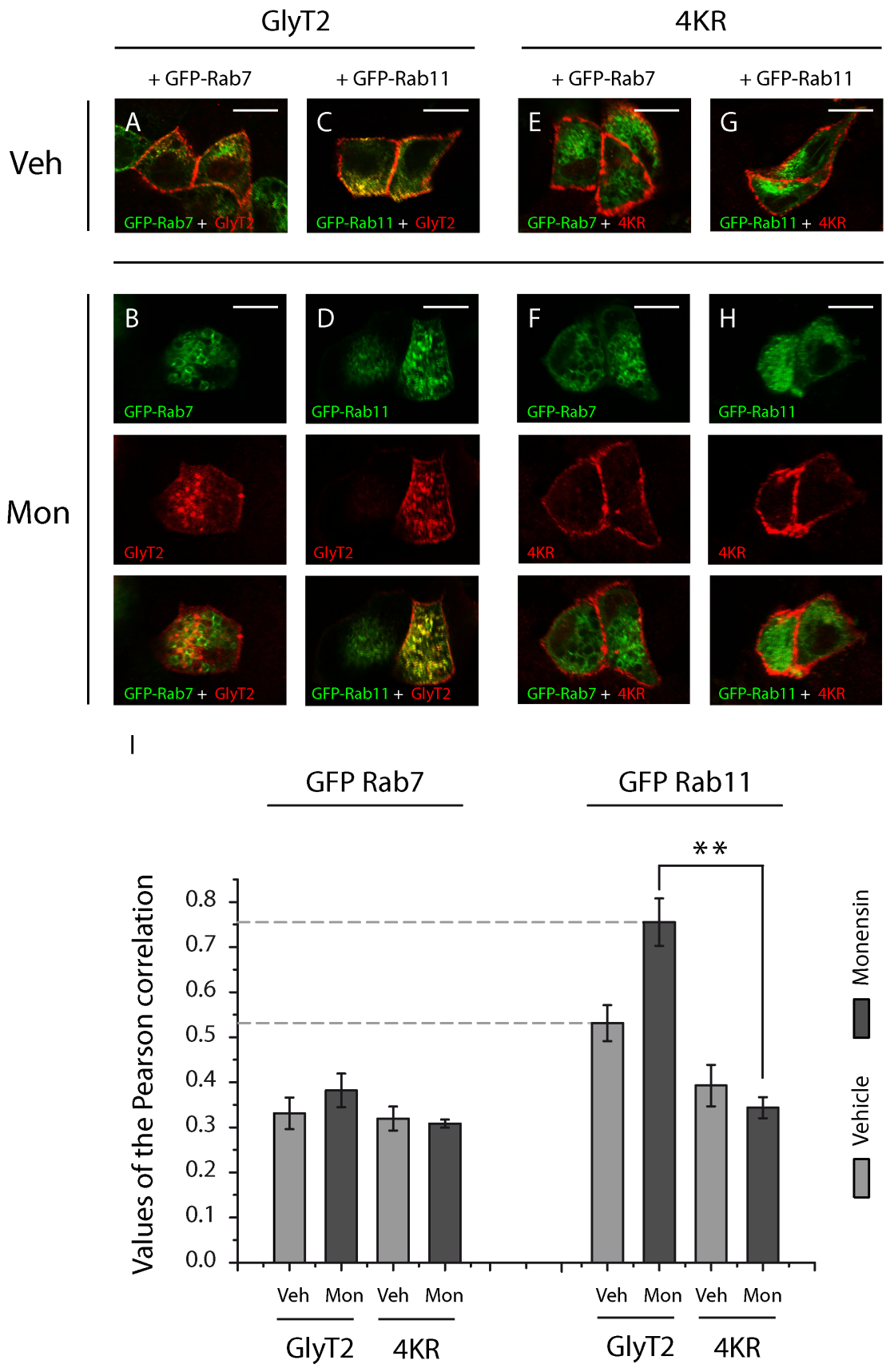
GlyT2
4KR
+ GFP-Rab7
+ GFP-Rab11
+ GFP-Rab7
+ GFP-Rab11
Veh
Mon
A
C
E
G
B
D
F
H
GFP-Rab7 + GlyT2
GFP-Rab11 + GlyT2
GFP-Rab7 + 4KR
GFP-Rab11 + 4KR
GFP-Rab7
GFP-Rab11
GlyT2
4KR
I
GFP Rab7
GFP Rab11
**
Values of the Pearson correlation
0.0
0.1
0.2
0.3
0.4
0.5
0.6
0.7
0.8
Veh
Mon
Veh
Mon
Veh
Mon
Veh
Mon
GlyT2
4KR
GlyT2
4KR
Monensin
Vehicle

Figure 6

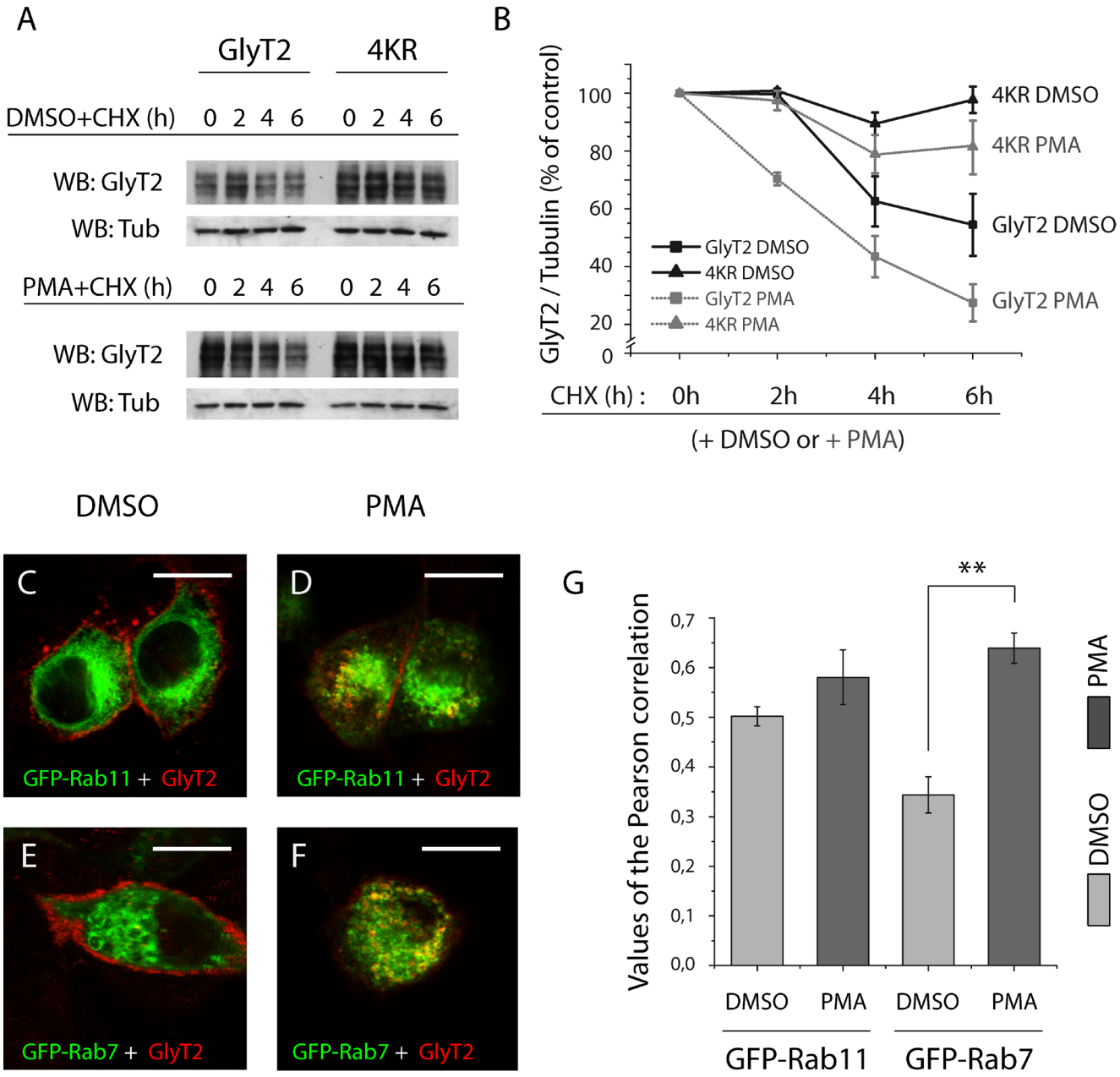
A
GlyT2
4KR
DMSO+CHX (h) 0 2 4 6 0 2 4 6
WB: GlyT2
WB: Tub
PMA+CHX (h) 0 2 4 6 0 2 4 6
WB: GlyT2
WB: Tub
B
GlyT2 / Tubulin (% of control)
100
80
60
40
20
0
GlyT2 DMSO
4KR DMSO
GlyT2 PMA
4KR PMA
4KR DMSO
4KR PMA
GlyT2 DMSO
GlyT2 PMA
CHX (h) : 0h 2h 4h 6h
(+ DMSO or + PMA)
DMSO
PMA
C
GFP-Rab11 + GlyT2
D
GFP-Rab11 + GlyT2
E
GFP-Rab7 + GlyT2
F
GFP-Rab7 + GlyT2
G
**
Values of the Pearson correlation
0,7
0,6
0,5
0,4
0,3
0,2
0,1
0,0
DMSO PMA DMSO PMA
GFP-Rab11 GFP-Rab7
PMA
DMSO

Figure 7

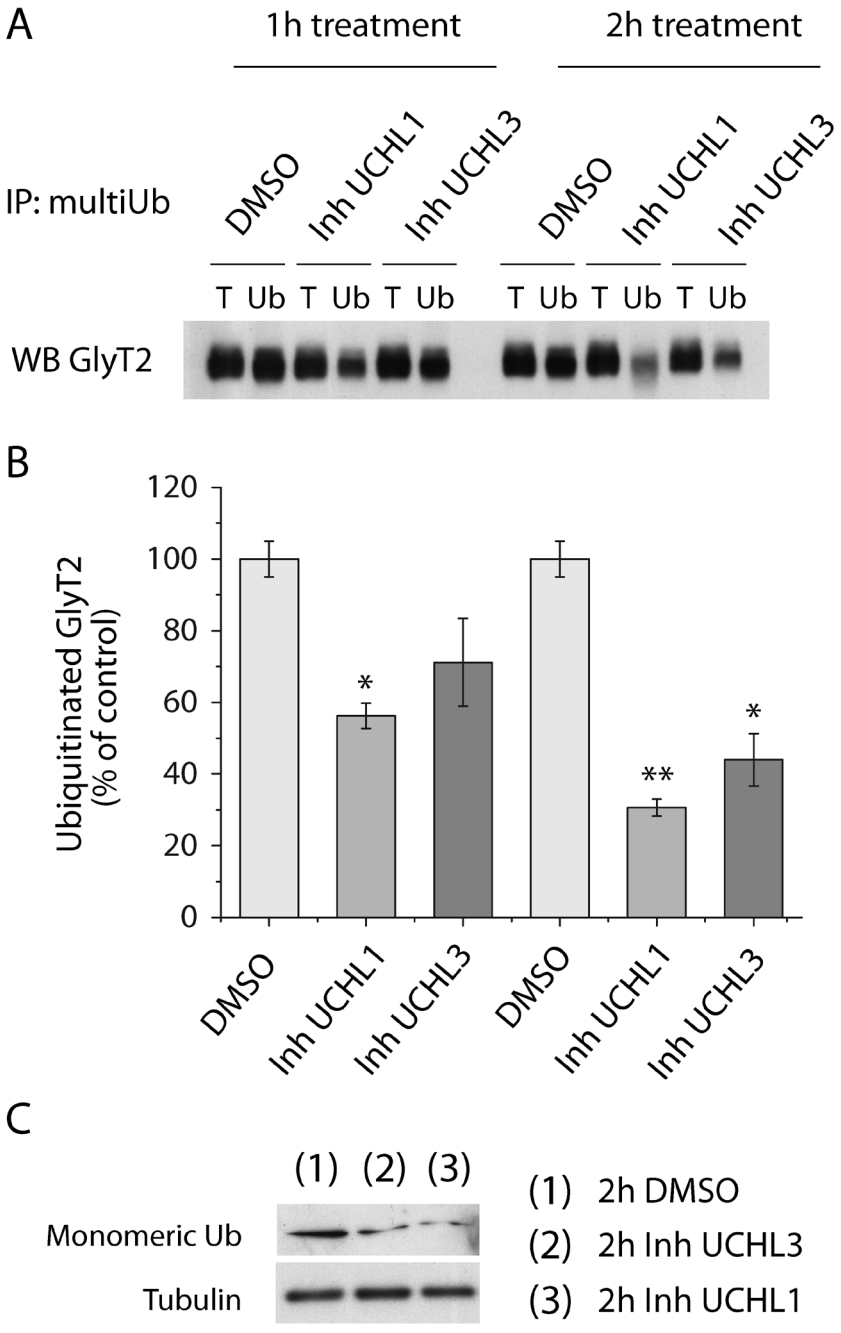
A
1h treatment
2h treatment
IP: multiUb
DMSO
Inh UCHL1
Inh UCHL3
DMSO
Inh UCHL1
Inh UCHL3
T Ub T Ub T Ub T Ub T Ub T Ub
WB GlyT2
B
Ubiquitinated GlyT2
(% of control)
120
100
80
60
40
20
0
*
**
*
DMSO
Inh UCHL1
Inh UCHL3
DMSO
Inh UCHL1
Inh UCHL3
C
(1) (2) (3)
Monomeric Ub
Tubulin
(1) 2h DMSO
(2) 2h Inh UCHL3
(3) 2h Inh UCHL1

Figure 8

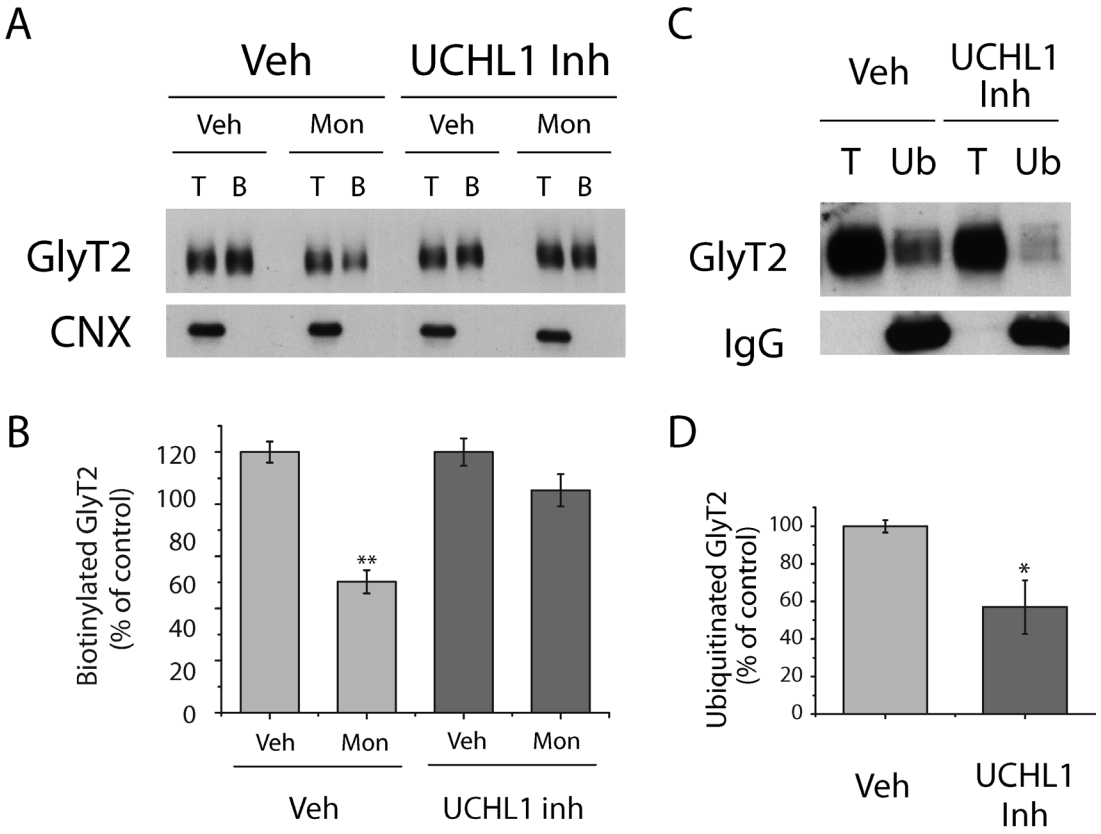
A
Veh
UCHL1 Inh
Veh
Mon
Veh
Mon
T B T B T B T B
GlyT2
CNX
C
Veh
UCHL1 Inh
T Ub T Ub
GlyT2
IgG
B
Biotinylated GlyT2 (% of control)
120
100
80
60
40
20
0
**
Veh
Mon
Veh
Mon
Veh
UCHL1 inh
D
Ubiquitinated GlyT2 (% of control)
100
80
60
40
20
0
*
Veh
UCHL1 Inh

Artículo #3

A novel dominant hyperekplexia mutation Y705C alters trafficking and biochemical properties of the presynaptic glycine transporter GlyT2.

Giménez C, Pérez-Siles G, Martínez-Villarreal J, Arribas-González E, Jiménez E, Núñez E, **de Juan-Sanz J**, Fernández-Sánchez E, García-Tardón N, Ibáñez I, Romanelli V, Nevado J, James VM, Topf M, Chung SK, Thomas RH, Desviat LR, Aragón C, Zafra F, Rees MI, Lapunzina P, Harvey RJ, López-Corcuera B. (2012). *J Biol Chem.* 287:28986-9002.

THE JOURNAL OF BIOLOGICAL CHEMISTRY VOL. 287, NO. 34, pp. 28986–29002, August 17, 2012

A Novel Dominant Hyperekplexia Mutation Y705C Alters Trafficking and Biochemical Properties of the Presynaptic Glycine Transporter GlyT2*

Received for publication, October 31, 2011, and in revised form, June 18, 2012 Published, JBC Papers in Press, June 29, 2012, DOI 10.1074/jbc.M111.319244

Cecilio Giménez[‡§¶], Gonzalo Pérez-Siles[‡§], Jaime Martínez-Villarreal[‡§¶], Esther Arribas-González[‡¶], Esperanza Jiménez[‡§¶], Enrique Núñez[‡§¶], Jaime de Juan-Sanz[‡§¶], Enrique Fernández-Sánchez[‡], Noemí García-Tardón[‡§¶], Ignacio Ibáñez[‡], Valeria Romanelli[§‖], Julián Nevado[§‖], Victoria M. James[**], Maya Topf[‡‡], Seo-Kyung Chung[§§], Rhys H. Thomas[§§], Lourdes R. Desviat[‡], Carmen Aragón[‡§¶], Francisco Zafra[‡§¶], Mark I. Rees[§§], Pablo Lapunzina[§‖], Robert J. Harvey[**], and Beatriz López-Corcuera[‡§¶1]

From the [‡]Departamento de Biología Molecular and Centro de Biología Molecular "Severo Ochoa," (Consejo Superior de Investigaciones Científicas-Universidad Autónoma de Madrid), Madrid 28049, Spain, the [§]Centro de Investigación Biomédica en Red de Enfermedades Raras, Instituto de Salud Carlos III, Madrid 28029, Spain, the [¶]IdiPAZ-Hospital Universitario La Paz, the [‖]Instituto de Genética Médica y Molecular, IdiPAZ-Hospital Universitario La Paz, Universidad Autónoma de Madrid, Madrid 28046, Spain, the [**]Department of Pharmacology, University College London School of Pharmacy, London WC1N 1AX, United Kingdom, the [‡‡]Institute of Structural and Molecular Biology, Crystallography, Birkbeck College, London WC1E 7HX, United Kingdom, and the [§§]Institute of Life Science, College of Medicine, Swansea University, Swansea SA2 8PP, United Kingdom

Background: Hyperekplexia or startle disease is caused by defects in glycinergic transmission.
Results: A new mutation pY705C in the glycine transporter GlyT2 alters protein trafficking and H^+ and Zn^{2+} transport modulation.
Conclusion: Multiple pathogenic mechanisms may contribute to the complex phenotype of individuals with the Y705C mutation.
Significance: This is the first common dominant mutation associated with hyperekplexia affecting the presynaptic glycine transporter GlyT2.

Hyperekplexia or startle disease is characterized by an exaggerated startle response, evoked by tactile or auditory stimuli, producing hypertonia and apnea episodes. Although rare, this orphan disorder can have serious consequences, including sudden infant death. Dominant and recessive mutations in the human glycine receptor (GlyR) α1 gene (*GLRA1*) are the major cause of this disorder. However, recessive mutations in the presynaptic Na^+/Cl^--dependent glycine transporter GlyT2 gene (*SLC6A5*) are rapidly emerging as a second major cause of startle disease. In this study, systematic DNA sequencing of *SLC6A5* revealed a new dominant GlyT2 mutation: pY705C (c.2114A→G) in transmembrane domain 11, in eight individuals from Spain and the United Kingdom. Curiously, individuals harboring this mutation show significant variation in clinical presentation. In addition to classical hyperekplexia symptoms, some individuals had abnormal respiration, facial dysmorphism, delayed motor development, or intellectual disability. We functionally characterized this mutation using molecular modeling, electrophysiology, [^{3}H]glycine transport, cell surface expression, and cysteine labeling assays. We found that the introduced cysteine interacts with the cysteine pair Cys-311–Cys-320 in the second external loop of GlyT2. This interaction impairs transporter maturation through the secretory pathway, reduces surface expression, and inhibits transport function. Additionally, Y705C presents altered H^+ and Zn^{2+} dependence of glycine transport that may affect the function of glycinergic neurotransmission *in vivo*.

The extracellular concentration of synaptic glycine is regulated by Na^+/Cl^--dependent glycine transporters. These proteins mediate reuptake of glycine into presynaptic terminals (GlyT2)[2] and glial cells adjacent to glycinergic inhibitory neurons (GlyT1) (1). Mouse knock-out studies have revealed that glial GlyT1 is the main regulator of the extracellular glycine concentrations (2). By contrast, neuronal GlyT2 is involved in the removal and recycling of synaptic glycine generating a vectorial flow from the synaptic cleft into the terminal, supplying substrate to the low affinity vesicular inhibitory amino acid transporter (2, 3). Inactivation of the GlyT2 gene (*Slc6a5*) pre-

* This work was supported by Spanish Dirección General de Enseñanza Superior e Investigación Científica Grants BFU2005-05931/BMC and BIO2005-05786, Ministerio de Ciencia e Innovación Grant SAF2008-05436, Comunidad Autónoma de Madrid Grants 11/BCB/010 and S-SAL-0253/2006, Ministerio de Economia y Competitividad Grant SAF2011-28674, Centro de Investigación Biomédica en Red de Enfermedades Raras Intramural Project U-751/U-753, an institutional grant from the Fundación Ramón Areces, Medical Research Council Grant G0601585, and Action Medical Research Grant 1966. The group is member of the European Regional Development Fund Grant BFU2007-30688-E/BFI.

[1] To whom correspondence should be addressed: Dept. de Biología Molecular, Centro de Biología Molecular "Severo Ochoa," Universidad Autónoma de Madrid, 28049 Madrid, Spain. Tel.: 34-91-1964631; Fax: 34-91-1964420; E-mail: blopez@cbm.uam.es.

[2] The abbreviations used are: GlyT, glycine transporter; GlyR, glycine receptor; GLR, glycine receptor subunit; HBS, Hepes-buffered saline; $LeuT_{Aa}$, leucine transporter from *A. aeolicus*; MesNa, sodium methanethiosulfonate; MTSEA, 2 aminoethyl methanethiosulfonate; SLC, solute carrier; TCEP, tris(2-carboxyethyl) phosphine; TM, transmembrane domain; HBS, Hepes-buffered saline; MDCK, Madin-Darby canine kidney.

vents glycine loading into synaptic vesicles, impairing inhibitory glycinergic neurotransmission (4). GlyT2 knock-out mice have a complex motor phenotype (4, 5) that mimics clinical signs of hyperekplexia or startle disease (OMIM 149400). This rare human disorder is characterized by an exaggerated startle response to acoustic or tactile stimuli (6). Startle disease can have serious consequences for neonates, including brain damage and/or sudden death caused by apnea episodes. The abnormal startle response, which can provoke unprotected falls resulting in injury, can persist throughout development and into adulthood (7). However, unlike rodent, cattle, and canine defects (6), humans with *SLC6A5* mutations survive, and clinical signs often resolve after the neonatal and infantile risk period (8).

Genetic analysis of individuals with human hyperekplexia has revealed mutations in genes for postsynaptic proteins involved in glycinergic neurotransmission. These include the GlyR α1 and β subunits (*GLRA1* and *GLRB*) and proteins that assist receptor trafficking to the synaptic membrane (9–11). Sequencing the 16 exons of the human GlyT2 gene (*SLC6A5*) also revealed that missense, nonsense, and frameshift mutations affecting presynaptic glycine transport can cause hyperekplexia (8, 12). The structure of a prokaryotic homologue ($LeuT_{Aa}$) of the SLC6 family (13) has provided a useful model for explaining the effects of selected missense mutations on Na^+ and glycine-binding residues crucial for transport activity (6, 8, 12). It is also noteworthy that the majority of GlyT2 mutations were recessive, producing bi-allelic loss of function caused by the absence of protein in the plasma membrane or by production of an inactive transporter (6). In the present study, we report the identification of a novel dominant mutation (c.2114A→G, pY705C) in exon 15 of *SLC6A5*. This change was found in eight individuals from three families in two cohorts of hyperekplexia patients that were devoid of GlyR gene mutations. Functional characterization of this GlyT2 substitution revealed the introduced cysteine impacts on transporter protein maturation through the secretory pathway and alters the H^+ and Zn^{2+} dependence of glycine transport. The biochemical features of the mutant transporter may produce detrimental effects on glycinergic inhibition *in vivo*.

EXPERIMENTAL PROCEDURES

Molecular Genetic Analysis of the Human GlyT2 Gene (SLC6A5)—Informed consent was obtained from all individuals using guidelines approved by the local ethical committees. Patients of both sexes were studied. Patient genomic DNA was amplified using primers for the 16 exons of the *SLC6A5* gene as previously described (8). 60 ng of genomic DNA were amplified using an Expand high fidelity PCR system (Roche Applied Science) in 25-μl reactions containing 10 pmol of each primer, 1× buffer with 1.5 mM $MgCl_2$, 200 μM dNTPs, and 1 unit of Taq polymerase (Roche Applied Science). PCR conditions were 94 °C for 5 min followed by 35 cycles of 30 s at 94 °C, 30 s at 60 °C, and 30 s at 72 °C. Amplification products were analyzed on 2% agarose gels, extracted with a QIAQuick gel extraction kit (Qiagen), and sequenced employing BigDye Terminator v.3.1 mix (Applied Biosystems Foster City, CA). Genomic DNA from 200 commercially available controls was obtained from the European Collection of Cell Cultures, human random control. Population analysis was conducted by DNA sequencing of control amplicons or using the artificially created restriction site method (14), where an NdeI site is introduced into control but not mutated amplicons during PCR. Electropherograms were analyzed using Sequencher (Gene Codes Corp., Ann Arbor, MI). Analysis of copy number variations in hyperekplexia genes was assessed by multiplex ligation-dependent probe amplification. Briefly, DNA (250 μg) was tested using the SALSA multiplex ligation-dependent probe amplification kit P274 (MRC Holland), which evaluates several regions of *GLRA1*, *GLRB*, and *SLC6A5*. No abnormalities (deletions nor duplications) were observed in any of the samples evaluated, ruling out copy number variations as a cause of hyperekplexia in these cases.

In Silico Analysis—Conservation of the mutated residues was assessed by alignment of orthologous and human protein sequences using ClustalW software (15). The putatively damaging effects of the predicted amino acid substitution was assessed using the PolyPhen-2 program (16) that gives the results as "benign," "possibly damaging," "probably damaging," or "unknown." A GlyT2 homology model was obtained using MODELLER (17) as previously reported (6, 18), based on the crystal structure of $LeuT_{Aa}$ from the bacterium *Aquifex aeolicus* (Protein Data Bank code 2A65) (13).

Mutagenesis and Expression of Human GlyT2 cDNA in Mammalian Cells—The human GlyT2 cDNA was cloned into the vectors pRC-CMV (Invitrogen) and pEGFP-C1 (Clontech) as previously described (8). Missense mutations were generated in pRC-CMV GlyT2 by site-directed mutagenesis using the QuikChange kit (Stratagene). Two independent *Escherichia coli* colonies carrying the mutant plasmids were characterized by DNA sequencing and [^{3}H]glycine transport activity. We sequenced the full coding region of each construct to verify that only the desired mutation had been introduced. Transient expression in COS7 cells was performed as described (18) using Lipofectamine Plus (Invitrogen) or Neofectin^{TM} (MidAtlantic Biolabs). The cells were incubated for 48 h at 37 °C, unless otherwise indicated in the figure legends. For electrophysiological recordings, the human GlyT2 cDNA was subcloned into the vector pSP64T, generously provided by Dr. Carmen Montiel (Universidad Autónoma of Madrid, Madrid, Spain).

Glycine Transport Assays—Transport assays in COS7 cells were performed at 37 °C in 0.25 ml of Hepes-buffered saline (HBS: 150 mM NaCl, 10 mM Hepes-Tris, pH 7.4, 1 mM $CaCl_2$, 5 mM KCl, 1 mM $MgSO_4$, 10 mM glucose). 2 μCi/ml [^{3}H]glycine (1.6 TBq/mmol; PerkinElmer Life Sciences) isotopically diluted at 10 μM final glycine concentration was used (19), unless a different concentration is specified. The reactions were terminated after 10 min by aspiration followed by washing with HBS. Transport was measured by subtracting the glycine accumulation by mock-transfected COS7 cells from that of GlyT2 transfected cells and normalizing to the protein concentration. Kinetic analysis was performed by varying glycine concentration in the uptake medium between 10 and 1000 μM.

Expression of the Human GlyT2 cDNA in Xenopus Oocytes—Wild-type and mutant GlyT2 cDNAs were cloned in the vector pSP64T, which contains a β1-globin promoter. Constructs

were linearized with XbaI, and cRNA was transcribed with SP6 polymerase and capped with 5′7-methylguanosine using the mMESSAGE mMACHINE SP6 RNA kit (Ambion Inc.). *Xenopus laevis* females were obtained from *Xenopus* Express (France). The oocytes were harvested from *X. laevis* anesthetized in tricaine methasulfonate 0.10% (w/v) solution in tap water. All of the procedures were in accordance with the Spanish and European guidelines for the prevention of cruelty to animals. The follicular membrane was removed by incubation in a medium (90 mM NaCl, 1 mM KCl, 1 mM $MgCl_2$, 5 mM Hepes, pH 7.4) containing 300 units/ml collagenase (Type 1; Sigma) for 1 h. Wild-type or mutant mRNAs (50 ng) were injected into defolliculated stage V and VI *X. laevis* oocytes. The oocytes were maintained in Barth's medium (88 mM NaCl, 1 mM KCl, 0.33 mM $Ca(NO_3)_2$, 0.41 mM $CaCl_2$, 0.82 mM $MgSO_4$, 2.4 mM $NaHCO_3$, and 10 mM Hepes, pH 7.4), and transport or electrophysiological experiments were assayed 5 days post-injection.

Two-microelectrode Voltage-Clamp Recordings from Xenopus Oocytes—Electrophysiological recordings were obtained after incubation of the injected oocytes at 18 °C in standard oocyte solution (100 mM NaCl, 2 mM KCl, 1 mM $CaCl_2$, 1 mM $MgCl_2$, 10 mM Hepes, pH adjusted to pH 7.5 with HCl). Two-electrode voltage clamp was used to measure and control the membrane potential and to monitor the capacitative currents using Axoclamp 900A (Axon Instruments), digitized using a Digidata 1440 (Axon Instruments). Both instruments were controlled by pCLAMP software (Axon Instruments), and the results were analyzed using Clampfit 10.2 software (Axon Instruments). Recordings were performed at room temperature using standard micropipettes filled with 3 M KCl (resistance varied between 0.5 and 2 MΩ). The oocytes were held at −40 mV, and to obtain current-voltage (I-V) relations, the pulse protocol consisted of 350-ms voltage steps between −130 and +50 mV in 20 mV steps. The currents were subjected to low pass filtering at 100 Hz.

Cell Surface Labeling—Thiol-specific biotinylation and total surface biotinylation was performed with MTSEA-biotin (Toronto Research Chemicals Inc., Toronto, Canada) and sulfo-NHS-SS-biotin (Pierce) on transfected COS7 cells as described (20, 21). 0.5 mM MTSEA-biotin or 1.5 mg/ml sulfo-NHS-SS-biotin and a 3-h incubation with streptavidin-agarose beads (Sigma) were used. Biotinylated proteins (B) were eluted from the beads with Laemmli buffer (40 mM Tris, pH 6.8, 2% SDS, 10% glycerol, 0.1 M DTT, 0.01% bromphenol blue) for 10 min at 70 °C and then analyzed in Western blots (7.5% SDS-PAGE) with anti-GlyT2 antibody (Santa Cruz). Protein bands were visualized by ECL and quantified on a GS-710 calibrated imaging densitometer from Bio-Rad with Quantity One software, using film exposures in the linear range. Loading controls were performed by reprobing Western blot membranes using an anti-calnexin antibody. Standard errors were calculated from at least three separate experiments.

GlyT2 Subcellular Localization—Wild-type or mutant GlyT2 in pEGFP-C1 were transfected in MDCK cells and 48 h later were subjected to immunofluorescence as described previously (22) using the antibody against the indicated marker protein. Secondary antibodies were coupled to Alexa Fluor® 555. Alternatively, the cells were transfected with pEGFP-C1 GlyT2 (23) and were fixed with 4% paraformaldehyde in PBS. The cells were visualized by confocal microscopy on a LSM510 confocal microscope (Zeiss) using a vertical microscope Axio Imager.Z1 M (Zeiss).

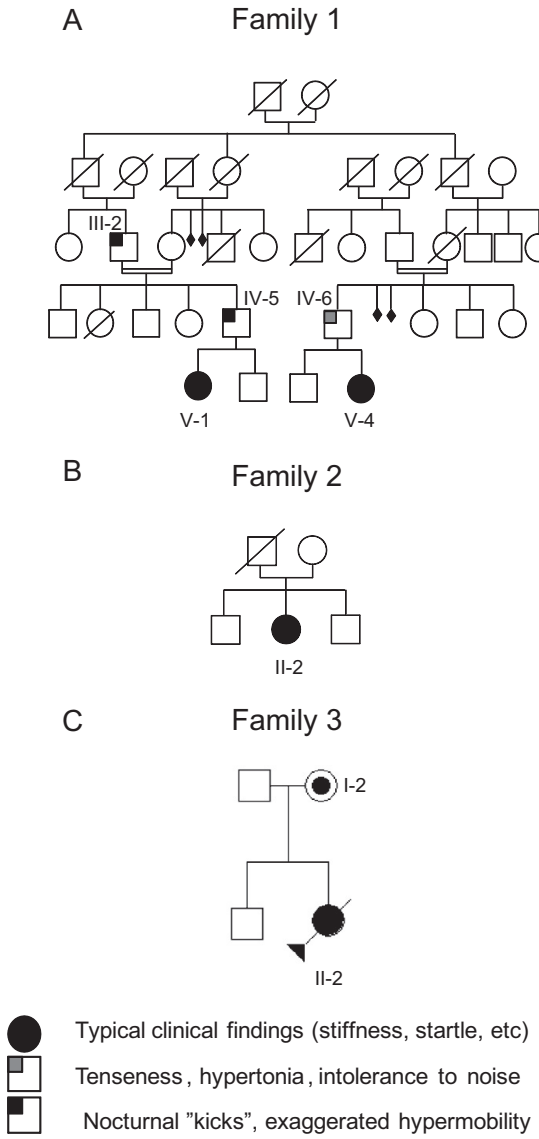

FIGURE 1. **Pedigree of families 1 (*A*), 2 (*B*), and 3 (*C*).** Individuals are numbered according to their position in the pedigree lines as I, II, III, and IV, and then each individual from left to right as 1, 2, 3, etc. Males and females are represented by *squares* and *circles*, respectively. *Shaded symbols* represent individuals with the Y705C mutation or who are/were affected, with clinical signs observed.

RESULTS

Patient Information—A total of 16 probands from Spain and 188 from the UK with clinical diagnosis of hyperekplexia, all of which had proved gene-negative in screens of *GLRA1* and *GLRB*, were provided from neurological units. Genomic DNA samples from the patients were screened for *SLC6A5* mutations. Clinical features of patients carrying the novel mutation in the *SLC6A5* gene are summarized below. Fig. 1 shows the pedigrees of the patient families.

The first patient from family 1, V-1, displayed perinatal onset persistent crying and hypertonia. This was ameliorated when she was removed from the neonatal intensive care unit and was placed in a quiet, low stimuli environment. Physical examination at day 7 revealed an exaggerated startle reaction and prominent head retraction. She had delayed motor development and showed a severe degree of intellectual disability. With the second patient from family 1, V-4, concern was raised when the child was 1 month old because of hypertonia and abnormal crying. Neurological evaluation demonstrated abnormal head retraction and hypertonia, which improved during sleep. Patient IV-5 from family 1 had similar neonatal behavior to V-1; he "kicked" and had exaggerated movements during rest at bed, mainly when sleeping. Patient IV-6 in family 1 showed some intolerance to noise and crowded places, and when he was a boy suffered from attacks of stiffness precipitated by surprise or school tests.

Patient II-2 in family 2 was a girl who presented with stiffness and frequent falling and was intellectually intact. Patient II-2 in family 3 had perinatal hypertonia with clonus (variable, partially resolving in sleep) and triggered startle episodes (paroxysmal clonic movements). In addition she had abnormal respiration with prominent apnea episodes. Physically she had several dysmorphic features: tongue protrusion, striking excess neck skin folds, large atrial-septal defect, short palpebral fissures, small carp-like mouth, subtly low set ears, single palmar crease, contractures at the knees, and overlapping clenched fingers and hands. Cranial calcification was also seen. Her MRI demonstrated small focal areas of signal change in the deep, subcortical white matter of both cerebral hemispheres and possible gyral swelling. She died aged 21 weeks having spent the majority of her life in pediatric intensive care. The mother is apparently asymptomatic. She was physically examined at the age of thirty-one and no abnormality or excessive startle was detected.

Genetic Analysis—Genomic DNA samples from 204 individuals with hyperekplexia who had tested negative for disease-causing mutations in *GLRA1* (5q33.1) and *GLRB* (4q32.1) were scanned on all 16 coding exons and extended flanking intronic regions of *SLC6A5* (11p15.1), encoding human GlyT2. Several single-nucleotide polymorphisms present in patients and controls were found. In addition, DNA sequence analysis revealed a heterozygous nonsynonymous change (c.2114A→G) in exon 15 in four of the patients analyzed (patients V-1 and V-2 of family 1, patient II-2 of family 2, and patient II-2 of family 3). Familial analysis revealed the presence of this sequence variant in four more individuals (Fig. 1). This change was not detected in 600 unrelated, normal control chromosomes (data from the United Kingdom; not detected in 400 normal control chromosomes, Caucasian samples), as assessed using two different techniques (see "Experimental Procedures"). This mutation resulted in a tyrosine (T*A*T) to cysteine (T*G*T) substitution at position 705 (pY705C) in transmembrane domain 11 (TM11; Fig. 2). Homology modeling of GlyT2 using the crystal structure of the $LeuT_{Aa}$ (13) located Tyr-705 at the carboxyl-terminal portion of the TM11, near the extracellular face of the transporter (Fig. 2*B*). A loss of a hydrogen bond with the side chain of Glu-701 is predicted. Phylogenetic comparisons of the TM11 region of GlyT2 show high evolutionary conservation of Tyr-705 (Fig. 2*C*). Alignment of GlyT2 with other Na^+/Cl^--dependent neurotransmitter transporters of the SLC6 family demonstrates that a tyrosine is found at the equivalent position in most human neurotransmitter transporters from the GABA, amino acid, and monoamine subfamilies (norepinephrine transporter and dopamine transporter) with the exception of GABA transporter 1 and serotonin transporter (Fig. 2*D*). This suggests that Tyr-705 has a relevant role for transporter function within this superfamily and accordingly, the Y705C substitution was predicted to be "probably damaging" in PolyPhen-2 analysis, with a score of 1.000.

Mutagenesis and Functional Characterization—Functional consequences of the Y705C mutation were initially assessed by assaying [^{3}H]glycine uptake of recombinant wild-type and mutant GlyT2 after transient expression in COS7 cells (Fig. 3*A*). The V_{max} of glycine transport by the Y705C mutant was reduced to ~60% as compared with wild-type GlyT2 (23 ± 2.5 for the Y705C *versus* 38 ± 3.2 nmol of Gly/mg of protein/5 min for wild type). The co-expression of wild-type and Y705C transporters resulted in a V_{max} of 30 ± 3.1 nmol of Gly/mg of protein/5 min, representing 79% of wild-type GlyT2. This value is close to the predicted average value of the activity of each transporter population. A slight but significant increase of the K_m for glycine was observed in the Y705C mutant when expressed alone. Investigation of other features of glycine transport by GlyT2 indicated that sensitivity to Na^+ and Cl^-, the ions required for transport, was unaffected in Y705C mutant, and the sensitivity of the mutant transporter to the inhibition by the selective GlyT2 inhibitor ALX1393 was unchanged as compared with wild-type GlyT2 (data not shown).

Additional functional characterization was performed by overexpressing wild-type and mutant GlyT2 in *Xenopus* oocytes to examine the electrophysiological properties of both proteins. As shown in Fig. 3*B*, glycine-induced inward currents were observed in oocytes expressing either wild-type GlyT2 or the Y705C mutant. In agreement with the reduced V_{max} for glycine transport observed in COS cells, maximal currents recorded from oocytes were ~35% lower than observed for wild-type GlyT2. We also studied the voltage dependence of the observed currents by employing a voltage-clamp protocol consisting of long square pulses from −130 to +50 mV. The current triggered by glycine showed inward rectification for both transporters (Fig. 3*C*). The *I-V* relationships were similar in shape, suggesting no alteration of the voltage dependence of glycine transport. However, at each voltage examined, the current mediated by wild-type GlyT2 was larger than that of the Y705C mutant.

Plasma Membrane Expression—One possible explanation for the reduction in V_{max} for glycine transport of the Y705C mutant could be impaired plasma membrane expression. We determined the levels of transporters present in the plasma membrane using two different approaches. First, we expressed EGFP-tagged wild-type GlyT2 or the Y705C mutant in MDCK cells (Fig. 4*A*), immunolabeling the cells for the plasma membrane marker protein E-cadherin (22, 24). The percentage of Y705C co-localization with the plasma membrane marker was

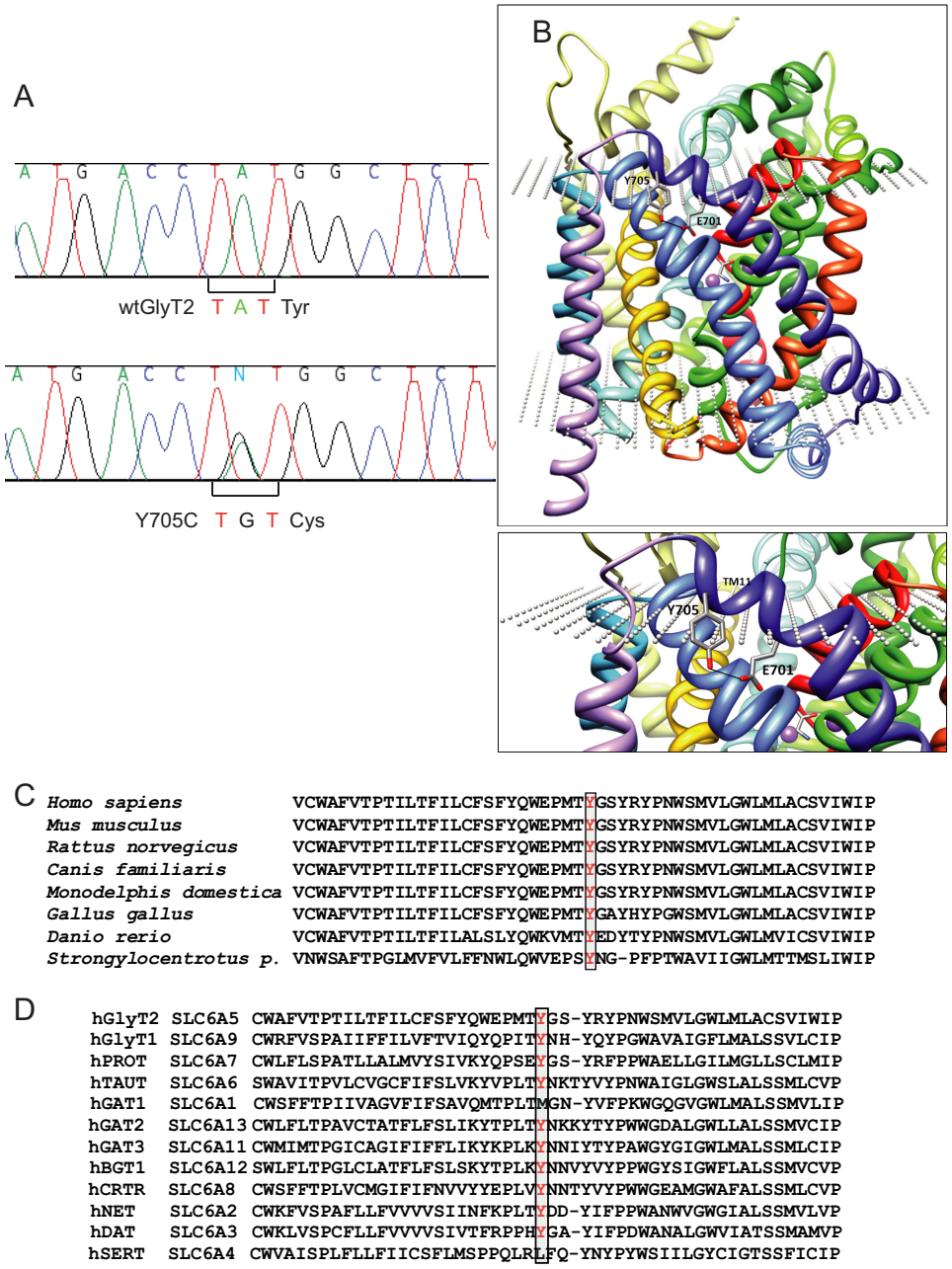

FIGURE 2. **Genetic and structural analysis of the Y705C mutant.** *A*, partial sequences of exon 15 from control and patient 1 DNAs, respectively. Note the heterozygous single-nucleotide polymorphism c.2114A→G changes the codon TAT to TGT, resulting in a pY705C substitution in GlyT2. *B*, molecular model of GlyT2 showing the localization of Tyr-705 in TM11. *C*, phylogenetic comparison of TM11 regions of GlyT2 containing the amino acid Tyr-705 (in *red*). *D*, sequence alignment of GlyT2 TM11 region in human SLC6 family members. Sequences were obtained from NCBI (www.ncbi.nlm.nih.gov) and were aligned using ClustalW software and MUSCLE alignment server.

76.8 ± 2.3% compared with wild-type GlyT2. In addition, surface labeling with the nonpermeant reagent Sulfo-NHS-SS-biotin of the proteins expressed in the plasma membrane of COS7 cells allowed the isolation and quantification of the surface-resident transporters. In agreement with this finding, the Y705C mutant amounted for 68.9 ± 5.7% of wild-type GlyT2 levels (Fig. 4*B*). GlyT2 protein expressed in cultured cells appears as a mature 100-kDa protein band, which is the form present on the plasma membrane, and a 75-kDa underglycosylated immature transporter (25). As shown in Fig. 4*B*, the Y705C mutant showed a higher proportion of immature precursor compared with wild-type GlyT2, so that the mature/immature protein ratio was 50% reduced for the mutant. This is highly suggestive of a deficiency in the biogenesis and processing of the Y705C mutant along the secretory pathway, slowing the transformation of the immature precursor into the mature protein. However, we did not observe clear co-localization of the transporter mutant with the endoplasmic reticulum marker (calnexin), nor with other cellular markers such as TGN38, Rab5, or the early endosome marker EEA1 as compared with wild-type GlyT2 (Fig. 4*C*). This suggests that the mutant protein is not arrested in a precise compartment of the secretory pathway but perhaps progresses slowly along the endomembrane system. In addition, no alteration of the typical GlyT2

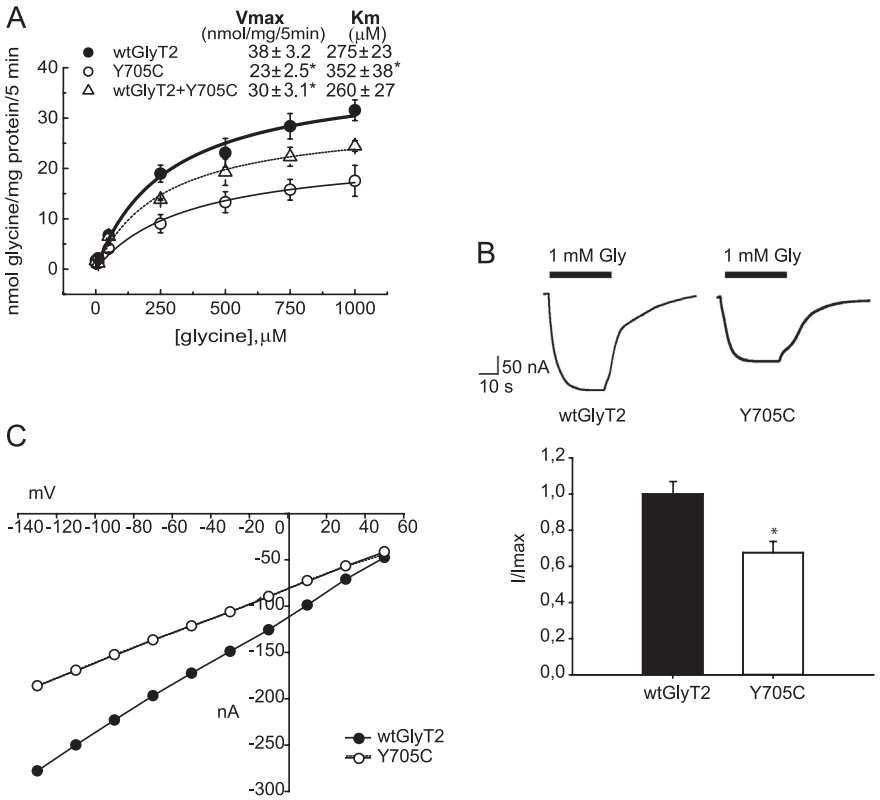

FIGURE 3. **Glycine transport and electrophysiological characterization of wild-type GlyT2 and the Y705C mutant.** *A*, COS7 cells expressing the indicated transporters were assayed for ^{3}[H]glycine transport during 10 min in HBS containing 150 mM NaCl in the presence of increasing glycine concentrations from 0.5 to 1 mM. Experimental data were fitted to hyperbolae. Kinetic parameters are indicated on the graph. *, significantly different from wild-type GlyT2, $p < 0.05$ in Student's *t* test. *B*, inward currents evoked by glycine in representative oocytes expressing wild-type GlyT2 or the Y705C mutant. The cells were voltage-clamped at −40 mV, and 1 mM glycine was superfused for the period indicated by the *solid bar*. Histogram represents arithmetic means ± S.E. (n = 5–10 oocytes) of normalized inward currents for wild-type GlyT2 and the Y705C mutant. *, significantly different from wild-type GlyT2, $p < 0.05$ in Student's *t* test. *C*, current-voltage plots of the glycine-mediated inward currents of wild-type GlyT2 and Y705C mutant determined by subtracting, in each case, the currents observed in the absence of glycine.

apical sorting (26) was observed in polarized MDCK cells growing in Transwells (Fig. 4*D*), because the asymmetric distribution of the Y705C mutant was coincident with that of wild-type GlyT2.

Substitution Analysis of Tyr-705—Multiple amino acid substitutions at Tyr-705 showed a comparable, although smaller impairment of plasma membrane localization than that observed for Y705C (Fig. 5*A*). This suggests that the defect in transporter biogenesis is not only due to the introduction of Cys-705 but also due to Tyr-705 removal. Moreover, different Tyr-705 substitutions had heterogeneous effects on glycine transport (Fig. 5*B*). Y705F or Y705A had no or low impact, showing 100 ± 12 and 80 ± 10% of wild-type transport, respectively. By contrast, Y705K and Y705S surpassed wild-type activity by 108 ± 11 and 135 ± 10%, respectively. Remarkably, substitution by glutamic acid (Y705E) profoundly impaired function resulting in 37 ± 4% of wild-type transport. Because transport activity of these mutants does not correlate with membrane expression, Tyr-705 substitutions affect the activity of surface transporters in addition to membrane trafficking.

To further investigate the effect of the cysteine substitution found in the hyperekplexia patients and taking into account that this residue can potentially form disulfide bonds with other cysteines, we performed DTT treatment on cells expressing Tyr-705 mutants. Interestingly, DTT rescued the transport activity of the Y705C mutant from 61 ± 6 to 100 ± 7% of wild-type transport (Fig. 5*B*). As expected, this effect was specific for the Y705C mutant, suggesting that glycine transport activity was restored by reduction of a disulfide bond involving Cys-705. DTT can readily cross the plasma membrane and may affect both transporter trafficking and transport activity. To distinguish between these two possibilities, we used the non-permeant reducing agents MesNa (27) and TCEP (28) (Fig. 5, *C* and *D*). Both reagents consistently produced lower recovery of Y705C function than DTT. This suggests the internal access of the reagent is important for the activation. The small activation produced by the negatively charged MesNa might be due to its decreased reactivity compared with the uncharged TCEP. However, none of the nonpermeant reagents reached the activation produced by DTT. We therefore assumed that DTT can improve a defect in the processing/folding of the transporter during biogenesis, whereas MesNa or TCEP can only "activate" plasma membrane-localized Y705C. Consistent with this theory, Fig. 5*D* shows that MesNa and TCEP promoted higher activation of the Y705C mutant than wild-type GlyT2 or the Y705A mutant.

DTT Increases Plasma Membrane Expression of the Y705C Mutant—Next, we wished to know whether DTT activation targets the intracellular Y705C transporter and increases

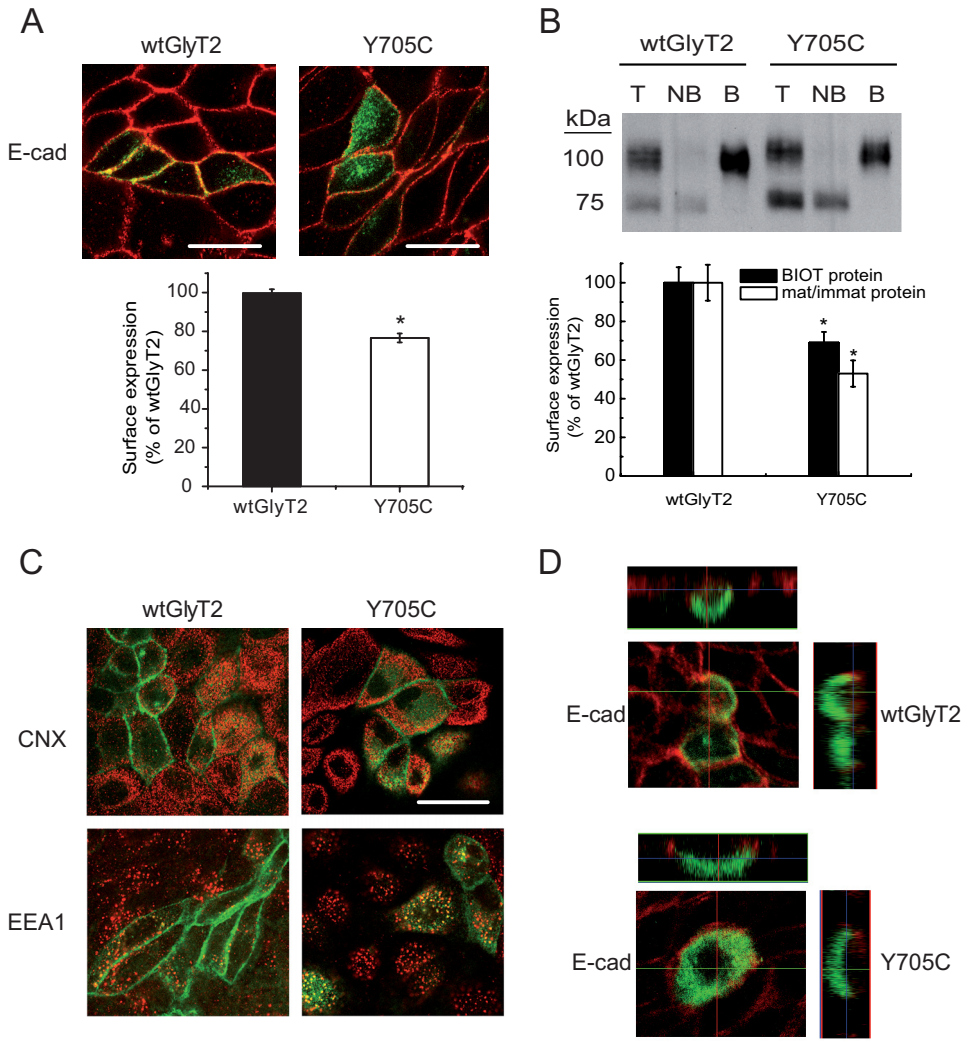

FIGURE 4. **Cell and plasma membrane expression of wild-type GlyT2 and Y705C.** *A*, immunofluorescence quantification of plasma membrane transporters. Wild-type EGFP-tagged GlyT2 or Y705C expressed in MDCK cells for 48 h were immunolabeled for the plasma membrane marker E-cadherin (*E-cad*). Two channel confocal images were obtained (*green* for GlyT2 and *red* for E-cadherin), and regions occupied by E-cadherin were taken as plasma membrane and regions inside the cadherin staining were taken as intracellular, using the Image J ROI manager. After applying an automatic threshold to adjust images, the fluorescence intensity was measured separately for membrane and intracellular regions, and the percentage of transporter in plasma membrane was calculated (histogram). This process was performed at least in 150 cells/condition. *, $p < 0.05$ values calculated using Student's *t* test by comparing wild-type GlyT2 with the Y705C mutant. *B*, COS7 cells expressing wild-type GlyT2 or Y705C mutant were subjected to biotinylation as described under "Experimental Procedures." 8 μg of total (*lanes T*) and nonbiotinylated proteins (*lanes NB*) and 24 μg of biotinylated proteins (*lanes B*) were subjected to Western blotting for GlyT2 detection, and the membranes were reprobed for calnexin immunoreactivity as a loading control. *Lower panel*, densitometric analysis. *Black bars*, total transporter that was biotin-labeled (*B* as a % of *T*) as percentage of that of wild-type GlyT2. *Open bars*, mature/immature transporter ratio (100 kDa/75 kDa) as a percentage of the ratio (100 kDa/75 kDa) for wild-type GlyT2. *, $p < 0.05$ in Student's *t* test. *C*, MDCK cells expressing wild-type EGFP-tagged GlyT2 or Y705C were immunolabeled for calnexin (*CNX*, endoplasmic reticulum marker) or early endosome antigen 1 (*EEA1*, early endosome marker). No significantly difference in co-localization was observed. *D*, MDCK cells transfected with wild-type EGFP-tagged GlyT2 or Y705C were plated on cell culture filter inserts and grown to confluence. Samples were examined by laser scanning confocal microscopy. *Left panel*, en face views. *Right panel*, *x-z* cross-sections. The *x-z* cross-sections are derived from the indicated transept lines.

plasma membrane levels sufficiently to restore the wild-type levels of surface-active GlyT2. For this purpose, we treated COS7 cells expressing wild-type GlyT2 or the Y705C mutant with DTT for increasing periods of time up to 30 min and measured [^{3}H]glycine transport and surface biotinylation in parallel (Fig. 6, *A* and *B*). As shown above, glycine transport by the Y705C mutant was rapidly increased by DTT, reaching wild-type levels of activity in 3–4 min and continuing up to 10 min before reaching a plateau (Fig. 6*A*). A 10-min period has been shown to be sufficient for trafficking to the Golgi of polytopic proteins expressed in mammalian cells (29). We have measured comparable time courses of plasma membrane expression for GlyT2.[3] In fact, extended time periods in DTT increased the amount of surface mutant transporter with a slightly delayed time course. This indicates a fast activation of surface-inserted transporter (5 min) followed by a slower increase in the amount of plasma membrane protein (10–30 min; Fig. 6*B*, *left histogram*). A decrease in the levels of the immature protein was also observed (Fig. 6*B*, *right histogram*). By contrast, the quantity of wild-type GlyT2 present in the plasma membrane was slightly diminished by DTT, and the transport activity was only slightly

[3] E. Arribas-González, P. Alonso-Torres, C. Aragón, and B. López-Corcuera, manuscript in preparation.

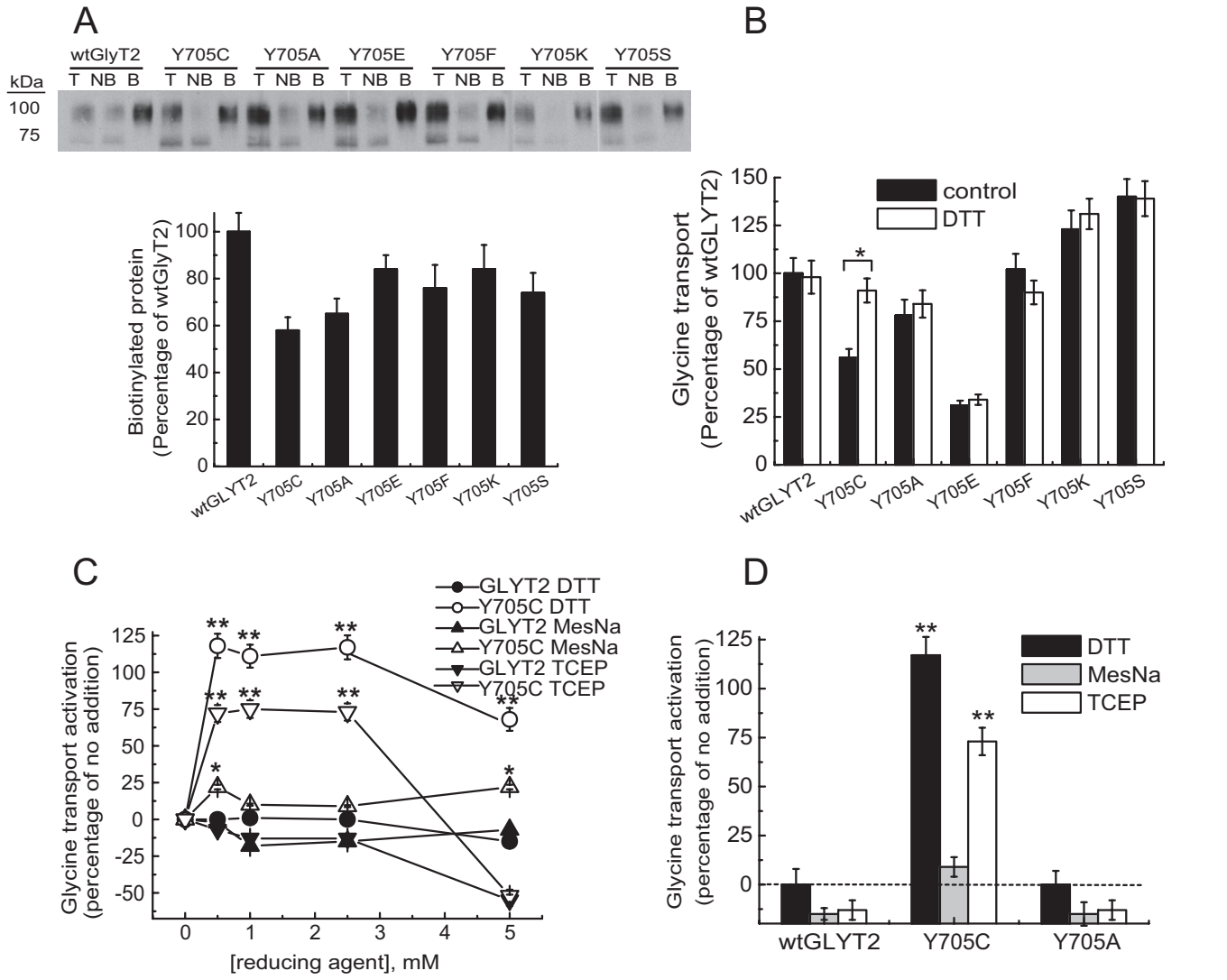

FIGURE 5. **Substitution analysis of Tyr-705 and effect of DTT on glycine transport.** Transiently transfected COS7 cells expressing wild-type GlyT2 or mutants with the indicated amino acids at position 705, were subjected to biotinylation as described in Fig. 4 to determine plasma membrane expression (*A*) or treated with vehicle or 12 mM DTT (*B*) or 2.5 mM DTT (*D*) or the specified concentrations of the indicated reducing agents (*C*) and then assayed for [^{3}H]glycine transport. In *B*, * indicates significantly different from wild-type GlyT2, $p < 0.05$ in Student's *t* test. In *C* and *D*, ** indicates $p < 0.01$, and * indicates $p < 0.05$ by analysis of variance. *Lanes T*, total proteins; *lanes NB*, nonbiotinylated proteins; *lanes B*, biotinylated proteins.

increased. To confirm that DTT can induce Y705C exocytosis, we treated MDCK cells expressing EGFP-tagged transporters with DTT and monitored co-localization with the plasma membrane marker E-cadherin (Fig. 6, *C* and *D*). As shown in Fig. 4*A*, the percentage of Y705C co-localization with the plasma membrane marker was ~65% compared with wild-type GlyT2, and the co-localization was increased by 40% by DTT (Fig. 6*D*).

Y705C Forms an Aberrant Disulfide Bond Interfering with the Cys-311–Cys-320 Pair—One possible explanation of the recovery of Y705C function with DTT could be that Cys-705 forms a disulfide bond with one of the 23 endogenous cysteines present in GlyT2 (Fig. 7*B*). Such a covalent bond could impair glycine transport and/or transporter trafficking. Cleavage of this bond by DTT could restore mutant membrane expression and transport activity. To test this possibility, we took advantage of the predicted external accessibility of Cys-705 and labeled the cells expressing the transporters with the nonpermeable SH-specific reagent MTSEA-biotin (Fig. 7, *A*, *E*, and *F*). This probe reacts with externally accessible free thiol groups in an aqueous environment. In control conditions, the fraction of SH-labeled Y705C mutant was higher than that of wild-type GlyT2 (~2 ± 0.5-fold; Fig. 7, *A* and *E*). Taking into account that the membrane expression of Y705C is ~65% of wild-type GlyT2 (Fig. 4), this means the cysteine specific label is ~3-fold higher in the Y705C mutant than in wild-type GlyT2. In fact, pretreatment with DTT, which increases mutant membrane expression to wild-type levels (Fig. 6), yielded ~3-fold higher labeling for Y705C compared with wild-type GlyT2 (Fig. 7, *A*, *E*, and *F*). This suggests that the Y705C mutation involves structural effects that increase cysteine availability. When the cells were pretreated with *N*-ethylmaleimide in the absence of DTT to prevent SH reagent reaction with the free cysteines, both transporters showed reduced labeling (Fig. 7*A*). Under this condition, the Y705C labeling was ~65% of that of wild-type GlyT2, reflecting lower membrane expression. Moreover, if *N*-ethyl-

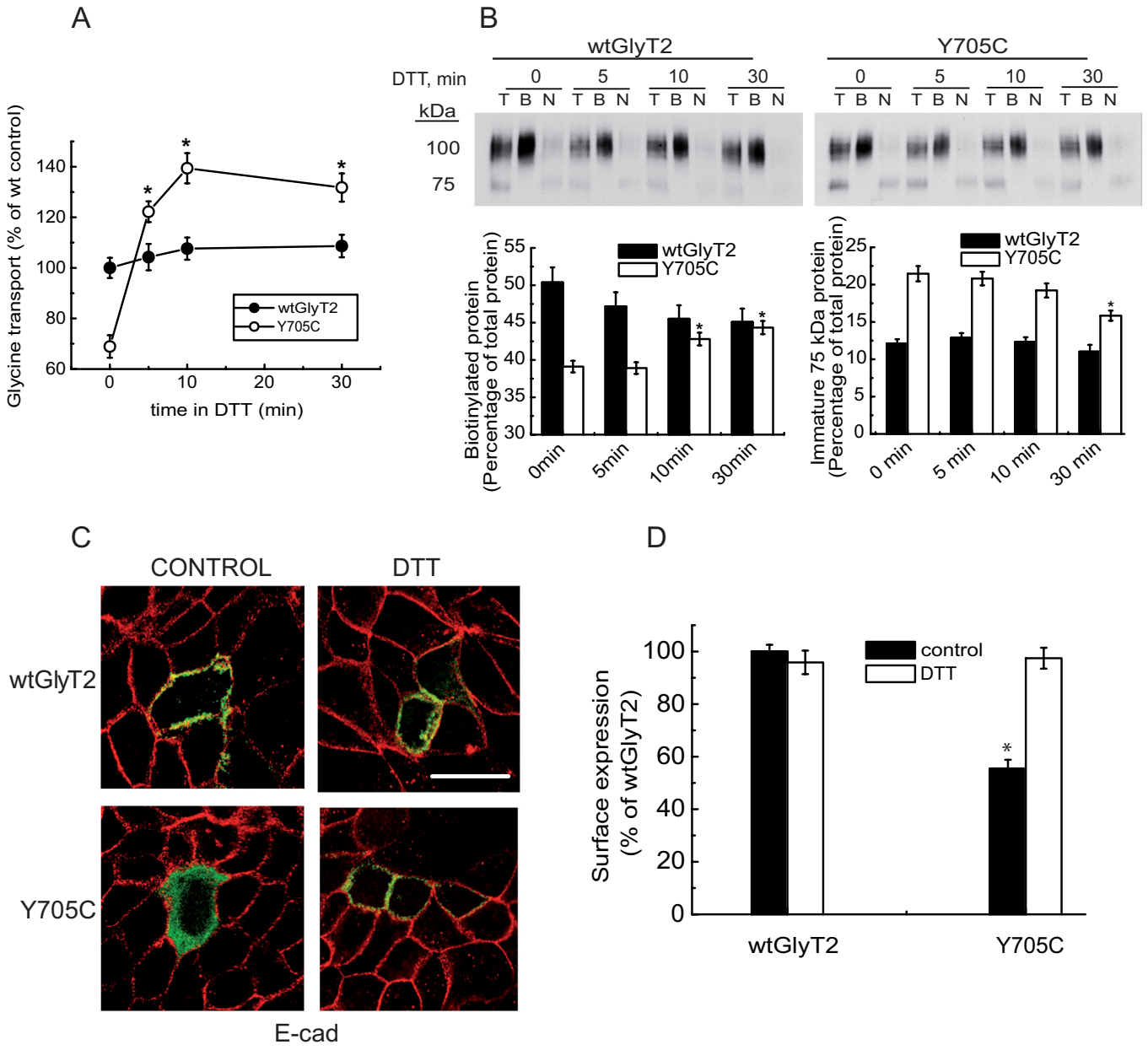

FIGURE 6. **Effect of DTT on Y705C plasma membrane expression.** COS7 cells expressing wild-type GlyT2 or Y705C were treated with 12 mM DTT at 22 °C for the indicated times and then assayed for [^{3}H]glycine transport for 10 min (*A*) or subjected to sulfo-NHS-SS-biotinylation as described under "Experimental Procedures" (*B*). *A*, transport data are expressed as percentages of wild-type GlyT2 transport activity, which was 2.8 ± 0.3 nmol of Gly/mg of protein/10 min. *, significantly different from no DTT, $p < 0.05$ in Student's *t* test. *B*, *upper panel*, Western blot for GlyT2 detection of a SDS-PAGE loaded with 8 μg of total (*lanes T*) and nonbiotinylated proteins (*lanes N*) and 24 μg of biotinylated proteins (*lanes B*). *Lower panel*, densitometric analysis. *, significantly different from no DTT, $p < 0.05$ in Student's *t* test. *C*, MDCK cells expressing wild-type EGFP-tagged GlyT2 or Y705C were treated for 30 min with 12 mM DTT, placed on ice to stop trafficking, and immunolabeled for the plasma membrane marker E-cadherin (*E-cad*). *D*, co-localization of transporter and marker was performed as described for Fig. 4. *, $p < 0.05$ values calculated using Student's *t* test by comparing wild-type GlyT2 with the Y705C mutant.

maleimide pretreatment was performed, and then DTT was added to release cysteines from disulfides, the DTT-induced increase in SH-specific label of the Y705C mutant was higher than that of wild-type GlyT2 (Fig. 7*A*). This result suggests the presence of an additional disulfide bond in the Y705C mutant. To identify the binding partner for Cys-705, we inspected the three-dimensional structure of GlyT2 and selected several cysteine residues based on location that might permit the formation of an intra- or intermolecular disulfide bond with Cys-705 (Fig. 7*B*). Selected cysteines were individually substituted to serine to form Cys → Ser mutants. Single substitutions were introduced into the Cys-705 background to generate double mutants (*CXS/Y705C*), which were tested for DTT activation of glycine transport (Fig. 7, *C* and *D*). Two of the mutants (C311S/Y705C and C320S/Y705C) were activated to a smaller extent than the other mutants (Fig. 7*D*). This result supports a potential interaction between a cysteine at position 705 and cysteines at positions 311 and 320. Accordingly, C311S/Y705C or C320S/Y705C double mutants display a significantly reduced MTSEA-biotin labeling compared with the Y705C mutant, indicating that Cys-705 can interact with either Cys-311 or Cys-320 (Fig. 7, *E* and *F*). Cysteines 311 and 320 are located in the second

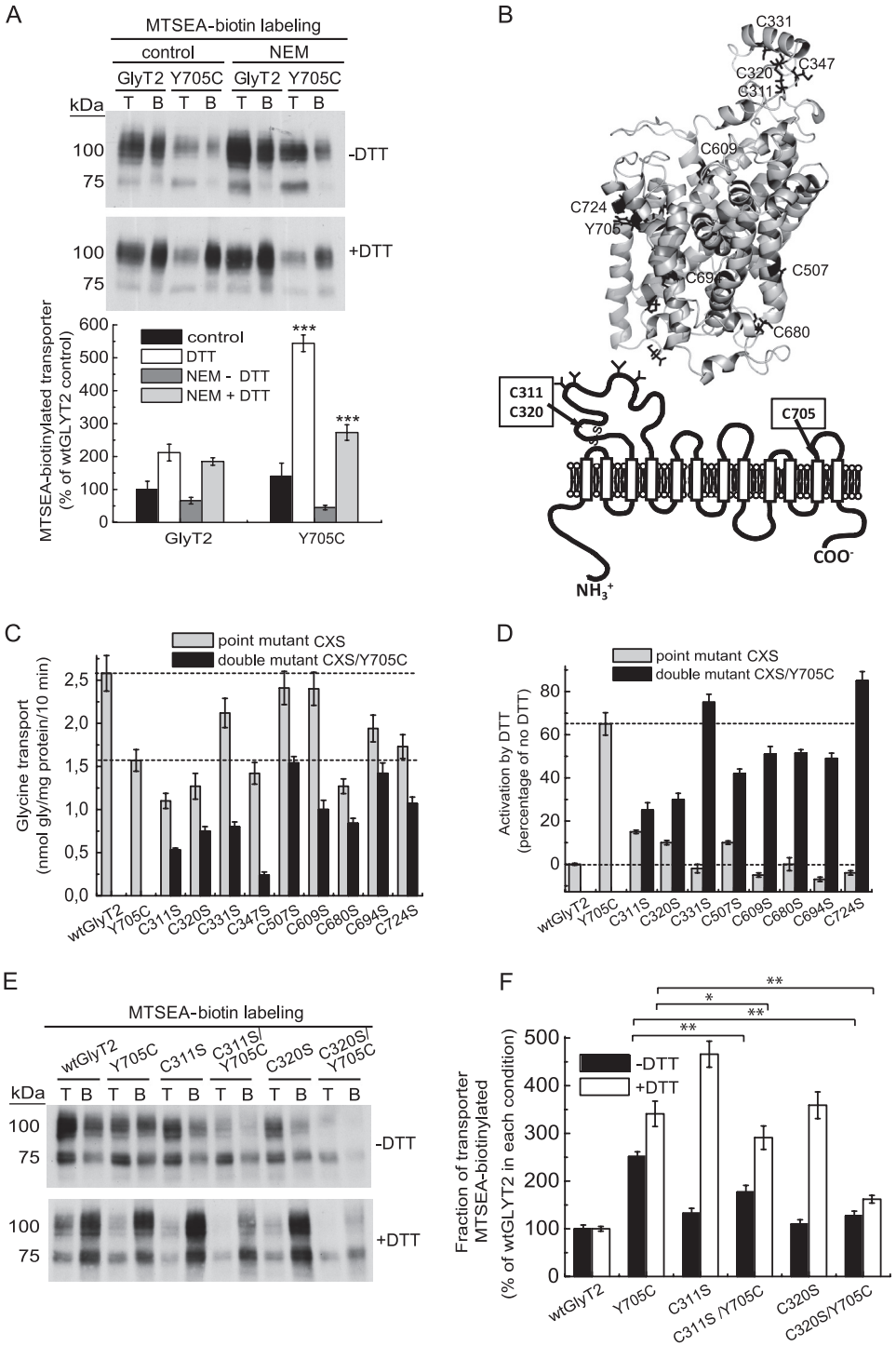

FIGURE 7. **MTSEA-biotin labeling and transport activity of Y705C and GlyT2 cysteine mutants.** *A*, COS7 cells expressing wild-type GlyT2 or Y705C were treated with vehicle or 50 mM *N*-ethylmaleimide (*NEM*) for 10 min, washed, and treated with HBS or 12 mM DTT in HBS for 30 min, washed, and subjected to MTSEA-biotinylation as described under "Experimental Procedures." *Upper panel*, Western blot for GlyT2 detection of a SDS-PAGE loaded with 10 μg of total (*lanes T*) and 100 μg of biotinylated proteins (*lanes B*). *Lower panel*, densitometric analysis of the percentage of total transporter (*B* as a % of *T*) that was MTSEA-biotin-labeled in each condition as percentage of control wild-type GlyT2. ***, Significantly different from wild-type GlyT2, $p < 0.001$ in Student's *t* test. *B*, *upper panel*, molecular model of GlyT2 showing the localization of Tyr-705 and some of the endogenous cysteines (*black*). *Lower panel*, location of the Cys-311–Cys-320 pair in the second external loop as compared with Cys-705 on schematic GlyT2 secondary structure. *C* and *D*, effect of DTT on glycine transport by cysteine to serine mutants in the background of wild-type GlyT2 or the Y705C mutant. COS7 cells expressing wild-type GlyT2, Y705C, cysteine to serine mutants (*CXS*), or Y705C/cysteine to serine double mutants (*CXS/Y705C*) for 48 h were assayed for [^{3}H]glycine transport for 10 min after being treated with vehicle (*C*) or with 12 mM DTT at 22 °C for 5 min (*D*). *E*, COS7 cells expressing the indicated transporters were treated with vehicle (−DTT) or DTT (+DTT) for 30 min, washed, and MTSEA-biotin-labeled; streptavidin-agarose bound proteins were run in nonreducing (−*DTT*) or reducing (+*DTT*) SDS-PAGE and subjected to Western blotting as above. *F*, densitometric analysis of the percentage of total transporter that was MTSEA-biotin-labeled in each condition. For clarity, this was expressed as percentage of the respective wild-type GlyT2 in each condition. Significantly different from the Y705C single mutant: *, $p < 0.05$; **, $p < 0.01$ in Student's *t* test.

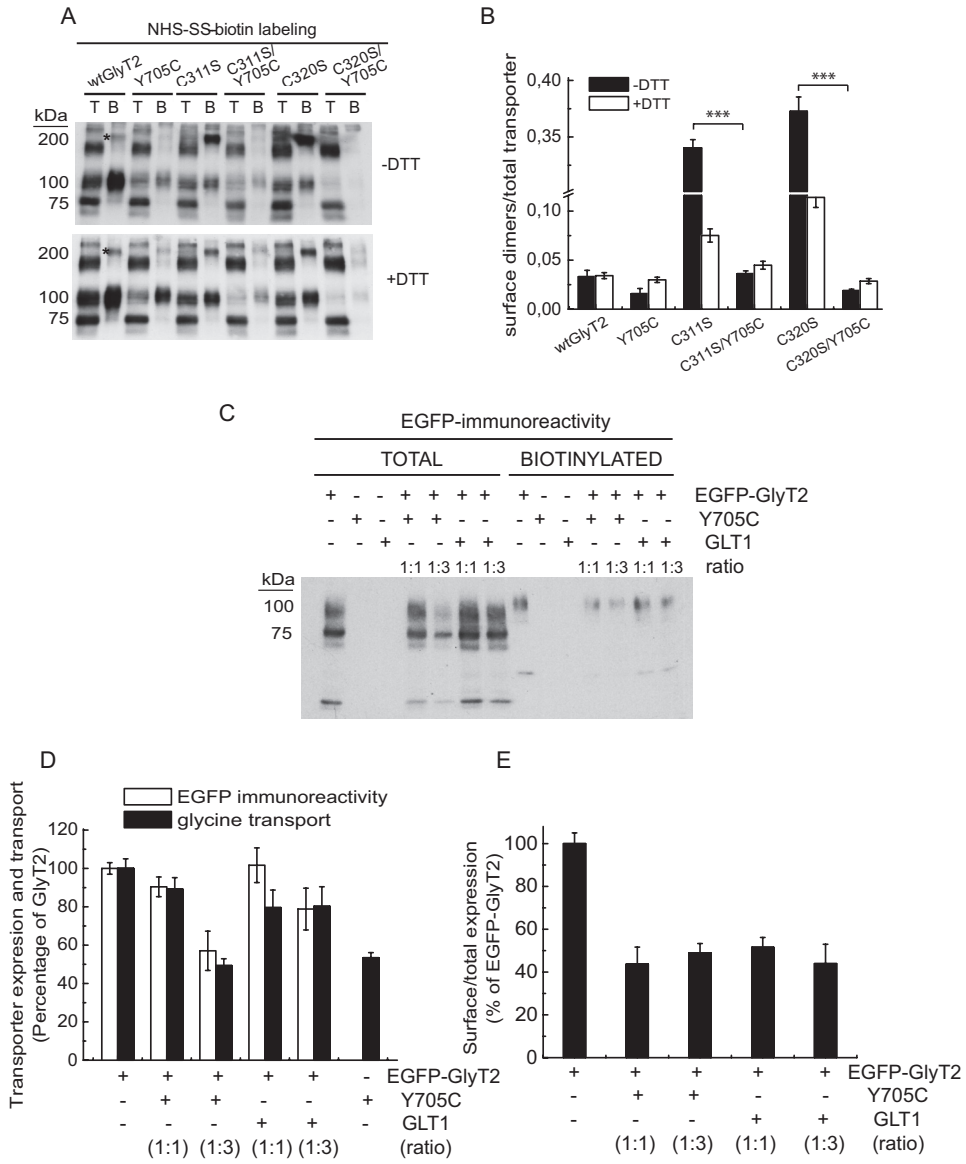

FIGURE 8. **Surface labeling and co-expression of Y705C and GlyT2 cysteine mutants.** *A*, COS7 cells expressing the indicated transporters were treated with vehicle (−*DTT*) or DTT (+*DTT*) for 30 min, washed, and subjected to NHS-SS-biotinylation as in Fig. 4*B*. *Lanes T*, total proteins; *lanes B*, biotinylated proteins. *B*, densitometric analysis of three blots as in *A* showing the immunoreactivity of 200-kDa dimers (*band* marked with *asterisk* in *A*) normalized by the total transporter immunoreactivity. ***, significantly different from the respective single mutant, $p < 0.01$ in Student's *t* test. *C*, effect of wild-type GlyT2 and Y705C on transporter expression. COS7 cells expressing wild-type GlyT2 or Y705C tagged with EGFP as described in Ref. 24 at the indicated ratios (increasing mutant cDNA) were assayed for [^{3}H]glycine transport and in parallel subjected to NHS-SS-biotinylation as described under "Experimental Procedures" except anti-EGFP antibody was used for the Western blots. *D*, effect of the expression of Y705C on EGFP-GlyT2 expression (densitometric analysis of blots as in *C*) and transport activity. *E*, effect of the expression of Y705C on EGFP-GlyT2 surface expression.

external loop (EL2) of GlyT2 (Fig. 7*B*). This region cannot currently be accurately modeled because of significant divergence in sequence and length compared with $LeuT_{Aa}$ (18, 21). However, equivalent conserved cysteines have been shown to form a disulfide bond in other members of the SLC6 family (30, 31). Unexpectedly, although C311S and C320S mutants should both have a single unpaired extracellular cysteine like Y705C, they have much lower cysteine labeling in the absence of DTT. In addition, they display very high MTSEA-biotin label after DTT treatment (Fig. 7, *E* and *F*). This unexpected result made us consider the possibility that the unpaired cysteine from the Cys-311–Cys-320 disulfide might form a disulfide bond with another monomer, creating disulfide-linked dimers. Fig. 8*A* shows that C311S and C320S mutants form disulfide-mediated dimers on the cell surface (band indicated by an *asterisk*), which are cleaved to monomers in the double C311S/Y705C or C320S/Y705C mutants. This reinforces the evidence that Cys-705 interacts with Cys-311 and Cys-320 (Fig. 8*B*).

A further relevant question is whether the trafficking defect of Y705C affects the expression of wild-type GlyT2. To answer this, we co-expressed wild-type and mutant GlyT2 differentially tagged with EGFP (Fig. 8*C*). The Y705C mutant reduces total wild-type GlyT2 expression by 10–20% when expressed at 1:1 ratio. This is comparable with the effect of a nonrelevant protein, the glutamate transporter GLT1 (Fig. 8*D*). At a higher GlyT2-Y705C ratio (1:3), a slight reduction of GlyT2 expression by the Y705C mutant was observed, although this effect was not due to a reduced delivery to the plasma membrane (Fig. 8*E*). Moreover, wild-type GlyT2 co-

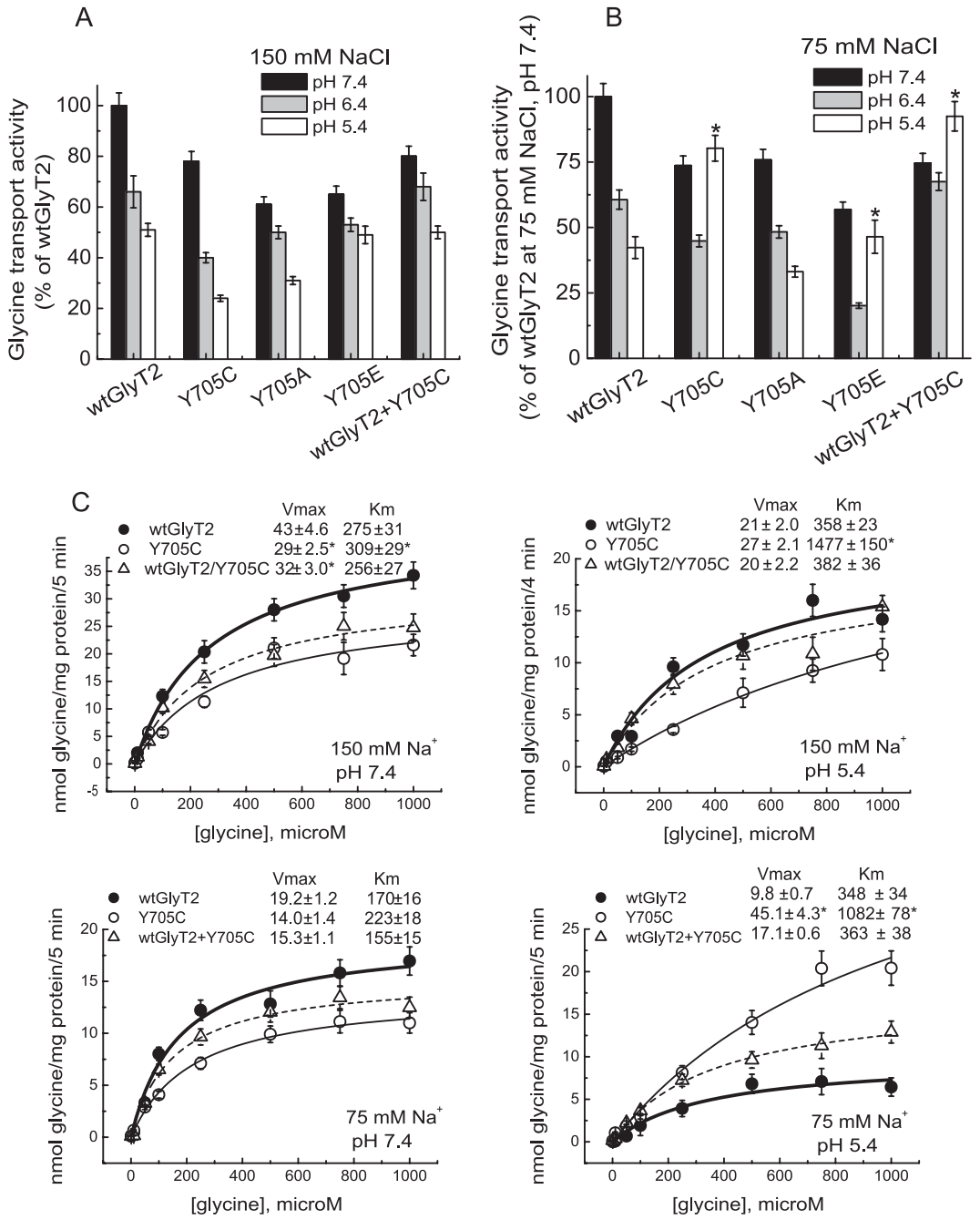

FIGURE 9. **Effect of pH on glycine transport by wild-type GlyT2 and the Tyr-705 mutant.** Transiently transfected COS7 cells expressing wild-type GlyT2 or mutants with the indicated amino acid substitutions at position 705 were assayed for [^{3}H]glycine transport for 5 min in HBS containing 150 (*A* and *C*) or 75 (*B* and *C*) mM NaCl at 10 μM or the indicated final glycine concentration and pH. Control GlyT2 transport values at pH 7.4 were 1.4 $\pm$ 0.2 and 0.73 $\pm$ 0.1 nmol of Gly/mg of protein/5 min at 150 and 75 mM NaCl, respectively. Mean pH change was significantly different from wild-type GlyT2. *, $p < 0.05$ by analysis of variance with Dunnett's post hoc test. *C*, kinetics of glycine transport at low pH. COS7 cells expressing wild-type GlyT2, the Y705C mutant, or the indicated combination of the respective cDNAs were assayed for [^{3}H]glycine transport at pH 7.4 or 5.4 for 5 min in HBS containing 150 or 75 mM NaCl and glycine concentrations increasing from 0.5 μM to 1 mM. Experimental data were fitted to hyperbolae. The kinetic parameters are indicated on the graphs. Mean pH change significantly different from wild-type GlyT2. *, $p < 0.05$ in Student's *t* test.

expressed with Y705C reduces the expression of the mutant by ~10–20% (data not shown). These results indicate that the traffic defect of the Y705C mutant is not dominant when it is co-expressed at the same dose as wild-type GlyT2.

H^+ Dependence of Glycine Transport Is Inverted in the Y705C Mutant—According to the above data, DTT is likely to disrupt an aberrant disulfide bond in the Y705C mutant. This facilitates exocytosis and induces the emergence of the mutant transporter on the cell surface. In addition, the Y705C substitution predicts the introduction of a local negative charge on the surface of the transporter because of the more acidic nature of the cysteine side chain (pK_a of 8.3 *versus* 10.3 for tyrosine). Because the protonation state of protein ionizable groups is dependent on pH, we tested the pH dependence of Tyr-705 mutants containing titratable side chains (Fig. 9). In agreement with published data on GABA transporters (32, 33), wild-type GlyT2 is

inhibited at low pH, showing ~50–60% transport activity at pH 5.4. The inhibition was even higher when assayed in low external sodium (Fig. 9, *A* and *B*). This is in agreement with the proposed competition of the two cations in the external transporter vestibule (32, 33). When the assay was performed at the physiological NaCl concentration (150 mM), the wild-type response to low pH was also observed for the Y705C, Y705E, and Y705A mutants (Fig. 9*A*). However, lowering the external pH in the presence of low NaCl concentrations (75 mM) produced a differential response in the Y705C and Y705E mutants. They became activated at pH 5.4 instead of inhibited, indicating an altered proton dependence of transport in these Tyr-705 substitutions (Fig. 9*B*). Furthermore, the pH dependence of wild-type GlyT2 co-transfected at a 1:1 cDNA ratio with the Y705C mutant resembled that of the mutant rather than wild-type GlyT2. This suggests a dominant phenotype for Y705C (Fig. 9, *A* and *B*). Therefore, we characterized the transport kinetics at acidic pH (Fig. 9*C*). The Y705C mutant had increased V_{max} at pH 5.4 when expressed alone and in co-expression with wild-type, especially at low sodium. This is in contrast to wild-type GlyT2 that showed a ~50% reduction in V_{max} value at acidic *versus* neutral pH. In addition, a general increase in K_m at low pH was observed for all the transporters. This was more pronounced for Y705C and the co-expression, especially at low sodium (~2-, 5-, and 2.5-fold for wild-type GlyT2, Y705C, and Y705C+wild-type GlyT2, respectively). Taken together, these data indicate that the Y705C mutation in GlyT2 induces an altered response to proton modulation of glycine transport.

Y705C Mutant Is Partially Resistant to Zn^{2+} Inhibition of Glycine Transport—Protons and metal transition dications are competitive inhibitors of several crucial mediators of glycinergic neurotransmission, such as the glycine receptor (34–36) and the glycine transporter GlyT1 (37, 38). Because H^+ and Zn^{2+} frequently bind to overlapping intersubunit sites (39–41), and the binding of transition dications can induce cysteine deprotonation (42), we tested the effect of Y705C substitution on the sensitivity of GlyT2 to Zn^{2+}. Although GlyT2 is not very sensitive to this cation (38), we observed a low but significant inhibition of GlyT2 transport by Zn^{2+} (Fig. 10). As expected, we found that Zn^{2+} sensitivity of wild-type transport was pH-dependent, being higher at pH 7.4 than 5.4, in agreement with the competitive nature of H^+ and Zn^{2+} inhibition (35, 38, 39). By contrast, the inhibition by Zn^{2+} of the Y705C mutant was much less sensitive to the presence of protons and slightly more pronounced at acidic pH. As expected from the proton response shown above, the co-expression of wild-type GlyT2 and the Y705C mutant also resulted in Y705C behavior, confirming a dominant phenotype (Fig. 10*A*). Fig. 10*B* shows that the IC_{50} for Zn^{2+} inhibition of wild-type GlyT2 was significantly increased at acidic pH from 63 ± 10 at pH 7.4 to 466 ± 42 μM at pH 5.4. By contrast, the Y705C mutant had IC_{50} values of 100 ± 15 and 189 ± 19 μM at these same pH values. The co-expressed wild-type GlyT2 and Y705C mutant displayed IC_{50} values of 99 ± 10 and 198 ± 22 μM, which are close to those of Y705C mutants. Further kinetic analysis of glycine transport in the presence of Zn^{2+} showed a significantly lower decrease in the V_{max} of transport by the Y705C-containing transporters than for wild-type GlyT2. In addition, a higher increase in K_m was observed. These data confirm the reduced sensitivity of Y705C-containing glycine transporters to Zn^{2+} inhibition (Fig. 10*C*).

DISCUSSION

We have identified a novel missense mutation in *SLC6A5*, encoding GlyT2, present in eight individuals from three families in two cohorts of hyperekplexia patients from Spain and the United Kingdom. The mutation results in a tyrosine to cysteine substitution at residue 705 (Y705C) in transmembrane domain 11 (TM11). This change was found in the heterozygous state in all positive cases suggesting a dominant mode of inheritance. This contrasts with the majority of the previously characterized GlyT2 mutations that were inherited in a recessive or compound heterozygous state (11). Y705C-harboring patients show significant variability in clinical presentation. As well as classical hyperekplexia symptoms, certain individuals exhibited abnormal respiration, facial dysmorphism, delayed motor development, or intellectual disability. This may be due to a complex phenotype caused by the mutation or to the presence of additional unknown mutations or modifiers. However, no other potential disease-causing mutations were detected in *SLC6A5*. Study of the biochemical properties of the mutant transporter in cultured cells revealed that the introduced cysteine affects several aspects of transporter biochemistry. These include impaired transporter protein maturation through the secretory pathway and an alteration of H^+ and Zn^{2+} dependence of glycine transport. The latter feature constitutes a dominant effect, because it is observed when the mutant is expressed alone and also when mutant and wild-type transporters are co-expressed.

The Y705C substitution introduces a free thiol in the place of a hydroxyl-containing side chain. Thiol labeling with impermeant cysteine MTS reagents confirmed that Cys-705 is accessible from the exterior of the plasma membrane, as predicted by molecular modeling. Therefore, the Y705C mutant exposes the introduced cysteine to the lumen of the secretory pathway cisternae during trafficking. This seems to be detrimental for transporter biogenesis, because Y705C has reduced expression at the plasma membrane, together with a higher proportion of immature precursor compared with wild-type GlyT2. This is in agreement with recent reports indicating that polymorphisms containing an uneven number of cysteine residues in extracellular loops impair the expression of G-protein-coupled receptors and other plasma membrane proteins. This feature has frequently been associated with disease states (29, 43–45). Restoration of Y705C membrane expression to wild-type levels with the permeable thiol reagent DTT and experiments using SH-specific and surface labeling of cells expressing the transporters suggest that Cys-705 is involved in aberrant disulfide bond formation. Cys-705 binding partners are either of two EL2 cysteines that are likely to form a disulfide bond in wild-type GlyT2 (C311-C320 pair) (30, 31). This interference is probably conformation-dependent, because EL2 may approach TM11 during the inward-facing conformation (46). Disruption of this aberrant bond with reducing agents may facilitate plasma membrane arrival and/or the conformational movements needed for transport in the surface-resident transporter. How-

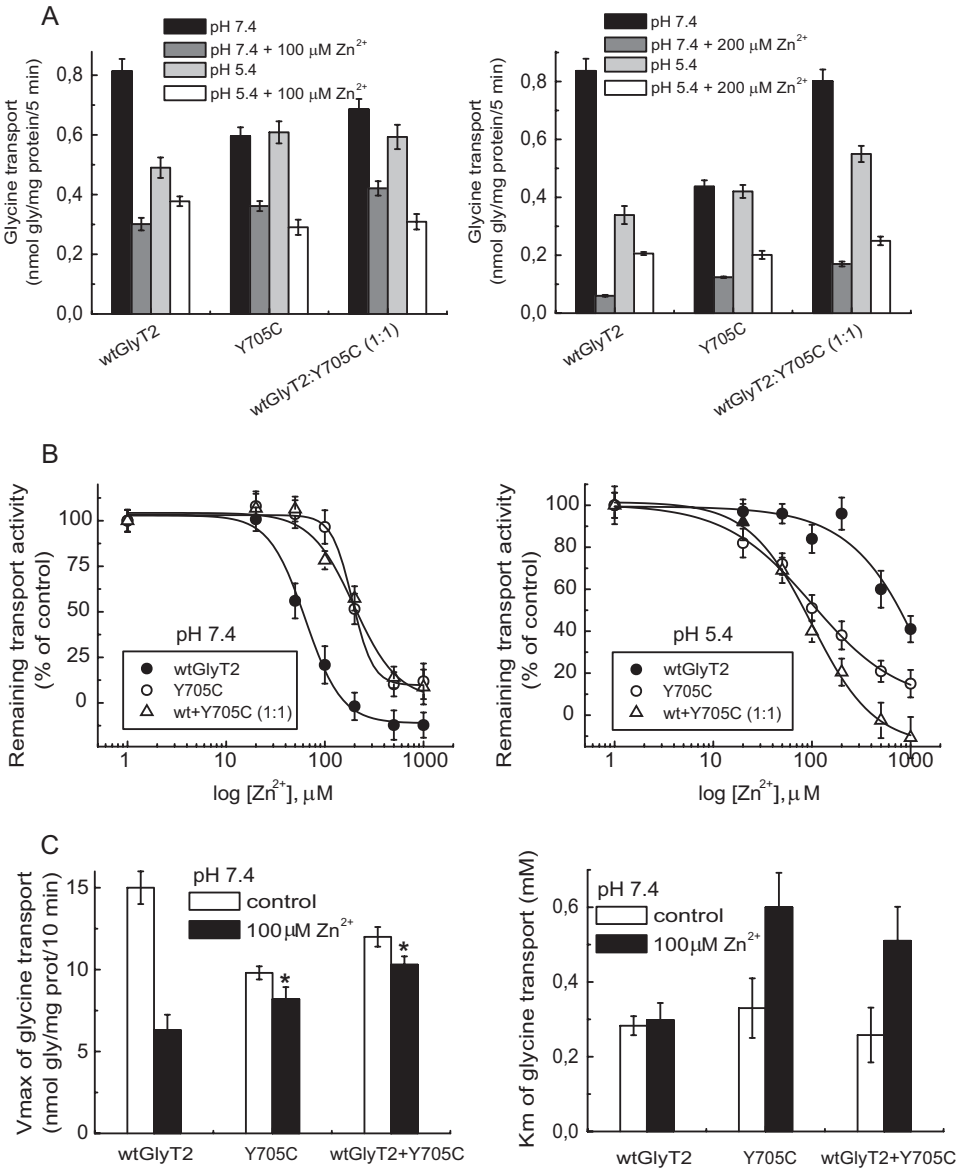

FIGURE 10. **Effect of Zn^{2+} on glycine transport by wild-type GlyT2 and the Y705C mutant.** Transiently transfected COS7 cells expressing wild-type GlyT2, the Y705C mutant, or the indicated combinations of the respective cDNAs were assayed for [^{3}H]glycine transport for 5 min in HBS containing 75 mM NaCl at the indicated pH and 10 μM final glycine concentration (*A* and *B*) or increasing glycine concentrations (*C*) in the presence of the indicated ZnCl concentrations (*A–C*). NaCl was isotonically substituted by choline chloride. *B*, dose-response data were fit to logistic curves. *C*, transport data were fitted to hyperbolae, and kinetic parameters were obtained from the best fit. Mean change significantly different from wild-type GlyT2. *, $p < 0.05$ in Student's *t* test.

ever, it is not clear whether Y705C expression is lower because a proper disulfide bridge cannot be formed or because the aberrant disulfide bond distorts the protein structure, because both conditions are present in Y705C. The single C311S and C320S mutants show approximately half the membrane expression of wild-type GlyT2, suggesting that the lack of the endogenous disulfide bond is detrimental for surface expression. However, the unusual behavior of these mutants prevents us from drawing clear conclusions. The fact that Y705C and wild-type GlyT2 are differentially sensitive to low concentrations of reducing agents but are inhibited by higher concentrations (Fig. 5*C* and data not shown) suggests that the aberrant disulfide bond involving Cys-705 is more sensitive to cleavage than the Cys-311–Cys-320 disulfide bond. The recovery of the expression in the Y705C mutant might be due to the cleavage of aberrant disulfide bonds without affecting the Cys-311–Cys-320 pairing. It is also possible that GlyT2 requires disulfide-mediated dimerization for plasma membrane expression as has been suggested for other SLC6 transporters (31) and that this process is disrupted by the Y705C mutation. Because GlyT2 multimerization has been proposed to be required for plasma membrane localization (47), this is an issue that will require further study.

The Y705C substitution is also predicted to introduce a local negative charge at the transporter surface. The endogenous Tyr-705 residue with a typical pK_a value of ~10.3 would be mostly protonated at physiological pH. By contrast, the side chain of Cys-705 would, in theory, be also protonated, but the more acidic pK_a value (close to 8.3) makes the probability of ionization higher than for the tyrosine side chain. In addition, a high dielectric medium favors cysteine deprotonation, whereas

a low dielectric medium favors the protonated state (42). Because Cys-705 is extracellular, it is therefore likely to be in a high dielectric environment. Deprotonation is also favored by the presence of transition metal dications, which may perform a metal-assisted deprotonation of cysteine side chains, especially if bound to polarizable ligands (42). Other factors such as the possible hydrogen-bonding network including the cysteine may affect the pK_a (48). All of these factors may drive Cys-705 to be deprotonated at physiological pH. By contrast, acidic pH may displace the equilibrium toward the protonated form. GlyT2 transport activity seems to be sensitive to the protonation state of Cys-705, and protonation may activate the mutant transporter. Therefore, although glycine transport by wild-type GlyT2 is inhibited at low pH, the Y705C mutant is resistant to this inhibition.

Functional analysis of the Y705C mutant has revealed the existence of an unexpected fine-tuning mechanism of glycine transport by external H^+, with Tyr-705 playing a central role. Interestingly, the GlyR is also inhibited by protons and the proton-binding site also involves a hydroxyl-containing residue (Thr-112), which when substituted by a tyrosine (but not by a neutral amino acid) preserves the H^+ sensitivity of the receptor (49). Both Tyr-705 in GlyT2 and Thr-112 in GlyRs are highly conserved. A threonine is found at the equivalent position in all pH-sensitive GlyR, $GABA_A$, and $GABA_C$ receptors. Equally, a Tyr-705 equivalent is found in many SLC6 family members, suggesting that this tyrosine might have a general role in pH sensitivity of Na^+-and Cl^--dependent neurotransmitter transporters. The location of Tyr-705 in an extracellular accessible region of the transporter would fulfill one of the prerequisites for H^+-binding sites, which are usually located outside the membrane electric field (49, 50). Proton and transition dication binding sites are usually overlapping in pH- and Zn^{2+}-sensitive proteins (34–36, 38). In the GlyR, Thr-112 also forms part of the group of crucial residues involved in regulation by Zn^{2+} (35). In several plasma membrane proteins present in inhibitory synapses, H^+/Zn^{2+}-binding sites are contributed by several adjacent subunits (35, 49, 51, 52). This structural requirement might also hold true for GlyT2 and would sustain the dominant nature of the aberrant pH sensitivity and Zn^{2+} dependence of the Y705C mutant co-expressed with wild-type GlyT2.

In summary, we have identified a novel missense mutation in GlyT2 associated with hyperekplexia and described altered biochemical properties of the mutant transporter. The Y705C mutation affects several aspects of transporter biochemistry including impaired transporter protein maturation through the secretory pathway and an alteration of H^+ and Zn^{2+} dependence of glycine transport. Any of these features may contribute to the etiology of the disease. In addition to effects in pathophysiological conditions such as inflammation and ischemia, transient changes in extracellular pH occur under physiological conditions. For example, in synaptic transmission, the acidic contents of transmitter vesicles cause an extracellular acid shift within the synaptic cleft (53, 54) and may reduce the local Na^+ concentration. Different sources of protons have been suggested in the synapse: acidic contents after vesicle fusion, incorporation of the vesicular ATPase to the plasma membrane, or extrasynaptic sources such as H^+ ion exchangers and voltage-gated H^+ conductances (51). These pH changes are especially relevant during repetitive electrical stimulation that may produce acid shifts of ~30 s in duration (53). Acidification reduces the duration of glycinergic synaptic currents and accelerates desensitization of the receptor significantly affecting the kinetics of glycinergic neurotransmission (54). Increased external pH potentiated, whereas decrease inhibited both the amplitude and frequency of glycinergic miniature inhibitory postsynaptic potential currents, suggesting the involvement of both presynaptic and postsynaptic mechanisms (54). In addition, Zn^{2+} is highly enriched in synaptic vesicles, from which it can be co-released with glutamate in an activity-dependent manner (36). Zn^{2+} modulates both current responses mediated by excitatory and inhibitory neurotransmitter receptors and the efficacy of transporter-driven neurotransmitter reuptake (55). We hypothesize that Y705C mutant may alter the kinetics of glycinergic inhibition by taking up glycine when the transporter is supposed to be inhibited by synaptic H^+ or Zn^{2+}. This may disrupt the coordination of neurotransmitter release and subsequent reuptake, leading to a damaging effect, mainly during repetitive firing. In addition, the mutant transport activity, which is resistant to two "natural" synaptic inhibitors, may prevent or dampen the interaction of glycine with GlyRs by simple competition. Finally, defective trafficking of the mutant may reduce the uptake of glycine at neutral pH, thus reducing the availability of transmitter in the terminal for synaptic vesicle loading. Future work performed in neuronal preparations will reveal to what extent glycinergic neurotransmission is impaired by the Y705C mutation.

Acknowledgments—We acknowledge the expert technical assistance of the confocal microscopy facility at the Centro de Biología Molecular "Severo Ochoa" (Madrid, Spain). Carlos Ernesto Fernández García is also acknowledged.

REFERENCES

1. Aragón, C., and López-Corcuera, B. (2003) Structure, function and regulation of glycine neurotransporters. *Eur. J. Pharmacol.* **479,** 249–262
2. Gomeza, J., Hülsmann, S., Ohno, K., Eulenburg, V., Szöke, K., Richter, D., and Betz, H. (2003) Inactivation of the glycine transporter 1 gene discloses vital role of glial glycine uptake in glycinergic inhibition. *Neuron* **40,** 785–796
3. Aragón, C., and López-Corcuera, B. (2005) Glycine transporters. Crucial roles of pharmacological interest revealed by gene deletion. *Trends Pharmacol. Sci.* **26,** 283–286
4. Gomeza, J., Ohno, K., Hülsmann, S., Armsen, W., Eulenburg, V., Richter, D. W., Laube, B., and Betz, H. (2003) Deletion of the mouse glycine transporter 2 results in a hyperekplexia phenotype and postnatal lethality. *Neuron* **40,** 797–806
5. Gomeza, J., Ohno, K., and Betz, H. (2003) Glycine transporter isoforms in the mammalian central nervous system. Structures, functions and therapeutic promises. *Curr. Opin. Drug Discov. Devel.* **6,** 675–682
6. Harvey, R. J., Topf, M., Harvey, K., and Rees, M. I. (2008) The genetics of hyperekplexia. More than startle!. *Trends Genet.* **24,** 439–447
7. Andermann, F., Keene, D. L., Andermann, E., and Quesney, L. F. (1980) Startle disease or hyperekplexia. Further delineation of the syndrome. *Brain* **103,** 985–997
8. Rees, M. I., Harvey, K., Pearce, B. R., Chung, S. K., Duguid, I. C., Thomas, P., Beatty, S., Graham, G. E., Armstrong, L., Shiang, R., Abbott, K. J., Zuberi, S. M., Stephenson, J. B., Owen, M. J., Tijssen, M. A., van den Maagdenberg, A. M., Smart, T. G., Supplisson, S., and Harvey, R. J. (2006) Mutations in the gene encoding GlyT2 (*SLC6A5*) define a presynaptic

component of human startle disease. *Nat. Genet.* **38,** 801–806
9. Rees, M. I., Harvey, K., Ward, H., White, J. H., Evans, L., Duguid, I. C., Hsu, C. C., Coleman, S. L., Miller, J., Baer, K., Waldvogel, H. J., Gibbon, F., Smart, T. G., Owen, M. J., Harvey, R. J., and Snell, R. G. (2003) Isoform heterogeneity of the human gephyrin gene (*GPHN*), binding domains to the glycine receptor, and mutation analysis in hyperekplexia. *J. Biol. Chem.* **278,** 24688–24696
10. Harvey, R. J., Depner, U. B., Wässle, H., Ahmadi, S., Heindl, C., Reinold, H., Smart, T. G., Harvey, K., Schütz, B., Abo-Salem, O. M., Zimmer, A., Poisbeau, P., Welzl, H., Wolfer, D. P., Betz, H., Zeilhofer, H. U., and Müller, U. (2004) GlyR α3. An essential target for spinal PGE_2-mediated inflammatory pain sensitization. *Science* **304,** 884–887
11. Chung, S. K., Vanbellinghen, J. F., Mullins, J. G., Robinson, A., Hantke, J., Hammond, C. L., Gilbert, D. F., Freilinger, M., Ryan, M., Kruer, M. C., Masri, A., Gurses, C., Ferrie, C., Harvey, K., Shiang, R., Christodoulou, J., Andermann, F., Andermann, E., Thomas, R. H., Harvey, R. J., Lynch, J. W., and Rees, M. I. (2010) Pathophysiological mechanisms of dominant and recessive *GLRA1* mutations in hyperekplexia. *J. Neurosci.* **30,** 9612–9620
12. Eulenburg, V., Becker, K., Gomeza, J., Schmitt, B., Becker, C. M., and Betz, H. (2006) Mutations within the human GLYT2 (*SLC6A5*) gene associated with hyperekplexia. *Biochem. Biophys. Res. Commun.* **348,** 400–405
13. Yamashita, A., Singh, S. K., Kawate, T., Jin, Y., and Gouaux, E. (2005) Crystal structure of a bacterial homologue of Na^+/Cl^--dependent neurotransmitter transporters. *Nature* **437,** 215–223
14. Haliassos, A., Chomel, J. C., Tesson, L., Baudis, M., Kruh, J., Kaplan, J. C., and Kitzis, A. (1989) Modification of enzymatically amplified DNA for the detection of point mutations. *Nucleic Acids Res.* **17,** 3606
15. Larkin, M. A., Blackshields, G., Brown, N. P., Chenna, R., McGettigan, P. A., McWilliam, H., Valentin, F., Wallace, I. M., Wilm, A., Lopez, R., Thompson, J. D., Gibson, T. J., and Higgins, D. G. (2007) Clustal W and Clustal X version 2.0. *Bioinformatics* **23,** 2947–2948
16. Ramensky, V., Bork, P., and Sunyaev, S. (2002) Human non-synonymous SNPs. Server and survey. *Nucleic Acids Res.* **30,** 3894–3900
17. Sali, A., and Blundell, T. L. (1993) Comparative protein modelling by satisfaction of spatial restraints. *J. Mol. Biol.* **234,** 779–815
18. Pérez-Siles, G., Morreale, A., Leo-Macías, A., Pita, G., Ortíz, A. R., Aragón, C., and López-Corcuera, B. (2011) Molecular basis of the differential interaction with lithium of glycine transporters GLYT1 and GLYT2. *J. Neurochem.* **118,** 195–204
19. Fornés, A., Núñez, E., Aragón, C., and López-Corcuera, B. (2004) The second intracellular loop of the glycine transporter 2 contains crucial residues for glycine transport and phorbol ester-induced regulation. *J. Biol. Chem.* **279,** 22934–22943
20. Pérez-Siles, G., Núñez, E., Morreale, A., Jiménez, E., Leo-Macías, A., Pita, G., Cherubino, F., Sangaletti, R., Bossi, E., Ortíz, A. R., Aragón, C., and López-Corcuera, B. (2012) An aspartate residue in the external vestibule of GLYT2 (glycine transporter 2) controls cation access and transport coupling. *Biochem. J.* **442,** 323–334
21. Jiménez, E., Zafra, F., Pérez-Sen, R., Delicado, E. G., Miras-Portugal, M. T., Aragón, C., and López-Corcuera, B. (2011) P2Y purinergic regulation of the glycine neurotransmitter transporters. *J. Biol. Chem.* **286,** 10712–10724
22. Núñez, E., Pérez-Siles, G., Rodenstein, L., Alonso-Torres, P., Zafra, F., Jiménez, E., Aragón, C., and López-Corcuera, B. (2009) Subcellular localization of the neuronal glycine transporter GLYT2 in brainstem. *Traffic* **10,** 829–843
23. Fornés, A., Núñez, E., Alonso-Torres, P., Aragón, C., and López-Corcuera, B. (2008) Trafficking properties and activity regulation of the neuronal glycine transporter GLYT2 by protein kinase C. *Biochem. J.* **412,** 495–506
24. de Juan-Sanz, J., Zafra, F., López-Corcuera, B., and Aragón, C. (2011) Endocytosis of the neuronal glycine transporter GLYT2. Role of membrane rafts and protein kinase C-dependent ubiquitination. *Traffic* **12,** 1850–1867
25. López-Corcuera, B., Martínez-Maza, R., Núñez, E., Roux, M., Supplisson, S., and Aragón, C. (1998) Differential properties of two stably expressed brain-specific glycine transporters. *J. Neurochem.* **71,** 2211–2219
26. Martínez-Maza, R., Poyatos, I., López-Corcuera, B., Núñez, E., Giménez, C., Zafra, F., and Aragón, C. (2001) The role of *N*-glycosylation in transport to the plasma membrane and sorting of the neuronal glycine transporter GLYT2. *J. Biol. Chem.* **276,** 2168–2173
27. Dunn, S. M., Conti-Tronconi, B. M., and Raftery, M. A. (1986) Acetylcholine receptor dimers are stabilized by extracellular disulfide bonding. *Biochem. Biophys. Res. Commun.* **139,** 830–837
28. Hepojoki, J., Strandin, T., Vaheri, A., and Lankinen, H. (2010) Interactions and oligomerization of hantavirus glycoproteins. *J. Virol.* **84,** 227–242
29. Petäjä-Repo, U. E., Hogue, M., Bhalla, S., Laperrière, A., Morello, J. P., and Bouvier, M. (2002) Ligands act as pharmacological chaperones and increase the efficiency of delta opioid receptor maturation. *EMBO J.* **21,** 1628–1637
30. Chen, J. G., Liu-Chen, S., and Rudnick, G. (1997) External cysteine residues in the serotonin transporter. *Biochemistry* **36,** 1479–1486
31. Chen, R., Wei, H., Hill, E. R., Chen, L., Jiang, L., Han, D. D., and Gu, H. H. (2007) Direct evidence that two cysteines in the dopamine transporter form a disulfide bond. *Mol. Cell Biochem.* **298,** 41–48
32. Forlani, G., Bossi, E., Ghirardelli, R., Giovannardi, S., Binda, F., Bonadiman, L., Ielmini, L., and Peres, A. (2001) Mutation K448E in the external loop 5 of rat GABA transporter rGAT1 induces pH sensitivity and alters substrate interactions. *J. Physiol.* **536,** 479–494
33. Grossman, T. R., and Nelson, N. (2003) Effect of sodium lithium and proton concentrations on the electrophysiological properties of the four mouse GABA transporters expressed in *Xenopus* oocytes. *Neurochem. Int.* **43,** 431–443
34. Lynch, J. W., Jacques, P., Pierce, K. D., and Schofield, P. R. (1998) Zinc potentiation of the glycine receptor chloride channel is mediated by allosteric pathways. *J. Neurochem.* **71,** 2159–2168
35. Hirzel, K., Müller, U., Latal, A. T., Hülsmann, S., Grudzinska, J., Seeliger, M. W., Betz, H., and Laube, B. (2006) Hyperekplexia phenotype of glycine receptor α1 subunit mutant mice identifies Zn^{2+} as an essential endogenous modulator of glycinergic neurotransmission. *Neuron* **52,** 679–690
36. Tóth, K. (2011) Zinc in neurotransmission. *Annu. Rev. Nutr.* **31,** 139–153
37. Laube, B. (2002) Potentiation of inhibitory glycinergic neurotransmission by Zn^{2+}. A synergistic interplay between presynaptic $P2X_2$ and postsynaptic glycine receptors. *Eur. J. Neurosci.* **16,** 1025–1036
38. Ju, P., Aubrey, K. R., and Vandenberg, R. J. (2004) Zn^{2+} inhibits glycine transport by glycine transporter subtype 1b. *J. Biol. Chem.* **279,** 22983–22991
39. Chu, X. P., Wemmie, J. A., Wang, W. Z., Zhu, X. M., Saugstad, J. A., Price, M. P., Simon, R. P., and Xiong, Z. G. (2004) Subunit-dependent high-affinity zinc inhibition of acid-sensing ion channels. *J. Neurosci.* **24,** 8678–8689
40. Baron, A., Voilley, N., Lazdunski, M., and Lingueglia, E. (2008) Acid sensing ion channels in dorsal spinal cord neurons. *J. Neurosci.* **28,** 1498–1508
41. Chen, J., Myerburg, M. M., Passero, C. J., Winarski, K. L., and Sheng, S. (2011) External Cu^{2+} inhibits human epithelial Na^+ channels by binding at a subunit interface of extracellular domains. *J. Biol. Chem.* **286,** 27436–27446
42. Dudev, T., and Lim, C. (2002) Factors governing the protonation state of cysteines in proteins. An *ab initio*/CDM study. *J. Am. Chem. Soc.* **124,** 6759–6766
43. Leskelä, T. T., Markkanen, P. M., Alahuhta, I. A., Tuusa, J. T., and Petäjä-Repo, U. E. (2009) Phe27Cys polymorphism alters the maturation and subcellular localization of the human delta opioid receptor. *Traffic* **10,** 116–129
44. Schülein, R., Zühlke, K., Krause, G., and Rosenthal, W. (2001) Functional rescue of the nephrogenic diabetes insipidus-causing vasopressin V2 receptor mutants G185C and R202C by a second site suppressor mutation. *J. Biol. Chem.* **276,** 8384–8392
45. Williams, S. E., Reed, A. A., Galvanovskis, J., Antignac, C., Goodship, T., Karet, F. E., Kotanko, P., Lhotta, K., Morinière, V., Williams, P., Wong, W., Rorsman, P., and Thakker, R. V. (2009) Uromodulin mutations causing familial juvenile hyperuricaemic nephropathy lead to protein maturation defects and retention in the endoplasmic reticulum. *Hum. Mol. Genet.* **18,** 2963–2974
46. Krishnamurthy, H., and Gouaux, E. (2012) X-ray structures of LeuT in substrate-free outward-open and apo inward-open states. *Nature* **481,** 469–474

47. Bartholomäus, I., Milan-Lobo, L., Nicke, A., Dutertre, S., Hastrup, H., Jha, A., Gether, U., Sitte, H. H., Betz, H., and Eulenburg, V. (2008) Glycine transporter dimers. Evidence for occurrence in the plasma membrane. *J. Biol. Chem.* **283,** 10978–10991
48. Pace, C. N., Grimsley, G. R., and Scholtz, J. M. (2009) Protein ionizable groups. pK values and their contribution to protein stability and solubility. *J. Biol. Chem.* **284,** 13285–13289
49. Chen, Z., Dillon, G. H., and Huang, R. (2004) Molecular determinants of proton modulation of glycine receptors. *J. Biol. Chem.* **279,** 876–883
50. Aubrey, K. R., Mitrovic, A. D., and Vandenberg, R. J. (2000) Molecular basis for proton regulation of glycine transport by glycine transporter subtype 1b. *Mol. Pharmacol.* **58,** 129–135
51. Krishtal, O. (2003) The ASICs. Signaling molecules? Modulators? *Trends Neurosci.* **26,** 477–483
52. Jasti, J., Furukawa, H., Gonzales, E. B., and Gouaux, E. (2007) Structure of acid-sensing ion channel 1 at 1.9 Å resolution and low pH. *Nature* **449,** 316–323
53. Krishtal, O. A., Osipchuk, Y. V., Shelest, T. N., and Smirnoff, S. V. (1987) Rapid extracellular pH transients related to synaptic transmission in rat hippocampal slices. *Brain Res.* **436,** 352–356
54. Li, Y. F., Wu, L. J., Li, Y., Xu, L., and Xu, T. L. (2003) Mechanisms of H^+ modulation of glycinergic response in rat sacral dorsal commissural neurons. *J. Physiol.* **552,** 73–87
55. Smart, T. G., Hosie, A. M., and Miller, P. S. (2004) Zn^{2+} ions. Modulators of excitatory and inhibitory synaptic activity. *Neuroscientist* **10,** 432–442

Artículo #4

Na/K ATPase is a new interacting partner for the neuronal glycine transporter GlyT2 that downregulates its expression *in vitro* and *in vivo*.

de Juan-Sanz J, Nunez E, Villarejo-López L, Rodriguez-Fraticelli AE, Pérez-Hernández D, López-Corcuera B, Vazquez J, Aragón C. (2013). *In preparation.*

Na/K ATPase is a new interacting partner for the neuronal glycine transporter GlyT2 that downregulates its expression in vitro and in vivo

Jaime de Juan-Sanz[*†‡], Enrique Núñez[*†‡], Lucía Villarejo-López[*], Alejo E. Rodriguez-Fraticelli[*], Daniel Pérez-Hernández[ᵇ], Beatriz López-Corcuera[*†‡], Jesús Vázquez[#] and Carmen Aragón[*†‡1]

*Centro de Biología Molecular "Severo Ochoa", Universidad Autónoma de Madrid, Consejo Superior de Investigaciones Científicas, Madrid, Spain.
[#]Centro Nacional de Investigaciones Cardiovasculares (CNIC), Madrid, Spain.
[ᵇ]Max Delbruck Centrum (MDC), Berlin, Germany.
[†]Centro de Investigación Biomédica en Red de Enfermedades Raras (CIBERER), ISCIII; [‡]IdiPAZ-Hospital Universitario La Paz, Madrid, Spain.
[1]Corresponding author: Carmen Aragón, Centro de Biología Molecular "Severo Ochoa", Universidad Autónoma de Madrid, Madrid, Spain.
Telephone: +34-91-1964632; Fax: +34-91-1964420; Email: caragon@cbm.uam.es

INTRODUCTION

Glycine is the major inhibitory neurotransmitter in brainstem and spinal cord of the vertebrate central nervous system and it participates in the processing of motor and sensory information involved in movement, vision, audition and inflammatory and neuropathic pain perception (1). Inhibitory glycinergic neurotransmission is terminated by specific transporters, GlyTs (GlyT1 and GlyT2), which mediate the reuptake of glycine from the synaptic cleft. GlyTs, beside to most of the neurotransmitter transporters in the central nervous system, belong to the neurotransmitter:sodium symporter family (SLC6 gene family) (Aragón and López-Corcuera, 2003; Kristensen et. al. 2011). By mediating the synaptic recycling of glycine, the neuronal transporter GlyT2 preserves the quantal glycine content in synaptic vesicles and assists GlyT1 in regulating glycine levels at the synapsis. Gene deletion studies suggest that modification of glycine transporter activity may be beneficial in several human disorders, including neuromotor deficiencies (startle disease, myoclonus), pain and epilepsy (Gomeza et. al. 2003a; Gomeza et. al. 2003b; Aragón and López-Corcuera, 2005). Indeed, mutations in the gene encoding GlyT2 can cause hyperekplexia in humans and congenital muscular dystonia type 2 in calves (Rees et al., 2006; Eulenburg et al. 2006; Gimenez et al. 2012). Protein trafficking plays a fundamental role in the control of neuronal activity and it has been identified as a primary regulatory mechanism for several plasma membrane neurotransmitter transporters, providing a rapid and transient means to modulate their activity (Blakely and Bauman, 2010). GlyT2 is recycled between the cell surface and the cell interior by constitutive and regulated trafficking pathways and a large proportion of GlyT2 resides in intracellular endosomal membranes of rat brainstem neurons under steady-state conditions (Nunez et al., 2009). Modulation of GlyT2 trafficking is accomplished by a variety of factors (Geerlings et al., 2001; Fornes et al. 2008; de Juan-Sanz et al., 2011; de Juan-Sanz et al., 2013). One of them is the interaction between GlyT2 and the SNARE syntaxin 1A that is essential for constitutive and Ca^{2+}-triggered insertion of the transporter into the plasma membrane of neurons (Geerlings et al., 2001). In addition, two more proteins have been described as interacting partners of GlyT2; Ulip6, a member of the collapsin response mediator protein family and the PDZ domain protein syntenin-1 (Ohno et al., 2004; Horiuchi et al., 2005). Both proteins were identified by a yeast two-hybrid screening and a role for synaptic localization and/or GlyT2 trafficking has been suggested for syntenin-1 (Armsenet al., 2007). Glycine transporters are sodium-dependent proteins functionally coupled to the sodium electrochemical gradient actively generated and maintained principally by Na^+-K^+-ATPase. GlyTs catalyze Na^+/Cl^-/glycine co-transport with a stoichiometry of: 2 : 1 : 1 (GlyT1) and 3 : 1 : 1 (GlyT2) (Roux and Supplisson, 2000; Aragón and López-Corcuera, 2005). GlyT2 must actively reuptake and create a high intracellular concentration of glycine into the nerve terminal such that the neurotransmitter can be accumulated in the synaptic vesicles by the low-affinity vesicular transporter VIAAT (Gomeza et al., 2003b; Aragón and López-Corcuera, 2005). The large rises of intracellular Na^+ resulting from GlyT2 activity must be efficiently pumped out by the Na^+-K^+-ATPase to preserve ion homeostasis, therefore a close association between GlyT2 and the catalytic α subunit could provide an efficient device to coordinate their functions.

Na^+-K^+-ATPase is a ubiquitous integral membrane protein that couples ATP hydrolysis with the active transport of 3 Na^+ out of the cell in exchange for 2 K^+ during each enzyme cycle. Na^+/K^+ gradients across the plasma membrane are particularly important for neuronal excitability, conduction of action potential, Na+-coupled transport systems responsible for synaptic reuptake of neurotransmitters and also for regulation of cell volume, pH, and [Ca^{2+}]. This enzyme is mainly composed of the catalytic α-subunit, which contains the binding sites for ATP, Na^+, K^+, and cardiotonic steroid (CTS) selective inhibitors, and a heavily glycosylated β-subunit. In some tissues this enzyme is associated with another subunit, a member of the FXYD family named γ subunit. There are 4 different isoforms of α subunits encoded by different genes and their expression is developmentally regulated and tissue-specific. The ubiquitously expressed α1, the α2 expressed mainly in skeletal, heart, and smooth muscle, brain, lung and adipocytes, the α3 that occurs mainly in neurons and ovaries and the α4 expressed in testis. Besides their important physiological role as an ion pump, recent research has elucidat-

ed that Na^+,K^+-ATPase also functions as a receptor involved in many signaling events, most of them being regulated by interactions with other membrane proteins (see recent reviews: Lingrel, 2010; Liu and Xie, 2010; Benarroch, 2011; Reinhard et al., 2012). CTS are specific inhibitors of the Na+,K+-ATPase and are found in plants and vertebrates but ouabain and marinobufagenin are also produced by the human adrenal cortex and hypothalamus (Hamlyn et al., 1991; el-Masri et al., 2002) and can be detected at nanomolar concentrations in human blood acting as endogenous hormones (Ludens et al., 1991; Bagrov et al., 2009). In this regard, low concentrations of CTS, insufficient to affect the total pool of Na+,K+-ATPase significantly, bind to α-subunits and trigger downstream events which lead to modulation of different cellular processes. Given the enormous variety of reported interaction partners and the complexity of signaling cascades involved, the role of Na^+,K^+-ATPase as signal transducer is extremely complex. So far only a few interactions between the Na^+,K^+-ATPase and membrane proteins involved in central nervous system (CNS) neurotransmission have been described. Thus, dopamine D1 and D2 receptors appear directly interact with Na^+,K^+-ATPase α1-subunit resulting in a reciprocal modulation that control both dopamine signaling and cellular ion homeostasis (Hazelwood et al., 2008). Recent evidence indicates that α1 subunit of Na^+,K^+-ATPase co-localizes and interacts with the glutamate AMPA receptor and the inhibition of Na^+,K^+-ATPase by high levels of ouabain causes internalization and degradation of AMPAR, leading to long term suppression of AMPAR-mediated synaptic transmission (Zhang et al., 2009). In addition, it has been proposed the existence of a Na^+,K^+-ATPase/Src/glutamate transporter protein complex that operate as a functional unit to regulate glutamatergic neurotransmission (Rose et al., 2009). These findings suggest a tight functional coupling between CNS excitatory neurotransmission and the Na^+,K^+-ATPase through its dual role as ion pump and signal transducer.

By using mass spectroscopy analysis coupled with co-immunoprecipitation and co-localization studies, we have identified α subunits of the Na^+,K^+-ATPase as GlyT2-interacting proteins in synaptosomes and primary neuronal cultures from rat brainstem and spinal cord. Furthermore, we have shown that GlyT2-αNKA interaction is compartmentalized in lipid raft subdomains, where GlyT2 is optimally active (Nuñez et al., 2008), suggesting that Na^+,K^+-ATPase could mediate the regulation of the local presynaptic Na^+ increases produced during glycine recapture by GlyT2. In addition, the selective inhibition of the CTS-sensitive α2 and α3 Na^+,K^+-ATPase subunits by low levels of ouabain (1 μM) causes internalization of GlyT2, whereas the inhibition of general Na^+,K^+-ATPase activity by high levels of ouabain (50 μM) lead to more drastic effects producing lysosomal degradation of the lipid raft-associated optimally active transporter. Ouabain-mediated degradation of GlyT2 is also observed in vivo after high-dose incubation in zebrafish embryos and after intramedullar ouabain administration in adult rats, which suggests the existence of an important endogenous ouabain-mediated mechanism that regulates glycinergic neurotransmission by modulating GlyT2 expression in vivo.

RESULTS

Given the importance of GlyT2 in the pathophysiology of inhibitory glycinergic neurotransmission and considering the small number of transporter interacting proteins known to date, we decided to carry out a proteomic study in an attempt to identify new molecular partners involved in the functional modulation of GlyT2. The approach consisted of immunoprecipitation of the native transporter from brainstem and spinal cord synaptosomes with a specific GlyT2 antibody (Zafra et al., 1995) and further identification of the protein partners by mass spectrometry analysis. The more abundant peptides identified in the two performed experiments belong to a3 and a2NKA suggesting that GlyT2 may be associated with Na^+,K^+-ATPase α subunits (Fig 1A). Representative tandem mass spectrums of a2NKA and a3NKA specific peptides are shown (Fig 1B).

GlyT2 interacts with α subunits of Na^+,K^+-ATPase in synaptosomes

To test whether GlyT2 interacts with Na^+,K^+-ATPase, reverse coimmunoprecipitations from rat brainstem and spinal cord synaptosomes lysates were performed with specific antibodies directed against GlyT2 and α1, α2 and α3 subunits (Fig 2a, b). Western blot analysis showed that each antibody selectively immunoprecipitated the respective target protein. As shown in representative blots of Fig 2, GlyT2 was coimmunoprecipitated with Na^+,K^+-ATPase α subunits (Fig 2a, b), indicating that GlyT2 and Na^+,K^+-ATPase specifically interact at physiological levels of native proteins. A significant percentage of GlyT2 interacted with α3 (13.01% ± 1.92), in a lesser extent with α2 (4.90% ± 1.83) and sparsely with α1 (0.29% ± 0.18). Neurons express all three Na^+ pump isoforms in different amounts. The α3 isoform is widely distributed throughout the brain, but its expression is restricted to neurons (Sweadner, 1989; Juhaszova and Blaustein, 1997; Moseley et al,, 2007). Thus, the magnitude of the interaction between GlyT2 and α3 subunit is related to its specific neuronal expression. To further confirm the interaction between GlyT2 and the different α subunits of Na^+,K^+-ATPase, their colocalization was examined by immunocytochemical analyses in primary neuronal cultures from brainstem and spinal cord (Fig 3). Double labeling of GlyT2 and Na^+,K^+-ATPase α subunits (Fig 3A, B) indicates that a majority of GlyT2 immunosignals overlapped with α3 subunit and a more limited colocalization with α2 and α1 was detected. Taking into account that GlyT2 is expressed in axon and nerve terminals and NKA is enriched in synapses (Hilgenberg et al., 2006; Hazelwood et al., 2008) we further performed immunofluorescence assays in synaptosomes where the degree of synaptic coexistence of Na^+,K^+-ATPase and GlyT2 should be significantly higher. Indeed, in addition to increase the extent of colocalization between GlyT2 and α3 subunit, the quantitative differences in the colocalization of the transporter and each of the three subunits are more clearly manifested in this preparation (Fig. 4). Together, reverse immunoprecipitation and immunocytochemical assays suggest that in neurons GlyT2 specifically interacts with the catalytic component of the Na^+,K^+-ATPase, mainly with α3 subunit. Considering these results and the neuron-specific expression of the α3 subunit and GlyT2, our further study is focused on the GlyT2- Na^+,K^+-ATPase α3 subunit interaction.

GlyT2 - α3NKA interaction occurs in lipid rafts

We recently reported that GlyT2 displays optimal transport activity when associated with lipid rafts in plasma membrane, where most of the transporter resides in primary neurons and synaptosomes from the rat brainstem (Nuñez et al., 2008). Considering that Na^+,K^+-ATPase localizes in lipid rafts of several tissues (Welker et al., 2007; Taguchi et al., 2007; Fujii et al., 2008; Liu et al., 2011; Ta-

jima et al., 2011) we investigated whether the interaction between Na^+,K^+-ATPase and GlyT2 occurs in these membrane subdomains. Co-immunoprecipitation assays (Fig. 5A) performed from raft and non-raft fractions isolated through a sucrose gradient and using an anti- Na^+,K^+-ATPase α3 antibody unambiguously indicated that the interaction between the two proteins takes place only in lipid rafts, as showed by the raft and non-raft fraction markers distribution, flotillin1 and clathrin heavy chain proteins, respectively. With the aim of identifying proteins that could be mediating the raft GlyT2-α3 subunit interaction we next performed mass spectrometry analysis of separately GlyT2-immunoprecipitated from raft and non-raft fractions. Although the proteomic assay have provided us no qualitative differences to point out potential protein candidates, interestingly α subunits peptides were identified almost exclusively in immunoprecipitated raft fractions which confirms the absolute dependence of the GlyT2 - Na^+,K^+-ATPase interaction on lipid raft subdomains (Fig 5B). Additional support was provided by immunocytochemistry assays (Fig 6) using specific antibodies against GlyT2, α3 subunit and Thy-1, a neuronal raft marker (Madore et al., 1999). As fig 6 shows similar fluorescence patterns were display by the three proteins (Fig 6A-G) which leads to a high degree of triple colocalization (Fig 6H-I).

Ouabain effect on the transport activity and expression of GlyT2

Lipid rafts are considered as fluctuating nanoscale assemblies of sphingolipids, cholesterol and proteins that can be stabilized into platforms that are important in signalling, viral infection and membrane trafficking (Simons and Gerl, 2010). As indicated before (see Introduction), Na^+,K^+-ATPase also functions as a specific receptor for endogenous and exogenous cardiotonic steroids (CTS) through macromolecular complexes in which α-subunit acts as the anchorage site. CTS-activated Na^+,K^+-ATPase signaling depends on the formation of specific signaling microdomains that couple the receptor Na^+,K^+-ATPase to its down-stream effectors (Lingrel, 2010; Liu and Xie, 2010; Benarroch, 2011; Reinhard et al., 2012). The ouabain binding site in all Na^+,K^+-ATPase molecules resides in the α subunit and different isoforms show similar affinity except for the rat and mouse α1 subunit, which is relatively resistant to ouabain presenting a much lower affinity (10^3-10^4 fold) than the rest of isoforms (see Lingrel, 2010 for a review). Therefore we next examined the effect of different concentrations of ouabain on GlyT2 function and protein expression. As the cardiotonic steroid ouabain is known to inhibit NKA function we determined the effect of ouabain on Na^+,K^+-ATPase and GlyT2 transport activities in parallel experiments performed in brainstem and spinal cord neurons (Fig. 7). A dose–response analysis of ouabain on the activity of Na^+,K^+-ATPase was carried out by ^{86}Rb-flux experiments as a tracer for potassium. The results showed that ouabain inhibits both, ^{86}Rb and [^{3}H]-glycine uptake in a concentration-dependent manner (Fig. 7A). Substantial inhibition was observed with 20 μM ouabain (Na^+,K^+-ATPase: 55%, GlyT2: 45%) and concentrations above 50μM resulted in a nearly total inhibition. The tight correlation observed in the inhibition of both transporters by ouabain may be explained by the strict dependence of the GlyT2 function on the sodium electrochemical gradient generated and maintained principally by the Na^+,K^+-ATPase at the neuronal plasma membrane. Considering that GlyT2 co-transport Na+/Cl-/glycine with a stoichiometry of 3:1:1 (Roux and Supplisson, 2000; Aragón and López-Corcuera, 2005) a functional relationship between the two proteins, as suggested by results of Fig 7A, therefore is not unexpected.

To attempt to elucidate the physiological role of the GlyT2-NKA interaction we examined the effect of ouabain on the total expression and plasma membrane GlyT2 levels. We used low (1 μM) and high (50 μM) inhibitor concentrations to preserve almost unaltered activity or otherwise cause a significant inhibition of the ion pump, respectively. Quantitative biotinylation experiments with the impermeable sulfo-NHS-SS-biotin were carried out to detect changes in cell surface levels of GlyT2. By Western blot analysis we found that 1 μM ouabain, a concentration that hardly affects the GlyT2 activity, induced a decrease in the neuronal surface Glyt2 levels (Fig. 7B). The effect started within 1h of ouabain treatment and higher reductions were observed at longer times, whereas the total amount of GlyT2 was not affected after 3h of ouabain treatment. By contrast, general inhibition of Na^+,K^+-ATPase activity by high-dose ouabain (50 μM) produced a more drastic effect reducing total and neuronal surface GlyT2 expression. Since the reduction of total GlyT2 may be due to inhibited synthesis or increased degradation we assayed the effect of inhibitors of each cellular process in the presence or absence of ouabain in order to discern between the two possibilities (Fig. 7C). We found that ouabain-induced GlyT2 reduction was completely prevented by the incubation of neurons with leupeptin, a lysosomal protease inhibitor. The partial effect exerted by the proteasome inhibitor MG132 probably is due to decreased GlyT2 ubiquitination because of the depletion of intracellular free ubiquitin pool (Patnaik et al., 2000; Maria et al., 2006) or/and by the lysosomal proteases inhibition caused by MG132 (Longva et al., 2002). This conclusion is based on our recent results showing that endocytosis and further sorting to recycling or degradation pathways of GlyT2 in neurons depends on ubiquitination, and that the ubiquitination status of the transporter is highly sensitive to ubiquitin homeostasis (de Juan-Sanz et al., 2013). Moreover, the lack of effect observed by 3 hours ciclohexiimide treatment, an inhibitor of the protein synthesis, compared with the GlyT2 decrease caused by a similar treatment of ouabain suggest that degradation, but not protein synthesis, underlies to the reduction of GlyT2 (Fig. 7D). Together these results indicate that NKA-dependent GlyT2 reduction is mainly due to an increase in its lysosomal degradation.

To investigate if Glyt2 degradation exerted by ouabain is a more general effect, we test the expression of GlyT2 related neuronal proteins in the presence of 50 μM ouabain. Syntaxin 1A and CRMP5/Ulip6 have been identified as binding partners of GlyT2, the serotonin and GABA transporters (SERT, GAT1, respectively) are, like GlyT2, members of the SLC6 gene family and α1 and α3 are the more abundant NKA subunits in neurons. Interestingly, no changes were appreciated in expression levels of these proteins upon 3 h of 50 μM ouabain treatment (Fig. 7E), suggesting a selective downregulation of GlyT2 by NKA in this conditions.

Then we asked if the fact that GlyT2-NKA interaction takes place in rafts (see Fig 5) could have functional implications and hence participate in the ouabain-mediated degradation of GlyT2. For this purpose we isolated lipid rafts from primary cultures of brainstem and spinal cord neurons previously treated with 50 μM ouabain and GlyT2 levels in raft and non-raft fractions were immunodetected by Western blot (Fig. 8A). Interestingly, we found that most of Glyt2 degradation by ouabain occurs in raft fractions remaining nearly unaltered the transporter located outside of rafts. Considering that Glyt2 requires to be located in rafts for displaying its optimal transport activity, results shown in Fig 8 provide strong

support to suggest a functional regulatory role mediated by NKA selectively on the Glyt2 lipid raft-associated pool located in the cell surface. Furthermore, lipid raft disruption performed by treating neurons with the cholesterol chelator nystatin produced a total blockage of the ouabain-mediated GlyT2 degradation. Thereby, in addition to providing the appropriate environment for GlyT2 optimal activity and consistent with its function as signaling platforms, membrane rafts represent the neuron surface subdomains where the GlyT2-NKA interaction translates into a regulated endocytosis and subsequent degradation of GlyT2.

Ouabain-mediated degradation of GlyT2 occurs in vivo in different species.

Since ouabain is a compound that is produced endogenously, we asked if GlyT2 regulation observed in vitro in primary cultures of rat brainstem and spinal cord neurons was also occurring in an in vivo system. To test this hypothesis we first used the zebrafish embryo, which has been firmly established as a great model for neuroscience studies, being widely used to investigate drug effects, CNS development, neurological disease mechanisms or even behavioral neuroscience (see Levin and Cerutti, 2009; Cheng et al., 2011 and Xi et al., 2011 for a review). CNS drug tests must be performed before the complete formation of the blood-brain barrier (BBB) to ensure the compound reaches its neuronal targets. This process ends 3 days after fertilization (72 hpf) when the embryo is ready to hatch, thus usually screenings are performed using dechorionated embryos at earlier stages. GlyT2 expression in zebrafish embryos starts at 20hpf (Higashijima et al., 2004a) and increases over the time being nicely detected at 36-48hpf (Higashijima et al., 2004b; Cui et al., 2005; Moly and Hatta, 2011). As shown in figure 9 A-F, 48hpf zebrafish embryos express both α3NKA and GlyT2 showing an extensive co-localization in central brain, hindbrain and spinal cord, clearly observed in dorsal interneurons (Higashijima et al., 2004a; Higashijima et al., 2004b; Cui et al., 2005; Moly and Hatta, 2011). To confirm previous in vitro results, we treated dechorionated zebrafish embryos at 48hpf with high-dose ouabain during 6h and analyzed GlyT2 expression by western blot. Figure 9G-H shows that GlyT2 expression is significantly reduced, remaining only the 6.74% ± 4.54 SEM of the initial amount, whereas tubulin and α3NKA remained unaffected. These significant results indicate the importance of the GlyT2 regulation by NKA in vivo and suggest it is conserved among different vertebrate species.

To investigate in vivo ouabain-mediated degradation of GlyT2 also in mammals we decided to inject ouabain intramedullary in adult rats (figure 10). GlyT2 is expressed equally along the spinal cord, so we decided to perform the administration in a middle part at thoracic vertebra eight (T8). After 3 hours of the administration, the anesthetized animals were sacrificed and different sections of the spinal cord (cervical vertebra 4 (C4), thoracic vertebra 8 (T8) and thoracic vertebra 12 (T12)) were extracted, lysed and analyzed by western blot (figure 10A-B). Interestingly, we found that vehicle injection produced no effect on GlyT2 expression, whereas ouabain injected sections showed a reduced amount of GlyT2 without affecting the expression of the transporter in other different sections of the injected spinal cord. Taken together, these results indicate that GlyT2 is degradated in vivo in the presence of ouabain in adult rats and zebrafish embryos, suggesting an evolutionarily conserved GlyT2 downregulation mechanism through its interacting partner Na^+/K^+ ATPase and consequently that modulates the inhibitory glycinergic neurotransmission.

DISCUSSION

In the present study, we used mass spectroscopy analysis to identify GlyT2 interacting proteins in CNS preparations with the aim to deepen the mechanisms modulating the function of GLYT2. Our data have identified NKA α3 subunit and, in a minor extent NKA α2 subunit, as new protein partners of GlyT2. This novel interaction regulates endocytosis and total expression of Glyt2 in neurons. Our results of reciprocal co-immunoprecipitation and immunocytochemistry further confirmed the proteomic data demonstrating the GlyT2-NKA association and their co-localization in neurons and synaptosomes where GlyT2-NKAα3 is clearly appreciated as the major interaction. NKAα3 is specifically expressed in neurons (Dobretsov and Stimers, 2005) and is mainly located in pre- and post-synapses (Hilgenberg et al., 2006; Kim et al., 2007). This subunit plays a crucial role in the control of membrane potential and carries out the fast recovering of high intracellular concentration of Na+ following intense synaptic activity (Kim et al., 2007; Azarias et al., 2013). Thus, it is not surprising the severe neurological disorders of human α3 mutations such as rapid-onset dystonia parkinsonism (de Carvalho Aguiar et al., 2004; Brashear et al., 2007), cognitive defects (Lingrel et al., 2007; Moseley et al., 2007), mood disorders (Kirshenbaum et al., 2011a; Kirshenbaum et al. 2011b) or alternating hemiplegia of childhood (Heinzen et al., 2012).

One important finding in this work is that GlyT2-α3NKA interaction is restricted to rafts subdomains as we proved by co-immunoprecipitation from rafts fractions and triple co-localization between GlyT2, α3NKA and the neuronal raft marker, Thy-1 by immunocytochemistry. These results were further confirmed by proteomic analysis upon detection α subunit specific peptides only in immunoprecipitated raft fractions by Glyt2 antibodies. This GlyT2-α3NKA membrane compartmentalization favors the interaction by increasing their likelihood of meeting and may have functional implications in the maintaining of local synaptic sodium homeostasis. Thus, the presence of α3NKA in rafts, by providing the needed energy to glycine transport, is essential for the efficient functioning of Glyt2. Furthermore, the interaction with the active population of GlyT2 in rafts allows to α3NKA restore the accumulation of intracellular Na+ close to the transporter in the presynaptic terminal during an active reuptake of the neurotransmitter from the synaptic cleft. As previously described (Roux and Supplisson, 2000), GlyT2 co-transport 3Na+ for each glycine recovered from synaptic cleft, being the only transporter of SLC6 family that need more than two Na+ for transport coupling. During activity conditions in the nerve terminal the neurotransmitter exocytosis occurs along with a rapid and transient increase in the amount of GlyT2 in the plasma membrane that favors a rapid reuptake and recycling of glycine in the terminal (Geerlings et al., 2001). In this situation a rapid local increase in the intracellular [Na+] takes place due to the action of GlyT2 and α3NKA by expelling Na+, to the expense of ATP, will balance rapidly the electrochemical gradient of Na + ions, according with their crucial role in the control of membrane potential and fast recovering of high intracellular concentration of Na+ following intense synaptic activity (Kim et al., 2007; Azarias et al., 2013).

In addition as ion pump, Na+,K+-ATPase also functions as an specific receptor for cardiotonic steroids (CTS) forming signaling complexes that couple the receptor to its down-stream effectors inducing different cellular effects (see recent reviews: Lingrel, 2010; Liu and Xie, 2010; Benarroch, 2011; Reinhard et al., 2012). CTS and related compounds are found in plants and vertebrates

and some of them as ouabain and marinobufagenin are also synthesized in the human adrenal cortex and hypothalamus (Hamlyn et al., 1991; el-Masri et al., 2002). Nanomolar concentrations of these compounds are detected in human blood (Ludens et al., 1991; Bagrov et al., 2009). The affinity for ouabain of the Na+,K+-ATPase depends on the isoform α and the specie. Thus, in rodents α1 subunit has come to define as resistant to oubaina with an IC50 of 48μM, but α2 and α3 subunits have greater affinity with IC50 of 58nM and 6.7 nM, respectively (Lingrel, 2010). This different affinity allows the study of the ouabain effect solely mediated through α2 and α3 by using low concentrations of the compound (0.1-1 μM) (Tymiak et al., 1993).

Our 86Rb-flux and glycine transport experiments show a tight correlation in the inhibition of Na^+,K^+-ATPase and GlyT2 activities by ouabain that is indicative of the strict functional dependence of GlyT2 on the sodium electrochemical gradient generated by the ion pump (Fig 7A). Considering that GlyT2 co-transports 3Na+/Cl-/glycine (Roux and Supplisson, 2000; Aragón and López-Corcuera, 2005) and the stoichiometry of NKA catalytic cycle is: 3Na+/2K+/ATP, which means that the transport of 1 molecule of glycine by GlyT2 needs the hydrolysis of 1ATP by NKA, a functional relationship and physical associationbetween the two proteins may represent a suitable molecular device for glycinergic synapse.

Low concentrations of ouabain (1 μM), unable to significantly affect the global Na+ gradient (Fig 7A) induced GlyT2 endocytosis, an slow effect that only can be detected in neurons after 1 hour of ouabain treatment. When the overall gradient of sodium in the neuron is severely compromised by high concentrations of ouabain (50 μM), besides GlyT2 endocytosis is also observed a significant time dependent lysosomal degradation of transporter. Thus, when α3NKA is inhibited by 1 μM ouabain, GlyT2 is removed from the cell surface to locally prevent further depolarization and dissipation of the gradient of Na + in the presynaptic membrane. The decrease in the GlyT2 stability induced by high ouabain levels prevents irreversibly the recycling back to the membrane of GlyT2. Our data suggest that NKA regulates recycling and turnover of GlyT2 in the glycinergic synapse by a feedback mechanism to maintain membrane potential and intracellular sodium homeostasis. As stated previously, α3NKA is considered the main responsible for control of membrane potential and recovery of Na+ gradient under increased [Na+]i, such that in hippocampal and striatal neurons over 90% of the pump activity is due to α3NKA (Azarias et al., 2013).

Given that α3NKA is the main interacting partner of GlyT2, as demonstrate in this study, and considering the important role that this subunit plays in high [Na+] intracellular situations, otherwise equivalent to the experimental situation generated by 50 μM ouabain, our results point to α3NKA as principal mediator of the GlyT2 downregulation by low and high ouabain concentrations found in the present work. Although GlyT2 appears to be selectively degradated by ouabain, as is not observed for other neuronal proteins (α1NKA, α3 NKA, syntaxin1A, Ulip6, SERT, GAT1), however, GluR1 subunit of the AMPA receptor in hippocampal neurons is downregulated by a surface and total expression decreasing of the receptor as response to ouabain through NKA-GluR1 interaction (Zhang et al., 2009). Together these data suggest that the mechanism described in this work and in the others could represent a more general regulation by NKA that control neuronal proteins whose operation in the synaptic membrane contributes to increase intracellular Na^{+} which requires of the rapid and efficient action of NKA.

The physiologically relevant role of rafts in regulating GLYT2 through its interaction with NKA is even most apparent when verifying that the ouabain-mediated degradation affects almost uniquely to the transporter associated with these subdomains, allowing act only on the functionally active GlyT2 population.

The fact that both, endocytosis and degradation of GlyT2 are slow responses to ouabain action is not consistent with the rapid Na^+ gradient depletion observed (20 min of ouabain treatment, Fig 7A) suggesting that the mechanism underlying the down-regulation of Glyt2 by NKA does not directly depend on ion gradient changes in the neuronal membrane but, rather, involves a process that takes more time to activate. In this regard it is noteworthy that the two functional roles played by NKA as ion pumping and as CTS receptor coupled to signaling pathways are not mutually exclusive being able to work in concert in the regulation of cellular function (Li and Xie, 2009) as the Glyt2 down-regulation shown in this study. However, the identification of such molecular mechanism, probably through signaling pathways downstream NKA receptor needs further study.

Finally and interestingly we have demonstrated that downregulation of GlyT2 by degradation in response to ouabain also occurs in an in vivo situation in adult rats and zebrafish embryos indicating an evolutionarily conserved GlyT2 regulatory mechanism through its interacting partner Na^+/K^+ATPase. Changes in the amount of GlyT2 at the plasma membrane produces large variations in inhibitory glycinergic neurotransmission, so that increases in the amount of ouabain at glycinergic synapses could induce two effects: 1) a short term effect decreasing GlyT2 at the cell surface that will lead to an increase of glycine in the synaptic cleft, which will bind to the receptor further increasing GlyR glycinergic neurotransmission, and 2) a long term effect by GlyT2 downregulation that will cause a depletion in glycine refilling of synaptic vesicles further decreasing the glycinergic neurotransmission. Future studies are needed to determine the physiological relevance of this new regulatory mechanism of this pathophysiologically important glycine neuronal transporter.

MATERIALS

Zebrafish and wistar rats were bred under standard conditions at the Centro de Biología Molecular Severo Ochoa in accordance with the current guidelines for the use of animals in neuroscientific research. Antibodies against GlyT2 were obtained in the laboratory (rabbit and rat: Nuñez et al., 2009; Zafra et sl., 1995). The other primary antibodies used were as follows: anti-α1 Na,K-ATPase (1:500, mouse monoclonal, clone C464.6; Millipore Bioscience Research Reagents), anti-α1 Na,K-ATPase (goat polyclonal; Santa Cruz Biotechnology), anti-α1 Na,K-ATPase (mouse monoclonal, clone α6F; DHSB. Only used for IP), anti-α2 Na,K-ATPase (1:500, rabbit polyclonal; Millipore Bioscience Research Reagents), anti-α3 Na,K-ATPase used for zebrafish (1:1000, mouse monoclonal; Affinity BioReagents), anti-α3 Na,K-ATPase (1:500, goat polyclonal; Santa Cruz Biotechnology), anti Thy-1 (1:500, mouse monoclonal; BD Pharmingen) anti-calnexin (1:1000, rabbit polyclonal; Stressgen), anti-SRC (1:500, rabbit polyclonal; santa cruz), anti-phosphoSRC (1:500, rabbit polyclonal; cell signalling), anti-ERK 1/2 ((1:500, rabbit polyclonal; cell signalling), anti-phosphoERK 1/2 (1:500, rabbit

polyclonal; cell signalling), anti-flotillin1 (1:500, mouse monoclonal; BD Biosciences), anti-clathrin heavy chain (1:500, mouse monoclonal; BD Transduction), anti-β3tubulin (1:1000, mouse monoclonal; Sigma-Aldrich), anti-tubulin for zebrafish (mouse monoclonal, clone 6G7s; DHSB). Fluorophore-coupled secondary antibodies were acquired from Molecular Probes and all chemicals used were from Sigma Aldrich. Neurobasal medium and B-27 supplement were from Invitrogen. Expression vectors for rat α1, α2 and α3 Na,K-ATPases were generously donated by doctor Jerry B. Lingrel.

Protein Identification by Liquid Chromatography Coupled to Tandem Mass Spectrometry:

Protein digestion was performed by using a previously-described protocol (Bonzon-Kulichenko et al., 2011). Briefly, approximately 40 µl of beads were suspended in 10 µl sample buffer (5% SDS, 10% glycerol, 25 mM Tris-Cl, pH 6.8, 10 mM DTT, 0.01% bromophenol blue). The samples were applied onto 2.8-cm wide wells of a conventional SDS-PAGE gel (0.5 mm-thick, 4% stacking, 10% resolving). The run was stopped as soon as the front entered 3 mm into the resolving gel, so that the whole proteome became concentrated in the stacking/resolving gel interface. The protein band was visualized by Coomassie staining, excised, cut into cubes and digested overnight at 37ºC with 60 ng/µl trypsin at 5:1 protein:trypsin (w/w) ratio in 50 mM ammonium bicarbonate, pH 8.8 containing 10% ACN and 0.01% 5-cyclohexyl-1-pentyl-ß-D-maltoside. The resulting tryptic peptides from each proteome were extracted by 1h-incubation in 12mM ammonium bicarbonate, pH 8.8. TFA was added to a final concentration of 1% and the peptides were finally desalted onto C18 Oasis cartridges and dried-down. The resulting peptides from each gel slice were analyzed separately by RP-HPLC-LIT for protein identification.

Mass spectrometry and data analysis.

To identify proteins, the resulting tryptic peptide mixtures were analyzed by nanoliquid chromatography coupled to mass spectrometry. Peptides were injected onto a C-18 reversed phase (RP) nanocolumn (100 µm I.D. And 15 cm, Mediterranea Sea, Teknokroma) and analyzed on a continuous acetonitrile gradient consisting of 0%–43% B for 90 min and 50%–90% B for 1min (B=95% acetonitrile, 0.1% formic acid). Peptides were eluted from the RP nanocolumn at a flow rate of 200 nl/min for real-time ionization and peptide fragmentation on an LTQ-Orbitrap mass spectrometer (Thermo Fisher, San Jose, CA). An enhanced FT-resolution spectrum (resolution = 30,000) and the MS/MS spectra of the fifteen most-intense parent ions were analyzed during the chromatographic run (150 min). Dynamic exclusion was set at 0.5 min.

For protein identification, The MS/MS raw files were searched against the Human Swissprot database (Uniprot release 14.0, 19929 sequence entries for human) supplemented with porcine trypsin, with Proteome Discoverer 1.2.0.207 (Thermo Fisher Scientific). All MS/MS samples were analyzed by SEQUEST (Thermo Fisher Scientific, version 1.0.43.2). Two mixed cleavages were allowed, and errors of 20 ppm or 0.8 Da were set for full MS and MS/MS spectra searches, respectively. Oxidation of M (15.9949 Da) was selected as dynamic modification and carbamidomethylation in C (57.021 Da) as fixed modification. SEQUEST results were validated using the probability ratio method (Martínez-Bartolomé et al., 2008) and false discovery rates (FDR) calculated using the refined method (Navarro and Vazquez, 2009). Peptide counting was performed assuming as positive events those with a FDR equal or lower than 5%.

Rubidium-86 uptake into neurons:

Rubidium-86 uptake into neurons was used to measure the potassium ion pumping activity of Na,KATPase. Neurons were treated in Neurobasal medium with diferent concentrations of ouabain during 15 minutes at 37ºC. Then the medium was replaced with new Neurobasal medium containing 1.5 µCi/ml (55.5 µBq/ml) of rubidium-86 (PerkinElmer Life and Analytical Sciences) mantainig the previous concentrations of ouabain. The uptake assay was allowed to proceed for 10 minutes and the incubation was stopped by rinsing the plate four times with cold PBS. Cells were extracted with 0.25 ml of 0.2 mmol/l NaOH for 10 minutes, and samples were counted in a liquid scintillation counter to measure radiation from beta-emitting rubidium-86 isotopes incorporated. Each data point represents the average of the radioactivity present in nine separate wells from three diferent experiments.

Immunoprecipitation:

Brainstem and spinal cord synaptosomes or primary neurons (100 µg) were lysed for 30 min at room temperature (RT) at a concentration of 0.35 mg of protein/ml in TN buffer (25 mM TrisHCl and 150 mM NaCl, pH 7.4) containing 0.25% Nonidet P-40 (NP-40) and protease inhibitors (PIs: 0.4 mM phenylmethylsulfonyl fluoride [PMSF] + Sigma cocktail). After 15 min of centrifugation in microfuge to remove cell debris, 4µg were separated to quantify total protein (T), and 5-10 µl of primary antibody were added and incubated over night at 4ºC. Antibodies used for immunoprecipitation were: rat or rabbit anti-GlyT2, goat anti-α1 Na,K-ATPase, rabbit anti-α2 Na,K-ATPase or goat anti-α3 Na,K-ATPase, always maintaining a condition without adding any antibody, denoted as minus Ab (-Ab). Then 20 µl of 50% protein A sepharose (PAS) for rabbit antibodies or protein G sepharose (PGS) for rat or goat antibodies were added and incubated 45 min at 4ºC. The beads were collected by mild centrifugation and washed 2 times for 7 minutes with lysis buffer at RT. Finally, the beads were pelleted and the immunprecipitated proteins were eluted in Laemmli buffer at 75°C for 10 min, resolved in SDS/PAGE gels (7.5%), detected in Western blots with enhanced chemiluminescence (ECL) and quantified on a GS-710 calibrated imaging densitometer (Bio-Rad).

Lipid rafts isolation:

Membrane rafts from brainstem and spinal cord synaptosomes or primary neurons were isolated as described previously (de Juan-Sanz et al., 2011). Briefly, scrapped washed neurons or purified synaptosomes were lysed at 2 mg of protein/ml in MBS buffer [25 mM Mes and 150 mM NaCl (pH 6.5)], containing 0.35% Triton X-100 and protease inhibitors (PI, 0.4 mM PMSF+Sigma cocktail). Samples were solubilized by passing them through a 25-gauge-needle and incubating those during 30min at 4ªC. Equal volumes of 70% (w/v) sucrose were added to the lysates and mixed thoroughly. Lysed samples (1ml) in 35% sucrose were overlaid successively with 2 ml of 30% and 1ml of 5% sucrose (in MBS+PI) in Ultra-Clear™ Beckman tubes for TST 60.4 rotor. After 18h of 52000 r.p.m ultracentrifugation at 4 °C, raft fractions (R) were collected from 5-30% interphase, and non-raft fractions from last 35% phase (NR). Both R and NR were solubilized for 30 min at room temperature (RT) with 0.25% Nonidet P-40 (NP-40) to disrupt raft structure, and proteins were analyzed by Western Blot or immunoprecipitated following the protocol described above. Flotillin1 and clathrin heavy chain were used as raft and non-raft markers respectively to control that isolation was correct.

Primary cultures of brainstem and spinal cord neurons.
Primary cultures of brainstem and spinal cord neurons were prepared as described previously (de Juan-Sanz et al. PLoS One?? 2012). Briefly, brainstems and spinal cords from Wistar rats foetuses at the 16th of gestation were obtained. The tissue was then mechanically disaggregated in Hanks' balanced salt solution (HBSS, Invitrogen) containing 0.25% trypsin (Invitrogen) and 4 mg/ml DNase (Sigma). Cells were plated at a density of 500,000 cells/well in Multiwell™ 12 well (Falcon) and incubated for 4 h in Dulbecco's modified Eagle's medium containing 10% fetal calf serum, 10 mM glucose, 10 mM sodium pyruvate, 0.5 mM glutamine, 0.05 mg/ml gentamicin, 0.01% streptomycin and 100 microU/ml penicillin G. After 4 hours this buffer was then replaced by culture medium (Neurobasal/B27 50:1 by volume, Invitrogen, containing 0.5 mM glutamine). After 2 days, cytosine arabinoside (2.5-5 μM) was added to inhibit further glial growth and the primary neurons were studied after 14 days in culture.

Immunofluorescence of brainstem and spinal cord primary neurons.
Primary neurons were fixed with 4% paraformaldehyde in PBS, washed three times with 1 ml PBS, and blocked for 30 min with 10% serum in TNT (0.1 M Tris/HCl pH 7.5, 0.3 M NaCl and 0.2% Triton). The neurons were then incubated with the primary anti-GlyT2 rat antibody (1:500) together with anti-α1 Na,K-ATPase (1:500), anti-α2 Na,K-ATPase (1:500), anti-α3 Na,K-ATPase (1:500) or Thy-1 (1.500) in TNT containing 1% serum for 2h. The cells were then washed three times with TNT buffer and incubated for 2h with the secondary antibody (anti-rat alexa 594, red, 1:500, anti-mouse Alexa 488 1:500, anti-rabbit alexa 594, 1:500, green) in TNT with 1% serum. After three washes with TNT, the coverslips were mounted on microscope slides with Vectashield (Vector Laboratories, Burlingame, CA). The cells were visualized by confocal microscopy using an inverted microscope AXIOVERT200 (Zeiss).

Immunofluorescence of brainstem and spinal cord synaptosomes
Purified brainstem-spinal cord synaptosomes were subjected to double immunofluorescence as reported previously (Jiménez et al., 2011) using primary antibodies against GlyT2 and the different α Na-K ATPase subunits. Samples were visualized in a confocal microscope as indicated above.

Immunofluorescence quantification and generation of colormaps-
At least 40 images of each condition were analyzed using IMAGEJ software (National Institutes of Health). Images were processed with a 2.0 pixel median filter, and threshold used was automatically determined by JACoP plugin (Bolte and Cordelières, 2006) . Pearson´s value was obtained with JACoP by comparing the two thresholded channels and measuring the correlation between them. The value can range from -1 to 1, being 1 the maximal colocalization possible (two identical images), and usually values from 0.5 to 1.0 can be considered as a valid colocalization (Zinchuk and Zinchuk, 2008). Colocalization colormaps were generated in ImageJ using the colocalization colormap plugin generated by Jaskolski F et. al (Jaskolski et al., 2005)

Zebrafish embryo wholemount immunofluorescence.
Manually dechorionated 48hpf zebrafish embryos were fixed in 4% PFA during 1 hour at RT, washed three times with 1 ml PBS, and blocked for 1h with 10% serum in PBS containing 0.55% Triton X-100. Then fixed entire embryos were incubated with the primary anti-GlyT2 rabbit antibody (1:200) together with anti-α3 Na,K-ATPase mouse antibody (1:200) in PBS containing 1% serum with gentle rotation for 3 days at 4ºC. The embryos were then washed three times with PBS and incubated for 4h with the secondary antibody (anti-rabbit alexa 594, red, 1:500, anti-mouse Alexa 488 1:500, green) in PBS with 1% serum. After three washes with PBS, embryos were visualized in a stereoscopic magnifying glass (Leica) or mounted in coverslips with Vectashield (Vector Laboratories, Burlingame, CA) and visualized by confocal microscopy using an inverted microscope AXIOVERT200 (Zeiss).

Zebrafish embryo incubations with ouabain.
Manually dechorionated 48hpf zebrafish embryos were incubated with vehicle or 100 uM ouabain diluted in E3 medium (5 mM NaCl, 0.17 mM Kcl, 0.33 mM $CaCl_2$, 0.33 mM $MgSO_4$ and 0.1% methylene blue), using seven embryos per point in triplicate. After six hours of incubation with slow shaking, the seven embryos per point were collected, sonicated, lysed together in 95ºC laemmli buffer during 5 minutes and resolved in SDS/PAGE gels (7.5%). GlyT2 expression was detected in Western blots using anti-GlyT2 rabbit primary antibody with a peroxidase-linked anti-rabbit IgG. Bands were visualized with the ECL (enhanced chemiluminescence) method and quantified on a GS-710 calibrated imaging densitometer (Bio-Rad).

Intramedullar administration of ouabain in adult wistar rats.
At 7–8 weeks of age, wistar rats (280–320 g) were anesthetized with intraperitoneal injections of 20 mg/kg of thiobarbital and body temperatures were kept within 37ºC using a heating pad. After breaking the skin, apophysis of thoracic vertebra 8 (T8) was removed, exposing the spinal cord. Intramedullar injections were administrated into this section using a Hamilton glass micro-needle syringe (Hamilton inc.) by injecting a volume of 2 μl of 1mM ouabain (or 2 μl of vehicle) per animal. Injection sites were identified by the deposition of a trypan blue dye (0.5 mg/ml, Sigma). After 3 hours of the administration, the animals were sacrificed and different sections of the spinal cord (cervical vertebra 4 (C4), thoracic vertebra 8 (T8) and thoracic vertebra 12 (T12)) were extracted, lysed and analyzed by western blot.

FIGURE LEGENDS

Figure legend 1. The neuronal glycine transporter GlyT2 associates with α subunits of Na/K ATPase.
A) The histogram represents the number of unique peptides corresponding to α1, α2 y α3 subunits of the Na/K ATPase indentified in protein A sepharose preclean control (light grey), rabbit IgG immunoprecipation control (medium grey) and anti-GlyT2 immunoprecipations (dark grey). Note the significantly increased number of αNKA peptides identified in GlyT2 immunoprecipation. β-V tubulin is shown as an example of inespecific peptides that are indentified equally in controls and in GlyT2 immunoprecipations. B) Representative MS/MS spectrum of unique peptides from α2 and α3 subunits of the Na/K ATPase indentified in GlyT2 immunoprecipations.

Figure legend 2. The neuronal glycine transporter GlyT2 copurifies with α subunits of Na/K ATPase.

A-B) Synaptosomes from rat brainstem and spinal cord were lysated and incubated at 4ºC with antibodies against GlyT2 (A), the α1, α2 or α3 NKA (B) subunit antibodies or the equivalent IgGs as control (A-B). After 1h of incubation with protein A beads (for rabbit antibodies) or protein G beads (for goat and mouse antibodies), samples were precipitated by mild centrifugation. The protein complexes were separated by SDS-PAGE and probed with anti-GlyT2 and α1, α2 or α3 NKA subunit antibodies. T: Total protein (4 µg), IP: Immunoprecipated sample (96 µg), IgG: IgG immunoprecipitation control (96 µg). Note the interaction can be detected with the three α isoforms, and no signal is observed in the IgG controls. C) Quantification of the percentage of GlyT2 interacting with the different α subunits was calculated from immunoprecipitations shown in (B). The histogram represents the mean ± SEM (IP α1, n=3; IP α2, n=5; IP α3, n=7)

Figure legend 3. GlyT2 colocalizes with α3 subunit of Na/K ATPase in brainstem and spinal cord primary neurons.

A-D) Primary cultures of spinal cord and brainstem neurons were grown in glass coverslips, fixed in -20ºC methanol and incubated with antibodies against GlyT2 and α1 (A), α2 (B) or α3 (C) NKA subunits. After incubation with secondary antibodies, samples were visualized by confocal microscopy, showing GlyT2 in red and αNKA subunits in green. D) Quantification of colocalization using Pearson´s value was performed as described in Materials and Methods. The histogram represents the mean ± SEM (n = 3; on average, 30 images per condition were analyzed in each experiment). *, significantly different, $p < 0.05$; ***, significantly different, $p < 0.001$ by ANOVA with Tukey's post hoc test. Note the significantly enriched colocalization between GlyT2 and α3 subunit of Na/K ATPase over α2 and α1 subunits.

Figure legend 4. GlyT2 colocalizes with α3 subunit of Na/K ATPase in synaptosomes from adult rat brainstem and spinal cord.

A-D) Synaptosomes isolated from adult rat brainstem and spinal cord were deposited in glass coverslips for 1h, fixed in -20ºC methanol and incubated with antibodies against GlyT2 and the α1 (A), α2 (B) or α3 (C) NKA subunits. After incubation with secondary antibodies, samples were visualized by confocal microscopy, showing GlyT2 in red and αNKA subunits in green. D) Quantification of colocalization using Pearson´s value was performed as described in Materials and Methods. The histogram represents the mean ± SEM (n = 3; on average, 30 images per condition were analyzed in each experiment). ###, significantly different, $p < 0.001$; ***, significantly different, $p < 0.001$ by ANOVA with Tukey's post hoc test. Note the significantly enriched colocalization between GlyT2 and α3 subunit of Na/K ATPase over α2 and α1 subunits.

Figure legend 5. GlyT2-αNKA interaction is compartimentalized in lipid raft subdomains.

A-C) Adult rat brainstem and spinal cord synaptosomes were lysed with ice-cold lysis buffer and lipid raft fractionswere isolated by discontinuous sucrose density gradient as described in Materials and Methods. A) Membrane raft or non-raft fractions were pooled, adjusted to 100µg in the same volume, lysed at 37ºC during 30 min in lysis buffer to disrupt remaining raft structures and incubated with the antibody against α3 NKA or with the equivalent amount of goat IgGs as control. After protein G sepharose incubation, protein complexes were separated by SDS-PAGE and probed with anti-GlyT2 antibody. T: Total protein (4 µg), IP: Immunoprecipated sample (96 µg), IgG: IgG-immunoprecipitation control (96 µg). Note that GlyT2 only copurifies with lipid raft-associated α3NKA isoform, and no signal is observed in the IgG controls or from the non-raft α3NKA immunoprecipitation. B) For each experiment performed as in (A), 10 µg of raft and non-raft fractions were run in SDS-PAGE and probed with anti-flotillin1 (raft marker) and anti-clathrin heavy chain (CHC, non-raft marker) to control the purity of the isolated fractions. C) Lipid raft and non-raft fractions isolated and lysed as in (A) were incubated with anti-GlyT2 or rabbit IgG and precipitated with protein A sepharose. Protein complexes were digested, and the resulting peptides were identified by high-throughput MS. The table shows the number of α1-, α2- and α3NKA unique peptides identified from raft (1) and non-raft fractions. Note that α NKA subunits are preferentially detected in lipid raft-associated GlyT2 immunoprecipitates.

Figure legend 6. Triple colocalization between GlyT2, α3NKA and the lipid raft marker Thy-1 in brainstem and spinal cord primary neurons.

A-C) Primary cultures of spinal cord and brainstem neurons were grown in glass coverslips, fixed in -20ºC methanol and incubated with primary and secondary antibodies against GlyT2 (green) α3NKA (red) and the lipid raft marker Thy-1 (blue). Samples were visualized by confocal microscopy, and triple colocalization maps were generated using a colocalization colormap plugin as described in Materials and Methods to denote triple colocalization regions, showing in red maximum colocalization pixels and in blue minimum colocalization pixels. Note that GlyT2-α3NKA colocalization co-compartimentalizes extensively with Thy-1 lipid raft clusters.

Figure legend 7. Functional coupling between Na/K ATPase and GlyT2.

A) Concentration-dependent inhibition of 86-rubidium uptake (Na/K ATPase activity) and [3H]-glycine transport (GlyT2 transport) by ouabain (20 min) in brainstem and spinal cord primary neurons. The results are expressed as percentage of control (without ouabain). Each point represents the mean ± SEM of four experiments done in triplicate. B-C) Representative immunoblot of primary brainstem and spinal cord neuronal cultures. Cells were treated with ouabain at 1µM (B) or 50µM (C) for the indicated times. After cell surface proteins were labeled with sulfo-NHS-SS-biotin the biotinylated proteins were pulled down with streptavidin-agarose beads and surface and total expression of GlyT2 and α3NKA were analyzed by western blot. Tubulin immunodetection was used as a non-biotinylated protein control. (2) and (4): biotinylated protein (16 µg); (1) and (3): total protein (8 µg). D) Degradation curves were generated by measuring GlyT2 band densities and normalizing them to corresponding tubulin band densities in total proteins (1) and (3), or normalizing them to corresponding surface α3NKA band densities in surface proteins (2) and (4), designating time zero as 100%. Black curves correspond to total GlyT2 after 1µM (1) or 50µM (3) ouabain treatments and grey curves correspond to surface GlyT2 after 1µM (2) or 50µM (4) ouabain treatments. Densitometric analysis of five independent Western blots as in B and C was performed, representing the means ± SEM. E-G) Representative immunoblots of primary brainstem and spinal cord neuronal cultures. E) Neurons were pre-treated with vehicle (veh), leupeptin (leupt) or MG132 for 3h. After that, vehicle or 50µM ouabain were added for 3h more mantaining previous pre-treatment and GlyT2

expression was analyzed by western blot. Note the significative blockage of GlyT2 degradation by leupeptine treatment. F) Neurons were treated with 10µg/ml cicloheximide or 50µM ouabain and with the respective vehicles (veh) during 3 hours and GlyT2 expression was analyzed by western blot. G) Neurons were treated with vehicle or 50µM ouabain and expression of GlyT2 related proteins was analyzed: α1NKA, syntaxin1A (STX1A), serotonin transporter (SERT), CRMP5 and gaba transporter 1 (GAT1).

Figure legend 8. Ouabain mediated degradation of lipid raft-associated GlyT2.
A-B) Brainstem and spinal cord primary neurons were treated with vehicle or 50µM ouabain during 3h, lysed with ice-cold lysis buffer and lipid raft fractionswere isolated by discontinuous sucrose density gradient as described in Materials and Methods. Membrane raft or non-raft fractions were pooled, adjusted to 100µg in the same volume, lysed at 37ºC during 30 min in lysis buffer and GlyT2 expression was analyzed. Flotillin1 was is shown to control the purity of the isolated fractions. Note the significative degradation of the lipid raft-associated GlyT2 pool. C-D) Neurons were pre-treated with vehicle (DMSO) or nystatin (Nys) for 3h. After that, vehicle or 50µM ouabain were added for 3h more mantaining previous pre-treatment and GlyT2 expression was analyzed by western blot. Note the significative blockage of GlyT2 degradation by nystatin-mediated disruption of raft subdomains.

Figure legend 9. GlyT2- α3NKA colocalization and *in vivo* ouabain-mediated degradation of GlyT2 in zebrafish embryos.
A-F) Dechorionated zebrafish embryos (48 hpf) were fixed in PFA 4%, permeabilized, immunostained against GlyT2 (green) and α3NKA (red) and visualized by confocal microscopy. A-C, whole-mount images of zebrafish embryos. D-F) Example detail showing colocalization between α3NKA and GlyT2 in dorsal interneurons. Scale bar 10 µm. E) Seven dechorionated zebrafish embryos (48 hpf) per condition were treated in E3 medium with or without 100 µM ouabain for 6h. After that, all embryos per condition were lysed together and GlyT2 expression was analyzed. Tubulin and α3NKA are shown as loading controls. Note significative reduction of GlyT2 expression whereas tubulin or α3NKA remained unaffected. F) The histogram represents the mean ± SEM of five experiments performed as in (E). ***, significantly different, p 0001 by student´s t-test.

Figure legend 10. Intramedullar administration of ouabain in adult rats produces in vivo degradation of GlyT2.
A-C) After anaesthesing the adult rats, 2 µl of vehicle or 2 µl of 1mM ouabain per animal were injected intramedullary at thoracic vertebra 8 (T8) spinal cord section. After 3 hours of the administration, the animals were sacrificed and different sections of the spinal cord were extracted, lysed and analyzed by western blot. These sections were from cervical vertebra 4 (C4), thoracic vertebra 8 (T8) and thoracic vertebra 12 (T12). B) The histogram represents the mean ± SEM (n = 4). *, significantly different, p 005 by ANOVA with Tukey's post hoc test. Note the reduced GlyT2 expression after ouabain administration in vivo. C) The cartoon shows different spinal cord sections extracted after ouabain administration in vivo and red colour denotes ouabain injection.

REFERENCES

Armsen W, Himmel B, Betz H, Eulenburg V (2007) The C-terminal PDZ-ligand motif of the neuronal glycine transporter GlyT2 is required for efficient synaptic localization. Mol Cell Neurosci 36:369-80.

Aragón C, Lopez-Corcuera B (2003) Structure,function and regulation of glycine neurotransporters. Eur J Pharmacol 479:249-262

Aragón C, López-Corcuera B (2005) Glycine transporters: crucial roles of pharmacological interest revealed by gene deletion. Trends Pharmacol Sci 26:283-286

Azarias G, Kruusmagi M, Connor S, Akkuratov EE, Liu XL, Lyons D, Brismar H, Broberger C, Aperia A (2013) A Specific and Essential Role for Na,K-ATPase α3 in Neurons Co-expressing α1 and α3. J Biol Chem 288:2734-43.

Bagrov AY, Shapiro JI, Fedorova OV (2005) Endogenous cardiotonic steroids: physiology, pharmacology, and novel therapeutic targets. Pharmacol Rev 61:9-38.

Benarroch EE (2011) Na+, K+ -ATPase: functions in the nervous system and involvement in
neurologic disease. Neurology 76:287-293.

Blakely RD, Bauman AL (2010) Biogenic amine transporters: regulation in flux. Curr Opin Neurobiol 10:328-336

Bolte S, Cordelières FP (2006) A guided tour into subcellular colocalization analysis in light microscopy. J Microsc 224:213-32.

Bonzon-Kulichenko E, Pérez-Hernández D, Núñez E, Martínez-Acedo P, Navarro P, Trevisan-Herraz M, Ramos Mdel C, Sierra S, Martínez-Martínez S, Ruiz-Meana M, Miró-Casas E, García-Dorado D, Redondo JM, Burgos JS, Vázquez J (2011) A robust method for quantitative high-throughput analysis of proteomes by 18O labeling. Mol Cell Proteomics 10:M110.003335.

Brashear A, Dobyns WB, de Carvalho Aguiar P, Bnorg M, Frijns CJ, Gollamudi S, Green A, Guimaraes J, Haake BC, Klein C, Linazasoro G, Munchau A, Raymond D, Riley D, Saunders-Pullman R, Tijssen MA, Webb D, Zaremba J, Bressman SB, Ozelius LJ (2007) The phenotypic spectrum of rapid-onset dystonia-parkinsonism (RDP) and mutations in the ATP1A3 gene. Brain 130:828-35.

Cheng RK, Jesuthasan S, Penney TB (2011) Time for zebrafish. Front Integr Neurosci. 5:40.

Cui WW, Low SE, Hirata H, Saint-Amant L, Geisler R, Hume RI, Kuwada JY (2005) The zebrafish shocked gene encodes a glycine transporter and is essential for the function of early neural circuits in the CNS. J Neurosci 25:6610-20.

de Carvalho Aguiar P, Sweadner KJ, Penniston JT, Zaremba J, Liu L, Caton M, Linazasoro G, Borg M, Tijssen MA, Bressman SB, Dobyns WB, Brashear A, Ozelius LJ (2004) Mutations in the Na+/ K+-ATPase alpha3 gene ATP1A3 are associated with rapid-onset dystonia parkinsonism. Neuron 43:169- 175

de Juan-Sanz J, Zafra F, López-Corcuera B, Aragón C (2011) Endocytosis of the neuronal glycine transporter GlyT2: role of membrane rafts and protein kinase C-dependent ubiquitination. Traffic 12:1850–1867

de Juan-Sanz J, Nunez E, López-Corcuera B, Aragón C (2013) Constitutive endocytosis and turnover of the neuronal glycine transporter GlyT2 is dependent on ubiquitination of a C-terminal lysine cluster. PLoS One. Feb 7. Doi: 10.1371/journal.pone.0058863. [In press]

Dobretsov M, Stimers JR (2005) Neuronal function and alpha3 isoform of the Na/K-ATPase. Front Biosci 10:2373-2396

el-Masri MA, Clark BJ, Qazzaz HM, and Valdes R Jr (2002) Human adrenal cells in culture produce both ouabain-like and dihydroouabain-like factors. Clin Chem 48:1720-1730.

Eulenburg V, Becker K, Gomeza J, Schmitt B, Becker CM, Betz H (2006) Mutations within the human GLYT2 (SLC6A5) gene associated with hyperekplexia. Biochem Biophys Res Commun 348:400-405

Fornes A, Nunez E, Alonso-Torres P, Aragon C, Lopez-Corcuera B (2008) Trafficking properties and activity regulation of the neuronal glycine transporter GlyT2 by protein kinase C. Biochem J 412:495-506

Fujii T, Takahashi Y, Itomi Y, Fujita K, Morii M, Tabuchi Y, Asano S, Tsukada K, Takeguchi N, Sakai H (2008) K+-Cl- Cotransporter-3a Up-regulates Na+,K+-ATPase in Lipid Rafts of Gastric Luminal Parietal Cells. J Biol Chem 283:6869-6877.

Geerlings A, Nunez E, Lopez-Corcuera B, Aragon C (2001) Calcium- and syntaxin 1-mediated trafficking of the neuronal glycine transporter GlyT2. J Biol Chem 276:17584-17590

Gimenez C, Perez-Siles G, Martinez-Villarreal J, Arribas-Gonzalez E, Jimenez E, Nunez E, de Juan-Sanz J, Fernandez-Sanchez E, Garcia-Tardon N, Ibanez I, Romanelli V, Nevado J, James VM, Topf M, Chung SK, Thomas RH, Desviat LR, Aragon C, Zafra F, Rees MI, Lapunzina P, Harvey RJ, Lopez-Corcuera B (2012) A novel dominant hyperekplexia mutation Y705C alters trafficking and biochemical properties of the presynaptic glycine transporter GlyT2. J Biol Chem 287:28986-29002

Gomeza J, Hulsmann S, Ohno K, Eulenburg V, Szoke K, Richter D, Betz H (2003a) Inactivation of the glycine transporter 1 gene discloses vital role of glial glycine uptake in glycinergic inhibition. Neuron. 40:785-796
Gomeza J, Ohno K, Hulsmann S, Armsen W, Eulenburg V, Richter DW, Laube B, Betz H (2003b) Deletion of the mouse glycine transporter 2 results in a hyperekplexia phenotype and postnatal lethality. Neuron 40:797-806

Hamlyn JM, Blaustein MP, Bova S, DuCharme DW, Harris DW, Mandel F, Mathews WR, Ludens JH (1991) Identification and characterization of a ouabain-like compound from human plasma. Proc Natl Acad Sci U S A 88:6259-6263.

Hazelwood LA, Free RB, Cabrera DM, Skinbjerg M, Sibley DR (2008) Reciprocal modulation of function between the D1 and D2 dopamine receptors and the Na+,K+-ATPase. J Biol Chem 283:36441-36453

Heinzen EL, Swoboda KJ, Hitomi Y, Gurrieri F, Nicole S, et. al. (2012) De novo mutations in ATP1A3 cause alternating hemiplegia of childhood. Nat Genet. 44:1030-4.

Higashijima S, Mandel G, Fetcho JR (2004a) Distribution of prospective glutamatergic, glycinergic, and GABAergic neurons in embryonic and larval zebrafish. J Comp Neurol. 480:1-18.

Higashijima S, Schaefer M, Fetcho JR (2004b) Neurotransmitter properties of spinal interneurons in embryonic and larval zebrafish J Comp Neurol 480:19-37.

Hilgenberg LG, Su H, Gu H, O'Dowd DK, Smith MA (2006) Alpha3Na+/K+-ATPase is a neuronal receptor for agrin. Cell 125:359-69.

Horiuchi M, Loebrich S, Brandstaetter JH, Kneussel M, Betz H (2005) Cellular localization and subcellular distribution of Unc-33-like protein 6, a brain-specific protein of the collapsin response mediator protein family that interacts with the neuronal glycine transporter 2. J Neurochem 94:307-315.

Jaskolski F, Mulle C, Manzoni OJ (2005) An automated method to quantify and visualize colocalized fluorescent signals. J Neurosci Methods 146:42-9.

Jiménez E, Zafra F, Pérez-Sen R, Delicado EG, Miras-Portugal MT, Aragón C, López-Corcuera B (2011) P2Y purinergic regulation of the glycine neurotransmitter transporters. J Biol Chem. 286:10712-24.

Juhaszova M, Blaustein MP (1997) Na+ pump low and high ouabain affinity a subunit isoforms are differently distributed in cells. Proc Natl Acad Sci USA 94:1800–1805.

Kim JH, Sizov I, Dobretsov M, von Gersdorff H (2007) Presynaptic Ca2+ buffers control the strength of a fast post-tetanic hyperpolarization mediated by the alpha3 Na(+)/K(+)-ATPase. Nat Neurosci 10:196-205.

Kirshenbaum GS, Clapcote SJ, Duffy S, Burgess CR, Petersen J, Jarowek KJ, Yucel YH, Cortez, MA, Snead OC, Vilsen B, Peever JH, Ralph MR, Roder JC (2011a) Mania-like behavior induced by genetic dysfunction of the neuron-specific Na+,K+- ATPase alpha3 sodium pump. Proc Natl Acad Sci U S A 108:18144-18149

Kirshenbaum GS, Saltzman K, Rose B, Petersen J, Vilsen B, Roder JC (2011b) Decreased neuronal Na+, K+ -ATPase activity in Atp1a3 heterozygous mice increases susceptibility to depression-like endophenotypes by chronic variable stress. Genes brain behav 10:542-550

Kristensen AS, Andersen J, Jørgensen TN, Sørensen L, Eriksen J, Loland CJ, Strømgaard K, Gether U (2011) SLC6 neurotransmitter transporters: structure, function, and regulation. Pharmacol Rev 63:585-640

Levin ED, Cerutti DT (2009) Behavioral Neuroscience of Zebrafish. Methods of Behavior Analysis in Neuroscience. 2nd edition. Boca Raton (FL): CRC Press. Chapter 15. Front in Neurosci

Li Z, Xie Z (2009) The Na/K-ATPase/Src complex and cardiotonic steroid-activated protein kinase cascades. Pflugers Arch. 457:635-44.

Lingrel JB (2010) The physiological significance of the cardiotonic steroid/ouabain-binding site of the Na,K-ATPase. Annu Rev Physiol 72:395-412.

Lingrel JB, Williams MT, Vorhees CV, Moseley AE (2007) Na,K-ATPase and the role of alpha isoforms in behavior. J Bioenerg Biomembr 39:385-389

Liu J, Xie, ZJ (2010) The sodium pump and cardiotonic steroids-induced signal transduction protein kinases and calcium-signaling microdomain in regulation of transporter trafficking. Biochim Biophys Acta 1802:1237-1245.
Liu L, Ivanov AV, Gable ME, Jolivel F, Morrill GA, Askari A (2011) Comparative properties of caveolar and noncaveolar preparations of kidney Na+/K+-ATPase. Biochemistry 50:8664-8673
Longva K, Blystad F, Stang E, Larsen A, Johannessen L, Madshus I (2002) Ubiquitination and proteasomal activity is required for transport of the EGF receptor to inner membranes of multivesicular bodies. J Biol Sci 156:843-854

Ludens JH, Clark MA, DuCharme DW, Harris DW, Lutzke BS, Mandel F, Mathews WR, Sutter DM, Hamlyn JM (1991) Purification of an endogenous digitalis-like factor from human plasma for structural analysis. Hypertension 17: 923-929.

Madore N, Smith KL, Graham CH, Jen A, Brady K, Hall S, Morris R (1999) Functionally different GPI proteins are organized in different domains on the neuronal surface. EMBO J 18:6917-6926.

Maria S. Melikova, Kirill A. Kondratov, Elena S. Kornilova (2006) Two different stages of epidermal growth factor (EGF) receptor endocytosis are sensitive to free ubiquitin depletion produced by proteasome inhibitor MG132. Cell Biol Int 30:31-43

Martínez-Bartolomé S, Navarro P, Martín-Maroto F, López-Ferrer D, Ramos-Fernández A, Villar M, García-Ruiz JP, Vázquez J (2008) Properties of average score distributions of SEQUEST: the probability ratio method. Mol Cell Proteomics 7:1135-45.

Moly PK, Hatta K (2011) Early glycinergic axon contact with the Mauthner neuron during zebrafish development. Neurosci Res 70:251-9.

Moseley AE, Williams MT, Schaefer TL, Bohanan CS, Neumann JC, Behbehani MM, Vorhees CV, Lingrel JB (2007) Deficiency in Na,K-ATPase alpha isoform genes alters spatial learning, motor activity, and anxiety in mice. J Neurosci 27:616-626.

Navarro P, Vázquez J (2009) A refined method to calculate false discovery rates for peptide identification using decoy databases. J Proteome Res. 8:1792-6.

Nuñez E, Alonso-Torres P, Fornes A, Aragon C, Lopez-Corcuera B. (2008) The neuronal glycine transporter GLYT2 associates with membrane rafts: functional modulation by lipid environment. J Neurochem 105:2080–2090.

Nuñez E, Perez-Siles G, Rodenstein L, Alonso-Torres P, Zafra F, Jimenez E, Aragon C, Lopez- Corcuera B (2009) Subcellular localization of the neuronal glycine transporter GlyT2 in brainstem. Traffic 10:829-843

Ohno K, Koroll M, El Far O, Scholze P, Gomeza J, Betz H (2004) The neuronal glycine transporter 2 interacts with the PDZ domain protein syntenin-1. Mol Cell Neurosci 26:518-529.

Patnaik A, Chau V, Wills JW (2000) Ubiquitin is part of the retrovirus budding machinery. Proc Natl Acad Sci U S A 97:13069-13074.

Rees MI, Harvey K, Pearce BR, Chung SK, Duguid IC, Thomas P, Beatty S, Graham GE, Armstrong L, Shiang R, Abbott KJ, Zuberi SM, Stephenson JB, Owen MJ, Tijssen MA, van den Maagdenberg AM, Smart TG, Supplisson S, Harvey RJ (2006) Mutations in the gene encoding GlyT2 (SLC6A5) define a presynaptic component of human startle disease. Nat Genet 38:801-806

Reinhard L, Tidow H, Clausen MJ, Nissen P (2013) Na+,K+-ATPase as a docking station: protein–protein complexes of the Na+,K+-ATPase. Cell Mol Life Sci 70:205-22.

Rose EM, Koo JC, Antflick JE, Ahmed SM, Angers S, Hampson DR. (2009) Glutamate transporter coupling to Na,K-ATPase. J Neurosci 29:8143-8155.

Roux MJ, Supplisson S (2000) Neuronal and glial glycine transporters have different stoichiometries. Neuron 25:373–383

Simons K, Gerl MJ (2010) Revitalizing membrane rafts: new tools and insights. Nat Rev Mol Cell Biol 11:688-99

Sweadner KJ (1989) Isozymes of the Na+/K+-ATPase. Biochem Biophys Acta 988:185–220.

Taguchi K , Kumanogoh H, Nakamura S, Maekawa S.(2007) Ouabain-induced isoform-specific localization change of the Na+,K+-ATPase subunit in the synaptic plasma membrane of rat brain. Neurosci Lett 413:42–45.

Tajima N, Itokazu Y, Korpi ER, Somerharju P, Käkelä R (2011) Activity of BK(Ca) channel is modulated by membrane cholesterol content and association with Na+/K+-ATPase in human melanoma IGR39 cells. J Biol Chem 286:5624-5638.

Tymiak AA, Norman JA, Bolgar M, DiDonato GC, Lee H, Parker WL, Lo LC, Berova N, Nakanishi K, and Haber E (1993) Physicochemical characterization of a ouabain isomer isolated from bovine hypothalamus. Proc Natl Acad Sci U S A 90: 8189-8193.

Welker P, Geist B, Frühauf JH, Salanova M, Groneberg DA, Krause E, Bachmann S (2007) Role of lipid rafts in membrane delivery of renal epithelial Na+-K+-ATPase, thick ascending limb. Am J Physiol Regul Integr Comp Physiol. 292:R1328-37.

Xi Y, Noble S, Ekker M (2011) Modeling neurodegeneration in zebrafish. Curr Neurol Neurosci Rep. 11:274-82

Zafra F, Aragon C, Olivares L, Danbolt NC, Gimenez C, et al. (1995) Glycine transporters are differentially expressed among CNS cells. J Neurosci 15:3952–3969.

Zhang D, Hou Q, Wang M, Lin A, Jarzylo L, Navis A, Raissi A, Liu F, Man HY (2009) Na+,K+-ATPase activity regulates AMPA receptor turnover through proteasome-mediated proteolysis. J Neurosci 29:4498-4511.

Zinchuk V, Zinchuk O (2008) Quantitative colocalization analysis of confocal fluorescence microscopy images. Curr Protoc Cell Biol. Chapter 4:Unit 4.19.

Figure 1

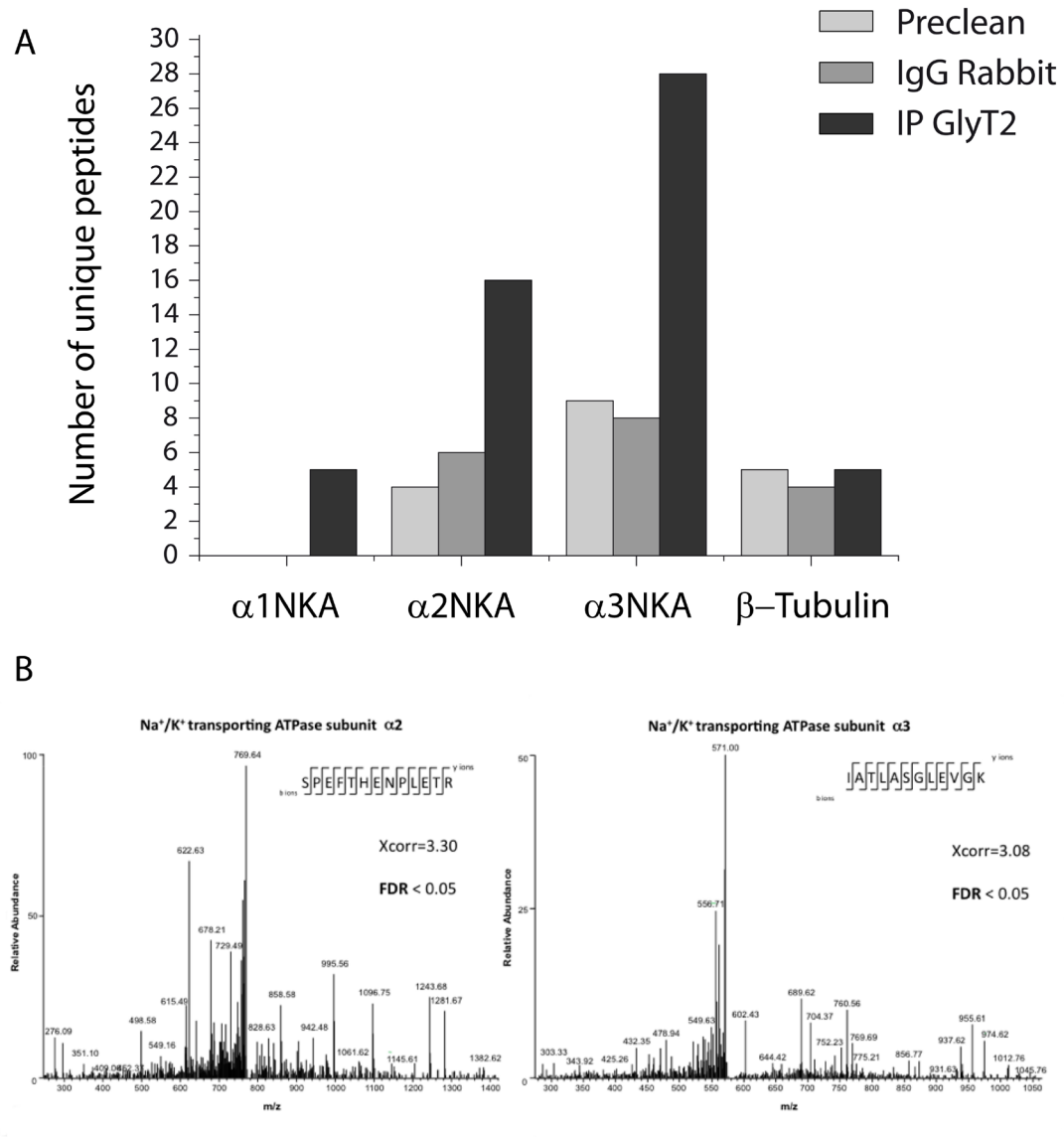
A
Number of unique peptides
30
28
26
24
22
20
18
16
14
12
10
8
6
4
2
0
Preclean
IgG Rabbit
IP GlyT2
α1NKA
α2NKA
α3NKA
β–Tubulin
B
Na+/K+ transporting ATPase subunit α2
SPEFTHENPLETR
Xcorr=3.30
FDR < 0.05
Relative Abundance
m/z
Na+/K+ transporting ATPase subunit α3
IATLASGLEVGK
Xcorr=3.08
FDR < 0.05
Relative Abundance
m/z

Figure 2

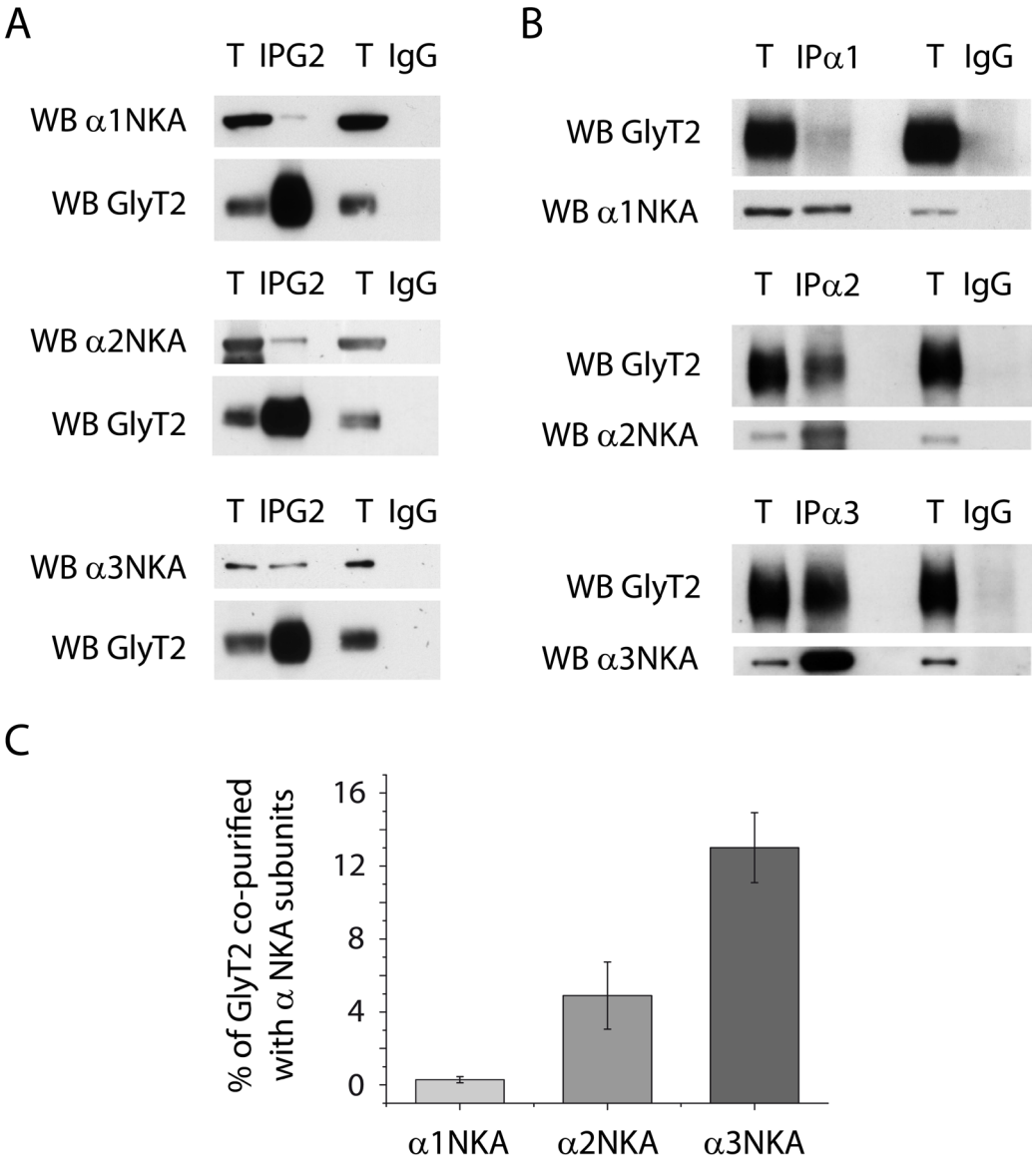
A
T IPG2 T IgG
WB α1NKA
WB GlyT2
T IPG2 T IgG
WB α2NKA
WB GlyT2
T IPG2 T IgG
WB α3NKA
WB GlyT2
B
T IPα1 T IgG
WB GlyT2
WB α1NKA
T IPα2 T IgG
WB GlyT2
WB α2NKA
T IPα3 T IgG
WB GlyT2
WB α3NKA
C
% of GlyT2 co-purified with α NKA subunits
16
12
8
4
0
α1NKA
α2NKA
α3NKA

Figure 3

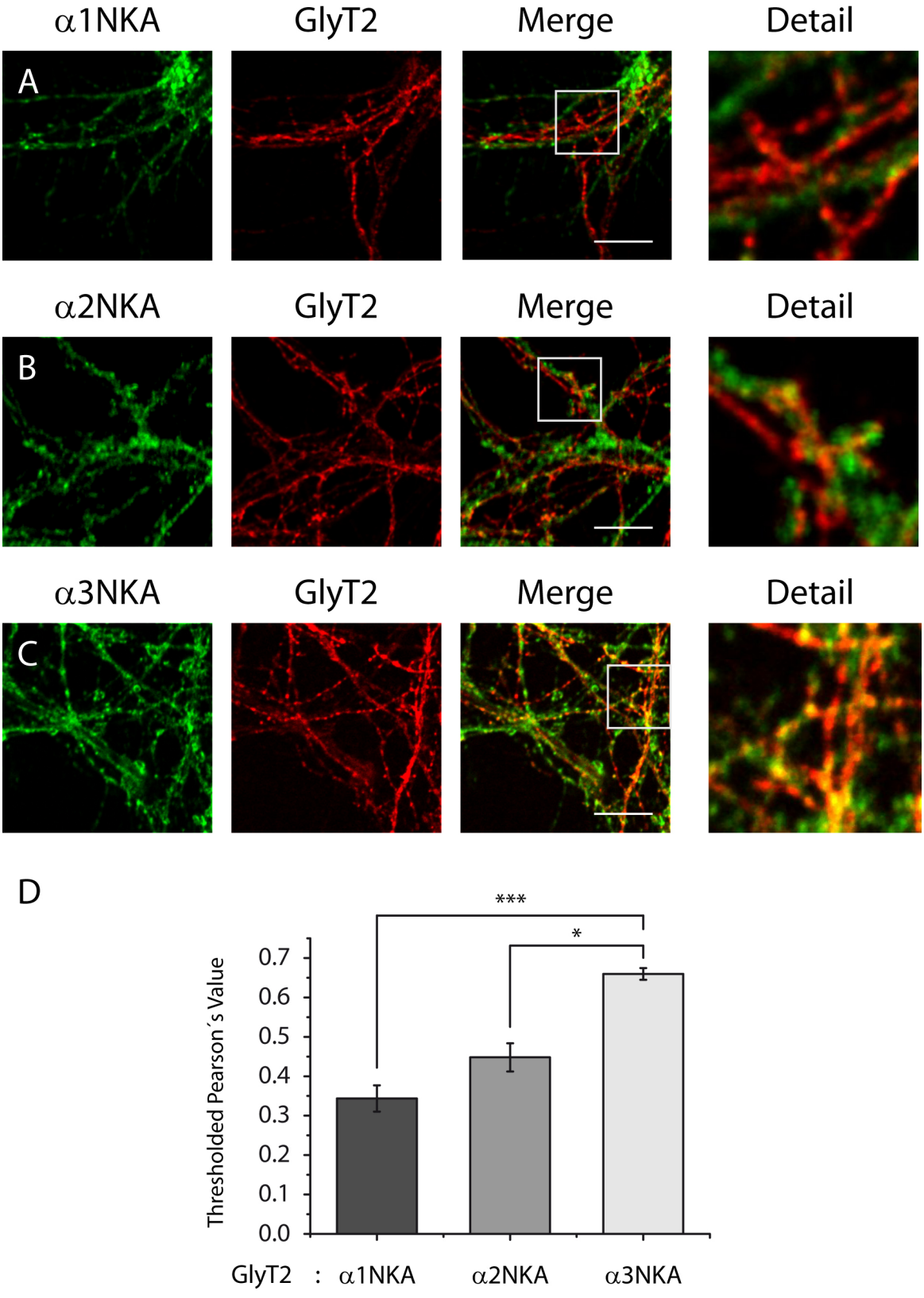
α1NKA
GlyT2
Merge
Detail
A
α2NKA
GlyT2
Merge
Detail
B
α3NKA
GlyT2
Merge
Detail
C
D
***
*
Thresholded Pearson´s Value
0.7
0.6
0.5
0.4
0.3
0.2
0.1
0.0
GlyT2 : α1NKA
α2NKA
α3NKA

Figure 4

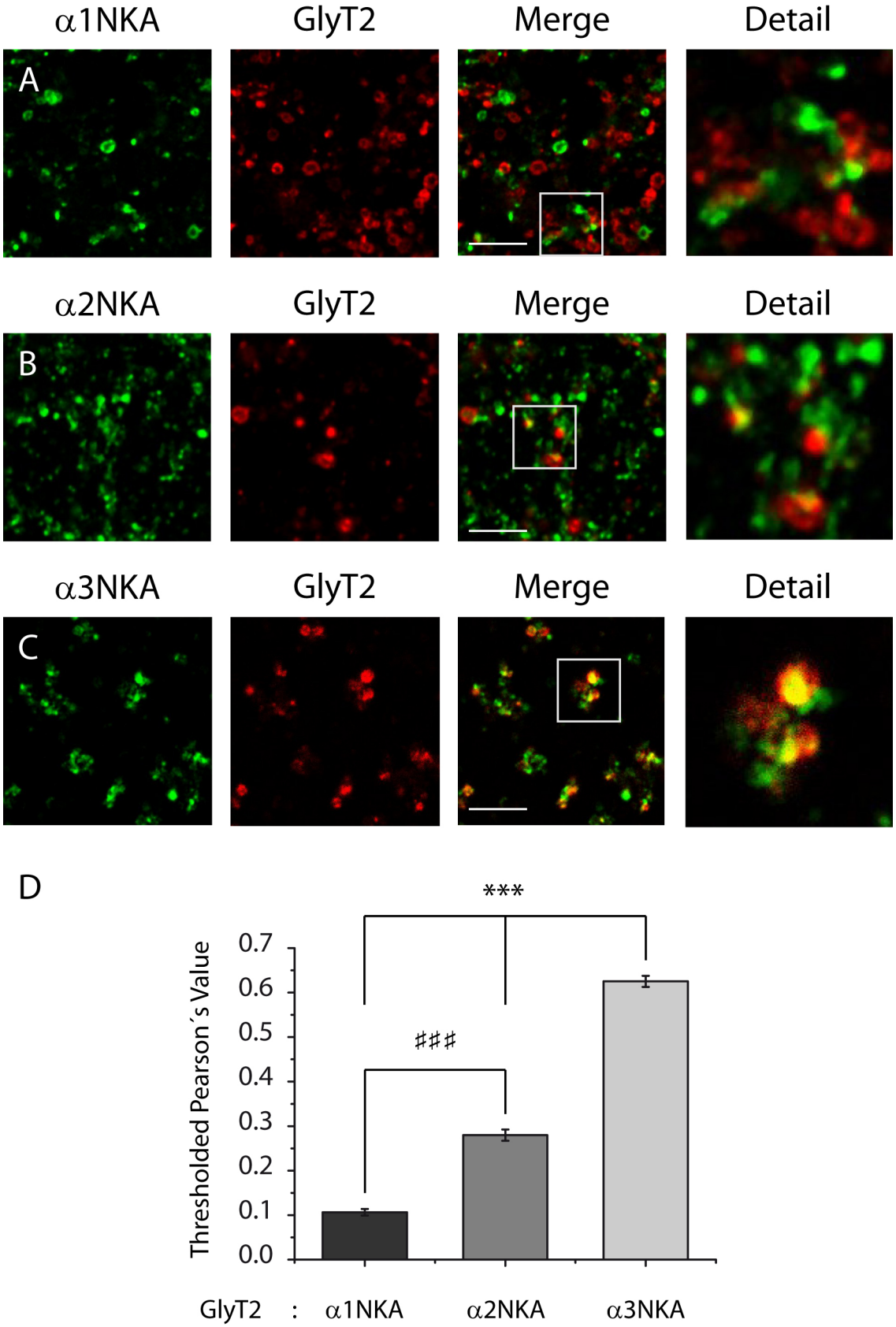
α1NKA
GlyT2
Merge
Detail
A
α2NKA
GlyT2
Merge
Detail
B
α3NKA
GlyT2
Merge
Detail
C
D
***
###
Thresholded Pearson´s Value
0.7
0.6
0.5
0.4
0.3
0.2
0.1
0.0
GlyT2 : α1NKA
α2NKA
α3NKA

Figure 5

A

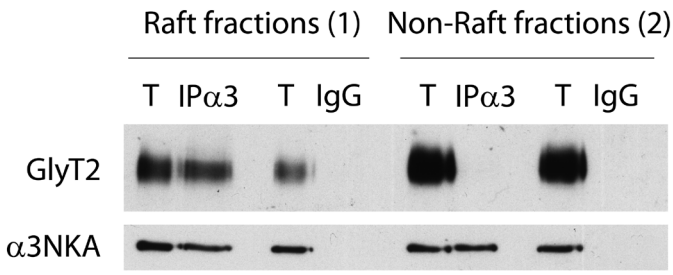

B

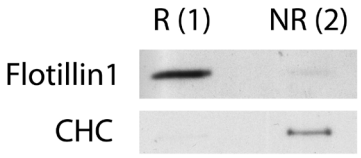

C Number of unique peptides: IP GlyT2 from R(1) and NR(2)

Acc. Number	Protein name	Raft fractions (1)		Non-Raft fractions (2)	
		IgG Rabbit	IP GlyT2	IgG Rabbit	IP GlyT2
P05023	α1NKA	0	**6**	0	0
P50993	α2NKA	1	**13**	0	2
P13637	α3NKA	4	**16**	0	0

Figure 6

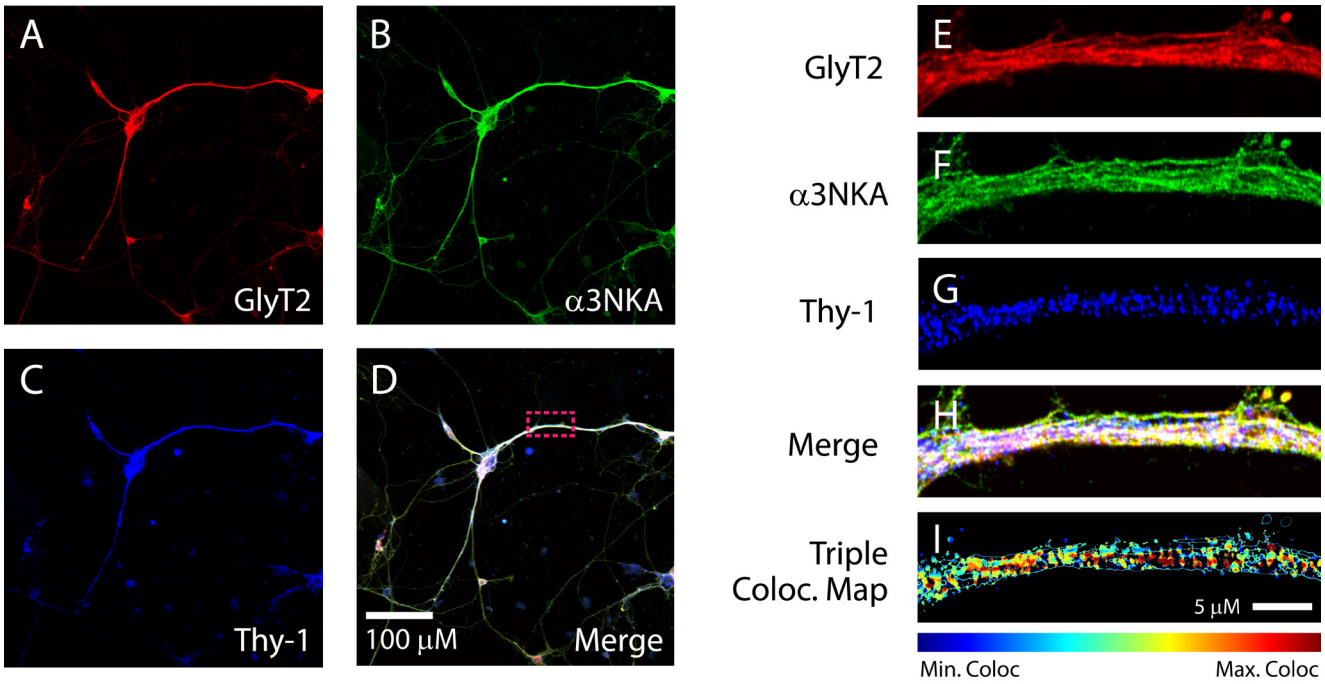
A
GlyT2
B
α3NKA
C
Thy-1
D
100 μM
Merge
GlyT2
E
α3NKA
F
Thy-1
G
Merge
H
Triple
Coloc. Map
I
5 μM
Min. Coloc
Max. Coloc

Figure 7

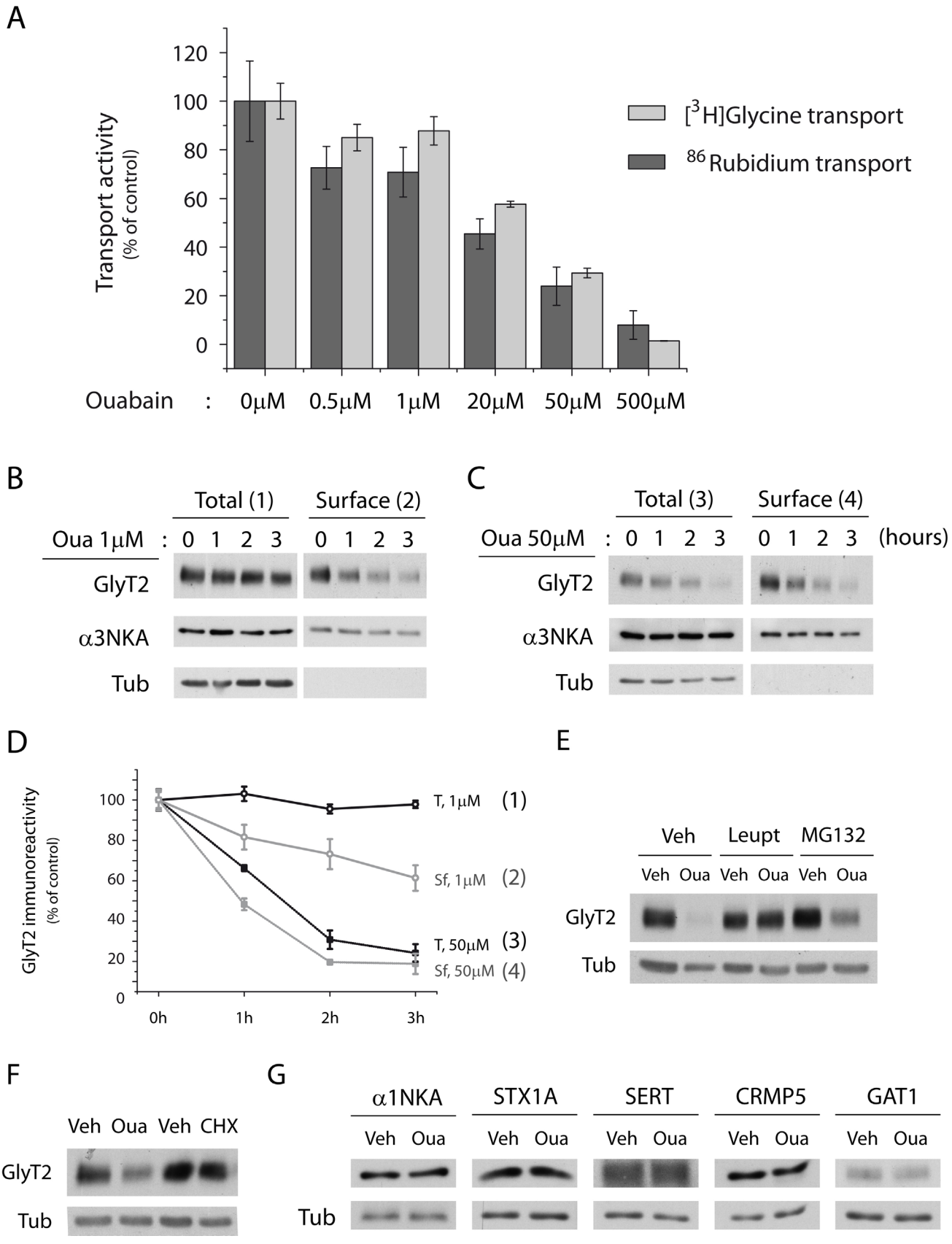
A
Transport activity
(% of control)
120
100
80
60
40
20
0
[3H]Glycine transport
86Rubidium transport
Ouabain : 0µM 0.5µM 1µM 20µM 50µM 500µM
B
Total (1)
Surface (2)
Oua 1µM : 0 1 2 3 0 1 2 3
GlyT2
α3NKA
Tub
C
Total (3)
Surface (4)
Oua 50µM : 0 1 2 3 0 1 2 3 (hours)
GlyT2
α3NKA
Tub
D
GlyT2 immunoreactivity
(% of control)
100
80
60
40
20
0
0h
1h
2h
3h
T, 1µM (1)
Sf, 1µM (2)
T, 50µM (3)
Sf, 50µM (4)
E
Veh
Leupt
MG132
Veh Oua Veh Oua Veh Oua
GlyT2
Tub
F
Veh Oua Veh CHX
GlyT2
Tub
G
α1NKA
STX1A
SERT
CRMP5
GAT1
Veh Oua Veh Oua Veh Oua Veh Oua Veh Oua
Tub

Figure 8

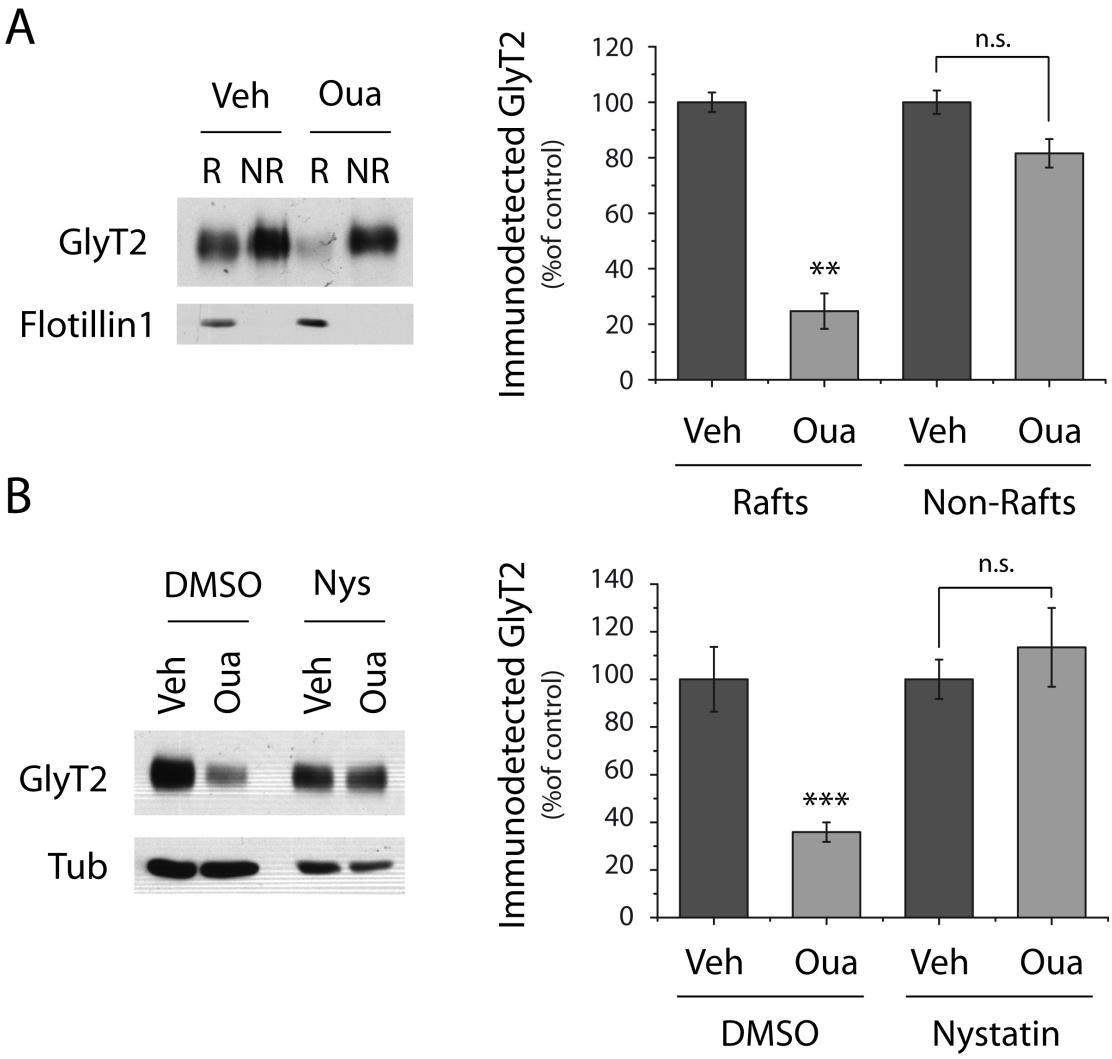
A
Veh
Oua
R NR R NR
GlyT2
Flotillin1
Immunodetected GlyT2
(%of control)
120
100
80
60
40
20
0
n.s.
**
Veh
Oua
Veh
Oua
Rafts
Non-Rafts
B
DMSO
Nys
Veh
Oua
Veh
Oua
GlyT2
Tub
Immunodetected GlyT2
(%of control)
140
120
100
80
60
40
20
0
n.s.
***
Veh
Oua
Veh
Oua
DMSO
Nystatin

Figure 9

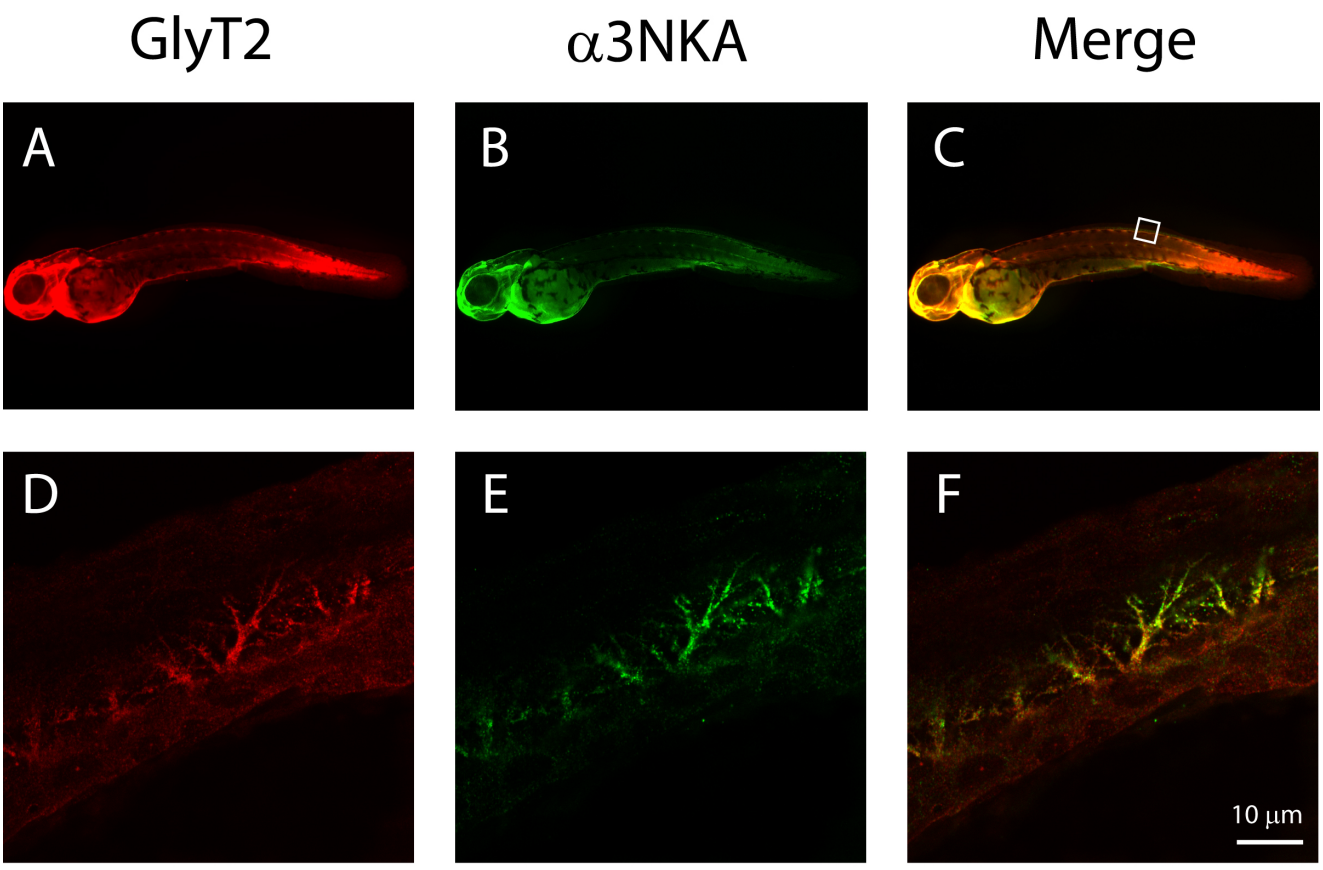
GlyT2
α3NKA
Merge
A
B
C
D
E
F
10 μm

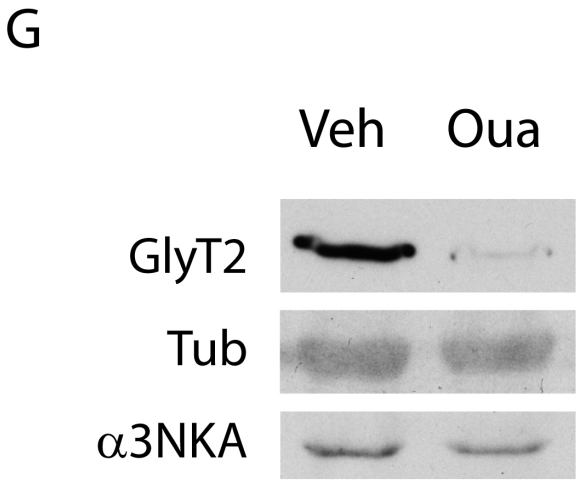
G
Veh
Oua
GlyT2
Tub
α3NKA

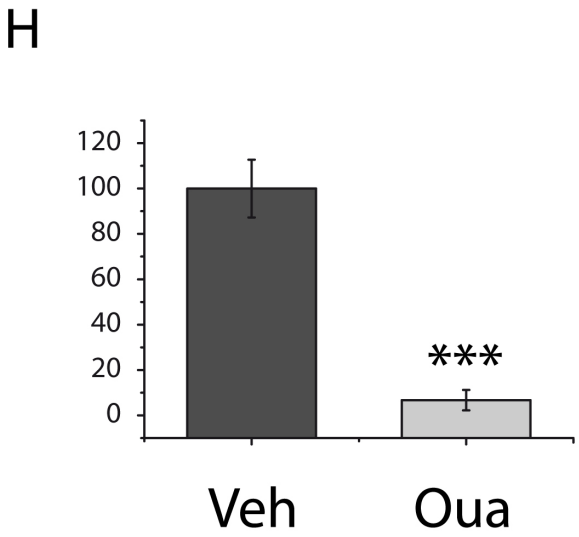
H
120
100
80
60
40
20
0
***
Veh
Oua

Figure 10

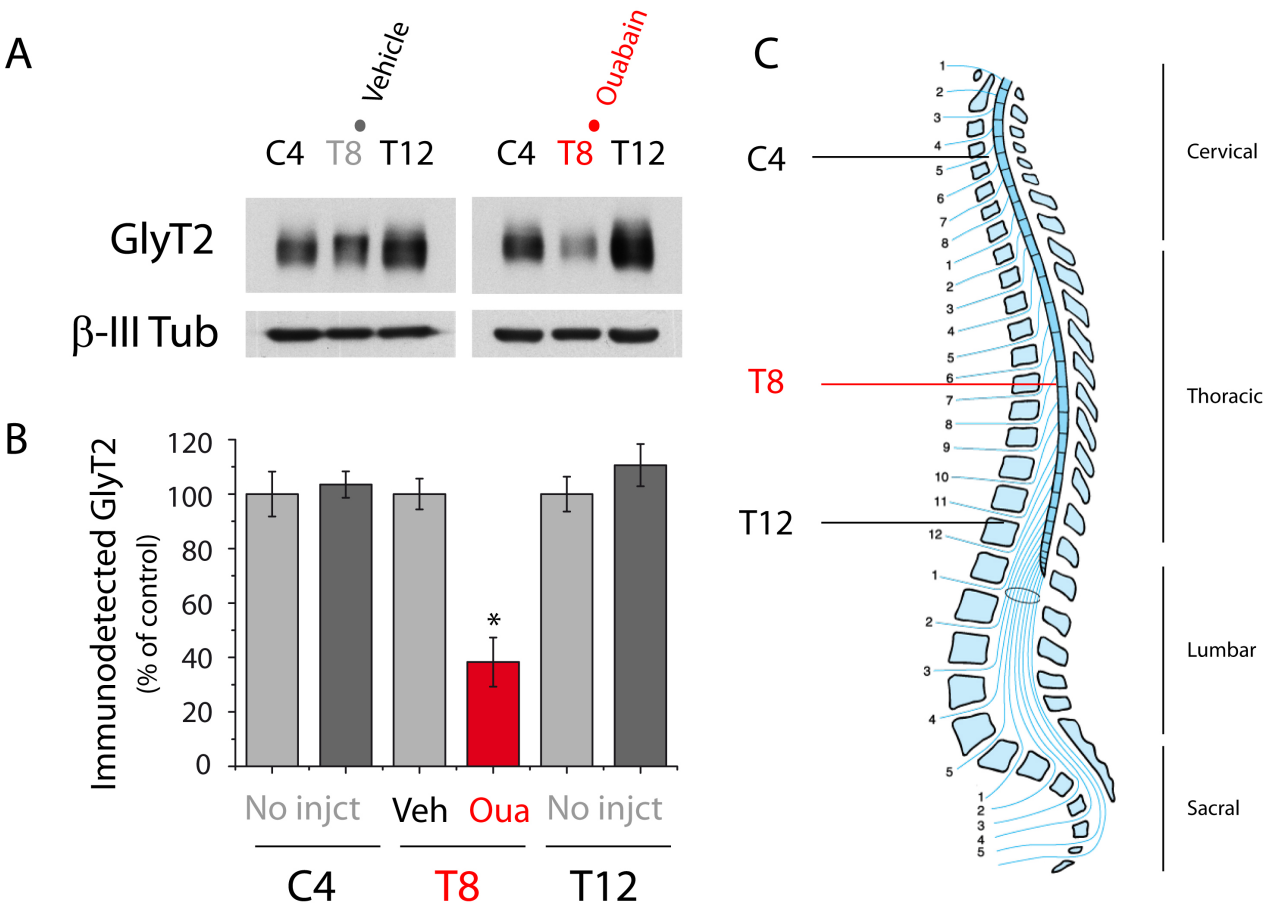
A
Vehicle
Ouabain
C4 T8 T12
C4 T8 T12
GlyT2
β-III Tub
B
Immunodetected GlyT2
(% of control)
120
100
80
60
40
20
0
*
No injct
Veh
Oua
No injct
C4
T8
T12
C
C4
T8
T12
Cervical
Thoracic
Lumbar
Sacral

Discusión

La generación y estudio de los ratones deficientes en los transportadores de glicina de alta afinidad GlyT1 y GlyT2 ha demostrado que la función de estos resulta crucial para el correcto funcionamiento de la neurotransmisión glicinérgica. Mientras que el transportador principalmente glial GlyT1 parece llevar a cabo una recaptación de glicina rápida en el espacio sináptico terminando así la inhibición mediada por glicina, el transportador neuronal GlyT2 se encarga del reciclaje del neurotransmisor hacia la neurona presináptica, lo que favorece el rellenado de la vesículas sinápticas y permite la posterior reutilización y liberación de la glicina al espacio sináptico. Esta función de GlyT2 resulta clave para el organismo, ya que mutaciones en su gen codificante *SLC6A5* producen la enfermedad denominada hiperplexia, también conocida como enfermedad del sobresalto o "síndrome del bebé entumecido". Esta enfermedad, cuyos síntomas aparecen muy pronto tras el nacimiento, se caracteriza por la rigidez de tronco y extremidades, puños apretados, frecuentes temblores y sobresaltos enérgicos y generalizados en respuesta a estímulos triviales generalmente acústicos o táctiles, que pueden llegar a producir la muerte súbita del neonato por parada cardiorespiratoria.

El estudio de diferentes mutaciones de GlyT2 encontradas en humanos muestra que una gran proporción de estas poseen fallos en su tráfico intracelular, uno de los mecanismos clave propuestos para la regulación de los transportadores de neurotransmisores (75,76), por lo que resulta de gran interés profundizar en el estudio de la modulación endógena de la actividad de GlyT2 a través de su presencia/ausencia en la membrana plasmática. De este modo, variaciones en la cantidad de moléculas de GlyT2 activas en la superficie celular modulan en gran medida la neurotransmisión glicinérgica inhibidora, básica para el correcto procesamiento sensorial, acústico y visual del entorno y necesaria para el control coordinado de la musculatura gracias a su implicación en los circuitos reflejos espinales de inhibición recíproca (1-5).

Pese al gran esfuerzo dedicado en la última década sobre el estudio del tráfico de GlyT2 (91-97), varias cuestiones clave permanecían sin resolver. En esta tesis doctoral nos hemos planteado profundizar en algunas de ellas, como son:

1. Indentificación de la vía principal de endocitosis del transportador en la internalización constitutiva e inducida por la activación de PKC.
2. Determinación del papel de los *lipid rafts* en el tráfico constitutivo y regulado por PKC de GlyT2.
3. Determinación del papel de la ubiquitinación sobre el tráfico constitutivo y regulado por PKC de GlyT2 y su implicación en la estabilidad del transportador.
4. Identificación de nuevas proteínas que interaccionen con GlyT2 y modulen su tráfico y actividad.

Gracias a los experimentos realizados, hemos contribuido a profundizar y describir nuevos mecanismos para la modulación de la actividad de GlyT2, 1) implicando a la vía dependiente de clatrina como el mecanismo molecular de internalización de GlyT2 (artículo #1), 2) describiendo el papel de la presencia de GlyT2 en *lipid rafts* y sus implicaciones diferenciales en el tráfico constitutivo y regulado por PKC (artículo #1) , 3) señalando al proceso de ubiquitinación en el carboxilo terminal de GlyT2 como un mecanismo implicado en la estabilidad y endocitosis del transportador (artículo #1 y artículo #2), 4) contribuyendo a la descripción de una nueva mutación en GlyT2 (Y705C) asociada a hiperplexia (artículo #3) y 5) señalando a la subunidad catalítica α de la Na/K ATPasa como un nuevo interactor de GlyT2 que es capaz de inducir su endocitosis y degradación en presencia de esteroides cardiotónicos como la ouabaína (artículo #4) .

A continuación se muestra el resumen de resultados y la discusión de los mismos siguiendo los apartados descritos anteriormente.

1

Identificación de la vía principal de endocitosis del transportador en la internalización constitutiva e inducida por PKC de GlyT2, presentado en el artículo #1.

Parte del estudio de tráfico intracelular presentado en esta tesis se ha realizado en células MDCK como modelo de expresión heterólogo, ya que expresan GlyT2 en la membrana apical de una manera asimétrica que se propone como reflejo de la distribución del transportador y otras proteínas de membrana en axones y terminales nerviosos (99). Además, es un tipo celular que no expresa GlyT2 endógenamente permitiendo la transfección y comparación de diversos mutantes frente al fenotipo silvestre.

El transportador GlyT2 sobrexpresado en estas células trafica de un modo constitutivo al igual que ocurre en neuronas, residiendo intracelularmente en endosomas de reciclaje rab11 positivos (93). Un método común para el estudio de la endocitosis constitutiva de proteínas de membrana en líneas celulares o en cultivos primarios de neuronas es el uso de del iónoforo de protones monensina que bloquea el reciclaje de vuelta a la membrana de las proteínas internalizadas, provocando su acumulación en endosomas (78, 89, 90, 100-102). Esta internalización constitutiva de GlyT2 puede ser acelerada en presencia de PMA, un activador general de las distintas isoformas de PKC, de tal modo que la adición simultánea de PMA y monensina se traduce en una bajada drástica de la cantidad de GlyT2 en membrana como resultado de la suma de la endocitosis constitutiva y la regulada por PKC (86).

El primer objetivo de nuestro proyecto sobre la endocitosis de GlyT2 fue determinar la vía principal de internalización utilizada y las moléculas implicadas en el proceso. Como un primer paso, mediante la sobreexpresión de GlyT2 en células MDCK junto al mutante dominante negativo K44A de la GTPasa dinamina2, determinamos la implicación de esta molécula de escisión tanto en la endocitosis constitutiva como en la endocitosis inducida por PKC. La dinamina es una proteína necesaria para las principales vías de endocitosis en MDCK; la vía dependiente de clatrina y la vía dependiente de caveolas, por lo que nos planteamos que GlyT2 podría estar utilizando cualquiera de las dos. Para diferenciar entre estas posibilidades, utilizamos un dominante negativo de caveolina1 cedido por el Dr. J. E. Pessin (*Albert Einstein College of Medicine ofYeshiva University*), que impide la internalización mediada por caveolas pero que no fue capaz de bloquear la internalización de GlyT2.

Pese a que el uso de dominantes negativos es una técnica ampliamente utilizada y aceptada, la depleción específica de proteínas mediante ARN de interferencia resulta más directa y fiable (103), por lo que decidimos medir la endocitosis de GlyT2 tras producir una depleción de caveolina1. Sin embargo, ni mediante técnicas de inmunocitoquímica ni usando técnicas de marcaje de proteínas de membrana por biotinilación observamos inhibición de la internalización del transportador.

El siguiente paso, por tanto, fue producir una depleción de clatrina, una proteína que media la internalización de una gran proporción de moléculas en los distintos tipos celulares mediante el proceso conocido como EMC (endocitosis mediada por clatrina) y que consituía la opción más probable dada la dependencia de dinamina2. La EMC es básica para el correcto funcionamiento de la sinápsis, ya que regula la cantidad en membrana plasmática de muchos tipos de receptores postsinápticos y transportadores de neurotransmisores gliales y neuronales (55, 56, 76). En el caso de GlyT2, tras la depleción de la cadena pesada de clatrina ("*clathrin heavy chain*", CHC), fuimos capaces de observar en células MDCK un bloqueo de la endocitosis constitutiva y regulada por PKC de GlyT2 mediante biotinilación y cuantificación de la proteína en membrana por inmunofluorescencia. Como aproximación adicional medimos el transporte de glicina tritiada ([^{3}H]-glicina) en células con y sin deficiencia en CHC y tras la activación de PKC observamos que la deficiencia en clatrina bloqueaba la reducción del transporte que es consecuencia de la endocitosis inducida por PKC.

Estos primeros indicios en células MDCK debían ser comprobados en el sistema endógeno. Para ello, testamos una batería de componentes descritos en la bibliografía como inhibidores específicos de la EMC (clorpromacina, concanavalina A, monodansilcadaverina) y de la endocitosis dependiente

de *rafts* (filipina, nistatina) sobre la internalización de GlyT2 en cultivos primarios de neuronas de médula espinal. En este caso, y de acuerdo con los resultados previos, observamos un reducción tanto de la endocitosis constitutiva como de la regulada por PKC en presencia de inhibidores específicos de la EMC. El mayor bloqueo se consiguió en presencia de clorpromazina, que era capaz de bloquear la internalización de GlyT2 en su totalidad. Este es un compuesto que previene la unión de la proteína adaptadora AP-2 y por tanto impide la formación de los recubrimientos de clatrina (104). Además, parece producir una relocalización de los complejos AP-2/clatrina desde la membrana hacia el interior celular (105) lo que bloquea completamente el proceso de EMC. Es un compuesto que se ha usado en humanos como antipsicótico y podría actuar favoreciendo la expresión en membrana plasmática del transportador de dopamina al inhibir su endocitosis, ya que se ha propuesto que la disminución de DAT en la superficie celular puede ser uno de los pasos previos a ciertos procesos psicóticos como la esquizofrenia (106).

La identificación de la vía principal de internalización de GlyT2 permitiría diseñar tratamientos similares a los realizados sobre DAT. Estrategias que modifiquen el funcionamiento de la EMC podrían tener aplicación en ciertos mutantes de hiperplexia cuya presencia está reducida en membrana, como puede ser el Y705C descrito por nuestro laboratorio. La inhibición de la endocitosis del transportador aumentaría su presencia en membrana, favoreciendo la recaptura y reciclaje de la glicina y mejorando la deficiente neurotransmisión glicinérgica de los pacientes. Sin embargo, esta aproximación no parece del todo acertada ya que la administración de un compuesto inhibidor de la EMC no es un tratamiento específico sobre el tráfico de GlyT2 y sus efectos secundarios pueden ser numerosos. Para ello resulta necesario profundizar en mecanismos adicionales relacionados con la EMC de GlyT2. Por ejemplo, en otros transportadores se está describiendo la importancia de ciertas modificaciones postraduccionales que modulen la selección de cargo, como puede ser la ubiquitinación de la proteína seleccionada para ser endocitada o la compartimentalización en subdominios de membrana que modulen la endocitosis. Estos conocimientos permitirían diseñar tratamientos más específicos que aumenten la presencia de GlyT2 en la superficie celular favoreciendo su actividad.

2 Determinación del papel de los *lipid rafts* en el tráfico constitutivo y regulado por PKC de GlyT2, presentado en el artículo #1.

Nuestro laboratorio había descrito previamente que GlyT2 se encuentra en subdominios especializados de membrana denominados balsas lipídicas, del inglés *lipid rafts*. Esta compartimentalización modula su actividad, ya que el transportador es más activo cuando se encuentra en este entorno lipídico (96). La asociación de GlyT2 a *rafts* es dinámica pudiendo ser desplazado a dominios *no raft* tras la activación de PKC en sinaptosomas (98).

Los *lipid rafts* modulan eventos de endocitosis, de tal forma que definen ciertas vías de internalización que dependen de su integridad. Sabiendo que GlyT2 endocita de una manera dependiente de clatrina, quisimos conocer la implicación de la asociación de GlyT2 a estos subdominios. Para ello comenzamos estudiando la implicación en la vía constitutiva. Como se ha comentado en el apartado anterior, un sistema muy utilizado para medir la endocitosis constitutiva se basa en el uso de monensina (78, 89, 90, 100-102). Como alternativa adicional a la monensina, decidimos utilizar la técnica no farmacológica denominada "*antibody feeding*", mediante la que se marca la proteína en membrana en células vivas a 4ºC (temperatura que detiene todos los eventos de tráfico) tras lo que se permite la endocitosis a 37ºC durante diferentes tiempos. Este marcaje se realiza mediante anticuerpos pero hasta la fecha no se dispone de ningún anticuerpo frente a un epítopo extracelular de GlyT2, por lo que nos vimos obligados a generar la quimera NGFR-GlyT2. Para ello añadimos el dominio amino terminal extracelular y el transmembrana siguiente del receptor del factor de crecimiento nervioso (NGFR) al extremo amino terminal de GlyT2, lo que nos permite el uso de anticuerpos frente a un epítopo extracelular de NGFR. Así, mediante esta técnica pudimos medir la endocitosis constitutiva de NGFR-GlyT2 en MDCK y comprobamos que la velocidad de internalización era muy similar a la obtenida mediante el uso de monensina.

Uno de los métodos más comunes para el estudio de *lipid rafts* se basa en el asilamiento de estos subdominios mediante su resistencia a la solubilización en frío con detergentes no iónicos a bajas

concentraciones y posterior separación por centrifugación en gradiente de sacarosa de las fracciones ligeras ricas en colesterol y esfingolípidos. Una alternativa reciente se basa en el mismo principio de solubilización en frío, pero realizado sobre células vivas, de tal modo que tras la solubilización se eliminan las proteínas no presentes en *lipid rafts* y se mantienen las proteínas asociadas a estos subdominios, observándose el resultado mediante inmunofluorescencia y microscopía confocal.

Utilizamos una combinación de ambas técnicas, midiendo la endocitosis constitutiva mediante el uso de NGFR-GlyT2 y solubilizando *in vivo* antes y después de la endocitosis. Observamos que GlyT2 se mantenía asociado a *lipid rafts* tanto en la membrana plasmática como en el interior celular tras 30 minutos de endocitosis constitutiva, lo que sugiere que GlyT2 internaliza constitutivamente sin abandonar estos subdominios. En estas mismas condiciones pudimos observar que el receptor de transferrina, una proteína no asociada a *lipid rafts*, perdía su señal tras la solubilización, mientras que el gangliósido GM1 (marcador de *rafts*), al igual que GlyT2, se mantenía en rafts tras endocitar. Así, GlyT2 endocita constitutivamente asociado a *lipid rafts* pero mediante la vía dependiente de clatrina, un mecanismo que cada vez se describe en más proteínas (107, 109, 110).

Además, nuestro laboratorio había descrito previamente que durante la endocitosis inducida por PKC se produce un desplazamiento de GlyT2 hacia zonas *no raft* reduciendo su actividad. Este desplazamiento podría ser un paso previo a la endocitosis, de tal modo que el transportador internalizaría fuera de los dominios *raft*, o podría ser un paso posterior a la endocitosis, de tal modo que internalizaría asociado a *rafts* y se disociaría de estos dominios en el interior celular. Para diferenciar entre estas dos posibilidades utlizamos células MDCK y cultivos primarios de neuronas en los que marcamos las proteínas de superficie mediante biotinilación, y después aislamos por métodos bioquímicos la totalidad de los dominios *raft* de las células. Desde estas fracciones aisladas *raft* y *no raft* se pueden recuperar mediante estreptavidina-agarosa las proteínas que estaban presentes o ausentes en la membrana plasmática, determinando la proporción del GlyT2 asociado a *lipid rafts* en la superficie celular. Dado que PKC produce internalización y desplazamiento del transportador, para poder observar únicamente el efecto de desplazamiento bloqueamos la endocitosis usando clorpromazina y determinamos la proporción de GlyT2 asociado a *lipid rafts* en la superficie. De este modo si el desplazamiento se produjese en el interior celular, el bloqueo de la endocitosis impediría el desplazamiento lateral, mientras que si el desplazamiento se sigue observando, este movimiento hacia dominios *no raft* se tiene que dar necesariamente en la membrana plasmática. En neuronas primarias tratadas con el activador de PKC (PMA) en presencia de clorpromazina observamos que la proporción de GlyT2 asociado a *rafts* disminuía significativamente, lo que indica que PKC induce este desplazamiento lateral como un paso previo a la internalización de GlyT2.

La asociación a estos subdominios parece compartimentalizar distintos reservorios de GlyT2 que se regulan de una manera diferente. En condiciones basales, GlyT2 endocita constitutivamente asociado a *rafts* para mantener disponible un reservorio funcional de transportador. GlyT2 es activo cuando está asociado a estos subdominios de tal forma que el reciclaje constitutivo por un lado permite a la neurona mantener un transporte basal de glicina más o menos constante y por otro además disponer de un reservorio intracelular de GlyT2 activo. Mediante exocitosis este reservorio del transportador puede incrementar rápidamente el número de moléculas activas en la membrana plasmática y por consiguiente favorecer la capacidad de recaptura del neurotransmisor dependiendo de la actividad de la sinápsis glicinérgica.

Por otro lado, la inhibición del transporte de GlyT2 por PKC ocurre a través de dos eventos independientes: 1) desplazamiento a zonas *no raft*, donde el transportador es mucho menos activo, y 2) endocitosis del transportador. Estos dos mecanismos se pueden desacoplar mediante inhibidores de la vía de clatrina y parecen ser secuenciales, produciéndose un desplazamiento a zonas *no raft* previo a la endocitosis del transportador. Mecanismos de regulación similares por diferentes factores ocurren en otras proteínas transmembrana como son el receptor del factor de crecimiento epidérmico (EGFR) (111) y el receptor adrenérgico α1a (112) o en otros casos como el de la internalización de la toxina tetánica (113).

Mediante el mecanismo de desplazamiento lateral, la célula puede producir una inhibición rápida del transporte de GlyT2. Esta inhibición es probablemente reversible, y ofrece una gran versatilidad a

la hora de modular la actividad de transporte ya que la inclusión/exclusión en este entorno lipídico modula a GlyT2 sin necesidad de procesos más lentos de internalización y actuando únicamente sobre la proteína en membrana. Coherentemente con este proceso, la activación de PKC produce la internalización del reservorio menos activo al disociarse de los *rafts* y que va a ser degradado posteriormente por el lisosoma. De este modo la compartimentalización de GlyT2 permite distinguir dos reservorios del transportador, uno activo asociado a *rafts* que recicla constitutivamente en endosomas rab11-positivos y otro inactivo no asociado a *rafts* cuya endocitosis mediada por PKC induce su degradación por el lisosoma previo paso por endosomas tardíos rab7-positivos (ver discusión más adelante, pag 126).

Estos resultados ayudan a clarificar la importancia de la presencia de GlyT2 en *lipid rafts*. La compartimentalización de proteínas transmembrana en *lipid rafts* usualmente es llevada a cabo por interacción con otras proteínas o lípidos enriquecidos en estos dominios. En el caso de GlyT2 está aún por establecer el mecanismo mediante el cual mantiene su asociación, pero es esperable que ciertos dominios de su secuencia sean necesarios. Una posibilidad aún por determinar es la implicación del dominio de interacción con colesterol CRAC (del inglés "*cholesterol recognition/interaction amino acid consensus*") (114) que posee GlyT2 entre los aminoácidos 485-493 de su secuencia. Este dominio está mutado en un residuo clave de su secuencia en pacientes de hiperplexia humana (mutación Y491C, ver tabla 1, introducción pag. 13). Tras el estudio de este mutante se ha visto que es capaz de alcanzar la membrana plasmática de manera normal pero una vez allí no es capaz de transportar glicina (26), lo que se podría explicar por una falta de compartimentalización que mantiene a GlyT2 fuera de su entorno lipídico óptimo impidiendo su transporte. Estudios futuros son necesarios para comprobar esta posible implicación de la presencia de GlyT2 en *lipid rafts*.

3 Determinación del papel de la ubiquitinación sobre el tráfico constitutivo y regulado por PKC de GlyT2: Implicaciones en la estabilidad del transportador y destino postendocítico, presentado en los artículos #1 y #2.

La ubiquitinación es una modificación postraduccional implicada en varios procesos celulares, entre los que se encuentran la endocitosis y degradación de proteínas. Ciertas proteínas de la maquinaria de la endocitosis mediada por clatrina, como las epsinas y Eps15/Eps15R, reconocen proteínas mono/multimonoubiquitinadas y las seleccionan para endocitar antes de la formación de la invaginación que dará lugar a la vesícula endocítica. Gracias a esto se produce una internalización selectiva de moléculas concretas que es regulada en ultima instancia por la enzima que añade la ubiquitina al sustrato (ubiquitin ligasa o E3) y por las enzimas que pueden revertir el proceso retirando la ubiquitina (deubiquitinasas o DUBs).

Mientras que para otros transportadores de neurotransmisores se había implicado a la ubiquitinación en el mecanismo de internalización, esto permanecía sin resolver en el caso de GlyT2. Para ello comenzamos utilizando Pyr-41, un compuesto que inhibe la actividad general de las enzimas activadoras de ubiquitina E1 (ver introducción pag. 17) y por tanto bloquea virtualmente todos los procesos de ubiquitinación de la célula. En presencia de este compuesto observamos una disminución de la ubiquitinación e internalización del transportador en células MDCK. Pyr-41 resultó altamente tóxico en neuronas y no nos permitió realizar los experimentos equivalentes en el sistema endógeno. Como estrategia alternativa utilizamos un inhibidor de la deubiquitinasa UCHL1 (del ingles "*Ubiquitin carboxyl-terminal hydrolase L1*"). Esta enzima es necesaria para la estabilidad de la sinápsis y la supervivencia neuronal. La función de UCHL1 resulta crucial en el mantenimiento de reservorios de ubiquitina monomérica libre, de tal forma que mantiene la disponibilidad de esta para los numerosos procesos de ubiquitinación en la neurona (72, 73). En el caso de GlyT2, tras inhibir UCHL1 y limitar el reservorio de ubiquitina libre, observamos una reducción de la ubiquitinación del transportador debido al desequilibrio en su ciclo ubiquitinación/desubiquitinación, lo que indica que GlyT2 es muy sensible a cambios en la cantidad de ubiquitina libre y parece estar sujeto a un proceso rápido de desubiquitinación.

Los resultados con Pyr-41 sugieren que la ubiquitinación de GlyT2 se requiere para su endocitosis tanto constitutiva como regulada por PKC, por lo que resulta de interés profundizar en el mecanismo tratando de determinar los residuos de lisina que unen ubiquitina para mediar estos procesos, ya que es precisamente la unión de ubiquitina a diferentes residuos de algunas proteínas lo que determina su destino final (116). Para ello generamos diferentes mutantes puntuales sustituyendo las cuatro últimas

lisinas del extremo carboxilo terminal de GlyT2 (K751, K773, K787, K791) y realizamos estudios de internalización del transportador mediante inmunocitoquímica y biotinilación.

En el caso de la endocitosis inducida por PKC, la sustitución de la última lisina del extremo carboxilo terminal por arginina (mutante K791R) bloqueaba la internalización. Mediante estudios de inmunoprecipitación anti-multiubiquitina en células MDCK pudimos observar que tras la activación de PKC aumenta la ubiquitinación de GlyT2 silvestre mientras que el mutante K791R es resistente a este efecto. Estos resultados indican que la lisina K791 es necesaria para la endocitosis inducida por PKC y que este mutante sufre un defecto de ubiquitinación en estas condiciones, lo que nos permite proponer que se requiere la ubiquitinación de esta lisina para que PKC induzca la endocitosis de GlyT2 (artículo #1). En el caso del otro transportador específico de glicina, GlyT1, la ubiquitinación de la última lisina en el extremo carboxilo terminal (K619) también es necesaria para su endocitosis inducida por PKC, lo que indica que ambas proteínas son internalizadas por mecanismos similares. GlyT1 y GlyT2 comparten el 65% de su secuencia de aminoácidos y tienen ciertas características en común, como por ejemplo la interacción con sintaxina1A. El hecho de que se requiera la ubiquitinación de la última lisina de su carboxilo terminal podría indicar que ambas proteínas comparten también la E3 ligasa que las reconoce de forma específica de tal modo que esta enzima, tras ser activada directa o indirectamente por PKC, podría reconocer una zona común del carboxilo terminal de ambos y producir la ubiquitinación de la lisina final.

Por otro lado, el estudio de la endocitosis constitutiva de los diferentes mutantes de GlyT2 (K751, K773, K787 y K791) indicó que ninguno de ellos es capaz de bloquear la internalización constitutiva lo que podría indicar la implicación de otras lisinas aún por determinar en otros dominios de la proteína. Sin embargo, en ciertas ocasiones se ha observado un fenómeno conocido como ubiquitinación redundante en el que tras la mutación del sitio preferente de unión de la ubiquitina ésta se puede enlazar a otros residuos de lisina cercanos para señalizar el destino final de la proteína ubiquitinada (115). Esto se ha observado para el transportador de glutamato GLT1, cuya endocitosis mediada por PKC depende de la ubiquitinación de un conjunto de 7 lisinas localizadas en su extremo carboxilo terminal (79) o para el transportador de dopamina DAT cuya endocitosis mediada por PKC depende de la ubiquitinación de 3 lisinas localizadas en su extremo amino terminal (88).

De este modo, quisimos averiguar si la endocitosis constitutiva de GlyT2 era dependiente de la ubiquitinación de las 4 lisinas del extremo carboxilo terminal para lo que generamos el mutante 4KR en el que se sustituyen a la vez las lisinas K751, K773, K787 y K791 por argininas. Este mutante es plenamente funcional y se expresa en la membrana plasmática correctamente. Mediante estudios de biotinilación y microscopía confocal pudimos comprobar que efectivamente la ubiquitinación de este grupo de lisinas era necesaria para la internalización constitutiva y que su sustitución producía una reducción parcial en la ubiquitinación basal de GlyT2. Esto parece indicar que existen otros sitios de ubiquitinación en el transportador, probablemente en el largo extremo amino terminal, con funciones diferentes como se ha observado en otras proteínas (116).

Por tanto, el mutante 4KR no internaliza constitutivamente ni de forma regulada por PKC ya que tiene mutada la lisina necesaria K791. Además, quisimos establecer la importancia de estas lisinas en la estabilidad, vida media y destino postendocítico del transportador. En preparaciones de tejido nervioso nuestro laboratorio indentificó a GlyT2 en endosomas de reciclaje Rab11 positivos (93). La proteína Rab11 pertenece a la familia de GTPasas Rab responsables de la regulación y organización del tráfico de proteínas en eucariotas (117) controlando el reciclaje lento a través de los compartimentos pericentriolares de reciclaje (118). Nuestros estudios en células MDCK concuerdan con los resultados previos realizados en tejido nervioso ya que en presencia de monensina se aprecia una elevada colocalización de GlyT2 con EGFP-Rab11, mientras que la colocalización con el marcador de endosomas tardíos Rab7 es mínima, lo que indica que una baja proporción del transportador internalizado constitutivamente va a ser degradado. Sin embargo, tras la activación de PKC se produce un aumento de la colocalización de GlyT2 con Rab7 y una marcada degradación de GlyT2 a tiempos largos (6 horas), lo que indica que los destinos de ambos tipos de endocitosis son diferentes. Mientras que GlyT2 recicla en endosomas Rab11 positivos asociado a *lipid rafts* con una baja proporción destinada a degradación, la activación de PKC lo desplaza a zonas *no raft* y lo envía a endosomas tardíos Rab7 positivos para su posterior degradación lisosomal. En estas condiciones sin embargo el mutante 4KR no se degrada probablemente debido a que no internaliza. Debido a la

menor ubiquitinación este mutante es más estable y posee una vida media más prolongada ya que es resistente a la degradación inducida por PKC y no endocita constitutivamente.

Por otro lado, GlyT2 con la proteína PDZ sintenina-1 a través de su dominio de unión PDZ presente en el extremo carboxilo terminal (119) lo que parece necesario para la correcta localización sináptica de GlyT2 (120). Para comprobar si las mutaciones introducidas en el transportador 4KR afectaban a este proceso expresamos GlyT2 silvestre y el mutante 4KR en neuronas de hipocampo, utilizando la ventaja de la ausencia de GlyT2 endógeno en este tipo neuronal. En estas condiciones analizamos la colocalización de ambos transportadores con sintenina1 por microscopía confocal, pero no encontramos diferencias significativas, lo que indica que la localización sináptica del mutante 4KR no se ve afectada. En otras proteínas neuronales la llegada a la membrana plasmática de mutantes de lisinas implicadas en endocitosis y degradación tampoco parece verse afectada (79, 88, 121), lo que indicaría que la ubiquitinación en estos residuos no se requiere para la exocitosis y correcta localización en la superficie celular.

Como se ha comentado al principio de este apartado, la inhibición de la desubiquitinasa UCHL1 produce una disminución de la ubiquitina libre monomérica, lo que limita los procesos de ubiquitinación en la neurona. GlyT2 resulta especialmente sensible a estos cambios, ya que pudimos comprobar que tras 2 horas de inhibición farmacológica de UCHL1 la proporción de GlyT2 ubiquitinado se reducía un 70%. La falta de ubiquitina monomérica produce un desequilibrio en el ciclo ubiquitinación/desubiquitinación de GlyT2 favoreciendo la especie desubiquitinada, y la rapidez con la que esto ocurre indica que existe una gran actividad desubiquitinasa sobre el transportador. Esta activa desubiquitinación de GlyT2 podría sugerir que su ubiquitinación se está realizando a la misma velocidad para mantener el equilibrio, lo que indica que este transportador está estrechamente regulado por su ciclo ubiquitinación/desubiquitinación pudiendo su tráfico intracelular ser modulado rápidamente por desequilibrios específicos inducidos sobre este ciclo.

El estudio de la endocitosis constitutiva de GlyT2 en presencia del inhibidor de UCHL1 en cultivos primarios de neuronas nos ha permitido comprobar la gran dependencia de la ubiquitinación de GlyT2 para que este proceso tenga lugar. La drástica disminución del transportador ubiquitinado en estas condiciones impide significativamente su internalización, lo que sugiere que en neuronas glicinérgicas el recilcaje constitutivo de GlyT2 es modulado por su estado de ubiquitinación (artículo #2).

La ubiquitinación juega un papel crucial en la función sináptica ya que modula gran cantidad de procesos entre los que se encuentran la regulación transcripcional, activación de quinasas implicadas en señalización celular, interacciones proteína-proteína, localización de proteínas y endocitosis y degradación de proteínas (66), por lo que se ha propuesto como un mecanismo necesario para la actividad y plasticidad de las conexiones sinápticas (67, 68). La neurotransmisión glicinérgica también se encuentra modulada por este proceso ya que la ubiquitinación regula la endocitosis del receptor de glicina GlyR (122) y la internalización constitutiva y regulada por PKC del transportador glial de glicina GlyT1 (78). Los datos presentados en esta tesis indican la importancia de este proceso en la endocitosis del transportador neuronal de glicina GlyT2, lo que contribuye a poner de manifiesto la relevancia de la ubiquitinación en la regulación de la función glicinérgica inhibidora.

Nuestros resultados plantean una nueva perspectiva de futuro en la que la actuación sobre el proceso de ubiquitinación de GlyT2 podría modificar la cantidad del transportador en membrana, aumentando su estabilidad y vida media, lo que podría ser de utilidad en los casos de hiperplexia causados por retenciones intracelulares parciales de GlyT2, como es el caso del mutante Y705C descrito por nuestro laboratorio (artículo #3). En estos casos, la disminución de la endocitosis del transportador podría aumentar el número de moléculas activas presentes en la membrana, lo que favorecería la recaptación y reciclaje del neurotransmisor permitiendo el rellenado de las vesículas sinápticas y por tanto normalizando la alterada neurotransmisión glicinérgica de los pacientes. Este objetivo podría lograrse mediante la activación específica de la deubiquitinasa encargada de editar/eliminar las cadenas de ubiquitina de GlyT2. Estudios futuros son necesarios para determinar que DUB actúa sobre GlyT2 y para diseñar estrategias que produzcan su activación. Resultados preliminares del laboratorio podrían implicar a la ataxina-3 como posible deubiquitinasa de GlyT2, aunque es necesario profundizar en esta posibilidad (de Juan-Sanz et. al, sin publicar).

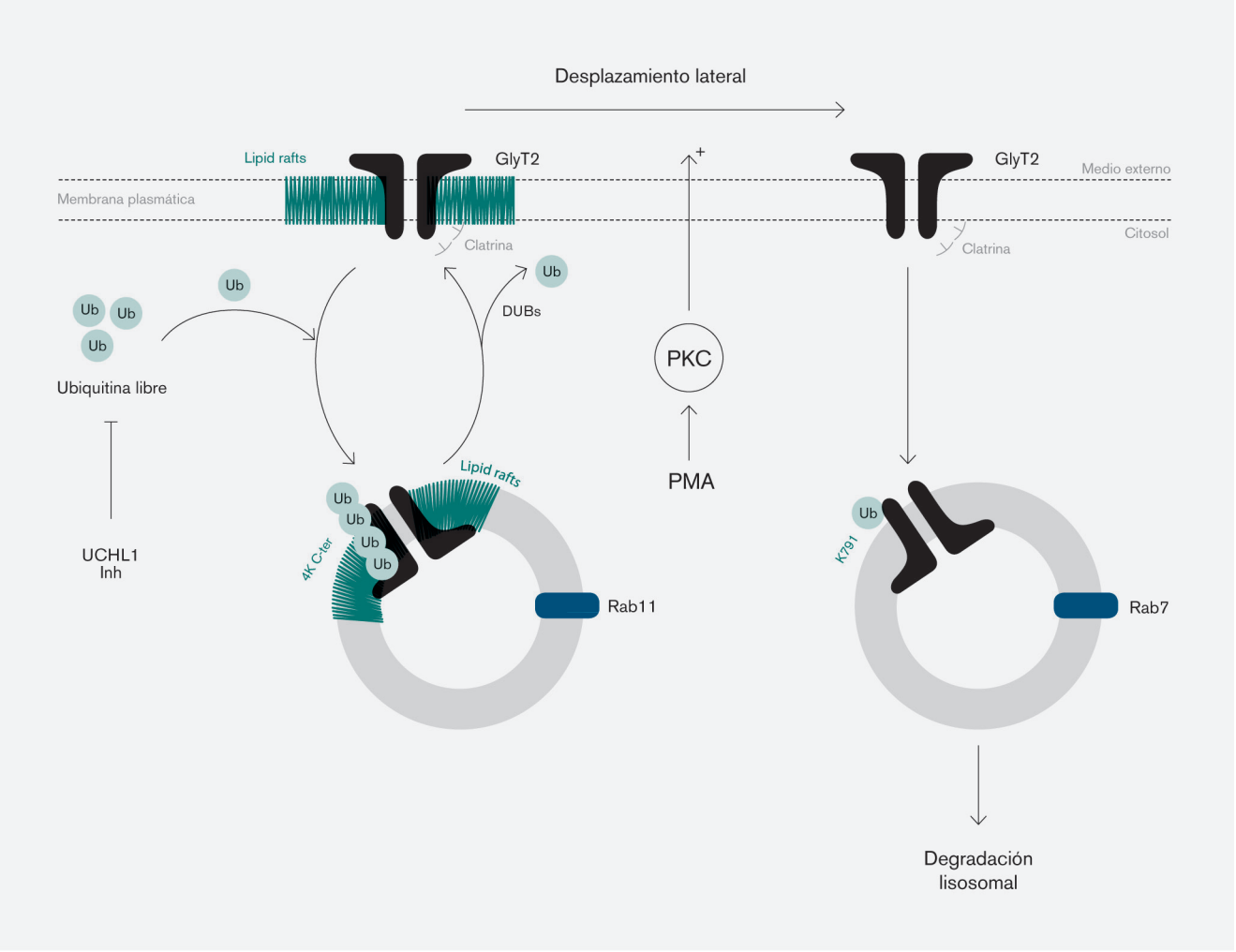

FIgura 10

Modelo del tráfico intracelular del transportador neuronal de glicina GlyT2.

GlyT2 es activo en superficie asociado a *lipid rafts*. Su endocitosis constitutiva a través de la vía de clatrina depende de la ubiquitinación del grupo de 4 lisinas del carboxilo terminal (4K C-ter) y se realiza sin abandonar estos subdominios hacia endosomas de reciclaje Rab11 positivos. Este reciclaje constitutivo se puede desequilibrar mediante la reducción de la disponibilidad de ubiquitina libre inhibiendo UCHL1, lo que aumenta la proporción de GlyT2 desubiquitinado reduciendo su endocitosis. Por otro lado, la activación por PMA de PKC produce un desplazamiento lateral en superficie de GlyT2 desde las fracciones raft a las fracciones no raft. Esto inhibe a GlyT2 ya que únicamente transporta asociado a ***rafts***, siendo un mecanismo de inhibición previo a la endocitosis del transportador que es internalizado a través de la vía dependiente de clatrina dependiendo de la ubiquitinación en la lisina K791, pasando por endosomas tardíos Rab7 positivos hasta terminar siendo degradado por el lisosoma.

Una alternativa a la activación de la DUB específica sería la inhibición de la ubiquitin ligasa que añade la ubiquitina a GlyT2. Del mismo modo, estudios futuros son necesarios para identificar esta enzima. Hasta la fecha para otros transportadores de neurotransmisores se ha determinado que NEDD 4-2 es la E3 responsable de la ubiquitinación de DAT (87) y GLT1 (77), pero en el caso de GlyT2 estudios preliminares realizados en nuestro laboratorio parecen indicar que esta enzima no ubiquitina al transportador (de Juan-Sanz et. al., sin publicar). Además, el conocimiento de la ubiquitin ligasa y la deubiquitinasa responsables del ciclo de ubiquitinación de GlyT2 permitiría sugerir nuevos genes que podrían estar implicados en enfermedades relacionadas con la neurotransmisión glicinérgica. Por ejemplo, mutaciones sobre la deubiquitinasa que actúe sobre GlyT2 favorecerían la forma ubiquitinada del transportador que internalizaría más rápidamente produciendo una disminución del número de moléculas activas en la superficie celular, lo que daría lugar a un fenotipo de hiperplexia similar al que producen mutantes de GlyT2 con defectos en el tráfico intracelular.

En conjunto, los resultados presentados en los artículos #1 y #2 permiten proponer el modelo de tráfico intracelular de GlyT2 que se muestra en la figura 10. El transportador se encuentra activo en la superficie celular asociado a *lipid rafts*. Esta subpoblación del transportador trafica constitutivamente en endosomas Rab11 positivos a través de la vía de endocitosis mediada por clatrina sin abandonar estos subdominios y dependiendo de la ubiquitinación del conjunto de 4 lisinas del extremo carboxilo terminal en las posiciones K751, K773, K787 y K791. Este estado estacionario se puede desequilibrar reduciendo la disponibilidad de ubiquitina libre mediante la inhibición de UCHL1, lo que aumenta la proporción de GlyT2 desubiquitinado en la superficie celular incapaz de endocitar. Por otro lado, la activación por PMA de PKC produce un desplazamiento lateral de GlyT2 en la superficie desde los dominios *raft* a los dominios *no raft*, lo que produce su inhibición debido a que GlyT2 es activo únicamente en los dominios *raft*. Este es un mecanismo de inhibición previo a la endocitosis del transportador, que internaliza a través de la vía de endocitosis mediada por clatrina dependiendo de la ubiquitinación en la lisina K791 siendo dirigido a endosomas tardíos Rab7 positivos para posteriormente ser degradado por el lisosoma.

4 Identificación de nuevas proteínas que interaccionen con GlyT2 y modulen su actividad y tráfico intracelular (artículo #4).

Uno de los mecanismos más comunes para la regulación de proteínas son las interacciones con otras moléculas que pueden modular entre otras funciones, su localización celular, conformación molecular o actividad. Hasta la fecha se han descrito 3 proteínas que interaccionan con GlyT2: 1) sintaxina1A una proteína SNARE que interacciona con el extremo amino terminal del transportador y está implicada en su llegada rápida a membrana al estimular la exocitosis de neurotransmisor (91, 92), 2) sintenina-1, cuya interacción con el dominio PDZ de GlyT2 en el carboxilo terminal controla la correcta localización presináptica del transportador (119, 120) y 3) Ulip6/CRMP5, que interacciona con la región de aminoácidos 134-185 del amino terminal de GlyT2 y podría modular la endocitosis del transportador (123). Esto se ha sugerido debido a su similitud con CRMP2, una proteína de la misma familia que comparte gran parte de su secuencia de aminoácidos con Ulip6/CRMP5 y que regula la endocitosis de algunas proteínas neuronales (124).

Con el objetivo de ampliar nuestros conocimientos sobre el interactoma de GlyT2 realizamos experimentos de inmunoprecipitación y detección por proteómica de las proteínas que puedan copurificar. En el análisis de los péptidos únicos detectados observamos la aparición de una gran cantidad de péptidos de la Na/K ATPasa, enzima encargada de la generación y mantenimiento del gradiente electroquímico de Na^+ necesario para el transporte de glicina mediado por GlyT2 (ver introducción, pág. 9). Estos péptidos provenían en su mayoría de las subunidades catalíticas α de la Na/K ATPasa (αNKA) siendo la subunidad específica de neuronas α3NKA la detectada con mayor número de péptidos. Para confirmar estos primeros resultados realizamos inmunoprecipitaciones anti-α1NKA, α2NKA y α3NKA con anticuerpos específicos de cada subunidad y comprobamos por western blot que GlyT2 copurifica con las tres subunidades, detectándose mayor cantidad del transportador en el inmunoprecipitado anti-α3NKA, seguido de α2NKA y en menor cuantía α1NKA. Además, realizamos inmuoprecipitaciones reversas con anticuerpos anti-GlyT2 obteniendo resultados similares.

Para confirmar los resultados anteriores realizamos ensayos de inmunocitoquímica en neuronas primarias y en sinaptosomas de cordón espinal de rata adulta para observar si existía colocalización de GlyT2 con la Na/K ATPasa. Los resultados demostraron una significativa colocalización de GlyT2 con α3NKA que era mayor que con α2NKA y α1NKA, de acuerdo con los resultados obtenidos en el análisis de proteómica y en experimentos de coinmuoprecipitación. El conjunto de estos resultados señala la existencia de una interacción entre GlyT2 y la Na/K ATPasa, favorecida especialmente con la subunidad α3 de la Na/K ATPasa.

La subunidad α3NKA es específica de neuronas localizándose principalmente en pre- y postsinápsis (125, 126, 127). Diferentes mutaciones de esta proteína están asociadas a distintos trastornos neurológicos como son la distonía-parkinsonismo de inicio rápido (DYT12) (128, 129), defectos cognitivos (130, 131), trastornos afectivos (132, 133) o la hemiplegia alternante infantil (OMIM 104290) (134). Esta subunidad parece ser responsable de la recuperación rápida

de la concentración intracelular de Na^+ en condiciones de actividad nerviosa intensa en la que se producen rápidos aumentos de Na^+ intracelular (126, 135). Esto se debe probablemente a su mayor afinidad por ATP y su menor afinidad por Na^+ respecto a las otras isoformas lo que favorece su acción al producirse grandes aumentos en la concentración de Na^+ intracelular que podrían estar saturando a las otras subunidades catalíticas (126, 136).

Como se ha descrito previamente GlyT2 co-transporta 3 iones Na^+ por cada molécula de glicina recuperada hacia el terminal presináptico, siendo el único transportador de la familia *SLC6* que necesita acoplar al transporte del sustrato más de dos iones Na^+ por ciclo funcional. Durante la actividad sináptica en el terminal se produce la exocitosis del neurotransmisor junto a un aumento rápido y transitorio de la cantidad de GlyT2 en la membrana plasmática que favorece la rápida recaptura y reciclaje de la glicina liberada (91). En esta situación el gran número de moléculas activas de GlyT2 en la superficie celular introduce $3Na^+$ por cada glicina recuperada, de tal modo que se produce un rápido aumento local del Na^+ intracelular en la presinápsis debido a la acción de GlyT2. Este aumento debe ser revertido ya que el incremento de Na^+ intracelular disminuye el gradiente electroquímico de este ion y por tanto la fuerza motriz necesaria para una gran cantidad de procesos neuronales. De este modo la subunidad α3NKA próxima a GlyT2 mediante el gasto de una molécula de ATP equilibraría el gradiente electroquímico de Na^+ expulsando rápidamente los iones Na^+ que han sido co-transportados con la glicina permitiendo que continuen funcionando los procesos dependientes del gradiente electroquímico de Na^+ en la presinápsis glicinérgica.

Como ya se ha comentado GlyT2 es activo cuando se encuentra asociado a *lipid rafts*, por lo que quisimos comprobar si la interacción GlyT2-α3NKA tenía lugar en estos subdominios. Para ello realizamos experimentos de coinmunoprecipitación con anticuerpos anti-α3NKA desde fracciones *raft* y *no raft* aisladas y observamos que GlyT2 únicamente copurificaba con α3NKA en los inmuoprecipitados provenientes de las fracciones ligeras raft, indicando que la interacción está restringida a estos subdominios. Como aproximación adicional en cultivos de neuronas primarias observamos que existe una triple colocalización en "*clusters*" entre α3NKA-GlyT2-Thy-1. Thy-1 (*Thymus cell surface antigen 1* o CD90) es una proteína asociada a *lipid rafts* mediante el grupo glicosilfosfatidilinositol (GPI) que es usada habitualmente como marcador de estos dominios en neuronas junto a flotilina1 (137, 138). La compartimentalización de GlyT2 y α3NKA en los subdominios *raft* Thy-1 positivos aumenta su probabilidad de encuentro y por tanto de interacción. De este modo α3NKA interacciona únicamente con la población activa de GlyT2 en *lipid rafts* (que es la que desequilibra el gradiente local de Na^+ al transportar glicina) restableciendo las concentraciones de Na^+ intracelular en el terminal presináptico.

Por otro lado, la presencia de ambas proteínas y su interacción en *lipid rafts* podría estar regulada y modulada por otras proteínas. Para intentar identificar estas proteínas y si forman parte del complejo GlyT2-α3NKA, realizamos experimentos de proteómica desde inmunoprecipitados anti-GlyT2 de fracciones *raft* y *no raft*. En estos experimentos comprobamos de nuevo que las distintas subunidades αNKA interaccionan con GlyT2 exclusivamente en estos subdominios, detectando un gran número de péptidos de αNKA en estas fracciones y muy pocos o ninguno en las fracciones *no raft*. Además, como control de especificidad del proceso, otras moléculas fueron halladas únicamente en las fracciones *no raft* o en ambas fracciones por igual. Sin embargo, las proteínas encontradas copurificando únicamente en fracciones raft no parecen ser relevantes para la interacción GlyT2-Na/K ATPasa según los datos bibliográficos, como es el caso de la proteína SNARE SNAP-25, aunque es necesario un estudio más detallado de estas proteínas y sus posibles implicaciones.

En resumen, estos resultados indican que la interacción GlyT2-αNKA en *lipid rafts* representa una ventaja funcional para GlyT2 al asociarse con la proteína que le suministra la energía necesaria (en forma de gradiente electroquímico de Na^+) para su función celular. Además, el mantenimiento de la homeostasis del Na^+, clave para la precisa actividad sináptica, se ve favorecida por esta interacción ya que permite sincronizar localmente en la membrana plasmática los ciclos catalíticos de ambos transportadores (fig 11-A). Los 3 Na^+ introducidos por GlyT2 por cada molécula de glicina transportada al interior celular son expulsados casi simultáneamente al exterior por la α3NKA con el gasto de una molécula de ATP.

Además, como se ha comentado en la introducción (pag. 9), esteroides cardiotónicos (del inglés "*cardiotonic steroids*", (CTS)) como la ouabaína son inhibidores específicos de la actividad Na/K ATPasa al unirse a la subunidad α. Esta unión además activa múltiples eventos de señalización celular que se inician con la activación de la tirosina quinasa Src, la transactivación de EGFR y que implican la subsecuente activación de: 1) la vía de las MAPKs, 2) PLCγ y PKC, 3) PI3K y Akt además de la 4) producción de especies reactivas de oxígeno y el 5) aumento de la concentración de Ca^{2+} intracelular, que en conjunto producen, entre otros procesos, cambios en la expresión génica. Hay que destacar que la activación de las diferentes vías de señalización inducidas por la función receptora de la Na/K ATPasa depende del tipo celular. En este sentido, el esquema que comentamos (ver introducción pag. 9, figura 6) se basa en los datos obtenidos principalmente en células renales y de músculo cardíaco, siendo todavía escasos los trabajos realizados en células neuronales.

La afinidad de la unión de la ouabaína a la Na/K ATPasa depende del tipo de isoforma α . Mientras que la subunidad α1 se ha llegado a definir como resistente a oubaina con una IC50 de 48μM, las subunidades α2 y α3 presentan una mayor afinidad con IC50 de 58nM y 6,7 nM respectivamente (139), lo que permite estudiar el efecto mediado únicamente por α2 y α3 en presencia de concentraciones bajas de ouabaína (0.1-1 μM) (140).

Así, nuestro siguiente paso fue comprobar si la unión de bajas (1μM) y altas (50μM) concentraciones de ouabaína a αNKA producían algún efecto sobre GlyT2. De este modo observamos que la presencia de 1μM ouabaína produce endocitosis del transportador y a altas concentraciones (50μM) se observa además de la endocitosis una degradación lisosomal de GlyT2. Paralelamente y para comprobar si las concentraciones utilizadas modificaban la actividad general de la Na/K ATPasa y la función de GlyT2, realizamos experimentos de transporte de ^{86}Rubidio y [^{3}H]-glicina en cultivos primarios de neuronas. Como era esperable, tras tratamientos cortos a concentración de 1μM ouabaina la actividad de las dos proteínas apenas se alteraba, indicando que el gradiente global de Na^+ no se veía afectado. Sin embargo, el tratamiento con ouabaina a 50μM inhibía aproximadamente un 70% de ambas actividades, de lo que deducimos que el efecto sobre GlyT2 en la superficie celular por 1μM ouabaina es independiente del gradiente global de Na^+. De estos resultados se deduce que parece existir una correlación entre la actividad Na/K ATPasa y la actividad de GlyT2, de tal modo que cuando se produce una inhibición de la α3NKA a 1μM, GlyT2 es retirado de la superficie celular probablemente con el objetivo de evitar que su presencia disipe el gradiente electroquímico local de Na^+ en la presinápsis. A concentraciones altas de oubabaína cuando el gradiente global Na^+ está seriamente comprometido este efecto se intensifica produciendo una degradación lisosomal del transportador que impedirá irreversiblemente su posible reciclaje de vuelta a la membrana.

La degradación a altas concentraciones de ouabaína no se observa en otras proteínas relacionadas como son: 1) sintaxina1A y Ulip6 (proteínas que interaccionan con GlyT2), 2) GAT1 y SERT (transportadores de la familia *SLC6*) o 3) las propias subunidades α de la Na/K ATPasa. Sin embargo, si se degrada por 50μM la subunidad GluR1 del receptor de AMPA en neuronas de hipocampo que también interacciona con la Na/K ATPasa (35), lo que sugiere que podría ser un mecanismo común que regule la expresión de proteínas que producen aumentos notables del Na^+ intracelular, aunque esta hipótesis ha de ser comprobada en estudios futuros.

Teniendo en cuenta que la Na/K ATPasa interacciona con GlyT2 únicamente en subdominios *raft* quisimos comprobar si la degradación por ouabaína se estaba produciendo únicamente sobre la población de GlyT2 activo. Tras el aislamiento de fracciones *raft* y *no raft* provenientes de neuronas primarias tratadas con altas dosis de ouabaína (50μM) observamos que el GlyT2 que se degrada era en su mayoría el asociado a *rafts*. De acuerdo con estos resultados pudimos observar también que la desestructuración de los *lipid rafts* mediante el uso del quelante de colesterol nistatina reducía la degradación de GlyT2, indicando una vez más la importancia de la compartimentalización en estos subdominios que permite actuar únicamente sobre la población de GlyT2 asociada a *lipid rafts*.

Por otro lado, la ouabaína y compuestos relacionados se producen endógenamente en la corteza suprarenal e hipotálamo (141, 142) encontrándose en concentraciones nanomolares en sangre en humanos en condiciones normales (143, 144). Dado que todas las células poseen Na/K ATPasa, la variedad de patologías humanas en las que se han detectado variaciones en la cantidad de ouabaína

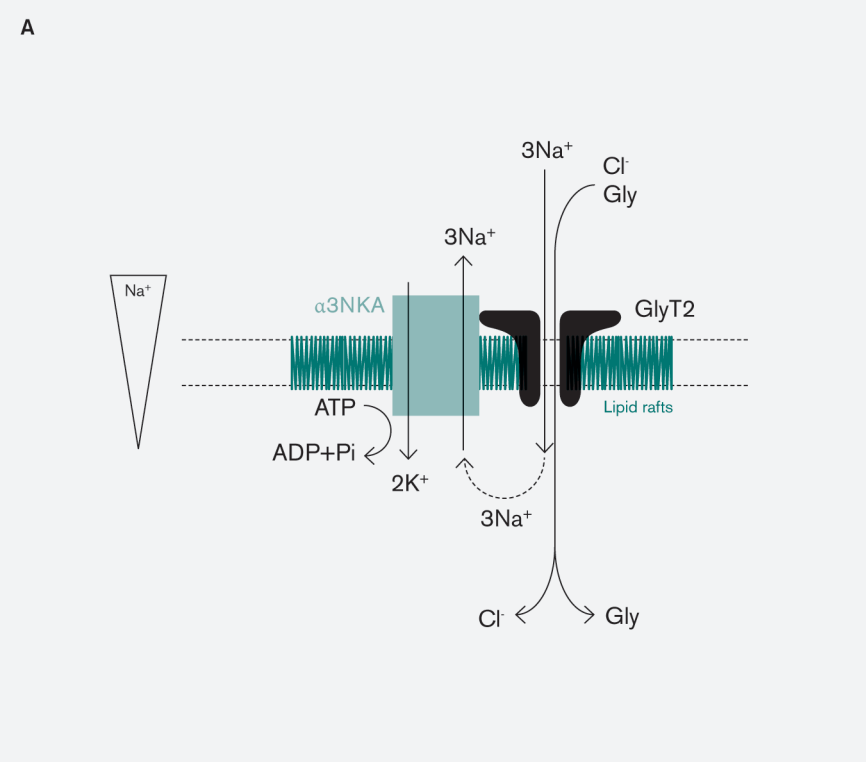

Figura 11-A
Modelo de la regulación del transportador neuronal GlyT2 por Na/K ATPasa.
A) GlyT2 es activo en membrana asociado a rafts, donde interacciona con la Na/K ATPasa, principalmente con la subunidad exclusiva neuronal α3NKA. Cada ciclo de transporte de glicina introduce una molécula de neurotransmisor, un ión cloruro y 3 iones Na^+. Un gran número de moléculas de GlyT2 transportando estos $3Na^+$ podrían desequilibrar el gradiente electroquímico local de Na^+ en la presinápsis, por lo que deben ser expulsados al espacio extracelular. Esto es realizado por la subunidad α3 de la Na/K ATPasa, introduciendo $2K^+$ y gastando una molécula de ATP.

en sangre es muy amplia abarcando fallos cardíacos, cáncer, diabetes mellitus, enfermedad renal en etapa terminal, apnea obstructiva del sueño o preeclampsia. Probablemente debido a la expresión específica de α3NKA en neuronas, también se han observado cambios en los niveles de ouabaína en sangre en casos de estrés emocional, adicción al alcohol, trastorno bipolar o depresión (145). Por tanto, la ouabaína endógena se considera como una hormona que parece regular multiples procesos en el organismo entre los cuales podría incluirse la modulación de la actividad de GlyT2.

Para tratar de comprobar el efecto *in vivo* de la ouabaína sobre GlyT2 decidimos utilizar en un principio el embrión del pez cebra (especie *Dario rerio*, conocido comunmente en inglés como "*zebrafish*"). El uso del embrión del pez cebra como modelo de estudio en neurociencia está emergiendo como un sistema *in vivo* versátil y poco costoso que se utiliza ampliamente en la actualidad en la búsqueda de fármacos, estudios de desarrollo del sistema nervioso, identificación de mecanismos de enfermedades neurológicas e incluso para estudios de comportamiento (146-148). La administración de cualquier fármaco o sustancia dirigida al sistema nervioso se debe realizar antes de la formación de la barrera hematoencefálica que se completa a las 72 horas post-fertilización (hpf). GlyT2 se expresa en el embrión del pez cebra a partir de las 20 hpf (149) siendo claramente detectado a las 36-48hpf (150-152). De acuerdo con esto, nuestros resultados indicaron que a las 48hpf los embriones de pez cebra expresan GlyT2 y α3NKA mostrando una clara colocalización entre ambas proteínas a lo largo de diferentes estructuras del embrión que se puede observar claramente en interneuronas dorsales. La administración de altas dosis de ouabaína a embriones en este estadío produjo una degradación significativa de GlyT2, lo que indica la importancia de este proceso *in vivo* y sugiere que está conservado entre distintas especies de vertebrados.

Para comprobar estos efectos *in vivo* en mamíferos decidimos administrar este compuesto intramedularmente a ratas. Varias horas tras la administración de ouabaína pudimos comprobar que se producía una disminución de la cantidad total de GlyT2 en las regiones medulares inyectadas pero no en otras zonas distantes o en las regiones inyectadas con el vehículo lo que indica que el efecto descrito en neuronas primarias y en embriones de pez cebra se produce también en ratas adultas. El conjunto de los resultados obtenidos en sistemas *in vivo* indica la importancia del proceso en el organismo completo y la conservación de este mecanismo a lo largo de especies muy diferentes. Evolutivamente la conservación de un mecanismo a lo largo de la escala filogenética indica la importancia del mismo, lo que nos permite proponer que este nuevo proceso de regulación de GlyT2 debe tener una importante relevancia fisiológica en la regulación endógena de la

neurotransmisión glicinérgica. Estudios futuros son necesarios para determinar en qué condiciones aumentos de ouabaína en sangre podrían modular la cantidad total de GlyT2 y su proporción en la superficie celular modulando la neurotransmisión glicinérgica. De este modo, aumentos en los niveles de ouabaína en las sinápsis glicinérgicas podrían producir dos efectos, 1) a corto plazo la disminución de GlyT2 en la membrana plasmática elevaría los niveles de glicina en la hendidura sináptica, que se uniría en mayor medida al receptor GlyR aumentando la neurotransmisión glicinérgica, y 2) a largo plazo la falta de reciclaje de glicina implicaría un rellenado deficiente de las vesículas sinápticas, inhibiendo la neurotransmisión glicinérgica por falta de liberación de

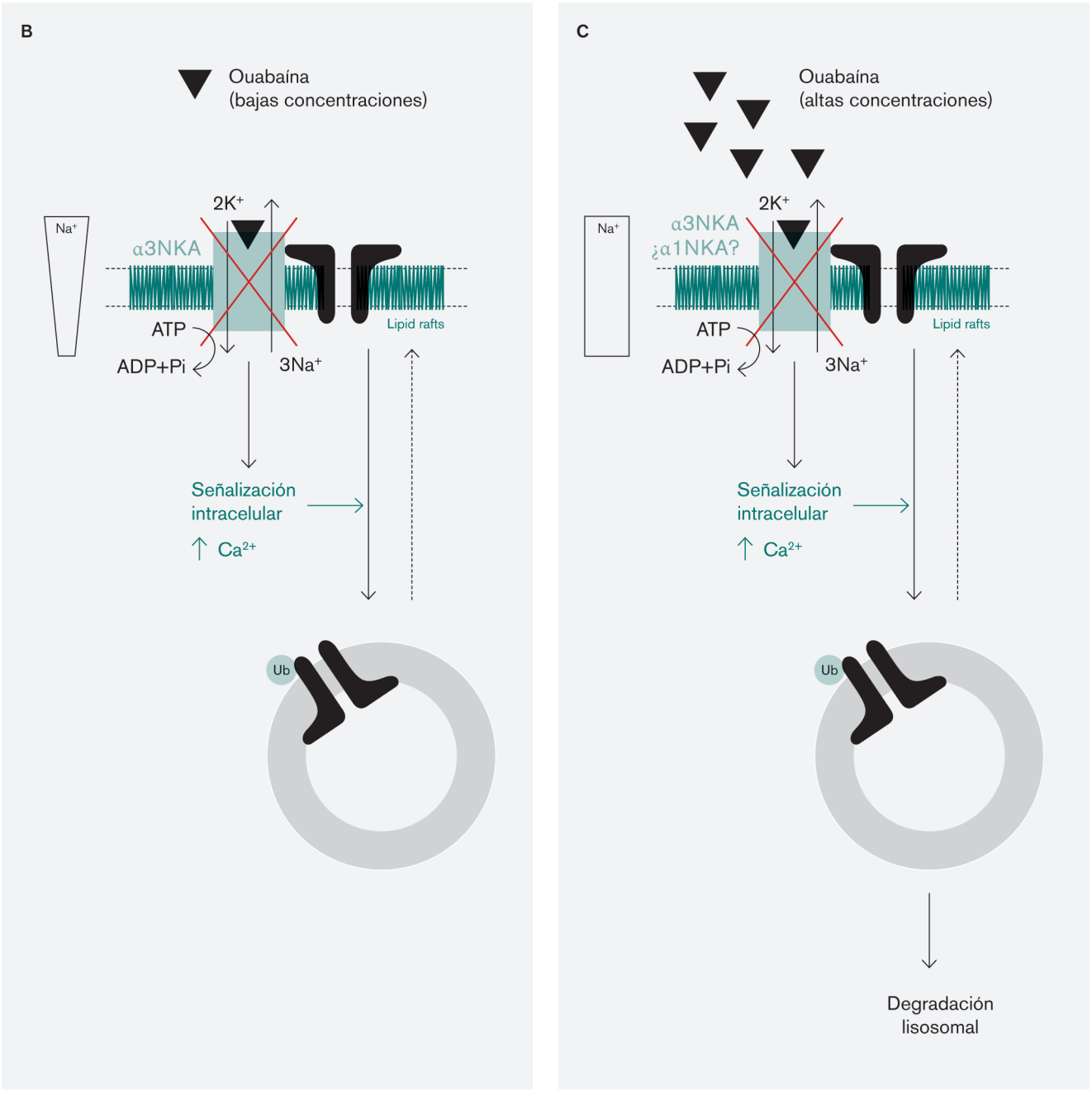

Figura 11- B y C

Modelo de la regulación del transportador neuronal GlyT2 por Na/K ATPasa.

B) La ouabaína se une a la subunidad α de la Na/K ATPasa, inhibiendo el gradiente electroquímico de Na^+ necesario para el transporte de GlyT2. Además, se produce una señalización intracelular determinada y un aumento de la concentración intracelular de Ca^{2+}. Estos eventos inducen (de una manera aún por determinar) la endocitosis de GlyT2 a bajas concentraciones de ouabaína.

C) Si estas concentraciones aumentan, el efecto de inhibición sobre la actividad de GlyT2 se intensifica, produciendo la degradación lisosomal del transportador.

neurotransmisor. Estudios futuros son necesarios para conocer la función en el organismo de este nuevo mecanismo de regulación del neurotransportador de glicina GlyT2.

En resumen, los resultados presentados en el artículo #4 identifican una nueva interacción entre GlyT2 y la Na/K ATPasa en dominios raft neuronales. Además, la inhibición de la Na/K ATPasa por ouabaína activa mecanismos de señalización celular que producen endocitosis y degradación del GlyT2 asociado a *rafts* regulando así principalmente la población de transportadores activos. Estos resultados describen un nuevo mecanismo de regulación del transportador por ouabaína, compuesto producido endógenamente por el organismo. Su unión específica a las subunidades α de la Na/K ATPasa modula *in vitro* e *in vivo* la cantidad de transportador activo en superficie celular, mecanismo que parece estar conservado evolutivamente (figura 11B-C).

En definitiva, el conjunto de los resultados presentados en esta tesis contribuye a aumentar el conocimiento sobre los mecanismos de tráfico intracelular del transportador neuronal de glicina GlyT2 y su regulación lo que puede contribuir al entendimiento de las patologías asociadas a las mutaciones del gen *SLC6A5* que presentan defectos de tráfico como algunas causantes de hiperplexia humana. Además, hemos descrito un nuevo mecanismo de regulación del transportador por Na/K ATPasa inducido por ouabaína, un esteroide cardiotónico producido endógenamente en el organismo y cuya concentración en sangre varía en diversas patologías del sistema nervioso. Estos resultados abren nuevas posibilidadades de estudio en el futuro para determinar la relación entre patologías asociadas a la neurotransmisión glicinérgica inhibitoria y la señalización de ouabaína mediada por Na/K ATPasa, pudiendo implicar por primera vez a ésta proteína ubícua en patologías relacionadas con la neurotransmisión glicinérgica.

Conclusiones

1. El transportador neuronal de glicina GlyT2 endocita de forma constitutiva y regulada por activación de PKC a través de la vía dependiente de clatrina (Artículo #1).

2. GlyT2 endocita constitutivamente asociado a *lipid rafts*. En la endocitosis regulada por PKC el transportador es desplazado a dominios "*no raft*" provocando su inactivación como un paso previo a la internalización (Artículo #1).

3. La endocitosis de GlyT2 regulada por PKC requiere la ubiquitinación de la lisina K791, mientras que la endocitosis constitutiva depende de la ubiquitinación del conjunto de lisinas K751, K773, K787 y K791 del extremo carboxilo terminal. La sustitución simultánea de estas cuatro lisinas impide su endocitosis aumentando considerablemente la estabilidad y vida media del transportador. La activación de PKC dirige a GlyT2 hacia la degradación lisosomal desviándolo de su reciclaje constitutivo (Artículos #1 y #2).

4. La reducción de la disponibilidad de ubiquitina monomérica libre por inhibición de la desubiquitinasa UCHL1 produce una desubiquitinación significativa de GlyT2 bloqueando su endocitosis (Artículo #2).

5. La sustitución Y705C (c.2114A→G) encontrada en el exón 15 del gen de GlyT2 (*SLC6A5*) en pacientes de hiperplexia humana produce defectos de trafico del transportador. (Artículo #3)

6. GlyT2 interacciona con las subunidades catalíticas α de la Na/K ATPasa en lipid rafts, principalmente con la isoforma especifica de neuronas α3NKA. Estas subunidades al actuar como receptores específicos de ouabaína activan mecanismos de señalización que inducen la endocitosis y degradación de la población activa de GlyT2 asociado a lipid rafts en neuronas in vitro (Articulo #4).

7. La regulación de GlyT2 a través de la Na/K ATPasa ocurre in vivo en embriones de pez cebra y en rata adulta tras la administración de ouabaina en el medio acuático o por vía intramedular en cordón espinal, respectivamente. El funcionamiento de este mecanismo en el organismo completo y su aparente conservación a lo largo de la escala evolutiva pone de manifiesto su importancia en el control de la neurotransmisión glicinérgica inhibidora (Articulo #4).

Resumen

Glycine is the main inhibitory neurotransmitter in the caudal areas of the brain, spinal cord and retina and plays an important role in the processing of sensory and motor information. In addition, glycine exerts a positive modulation in the excitatory glutamatergic neurotransmission by acting as a necessary co-agonist of glutamate in NMDA receptors. Glycine-mediated neurotransmission is terminated by neurotransmitter reuptake by plasma membrane glycine transporters GlyT1 and GlyT2. Mutations in the GlyT2 gene (*SLC6A5*) cause an impairment of glycinergic neurotransmission that produces hyperekplexia in humans because the neurotransmitter cannot be recaptured back to the presynaptic terminal to refill synaptic vesicles. Many of these mutations impair the normal intracellular trafficking of GlyT2, e.g. the substitution Y705C (c.2114A→G) described by our laboratory. Given the importance of GlyT2 intracellular trafficking, we have analysed the molecular mecanisms underling GlyT2 endocytosis, describing the dependence on dynamin and clathrin pathway of the constitutive and PKC-induced internalization of the transporter. Moreover, we have described that GlyT2 internalizes constitutively associated to *lipid rafts* whereas in the PKC-induced endocytosis a previous lateral displacement to non-raft domains is needed before GlyT2 internalizes to endosomal compartments. In addition, we have described that ubiquitination in the GlyT2 C-terminal end plays an important role in both internalization process. Whereas PKC-induced endocytosis of GlyT2 needs the ubiquitination of a single lysine in position K791, constitutive endocytosis of the transporter needs the ubiquitination of a cluster of lysines in positions K751, K773 ,K787, K791. Simultaneous mutation of this c-ter lysine cluster reduced basal ubiquitination of the transporter and increased notably its half-life and stability. Also, we have described that GlyT2 ubiquitination status is highly sensitive to ubiquitin homeostasis in neurons, since the reduction of the free monomeric ubiquitin pool achieved by UCHL1 inhibition reduces significantly GlyT2 ubiquitination. Moreover, in these conditions constitutive endocytosis of the transporter is impaired, denoting the importance of the ubiquitination mechanism in the GlyT2 internalization process.

In this work we have also described that Na/K ATPase is a new interacting partner for GlyT2. GlyT2 interacts with α catalytic subunits, especially with α3NKA subunit, and this interaction is restricted to lipid raft subdomains. α subunits bind ouabain, an endogenous cardiotonic steroid that induces the activation of many intracellular signaling events. In the presence of ouabain we have observed endocytosis and degradation of the lipid raft associated pool of GlyT2, which represents a drastic new pathway of transporter regulation. Further studies are needed to dilucidate the mechanisms underling this process, but these findings could help designing more effective actions in glycinergic neuromotor disorders including hyperekplexia and myoclonus, or other glycinergic-related dysfunctions as neuropathic pain or epilepsy.

Agradecimientos

Quería agradecer a las Doctoras Carmen Aragón y Beatriz López-Corcuera la oportunidad de haberme permitido realizar mi tesis doctoral en este laboratorio. He tenido la suerte de haber aprendido muchísimo de ellas durante todos estos años de trabajo compartido. Gracias especialmente a Carmen por su enorme implicación en todos los proyectos que hemos ido desarrollando, por conseguir motivarme cuando los resultados no eran los esperados y por darme la libertad de desarrollar mis propias ideas. Gracias por todo el apoyo, la entrega, la paciencia, las sugerencias, las discusiones científicas, la ilusión, los consejos y las conversaciones de la vida. Gracias por transmitirme que me ves que valgo para esto y por estar dispuesta a formar equipo conmigo. He aprendido muchísimo de ti durante todos estos años sobre ciencia y sobre muchas otras cosas. Gracias también al Dr. Francisco Zafra por la disponibilidad y el humor cada día y al Dr. Cecilio Giménez por las palabras de apoyo y confianza durante todos estos años.

Muchísimas gracias a todos los compañeros de laboratorio con los que he ido compartiendo el día a día durante estos años. Gracias por todo este tiempo, lo he disfrutado muchísimo y en una grandísima parte ha sido gracias a vosotros. Gracias a Enri, que no es por ponerme típico, pero me lo ha enseñado todo: a trabajar ordenado, con paciencia, meticulosamente y con tranquilidad. Muchas gracias por todo el apoyo estos años, por haberte preocupado y contribuido con todos los temas que he ido llevando, por la paciencia con todas las cosas que se me olvidan y con lo desastre que soy a veces y por todos los ratos compartidos que son muchos. Claramente habría sido una tesis muy diferente sin tu ayuda. Gracias a los antiguos compañeros: Jaime, que es un ejemplo de nobleza y que aunque vaya de duro todos sabemos que es un buenazo. Gracias por todas las conversaciones y coffenators compartiendo nuestra forma de ver las cosas. Gon, que es un tío único, con un buen humor incansable y claramente de las mejores personas que conozco. Gracias por todas esas horas juntos en el 304 compartiéndolo todo y por la tranquilidad con la que afrontas lo que vives que ayuda a relativizar casi cualquier cosa. Noe, que ha sido la alegría del laboratorio, del CBM y lo será de cualquier parte que vaya. Muchas gracias por hacer del trabajo un sitio donde poder disfrutar de la gente. Inma que siempre transmite su pasión por la ciencia y se preocupa de que vayamos encontrando nuestro sitio, Kike que es un pedazo de profe (y de comercial) y que nos descubrió el antimultiUb que nos salvó el Traffic y Aroa que aunque estuvo escasos meses (:P) nos ha dejado huella. Gracias por ser tan atenta y encantadora el tiempo que estuviste. Midi power!
Muchas gracias a todos los demás por esos ratos tan buenos: Guille, Rachel, Icíar, Iván.

Por supuesto, muchas gracias a las compis de ahora. Sobretodo a Esther, que siempre tiene esa buena cara todas las mañanas aunque el constructor no le ponga las ventanas de la casa o los oligómeros no se oligomericen y que nos hace a todos el día más fácil con su disponibilidad incondicional. Claramente nos hace falta en el mundo más gente como tú, y la verdad es que ha sido un placer compartir todos estos años. Gracias a Lucía por su implicación con los experimentos in vivo y las clases de anatomía, sin ti nunca habríamos sacado nada, y a Cris por ser tan agradable y dispuesta, estoy convencido de que te va a ir fenomenal. Gracias a los del 303, a Nacho que es un crack, a Espe que siempre transmite esa tranquilidad que hace mucha falta en la ciencia y en la vida, y a Cris, Valentina y Rocío. Muchas gracias por todos esos buenos momentos compartidos y los que quedan.

Gracias a las chicas del 306, sobretodo a Mónica, María y Argentina por ser tan majas, así da gusto. Argentina, muchísimas gracias por todos tus consejos, por decirme siempre que papel hay que entregar a quién, por tus correcciones del inglés, por enseñarme electrofisio una vez al mes y por la amistad de estos años. Por Dios no te vayas a Nebraska de postdoc, hay sitios que molan en el mundo! También gracias a Alfonsinho por las risas dentro y fuera del CBM, por ser tan crack y

afrontar la vida con ese buen humor, y a Alberto y Almudena por esas conversaciones en cultivos, sois lo más. Gracias a todos los compis de carrera, que sois todos unos apasionados de esto y me lo habéis ido pegando poco a poco. Gracias a Alejo, por todos los apuntes y consejos durante la carrera, por todo el buen humor y cachondeo que me has transmitido desde que nos conocemos, por los pececillos y sobretodo por tu amistad durante estos años. Muchas gracias a Lara. La amistad sigue después de tantísimos años, y seguirá muchos más. Gracias a los demás: Pilar, Marta, Elisa, Piñero, Foronda, Lucía, Cris (compi de prácticas forever!), Inés, Alfonso, Dani, Jaime, David. Ha sido genial coincidir con vosotros y a ver si hay suerte y nos vamos alguno de postdoc al mismo sitio! Y muchas gracias a todos los demás que hemos coincidido en el CBM: Guzmán, Amigo, Carlos (chaaaaaaarlie), Lagares, Óscar, Parras, Maribel, Javi K, Elena. Me llevo un gran recuerdo por haber compartido con vosotros estos años, habéis sido unos compañeros geniales, no se puede pedir más.

Por supuesto muchas gracias a todos los de la 103, por vuestro interés en saber qué hago exactamente aunque nunca sepa explicároslo bien. Gracias por tantísimos años de amistad y tantos momentos compartidos, en especial a los Ignacios, Urre, Julia, Curín, Ceb, ... donde me den trabajo tendréis vuestra casa! Gracias también a Guille, Jaco, Kike, Charlie, Fran y Nacho, por ser esa vía de escape donde nos morimos de risa aunque se hunda el mundo. Es una suerte teneros como amigos y poder contar con vosotros.

Gracias a mi familia. A mis hermanos: Víctor, que es un ejemplo de cómo hay que tomarse las cosas en la vida. Carlos, que el buen humor le sale solo, está siempre disponible para todo y es perseverante en las cosas que cree con una sonrisa y Fer, que es un ejemplo de hermano mayor, de científico crack y de buena gente. Pero sobretodo gracias a mis padres que me lo han dado todo. El cariño durante toda mi vida y el apoyo incondicional que me ha permitido ser quién soy hoy. Gracias por estar siempre ahí, sois geniales y todo esto es posible gracias a vosotros. Y gracias también a mi nueva familia: Nacha, Pedro, Marta, Gonzalo, Íñigo, Isa, Javi, Ana y los enanos Ana, Javi, Ignacio, Sofía y Mateo por tantos ratos tan buenos y los que nos quedan. Isa e Iñigo, no cerréis la fábrica!

Y por último gracias a Clara. Muchísmas gracias. Por todo. Se me queda grande poder escribir aquí algo que no se me quede corto. Muchas gracias por estar siempre ahí, por ser el descanso de todo lo demás, por todo lo que aprendo de ti cada día pero sobretodo gracias por apuntarte a la aventura de la vida conmigo. GRACIAS

Referencias

1 Legendre P. (2001) The glycinergic inhibitory synapse. *Cell Mol Life Sci* 58, 760-93

2 Ottersen OP, Storm-Mathisen, J. (1990) Immunocytochemistry of glycine and glycine receptors in the central auditory system (Eds.), Glycine Neurotransmission, Wiley, Chichester, pp. 391–415

3 Han Y, Zhang J, Slaughter MM. (1997) Partition of transient and sustained inhibitory glycinergic input to retinal ganglion cells. *J Neurosci* 17(10), 3392-400.

4 Protti DA, Gerschenfeld HM, Llano I. (1997) GABAergic and glycinergic IPSCs in ganglion cells of rat retinal slices. *J Neurosci* 17(16), 6075-85.

5 Aragón C, López-Corcuera B. (2003) Structure, function and regulation of glycine neurotransporters. *Eur J Pharmacol* 479, 249-262.

6 Melzack R, Wall PD. (1965) Pain mechanisms: a new theory. *Science* 150, 971-9.

7 Langosch D, Thomas L, Betz H. (1988) Conserved quaternary structure of ligand-gated ion channels: the postsynaptic glycine receptor is a pentamer. *Proc Natl Acad Sci U S A* 85(19), 7394-8.

8 Yang Z, Taran E, Webb TI, Lynch JW. (2012) Stoichiometry and subunit arrangement of $\alpha 1\beta$ glycine receptors as determined by atomic force microscopy. *Biochemistry* 51(26), 5229-31.

9 Moss SJ, Smart TG. (2001) Constructing inhibitory synapses. *Nat Rev Neurosci* 2, 240-250

10 Dutertre S, Becker CM, Betz H. (2012) Inhibitory glycine receptors: an update. *J Biol Chem* 287(48), 40216-23.

11 Zafra F, Aragón C, Olivares L, Danbolt NC, Giménez C, Storm-Mathisen J. (1995) Glycine transporters are differentially expressed among CNS cells. *J Neurosci* 2, 3952-69.

12 Gasnier B. (2004) The SLC32 transporter, a key protein for the synaptic release of inhibitory amino acids. *Pflugers Arch* 447(5), 756-9.

13 Madden RD. (2002) The structure and function of glutamate receptor ion channels. *Nat Rev Neurosci* 3, 91-101

14 Benveniste M, Mayer ML. (1991) Kinetic analysis of antagonist action at N-methyl-D-aspartic acid receptors. Two binding sites each for glutamate and glycine. *Biophys J* 59(3), 560-73.

15 Clements JD, Westbrook GL. (1991) Activation kinetics reveal the number of glutamate and glycine binding sites on the N-methyl-D-aspartate receptor. *Neuron* 7(4), 605-13.

16 Labrie V, Roder JC. (2010) The involvement of the NMDA receptor D-serine/glycine site in the pathophysiology and treatment of schizophrenia. *Neurosci Biobehav Rev* 34(3), 351-72.

17 Kristensen AS, Andersen J, Jørgensen TN, Sørensen L, Eriksen J, Loland CJ, Strømgaard K, Gether U. (2011) SLC6 neurotransmitter transporters: structure, function, and regulation. *Pharmacol Rev* 63(3), 585-640.

18 Dohi T, Morita K, Kitayama T, Motoyama N, Morioka N. (2009) Glycine transporter inhibitors as a novel drug discovery strategy for neuropathic pain. *Pharmacol Ther* 123(1), 54-79.

19 Eulenburg V, Armsen W, Betz H, Gomeza J. (2005) Glycine transporters: essential regulators of neurotransmission. *Trends Biochem Sci* 30(6), 325-33.

20 Adams RH, Sato K, Shimada S, Tohyama M, Püschel AW, Betz H. (1995) Gene structure and glial expression of the glycine transporter GlyT1 in embryonic and adult rodents. *J Neurosci* 15, 2524-32.

21 Cubelos B, Giménez C, Zafra F. (2005) Localization of the GLYT1 glycine transporter at glutamatergic synapses in the rat brain. *Cereb Cortex*15(4), 448-59.

22 Jursky F, Nelson N. (1995) Localization of glycine neurotransmitter transporter (GLYT2) reveals correlation with the distribution of glycine receptor. *J Neurochem* 64(3):1026-33.

23 Jones EM, Fernald A, Bell GI, Le Beau MM. (1995) Assignment of *SLC6A9* to human chromosome band 1p33 by in situ hybridization. *Cytogenet Cell Genet* 71, 211.

24 Kim KM, Kingsmore SF, Han H, Yang-Feng TL, Godinot N, Seldin MF, Caron MG, Giros B. (1994) Cloning of the human glycine transporter type 1: molecular and pharmacological characterization of novel isoform variants and chromosomal localization of the gene in the human and mouse genomes. *Mol Pharmacol* 45, 608–617

25 Hanley JG, Jones EM, Moss SJ. (2000) GABA receptor rho1 subunit interacts with a novel splice variant of the glycine transporter, GLYT-1. *J Biol Chem* 275, 840–846

26 Rees MI, Harvey K, Pearce BR, Chung SK, Duguid IC et al. (2006) Mutations in the gene encoding GlyT2 (*SLC6A5*) define a presynaptic component of human startle disease. Nat Genet. 38(7), 801-6.

27 Gomeza J, Armsen W, Betz H, Eulenburg V. (2006) Lessons from the knocked-out glycine transporters. *Handb Exp Pharmacol* 175, 457-83.

28 Baliova M, Betz H, Jursky F. (2004) Calpain-mediated proteolytic cleavage of the neuronal glycine transporter, GlyT2. *J Neurochem* 88(1), 227-32.

29 Roux MJ, Supplisson S. (2000) Neuronal and glial glycine transporters have different stoichiometries. Neuron. 25(2), 373-83.

30 Aubrey KR, Vandenberg RJ, Clements JD. (2005) Dynamics of forward and reverse transport by the glial glycine transporter, glyt1b. *Biophys J* 89(3):1657-68.

31 Lingrel JB. (2010) The physiological significance of the cardiotonic steroid/ouabain-binding site of the Na,K-ATPase. *Annu Rev Physiol* 72, 395-412.

32 Yuan Z, Cai T, Tian J, Ivanov AV, Giovannucci DR, Xie Z. (2005) Na/K-ATPase tethers phospholipase C and IP3 receptor into a calcium-regulatory complex. *Mol Biol Cell* 16(9), 4034-45.

33 Hazelwood LA, Free RB, Cabrera DM, Skinbjerg M, Sibley DR. (2008) Reciprocal modulation of function between the D1 and D2 dopamine receptors and the Na^+,K^+-ATPase. *J Biol Chem* 283, 36441-53.

34 Rose EM, Koo JC, Antflick JE, Ahmed SM, Angers S, Hampson DR. (2009) Glutamate transporter coupling to Na,K-ATPase. *J Neurosci* 29(25), 8143-55.

35 Zhang D, Hou Q, Wang M, Lin A, Jarzylo L, Navis A, Raissi A, Liu F, Man HY. (2009) Na,K-ATPase activity regulates AMPA receptor turnover through proteasome-mediated proteolysis. *J Neurosci* 29, 4498-511.

36 Gomeza J, Hülsmann S, Ohno K, Eulenburg V, Szöke K, Richter D, Betz H. (2003) Inactivation of the glycine transporter 1 gene discloses vital role of glial glycine uptake in glycinergic inhibition. *Neuron* 40, 785-96.

37 Gomeza J, Ohno K, Hülsmann S, Armsen W, Eulenburg V, Richter DW, Laube B, Betz H. (2003) Deletion of the mouse glycine transporter 2 results in a hyperekplexia phenotype and postnatal lethality. *Neuron* 40(4), 797-806.

38 Giménez C, Zafra F, López-Corcuera B, Aragón C. (2008) Molecular bases of hereditary hyperekplexia. *Rev Neurol* 47(12):648-52.

39 Bakker MJ, Peeters EA, Tijssen MA. (2009) Clonazepam is an effective treatment for hyperekplexia

due to a *SLC6A5* (GlyT2) mutation. *Mov Disord* 12, 1852-4.

40 Eulenburg V, Becker K, Gomeza J, Schmitt B, Becker CM, Betz H. (2006) Mutations within the human GLYT2 (*SLC6A5*) gene associated with hyperekplexia. *Biochem Biophys Res Commun* 348(2), 400-5.

41 Carta E, Chung SK, James VM, Robinson A, Gill JL, Remy N, Vanbellinghen JF, et. al. (2012) Mutations in the GlyT2 gene (*SLC6A5*) are a second major cause of startle disease. *J Biol Chem* 287(34), 28975-85.

42 Chung SK, Vanbellinghen JF, Mullins JG, Robinson A, Hantke J, Hammond CL, Gilbert DF, Freilinger M, Ryan M, et. al. (2010) Pathophysiological mechanisms of dominant and recessive GLRA1 mutations in hyperekplexia. *J Neurosci* 30(28), 9612-20.

43 del Giudice EM, Coppola G, Bellini G, Cirillo G, Scuccimarra G, Pascotto A. (2001) A mutation (V260M) in the middle of the M2 pore-lining domain of the glycine receptor causes hereditary hyperekplexia. *Eur J Hum Genet* 9(11), 873-6.

44 Rees MI, Andrew M, Jawad S, Owen MJ. (1994) Evidence for recessive as well as dominant forms of startle disease (hyperekplexia) caused by mutations in the alpha 1 subunit of the inhibitory glycine receptor. *Hum Mol Genet* 3, 2175–2179.

45 Giménez C, Pérez-Siles G, Martínez-Villarreal J, Arribas-González E, Jiménez E, Núñez E, de Juan-Sanz J, et. al. (2012) A novel dominant hyperekplexia mutation Y705C alters trafficking and biochemical properties of the presynaptic glycine transporter GlyT2. *J Biol Chem* 287(34), 28986-9002.

46 Nunez E, Lopez-Corcuera B, Martinez-Maza R, Aragon C. (2000a) Differential effects of ethanol on glycine uptake mediated by the recombinant GLYT1 and GLYT2 glycine transporters. *Br J Pharmacol* 129, 802–810.

47 Nunez E, Lopez-Corcuera B, Vazquez J, Gimenez C, Aragon C. (2000b) Differential effects of the tricyclic antidepressant amoxapine on glycine uptake mediated by the recombinant GLYT1 and GLYT2 glycine transporters. *Br J Pharmacol* 129, 200–206

48 Caulfield WL, Collie IT, Dickins RS, Epemolu O, McGuire R, Hill DR, McVey G, Morphy JR, Rankovic Z, Sundaram H. (2001) The first potent and selective inhibitors of the glycine transporter type 2. *J Med Chem* 44, 2679–2682

49 Xu TX, Gong N, and Xu, TL. (2005) Inhibitors of GlyT1 and GlyT2 differentially modulate inhibitory transmission. *NeuroReport* 16, 1227-1231.

50 Carland JE, Mansfield RE, Ryan RM, Vandenberg RJ. (2013) Oleoyl-L-Carnitine Inhibits Glycine Transport by GlyT2. *Br J Pharmacol* 168(4), 891-902

51 Blakely RD, Edwards RH. (2012) Vesicular and plasma membrane transporters for neurotransmitters. *Cold Spring Harb Perspect Biol* 1;4(2).

52 Kessels HW, Malinow R. (2009) Synaptic AMPA receptor plasticity and behavior. *Neuron* 61(3), 340-50.

53 Lim JP, Gleeson PA. (2011) Macropinocytosis: an endocytic pathway for internalising large gulps. *Immunol Cell Biol* 89(8), 836-43.

54 Deschamps C, Echard A, Niedergang F. (2013) Phagocytosis and cytokinesis: do cells use common tools to cut and to eat? Highlights on common themes and differences. *Traffic.* doi: 10.1111/tra.12045. *In press*

55 Jung N, Haucke V. (2007) Clathrin-mediated endocytosis at synapses. *Traffic* 8(9), 1129-36.

56 Royle SJ, Lagnado L. (2010) Clathrin-mediated endocytosis at the synaptic terminal: bridging the gap between physiology and molecules. *Traffic* 11, 1489-97.

57 Owen DJ, Collins BM, Evans PR. (2004) Adaptors for clathrin coats: structure and function. *Annu Rev Cell Dev Biol* 20, 153–91.

58 McMahon HT, Boucrot E. (2011) Molecular mechanism and physiological functions of clathrin-mediated endocytosis. *Nat Rev Mol Cell Biol* 12, 517-33.

59 Trushina E, Du Charme J, Parisi J, McMurray CT. (2006) Neurological abnormalities in caveolin-1 knock out mice. *Behav Brain Res* 172, 24–32.

60 Banning A, Tomasovic A, Tikkanen R. (2011) Functional aspects of membrane association of reggie/flotillin proteins. *Curr Protein Pept Sci* 12(8), 725-35.

61 Frank C, Giammarioli AM, Pepponi R, Fiorentini C, Rufini S. (2004) Cholesterol perturbing agents inhibit NMDA-dependent calcium influx in rat hippocampal primary culture. *FEBS Lett* 566, 25–29.

62 Dalskov SM, Immerdal L, Niels-Christiansen LL, Hansen GH, Schousboe A, Danielsen EM. Lipid raft localization of GABAA receptor and Na^+, K^+-ATPase in discrete microdomain clusters in rat cerebellar granule cells. *Neurochem Int* 46, 489–499.

63 Hering H, Lin CC, Sheng M. (2003) Lipid rafts in the maintenance of synapses, dendritic spines, and surface AMPA receptor stability. *J Neurosci* 23, 3262–3271.

64 Zhu D, Xiong WC, Mei L. (2006) Lipid rafts serve as a signaling platform for nicotinic acetylcholine receptor clustering. *J Neurosci* 26, 4841–4851.

65 Raiborg C, Stenmark H. (2009) The ESCRT machinery in endosomal sorting of ubiquitylated membrane proteins. *Nature* 458, 445-52.

66 Komander D, Rape M. (2012) The ubiquitin code. *Annu Rev Biochem* 81, 203-29.

67 DiAntonio A, Hicke L. (2004) Ubiquitin-dependent regulation of the synapse. *Annu Rev Neurosci* 27, 223-46.

68 Hegde AN, DiAntonio A. (2002) Ubiquitin and the synapse. *Nat Rev Neurosci* 3, 854-61.

69 Nijman SM, Luna-Vargas MP, Velds A, Brummelkamp TR, Dirac AM, Sixma TK, Bernards R. (2005) A genomic and functional inventory of deubiquitinating enzymes. *Cell* 123(5), 773-86.

70 Leroy E, Boyer R, Auburger G, Leube B, Ulm G, Mezey E, Harta G, Brownstein MJ, Jonnalagada S, Chernova T, Dehejia A, Lavedan C, Gasser T, Steinbach PJ, Wilkinson KD, Polymeropoulos MH. (1998) The ubiquitin pathway in Parkinson's disease. *Nature* 395(6701), 451-2.

71 Maraganore DM, Lesnick TG, Elbaz A, Chartier-Harlin MC, Gasser T, Krüger R, Hattori N, Mellick GD, Quattrone A, Satoh J, Toda T, Wang J, Ioannidis JP, de Andrade M, Rocca WA. (2004) UCHL1 is a Parkinson's disease susceptibility gene. *Ann Neurol* 55(4), 512-21.

72 Osaka H, Wang YL, Takada K, Takizawa S, Setsuie R, Li H, Sato Y, Nishikawa K, Sun YJ, Sakurai M, Harada T, Hara Y, Kimura I, Chiba S, Namikawa K, Kiyama H, Noda M, Aoki S, Wada K. (2003) Ubiquitin carboxy-terminal hydrolase L1 binds to and stabilizes monoubiquitin in neuron. *Hum Mol Genet* 12, 1945-58.

73 Chen F, Sugiura Y, Myers KG, Liu Y, Lin W. (2010) Ubiquitin carboxyl-terminal hydrolase L1 is required for maintaining the structure and function of the neuromuscular junction. *Proc Natl Acad Sci U S A* 107(4), 1636-41.

74 Gong B, Cao Z, Zheng P, Vitolo OV, Liu S, Staniszewski A, Moolman D, Zhang H, Shelanski M, Arancio O. (2006) Ubiquitin hydrolase Uch-L1 rescues beta-amyloid-induced decreases in synaptic function and contextual memory. *Cell* 126, 775-88.

75 Blakely RD, Bauman AL. (2000) Biogenic amine transporters: regulation in flux. *Curr Opin Neurobiol* 10, 328–336.

76 Chang MY, Lee SH, Kim JH, Lee KH, Kim YS, Son H, Lee YS (2001) Protein kinase C-mediated functional regulation of dopamine transporter is not achieved by direct phosphorylation of the dopamine transporter protein. J Neurochem 77, 754-61.

77 García-Tardón N, González-González IM, Martínez-Villarreal J, Fernández-Sánchez E, Giménez C, Zafra F. (2012) Protein kinase C (PKC)-promoted endocytosis of glutamate transporter GLT-1 requires ubiquitin ligase Nedd4-2-dependent ubiquitination but not phosphorylation. *J Biol Chem* 287(23), 19177-87.

78 Fernández-Sánchez E, Martínez-Villarreal J, Giménez C, Zafra F. (2009) Constitutive and regulated endocytosis of the glycine transporter GLYT1b is controlled by ubiquitination. *J Biol Chem* 284(29), 19482-92.

79 González-González IM, García-Tardón N, Giménez C, Zafra F. (2008) PKC-dependent endocytosis of the GLT1 glutamate transporter depends on ubiquitylation of lysines located in a C-terminal cluster. *Glia* 56(9), 963-74.

80 Holton KL, Loder MK, Melikian HE. (2005) Nonclassical, distinct endocytic signals dictate constitutive and PKC-regulated neurotransmitter transporter internalization. *Nat Neurosci* 8(7), 881-8.

81 Boudanova E, Navaroli DM, Stevens Z, Melikian HE. (2008) Dopamine transporter endocytic determinants: carboxy terminal residues critical for basal and PKC-stimulated internalization. *Mol Cell Neurosci* 39(2), 211-7.

82 Jayanthi LD, Samuvel DJ, Blakely RD, Ramamoorthy S. (2005) Evidence for biphasic effects of protein kinase C on serotonin transporter function, endocytosis, and phosphorylation. *Mol Pharmacol* 67(6), 2077-87.

83 Sato K, Betz H, Schloss P. (1995) The recombinant GABA transporter GAT1 is downregulated upon activation of protein kinase C. *FEBS Lett* 375, 99-102.

84 Corey JL, Davidson N, Lester HA, Brecha N, Quick MW. (1994) Protein kinase C modulates the activity of a cloned gamma-aminobutyric acid transporter expressed in Xenopus oocytes via regulated subcellular redistribution of the transporter. *J Biol Chem* 269, 14759-67.

85 Apparsundaram S, Schroeter S, Giovanetti E, Blakely RD. (1998) Acute regulation of norepinephrine transport: II. PKC-modulated surface expression of human norepinephrine transporter proteins. *J Pharmacol Exp Ther* 287, 744-51.

86 Fornés A, Núñez E, Alonso-Torres P, Aragón C, López-Corcuera B. (2008) Trafficking properties and activity

regulation of the neuronal glycine transporter GLYT2 by protein kinase C. *Biochem J* 412, 495-506.

87 Sorkina T, Miranda M, Dionne KR, Hoover BR, Zahniser NR, Sorkin A. (2006) RNA interference screen reveals an essential role of Nedd4-2 in dopamine transporter ubiquitination and endocytosis. *J Neurosci* 26, 8195-205.

88 Miranda M, Dionne KR, Sorkina T, Sorkin A. (2007) Three ubiquitin conjugation sites in the amino terminus of the dopamine transporter mediate protein kinase C-dependent endocytosis of the transporter. *Mol Biol Cell* 18, 313-323.

89 Martínez-Villarreal J, García Tardón N, Ibáñez I, Giménez C, Zafra F. (2012) Cell surface turnover of the glutamate transporter GLT-1 is mediated by ubiquitination/deubiquitination. *Glia* 60(9), 1356-65.

90 Eriksen J, Bjørn-Yoshimoto WE, Jørgensen TN, Newman AH, Gether U. (2010) Postendocytic sorting of constitutively internalized dopamine transporter in cell lines and dopaminergic neurons. *J Biol Chem* 285, 27289-27301.

91 Geerlings A, Núñez E, López-Corcuera B, Aragón C. (2001) Calcium- and syntaxin 1-mediated trafficking of the neuronal glycine transporter GLYT2. *J Biol Chem* 276(20), 17584-90.

92 Geerlings A, López-Corcuera B, Aragón C. (2000) Characterization of the interactions between the glycine transporters GLYT1 and GLYT2 and the SNARE protein syntaxin 1A. *FEBS Lett* 470(1), 51-4.

93 Núñez E, Pérez-Siles G, Rodenstein L, Alonso-Torres P, Zafra F, Jiménez E, Aragón C, López-Corcuera B. (2009) Subcellular localization of the neuronal glycine transporter GLYT2 in brainstem. *Traffic* 10(7), 829-43.

94 Geerlings A, Nunez E, Rodenstein L, Lopez-Corcuera B, Aragon C. (2002) Glycine transporter isoforms show differential subcellular localization in PC12 cells. *J Neurochem* 82, 58–65.

95 Fornes A, Nunez E, Aragon C, Lopez-Corcuera B. (2004) The second intracellular loop of the glycine transporter 2 contains crucial residues for glycine transport and phorbol ester-induced regulation. *J Biol Chem* 279, 22934–22943.

96 Fornés A, Núñez E, Alonso-Torres P, Aragón C, López-Corcuera B. (2008) Trafficking properties and activity regulation of the neuronal glycine transporter GLYT2 by protein kinase C. *Biochem J* 412(3), 495-506.

97 Núñez E, Alonso-Torres P, Fornés A, Aragón C, López-Corcuera B. (2008) The neuronal glycine transporter GLYT2 associates with membrane rafts: functional modulation by lipid environment. *J Neurochem* 105, 2080-90.

98 Tsui-Pierchala BA, Encinas M, Milbrandt J, Johnson EM Jr. (2002) Lipid rafts in neuronal signaling and function. *Trends Neurosci* 25(8), 412-7

99 Martínez-Maza R, Poyatos I, López-Corcuera B, Nuñez E, Giménez C, Zafra F, Aragón C. (2001) The role of N-glycosylation in transport to the plasma membrane and sorting of the neuronal glycine transporter GLYT2. *J Biol Chem* 276(3), 2168-73.

100 Dang VC, Williams JT. (2004) Chronicmorphine treatment reduces recovery from opioid desensitization. *J Neurosci* 24, 7699-7706.

101 Michaely P, Zhao Z, Li WP, Garuti R, Huang LJ, Hobbs HH, Cohen JC. (2007) Identification of a VLDL-induced, FDNPVY independent internalization mechanism for the LDLR. *EMBO J* 26, 3273-3282.

102 Magalhaes AC, Holmes KD, Dale LB, Comps-Agrar L, Lee D, Yadav PN, Drysdale L, Poulter MO, Roth BL, Pin JP, Anisman H, Ferguson SS. (2010) CRF receptor 1 regulates anxiety behaviour via sensitization of 5-HT2 receptor signaling. *Nat Neurosci* 13, 622-629.

103 [Editorial] (2003) Whither RNAi?. *Nat Cell Biol* 5(6), 489-90.

104 Rodemer C, Haucke V. (2008) Clathrin/AP-2-dependent endocytosis: a novel playground for the pharmacological toolbox? *Handb Exp Pharmacol* 186, 105-122.

105 Wang LH, Rothberg KG, Anderson RG. (1993) Mis-assembly of clathrin lattices on endosomes reveals a regulatory switch for coated pit formation. *J Cell Biol* 123, 1107-1117.

106 Schmitt GJ, la Fougère C, Dresel S, Frodl T, Hahn K, Möller HJ. (2008) Dual-isotope SPECT imaging of striatal dopamine: first episode, drug naïve schizophrenic patients. *Schizophr Res* 101, 133-14.

107 Masuyama N, Kuronita T, Tanaka R, Muto T, Hirota Y, Takigawa A, Fujita H, Aso Y, Amano J, Tanaka Y. (2009) HM1.24 is internalized from lipid rafts by clathrin-mediated endocytosis through interaction with alpha-adaptin. *J Biol Chem* 284, 15927-15941.

108 Fattakhova G, Masilamani M, Borrego F, Gilfillan AM, Metcalfe DD, Coligan JE. (2006) The high affinity immunoglobulin-E receptor (FcepsilonRI) is endocytosed by an AP-2/clathrin-independent, dynamin-dependent mechanism. *Traffic* 7, 673–685.

109 Sarnataro D, Caputo A, Casanova P, Puri C, Paladino S, Tivodar SS, Campana V, Tacchetti C, Zurzolo C. (2009) Lipid rafts and clathrin cooperate in the internalization of PrP in epithelial FRT cells. *PloS One* 4, e5829.

110 Cuitino L, Matute R, Retamal C, Bu G, Inestrosa NC, Marzolo MP. (2005) ApoER2 is endocytosed by a clathrin-mediated process involving the adaptor protein Dab2 independent of its Rafts' association. *Traffic* 6, 820-838.

111 Mineo C, Gill GN, Anderson RG. (1999) Regulated migration of epidermal growth factor receptor from caveolae. *J Biol Chem* 274, 30636-30643.

112 Morris DP, Lei B, Wu YX, Michelotti GA, Schwinn DA. (2008) The alpha 1a adrenergic receptor occupies membrane rafts with its G protein effectors but internalizes via clathrin-coated pits. *J Biol Chem* 283, 2973-2985.

113 Deinhardt K, Berninghausen O, Willison HJ, Hopkins CR, Schiavo G. (2006) Tetanus toxin is internalized by a sequential clathrin-dependent mechanism initiated within lipid microdomains and independent of epsin1. *J Cell Biol* 174, 459-471.

114 Epand RM. (2008) Proteins and cholesterol-rich domains. Biochim Biophys Acta. 1778(7-8), 1576-82.

115 Miranda M, Sorkin A. (2007) Regulation of receptors and transporters by ubiquitination: new insights into surprisingly similar mechanisms. Mol Interv 7, 157-67.

116 Sadowski M, Sarcevic B. (2010) Mechanisms of mono- and poly-ubiquitination: Ubiquitination specificity depends on compatibility between the E2 catalytic core and amino acid residues proximal to the lysine. *Cell Div* 13, 5-19.

117 Zerial M, McBride H. (2001) Rab proteins as membrane organizers. *Nat Rev Mol Cell Biol* 2, 107-117.

118 Jones MC, Caswell PT, Norman JC (2006) Endocytic recycling pathways: emerging regulators of cell migration. *Curr Opin Cell Biol* 18, 549-557.

119 Ohno K, Koroll M, El Far O, Scholze P, Gomeza J, Betz H. (2004) The neuronal glycine transporter 2 interacts with the PDZ domain protein syntenin-1. *Mol Cell Neurosci* 26(4), 518-29.

120 Armsen W, Himmel B, Betz H, Eulenburg V. (2007) The C-terminal PDZ-ligand motif of the neuronal glycine transporter GlyT2 is required for efficient synaptic localization. *Mol Cell Neurosci* 36(3), 369-80.

121 Schwarz LA, Hall BJ, Patrick GN. (2010) Activity-dependent ubiquitination of GluA1 mediates a distinct AMPA receptor endocytosis and sorting pathway. *J Neurosci* 30, 16718-29.

122 Büttner C, Sadtler S, Leyendecker A, Laube B, Griffon N, Betz H, Schmalzing G. (2001) Ubiquitination precedes internalization and proteolytic cleavage of plasma membrane-bound glycine receptors. *J Biol Chem* 276(46), 42978-85.

123 Horiuchi M, Loebrich S, Brandstaetter JH, Kneussel M, Betz H. (2005) Cellular localization and subcellular distribution of Unc-33-like protein 6, a brain-specific protein of the collapsin response mediator protein family that interacts with the neuronal glycine transporter 2. *J Neurochem* 94, 307-15.

124 Nishimura T, Fukata Y, Kato K, Yamaguchi T, Matsuura Y, Kamiguchi H, Kaibuchi K. (2003) CRMP-2 regulates polarized Numb-mediated endocytosis for axon growth. *Nat Cell Biol* 5, 819-26.

125 Hilgenberg LG, Su H, Gu H, O'Dowd DK, Smith MA. (2006) Alpha3 Na^+/K^+-ATPase is a neuronal receptor for agrin. *Cell* 125(2), 359-69.

126 Kim JH, Sizov I, Dobretsov M, von Gersdorff H. (2007) Presynaptic Ca^{2+} buffers control the strength of a fast post-tetanic hyperpolarization mediated by the alpha3 $Na(^+)/K(^+)$-ATPase. *Nat Neurosci* 10, 196-205.

127 Blom H, Rönnlund D, Scott L, Spicarova Z, Widengren J, Bondar A, Aperia A, Brismar H. (2011) Spatial distribution of Na^+-K^+-ATPase in dendritic spines dissected by nanoscale superresolution STED microscopy. *BMC Neurosci* 1, 12-16.

128 de Carvalho Aguiar P, Sweadner KJ, Penniston JT, Zaremba J, Liu L, Caton M, Linazasoro G, Borg M, Tijssen MA, Bressman SB, Dobyns WB, Brashear A, Ozelius LJ. (2004) Mutations in the Na^+/K^+-ATPase alpha3 gene ATP1A3 are associated with rapid-onset dystonia parkinsonism. *Neuron* 43, 169-175

129 Brashear A, Dobyns WB, de Carvalho Aguiar P, Bnorg M, Frijns CJ, Gollamudi S, Green A, Guimaraes J, Haake BC, Klein C, Linazasoro G, Münchau A, Raymond D, Riley D, Saunders-Pullman R, Tijssen MA, Webb D, Zaremba J, Bressman SB, Ozelius LJ. (2007) The phenotypic spectrum of rapid-onset dystonia-parkinsonism (RDP) and mutations in the ATP1A3 gene. *Brain* 130, 828-35.

130 Lingrel JB, Williams MT, Vorhees CV, Moseley AE. (2007) Na,K-ATPase and the role of alpha isoforms in behavior. *J Bioenerg Biomembr* 39, 385-389

131 Moseley AE, Williams MT, Schaefer TL, Bohanan CS, Neumann JC, Behbehani MM, Vorhees CV, Lingrel JB.

(2007) Deficiency in Na,K-ATPase alpha isoform genes alters spatial learning, motor activity, and anxiety in mice. *J Neurosci* 27, 616-626

132 Kirshenbaum GS, Saltzman K, Rose B, Petersen J, Vilsen B, Roder JC. (2011) Decreased neuronal Na^+, K^+ -ATPase activity in Atp1a3 heterozygous mice increases susceptibility to depression-like endophenotypes by chronic variable stress. *Genes Brain Behav* 10, 542-550

133 Kirshenbaum GS, Clapcote SJ, Duffy S, Burgess CR, Petersen J, Jarowek KJ, Yucel YH, Cortez MA, Snead OC, Vilsen B, Peever JH, Ralph MR, Roder JC. (2011) Mania-like behavior induced by genetic dysfunction of the neuron-specific Na^+,K^+-ATPase alpha3 sodium pump. *Proc Nat Acad Sci U S A* 108, 18144-18149

134 Heinzen EL, Swoboda KJ, Hitomi Y, Gurrieri F, Nicole S, et. al. (2012) De novo mutations in ATP1A3 cause alternating hemiplegia of childhood. *Nat Genet* 44, 1030-4.

135 Azarias G, Kruusmägi M, Connor S, Akkuratov EE, Liu XL, Lyons D, Brismar H, Broberger C, Aperia A. (2013) A Specific and Essential Role for Na,K-ATPase α3 in Neurons Co-expressing α1 and α3. *J Biol Chem* 288, 2734-43.

136 Zahler R, Zhang ZT, Manor M, Boron WF. (1997) Sodium kinetics of Na,KATPase alpha isoforms in intact transfected HeLa cells. *J Gen Physiol* 110, 201-213

137 Wilson BS, Steinberg SL, Liederman K, Pfeiffer JR, Surviladze Z, Zhang J, Samelson LE, Yang LH, Kotula PG, Oliver JM. (2004) Markers for detergent-resistant lipid rafts occupy distinct and dynamic domains in native membranes. *Mol Biol Cell* 15, 2580-92.

138 Stuermer CA. (2011) Reggie/flotillin and the targeted delivery of cargo. *J Neurochem* 116, 708-13.

139 O'Brien WJ, Lingrel JB, Wallick ET. (1994) Ouabain binding kinetics of the rat alpha two and alpha three isoforms of the sodium-potassium adenosine triphosphate. *Arch Biochem Biophy* 310, 32-39

140 Lingrel JB. (2010) The physiological significance of the cardiotonic steroid/ouabain-binding site of the Na,K-ATPase. *Annu Rev Physiol* 72, 395-412.

141 Tymiak AA, Norman JA, Bolgar M, DiDonato GC, Lee H, Parker WL, Lo LC, Berova N, Nakanishi K, and Haber E (1993). Physicochemical characterization of a ouabain isomer isolated from bovine hypothalamus. *Proc Natl Acad Sci U S A* 90, 8189-8193.

142 el-Masri MA, Clark BJ, Qazzaz HM, and Valdes R Jr (2002) Human adrenal cells in culture produce both ouabain-like and dihydroouabain-like factors. *Clin Chem* 48, 1720-1730.

143 Hamlyn JM, Blaustein MP, Bova S, DuCharme DW, Harris DW, Mandel F, Mathews WR, and Ludens JH (1991) Identification and characterization of a ouabain-like compound from human plasma. *Proc Natl Acad Sci U S A* 88, 6259-6263.

144 Ludens JH, Clark MA, DuCharme DW, Harris DW, Lutzke BS, Mandel F, Mathews WR, Sutter DM, and Hamlyn JM. (1991) Purification of an endogenous digitalis-like factor from human plasma for structural analysis. *Hypertension* 17, 923-929.

145 Bagrov AY, Shapiro JI, Fedorova OV. (2009) Endogenous cardiotonic steroids: physiology, pharmacology, and novel therapeutic targets. *Pharmacol Rev* 61, 9-38.

146 Cheng RK, Jesuthasan S, Penney TB. (2011) Time for zebrafish. *Front Integr Neurosci* 5-40.

147 Edward DL, Daniel TC. (2009) Chapter 15: Behavioral Neuroscience of Zebrafish. *Methods of Behavior Analysis in Neuroscience*. 2nd edition. Buccafusco JJ, editor. Boca Raton (FL): CRC Press.

148 Xi Y, Noble S, Ekker M. (2011) Modeling neurodegeneration in zebrafish. *Curr Neurol Neurosci Rep* 11, 274-82

149 Higashijima S, Mandel G, Fetcho JR. (2004) Distribution of prospective glutamatergic, glycinergic, and GABAergic neurons in embryonic and larval zebrafish. *J Comp Neurol* 480, 1-18.

150 Higashijima S, Schaefer M, Fetcho JR. (2004) Neurotransmitter properties of spinal interneurons in embryonic and larval zebrafish. *J Comp Neurol* 480, 19-37.

151 Cui WW, Low SE, Hirata H, Saint-Amant L, Geisler R, Hume RI, Kuwada JY. (2005) The zebrafish shocked gene encodes a glycine transporter and is essential for the function of early neural circuits in the CNS. *J Neurosci* 25, 6610-20.

152 Moly PK, Hatta K. (2011) Early glycinergic axon contact with the Mauthner neuron during zebrafish development. *Neurosci Res* 70, 251-9